

**Identification and functional characterization of
mPDCA-1 as a novel antigen-uptake receptor
on murine plasmacytoid dendritic cells
enabling (cross-) priming of naïve CD4⁺ and CD8⁺ T cells.**

INAUGURAL-DISSERTATION

zur

Erlangung des Doktorgrades

der Mathematisch-Naturwissenschaftlichen Fakultät

der Universität zu Köln

vorgelegt von

Jens A. A. Fischer

aus Leverkusen

Bergisch Gladbach, 2008

Berichtersteller/in:

Erstgutachter:

Prof. Dr. Manolis Pasparakis

Zweitgutachterin:

Prof. Dr. Dagmar Knebel-Mörsdorf

Tag der mündlichen Prüfung: 24. Oktober 2008

Für Virginia

ZUSAMMENFASSUNG

Plasmazytoide Dendritische Zellen (PDCs) repräsentieren eine Subpopulation Dendritischer Zellen und sind die Hauptproduzenten von Typ I Interferonen nach viraler oder mikrobieller Stimulation. Dadurch beeinflussen und verbinden sie die angeborene und adaptive Immunabwehr. Obwohl es immer mehr Anzeichen einer Beteiligung von PDCs an der Entstehung und Aufrechterhaltung von Autoimmunerkrankungen oder Krebs gibt, und ihnen auch eine Rolle bei der Induktion von Toleranz zugeschrieben wird, ist wenig über ihre exakte immunologische Funktion bekannt. Besonders ihre Rolle als Antigen-präsentierende Zellen bei der Induktion einer T-Zell-Antwort wird kontrovers diskutiert. Die funktionelle Charakterisierung von murinen PDCs wurde durch das Fehlen eines spezifischen Oberflächenrezeptors erschwert. PDCs wurden identifiziert anhand der Co-Expression von B220, Ly-6C, und CD11c.

In dieser Arbeit wurden verschiedene monoklonale Antikörper generiert, die alle ein Oberflächenantigen erkannten, das spezifisch auf PDCs in naiven Mäusen exprimiert war und das als „murines PDC Antigen 1“ (mPDCA-1) bezeichnet wurde. Mithilfe differentieller Genexpressionsanalyse konnte gezeigt werden, daß die anti-mPDCA-1 Antikörper das „Bone marrow stromal antigen 2“ (BST2) erkennen.

Weitere Experimente zeigten, daß Ligandierung des mPDCA-1 Rezeptors eine *Toll-like* Rezeptor-induzierte Produktion von Typ I Interferonen in PDCs inhibierte. Die Kreuzvernetzung des Rezeptors mit anti-mPDCA-1 Antikörpern resultierte in einer intrazellulären Kalzium-Mobilisierung sowie in einer allgemeinen Phosphorylierung von Proteintyrosinresten. Des Weiteren führte die Kreuzvernetzung sowohl *in vitro* als auch *in vivo* zu einer schnellen und effizienten Internalisierung des Rezeptor-Antikörperkomplexes.

Als nächstes wurde die potentielle Funktion des mPDCA-1 Moleküls als PDC-spezifischer Antigen-Aufnahmerezeptor untersucht. Da die Applikation des vollständigen anti-mPDCA-1 Antikörpers *in vivo* in Fc-vermittelter oder ADCC-abhängiger Depletion der PDCs resultierte, wurde Ovalbuminprotein kovalent an ein nichtdepletierendes F(ab')₂-Fragment des anti-PDCA-1 Antikörpers konjugiert. Somit konnten PDCs spezifisch *in vitro* und *in vivo* angefärbt werden. Über mPDCA-1 aufgenommenes Antigen wurde prozessiert und auf Klasse I und II MHC-Molekülen präsentiert. Dabei waren PDCs in der Lage, naive CD4⁺ and CD8⁺ T-Lymphozyten *in vitro* effizient zu *primen*. Sowohl das *Priming* als auch das *cross-priming* antigenspezifischer T-Zellen war abhängig von einer Aktivierung der PDCs, die mit einer verstärkten Expression costimulatorischer und MHC-Moleküle einherging. Dieser zusätzliche Stimulus schien auch die Antigenprozessierungs- und präsentationsmaschinerie zu aktivieren.

Letztlich wurde eine heterogene Expression des „Stem cell antigen 1“ (Sca-1) auf PDCs beobachtet, die organabhängig variierte. Sca-1⁺ PDCs erschienen früher in der Entwicklung der Zellen und produzierten mehr IFN α nach Stimulation. Aktivierte PDCs regulierten die Expression von Sca-1 hoch.

Zusammengefasst ist mPDCA-1 ein spezifischer Marker für die Identifizierung von PDCs. Die direkte Interaktion mit naïven T-Zellen unterstreicht die Rolle der PDCs in der Koordination von angeborener und adaptiver Immunantwort. Die Ergebnisse dieser Arbeit zeigen, daß PDCs ein viel versprechendes Ziel für die Entwicklung neuartiger Therapiemöglichkeiten und deren Untersuchung im Mausmodell sind, vor allem für die Behandlung von Tumor- oder Autoimmunerkrankungen, z.B. von SLE.

ABSTRACT

Plasmacytoid dendritic cells (PDCs) represent a distinct subset of dendritic cells in humans and mice. In the murine system PDCs were characterized by the co-expression of B220, Ly-6C, and CD11c. Due to their ability to produce large amounts of interferon (IFN)-alpha upon microbial challenge and due to their stimulatory capacity they are believed to link innate and adaptive immune responses. Although there is growing evidence of their contribution in the induction of anti-viral immune responses, autoimmune disorders and tolerance, less is known about their exact function. In particular their role as antigen-presenting cells in the induction of T cell responses is still controversially discussed.

In the present study, a panel of monoclonal antibodies (mAb) was generated, all recognizing a cell surface antigen specifically expressed on PDCs in naïve mice. The antigen was termed mPDCA-1. Differential gene expression analysis revealed that mPDCA-1 is identical to the bone marrow stromal antigen 2 (BST2). Triggering of mPDCA-1/BST2 with the mAb resulted in calcium mobilization and overall protein-tyrosine phosphorylation, which inhibited TLR-induced IFN-alpha production in PDCs. Cross-linking of mPDCA-1 also resulted in rapid internalization of the antibody-receptor complex *in vitro* and *in vivo*. Since the administration of the complete anti-mPDCA-1 mAb resulted in Fc-mediated or ADCC-dependent depletion of PDCs *in vivo*, Ovalbumin protein was covalently conjugated to a non-depleting anti-mPDCA-1-F(ab')₂ fragment. When targeted via mPDCA-1, antigens entered the MHC class I and II processing and presentation pathway and PDCs were shown to efficiently prime naïve CD4⁺ and CD8⁺ T cells *in vitro*. Interestingly, this process was dependent on stimulation of PDCs leading to the activation of their antigen processing and presentation machinery. In contrast, without activation PDCs failed to stimulate naïve T cells.

In summary, mPDCA-1/BST2 is a novel specific marker for PDCs in mice, influencing their innate and adaptive functions. Further experiments including the identification of the natural ligand of mPDCA-1/BST2 in mice will be needed for better understanding its *in vivo* function. The effect of IFN-alpha abrogation after mPDCA-1 triggering could be investigated in murine models of autoimmune disease (e.g. SLE) or in viral infections. Furthermore, targeting antigen via mPDCA-1 would be a promising system to study the role of PDCs in adaptive immunity including the initiation of cytotoxic T cell responses *in vivo*.

In the second part of the work, two subpopulations of PDC characterized by the differential expression of the stem cell antigen 1 (Sca-1) could be identified. Sca-1⁻ PDCs produced large amounts of IFN-alpha after stimulation with TLR9 ligands, appeared earlier in the development and were predominantly present in the bone marrow. In contrast, Sca-1⁺ PDCs were poor IFN-alpha producers, represented the majority of PDCs in the lymph nodes and seemed to develop from Sca-1⁻ PDCs upon *in vitro* activation or adoptive transfer. Further work will be necessary to elucidate whether Sca-1 expression characterizes developmental/activation stages or two different subpopulations of PDCs.

ABBREVIATIONS

aa	Amino acid
Ab	antibody
ADCC	Antibody-dependent cell-mediated cytotoxicity
Ag	Antigen
APC	Antigen-presenting cell
APC	Allophycocyanin
BDCA	Blood dendritic cell antigen, e.g. BDCA-2, -3, -4
BM	Bone marrow
bp	Base pair
BrdU	5-bromo-2-desoxyuridin (thymidine analoge)
BSA	Bovine serum albumin
BST2	Bone marrow-stromal antigen 2
$[Ca^{2+}]_i$	Intracellular calcium concentration
CD	Cluster of Differentiation
cDC	conventional (myeloid) dendritic cell
CCL	Chemokine (CC) motif ligand
CDS	Protein coding sequence
CLR	Ca^{+2} -dependent lectin receptor
CLSM	Confocal laser scanning microscopy
CpG ODNs	Cytosine-phosphate-guanine oligodeoxynucleotides
CRM	cysteine-rich motifs
CTL	Cytotoxic T lymphocyte
DAMP	Danger-associated molecular pattern
DC	Dendritic cell
DCIR	DC Immunoreceptor
DC-SIGN	Dendritic Cell-specific Intercellular Adhesion Molecule 3 (ICAM-3)-grabbing Nonintegrin (CD209)
Dectin-1/-2	DC-associated C type lectin 1 and 2
dH ₂ O	Deionized water
DNA	Deoxyribonucleic acid
ds RNA	Double-stranded ribonucleic acid
EEA-1	Early endosomes antigen 1
ELISA	Enzyme-linked immunosorbent assay
ER	Endoplasmic reticulum
F(ab') ₂	Fragment antigen binding region, based on two combined Fab domains, each composed of the variable and constant region of light and heavy chain (only CH ₁)
FACS	Flow cytometric cell sorting

Fc	Fragment crystallizable region of an antibody, constant part, based on the CH ₂ and CH ₃ domain of the heavy chain
FCS	Fetal calv serum
FITC	Fluorescein isothiocyanate
FLT-3L (FL)	FMS-related tyrosine kinase 3 ligand
Foxp3	Forkhead box p3
FSC	Forward scatter
GITR	Glucocorticoid-induced tumor necrosis factor receptor
GOC	Gene ontology clustering
HA	Hemagglutinin
HEV	High endothelial venule
HRP	Horseradish peroxidase
HSV	Herpex simplex virus
i.p.	Intraperitoneally
i.v.	Intravenously
ICOS	Inducible T cell costimulator
IDO	Indoleamine 2,3-dioxygenase
IFN	Interferon
IFN-I	Type I interferon
Ig	Immunoglobulin
imDC	Immature DC
IKK	Inhibitor of NF-kB kinase
IL	Interleukin
IP10	IFN-inducible 10kDa protein
ITAM/ITIM	Immunoreceptor tyrosine-based activation/inhibitory motif
IPC	Interferon-producing cells (syn. PDC)
IRAK1/4	IL1-receptor-associated kinase 1/4
IRF	Interferon regulatory factor
LCMV	Lymphocytic choriomeningitis virus
LN	Lymph node
LPS	Lipopolysaccharide
LRR	Leucine rich repeat
mAb	Monoclonal antibody
mar mAb	Mouse anti-rat mAb
MACS	Magnetic cell separation
MB	Microbead
MCMV	Murine cytomegalovirus
MHC	Major histocompatibility complex
MFI	Mean fluorescence intensity
MIP	Macrophage inflammatory protein

MMR	Macrophage mannose receptor
Mock control	Cells transfected with empty vector (without gene of interest)
mPDCA-1	Mouse plasmacytoid dendritic cell antigen 1
MPG1	Macrophage specific gene 1 (syn. MSP1, MPEG1)
MyD88	Myeloid differentiation primary-response protein 88
NEMO	NF- κ B essential modulator
NF- κ B	Nuclear factor-kappa B
NK cell	Natural killer cell
ODN	Oligodeoxynucleotide
ORF	Open reading frame
OVA	Ovalbumin (Hen egg white protein)
pAb	Polyclonal antibody
PAGE	Polyacryl-amide gel electrophoresis
PAMP	Pathogen-associated molecular pattern
PBMC	Peripheral blood mononuclear cells
PBS	Phosphate buffered saline
PCR	Polymerase chain reaction
PDC	Plasmacytoid dendritic cell
PD-1L	Programmed cell death receptor 1 ligand
PE	R-phycoerythrin
PerCP	Peridinin chlorophyll (A) protein
PIQOR	Parallel Identification and quantification of RNA
PMA	Phorbol-12-myristate-13-acetate
PMF	Peptide mass fingerprinting (phorbol ester)
PRR	Pattern recognition receptor
PVDF	Polyvinylidene Fluoride
ram mAb	rat anti-mouse mAb
RPMI	Rosewell Park Memorial Institute Medium
RSV	Respiratory syncytial virus
RT	Room temperature
RT-PCR	Reverse transcriptase PCR
s.c.	Subcutaneous
SDS	Sodium dodecyl sulfate
SEM	Standard error of measurement or mean
Siglec-H	Sialic acid binding Ig-like lectin H
SLE	Systemic lupus erythematosus
SSC	Side scatter
ss RNA	single-stranded ribonucleic acid
STAT-1	Signal transducer and activator of transcription-1
TAP	Transporters associated with antigen processing

ABBREVIATIONS

Tcm	Central memory T cell
TCR	T cell receptor
Tem	Effector memory T cell
TGF	Transforming growth factor beta
T _H	T helper cell
TIL	Tumor infiltrating lymphocyte
TIR	Toll/IL-1R
TLR	Toll-like receptor
TMD	Trans-membrane domain
TNF	Tumor necrosis factor
Th	T helper cell type
Tr1/reg	Regulatory T cell
TRAF	Tumor necrosis factor receptor-associated factor
TRIS	Tris(hydroxymethyl)aminomethane
UTR	Untranslated region

LIST OF FIGURES

Fig.1.1	Professional antigen-presenting cells process intracellular and extracellular pathogens differently.	5
Fig. 1.2	The role of PDCs bridging innate and adaptive immune responses.	11
Fig. 3.1	Differential gene expression analysis on Agilent microarrays.	27
Fig. 3.2	Cloning strategies for L20315 (MPG1) and BST2 (BC027328) as well as generation of a full-length transfectants.	30
Fig 4.1.1	Screening strategy to detect PDC-specific hybridoma clones.	38
Fig 4.1.2	Staining of spleen cells with the PDC-specific clone JF05-1C2.	39
Fig 4.1.3	Determination of the specificity of the generated anti-mPDCA-1 mAbs on Balb/c spleen cells.	41
Fig 4.1.4	Expression of mPDCA-1 on PDCs in different lymphoid organs.	42
Fig 4.1.5	Expression of mPDCA-1 on <i>in vitro</i> -generated PDCs.	43
Fig 4.1.6	Expression of mPDCA-1 on PDCs from different mouse strains.	43
Fig 4.1.7	Immuno-histochemical staining of mPDCA-1 on lymph node cryosections.	44
Fig 4.1.8	Effect of mPDCA-1 cross-linking on the <i>in vitro</i> cytokine production of PDCs.	45
Fig 4.1.9	<i>In vivo</i> depletion of PDCs.	47
Fig 4.1.10	Comparison of the depletion efficiency of four different anti-mPDCA-1 clones.	47
Fig 4.1.11	Titration of the anti-mPDCA-1 mAb effector dose for <i>in vivo</i> PDC depletion.	48
Fig 4.1.12	Depletion efficiency in different lymphoid organs after anti-mPDCA-1 mAb administration.	49
Fig 4.1.13	Impact of the application route on PDC depletion efficiency.	49
Fig 4.1.14	PDC depletion and repopulation kinetics.	50
Fig 4.1.15	PDC depletion capacity of complete or F(ab') ₂ anti-mPDCA-1 mAb.	51
Fig 4.1.16	Abrogation of IFN α production after <i>in vivo</i> PDC depletion.	52
Fig 4.1.17	Cross-linking of mPDCA-1 on PDCs results in calcium flux and overall tyrosine phosphorylation <i>in vitro</i> .	53
Fig 4.1.18	Internalization of the mPDCA-1 mAb:receptor complex <i>in vitro</i> and <i>in vivo</i> .	54
Fig 4.2.1	Upregulation of mPDCA-1 expression <i>in vivo</i> .	57
Fig 4.2.2	Upregulation of mPDCA-1 expression on Sp2/0 cells.	58
Fig 4.2.3	Kinetic of IFN α -induced upregulation of mPDCA-1 expression on Sp2/0 cells.	59
Fig. 4.2.4	LightCycler curves indicating crossing points for L20315 and NM_008331 performed on different mRNA templates.	63
Fig 4.2.5	Differential expression of L20315 (MPG1) and BC027328 (BST2) mRNA.	65
Fig 4.2.6	Cloning of L20315 (MPG1) and generation of a full-length transfectant.	66
Fig 4.2.7	Cloning of BC027328 (BST2) and generation of full-length transfectants.	67

Fig 4.3.1	Uptake and processing of DQ-OVA by PDCs <i>in vivo</i> .	70
Fig 4.3.2	<i>In vivo</i> PDC targeting via anti-mPDCA-1-F(ab') ₂ antibody fragment.	71
Fig 4.3.3	Characterization of selective PDC targeting and antigen delivery.	72
Fig 4.3.4	Capacity of murine PDCs to present antigen to naïve CD4 ⁺ T cells.	73
Fig 4.3.5	Murine PDCs targeted with OVA antigen via mPDCA-1 prime antigen-specific CD4 ⁺ T cells.	74
Fig 4.3.6	PDCs from different lymphoid organs have similar capacities to prime naïve CD4 ⁺ T cells <i>in vitro</i> .	75
Fig 4.3.7	CD8 ⁺ T cell proliferation showing the cross-priming capacity of murine PDCs.	76/77
Fig 4.3.8	Receptor blocking abolishes mPDCA-1-mediated priming of both CD4 ⁺ and CD8 ⁺ T cells.	78
Fig 4.3.9	<i>In vitro</i> activation and maturation of PDCs.	79/80
Fig 4.3.10	Influence of PDC activation on the T cell priming capacity	81
Fig 4.3.11	Detection of processed OVA antigen in the context of MHC-I on PDCs.	82
Fig 4.3.12	Cytokine profile of restimulated CD4 ⁺ T cells after PDC-mediated priming.	83/84
Fig 4.4.1	Heterogeneous expression of Sca-1 on PDCs.	86
Fig 4.4.2	Strain-specific expression of Sca-1 on spleen PDCs.	87
Fig 4.4.3	Correlation of Sca-1 expression and PDC proliferation.	87/88
Fig 4.4.4	Sca-1 upregulation on PDCs upon TLR-mediated activation.	89
Fig 4.4.5	Upregulation of Sca-1 expression on transferred PDCs.	91
Fig 4.4.6	Expression of co-stimulatory molecules in correlation with Sca-1 expression in both steady state and after CpG-activation.	92
Fig 4.4.7	Differential Gene regulation of Sca-1 ⁺ and Sca-1 ⁻ PDCs.	92,94-96
Fig 4.4.8	Functional correlation of the Sca-1 expression and cytokine production capacity of PDCs.	97/98
Fig 5.1	Predicted protein structure of the mPDCA-1/BST2 molecule.	103
Fig 5.2	Model of the Sca-1 expression during PDC development.	117
Fig 7.1	Pepsin digestion of anti-mPDCA-1 mAb to generate F(ab') ₂ fragments.	122
Fig 7.2	LightCycler standard curves for four murine house keeping genes: β-actin, GAPDH, PPIA, and Hprt-1.	123

LIST OF TABLES

Table 3.1	Cycler settings for standard PCR	25
Table 3.2	Overview of the hybridization scheme and setup for the gene expression analysis on Agilent microarrays.	28
Table 4.1.1	(A) Overview of the outcome of the cross-blocking experiments	40
	(B) Isotype and recognized epitopes of different anti-mPDCA-1 clones	40
Table 4.2.1	Schematic overview of regulated genes within the seven separate chip hybridizations	60
Table 4.2.2	Differentially regulated gene candidates after extensive Agilent microarray analysis.	61
Table 4.2.3	Validation of candidates by quantitative real time RT-PCR analysis.	62
Table 4.2.4	Final list of mPDCA-1 candidates after microarray and RT-PCR analysis.	64
Tab. 4.4.1	(A) Genes that are predominantly regulated on Sca-1 ⁻ PDCs	93
	(B) Genes that are predominantly regulated on Sca-1 ⁺ PDCs	93
Table 7.1	Primer sequences	124-125
Table 7.2	List of differentially regulated genes in Sca-1 ⁺ and Sca-1 ⁻ PDCs from spleen and LNs	126-134

TITLE	I
ZUSAMMENFASSUNG	IV
ABSTRACT	VI
ABREVIATIONS	VII
LIST OF FIGURES	XI
LIST OF TABLES	XIII
TABLE OF CONTENTS	XIV
1. INTRODUCTION	1
1.1 The immune system	1
1.2 Dendritic Cells	3
1.3 Plasmacytoid Dendritic Cells	7
2. OBJECTIVES OF THE WORK	13
3. MATERIALS AND METHODS	14
3.1 Mice	14
3.2 Reagents	14
3.3 Cell culture	18
3.4 Generation of monoclonal antibodies	18
3.5 Biochemical methods	19
3.6. Flow cytometric analysis	22
3.7 Biomolecular methods and gene expression analysis	24
3.8 Microscopic and histological analyses	31
3.9 Cell separation	32
3.10 Biological assays	33
3.11 Statistical analysis	36
4. RESULTS	37
4.1 Generation of monoclonal antibodies for the detection of PDC-specific cell surface receptors	37
4.1.1 Contralateral footpad immunization	37
4.1.2 Antibodies that identify murine PDCs	38
4.1.3 Isotype designation and epitope determination (blocking experiments)	39
4.1.4 Flow cytometric analysis of mPDCA-1 ⁺ cells in lymphoid organs	40
4.1.5 Immuno-histochemical staining of mPDCA-1	43
4.1.6 Effects of mPDCA-1 cross-linking on maturation and IFN α production of PDCs	44
4.1.7 <i>In vivo</i> PDC depletion	46
4.1.7.1 Depletion of PDCs after anti-mPDCA-1 administration	46
4.1.7.2 PDC depletion capacity of complete or F(ab') ₂ anti-mPDCA-1 antibodies	50

4.1.7.3 Effect of PDC depletion on <i>in vivo</i> cytokine production after viral challenge or CpG stimulation	51
4.1.8 Signal transduction via mPDCA-1	52
4.1.9 <i>In vitro</i> and <i>in vivo</i> internalization of mPDCA-1 receptor-antibody complex	54
4.2 Identification and molecular characterization of mPDCA-1	55
4.2.1 Biochemical approaches to identify the mPDCA-1 antigen	55
4.2.2 Induction of mPDCA-1 expression <i>in vivo</i> and <i>in vitro</i>	56
4.2.3 Identification of mPDCA-1 by differential gene expression analysis	59
4.2.4 Validation of mPDCA-1 candidates for PDC-specific expression by quantitative real time RT-PCR	61
4.2.5 Cloning and generation of transfectants of potential mPDCA-1 candidates	64
4.2.5.1 The macrophage-specific gene 1	65
4.2.5.2 The Bone marrow stromal antigen 2	66
4.3 Characterization of mPDCA-1 as novel antigen-uptake receptor on PDCs enabling priming and cross-priming of naïve T cells	68
4.3.1 Endocytosis of DQ-OVA demonstrated the antigen-uptake capacity of PDCs	69
4.3.2 Generation of a PDC-specific <i>in vitro</i> and <i>in vivo</i> antigen delivery strategy	70
4.3.3 Capacity of murine PDCs to prime antigen-specific CD4 ⁺ T cells <i>in vitro</i>	72
4.3.3.1 Peptide-pulsed PDCs are able to induce naïve CD4 ⁺ T cell proliferation	72
4.3.3.2 Activated PDCs prime naïve CD4 ⁺ T cells after antigen-uptake via mPDCA-1	73
4.3.3.3 Priming capacity of PDCs from different lymphoid organs	75
4.3.4 PDC-induced (cross-) priming of CD8 ⁺ T cells <i>in vitro</i>	76
4.3.4.1 Cross-presentation and -priming capacity of mouse PDCs	76
4.3.4.2 Cross-priming capacity of PDC from different lymphoid organs	77
4.3.5 Receptor blocking elucidates specificity of mPDCA-1-mediated antigen delivery for priming of CD4 ⁺ and CD8 ⁺ T cells	78
4.3.6 PDC activation: Up-regulation of co-stimulatory and MHC molecules (maturation)	78
4.3.7 PDC activation: Impact on antigen processing capacity?	80
4.3.8 Cytokine production of expanded CD4 ⁺ T cells after PDC-mediated priming	82
4.3.9 Conclusion	85
4.4 Heterogeneous Sca-1 expression defines two functional different PDC subsets	85
4.4.1 Sca-1 is differentially expressed on PDCs	85
4.4.2 The expression of Sca-1 correlates with the developmental stage of PDCs	87
4.4.3 The expression of Sca-1 correlates with the maturation level of PDCs	89
4.4.4 Correlation of the different Sca-1 expression with the cytokine production capacity of PDCs	96

5.	DISCUSSION	99
5.1	Generation of PDC-specific monoclonal antibodies and phenotyping of mPDCA-1 ⁺ cells	99
5.2	Identification and functional characterization of mPDCA-1	102
5.3	Heterogeneous expression of Sca-1 defines functionally different PDC subsets	115
6.	OUTLOOK	120
7.	APPENDIX	122
8.	REFERENCES	135
9.	PUBLICATIONS AND ABSTRACTS	151
10.	ACKNOWLEDGMENTS	158
11.	ERKLÄRUNG	160
12.	LEBENS LAUF	162

1. INTRODUCTION

1.1 The immune system

The invasion of pathogens (bacteria, viruses, parasites) influences the organism, often leading to the development of diseases and, finally, to its death. To counter and neutralize the multitude of pathogens the organism is confronted with constantly, the immune system developed different strategies. In vertebrates, and in particular in mammals, the immune system can be divided into the innate and the adaptive arm. The innate response works as the first line defense against various pathogens. The adaptive or acquired immune response is acting slower but builds up a specific response that clears the infection and offers the advantage of an immunological memory. This principle of a dual immune system in vertebrates has been evolutionary established and strengthens the immunological protection [Lo D, Immunol Rev 1999; Medzhitov R, Nature 2007].

The innate immune system comprises both cells and mechanisms that defend the host from pathogenic infections. Components of this system are physiological barriers, such as the skin, mucosa and the epithelium, that prevent the encounter, or the low gastric pH that inactivates invading microbes as well as the complement system. On the other cellular level a multitude of specialized cells recognize and respond to invading pathogens before they are able to replicate and cause serious damage to the host [Reis e Sousa C, Immunity 2001; Medzhitov R, Nat Rev Immunol 2000]. These inflammatory reactions include the activation of the complement cascade, which leads to the clearance of opsonized cells as well as the recruitment of immune cells to sites of infection, through the production of mediators, such as cytokines and chemokines secreted by mast cells and other cells of the innate immune system. Upon pathogen encounter the granulocyte family and NK cells produce toxic proteins (such as perforins or granzymes) that kill target cells (i.e. infected or tumor cells) by induction of apoptosis [Grundy MA, Cancer Immunol Immunother. 2007; Veugelers K, Mol Biol Cell. 2005]. So-called phagocytes, mainly macrophages, can ingest and thus remove foreign or degenerated cells [Ljunggren HG, Immunol Today 1990; Smyth MJ, Nat Rev Cancer 2002; Medzhitov R, Immunol Rev 2000/Semin Immunol. 2000].

Whereas the innate immune system becomes activated upon recognition of few, highly conserved pathogen structures, adaptive immunity is able to detect an almost unlimited number of structures. This diversity is based on the recombination of antigen receptor gene segments, generating a large number of lymphocytes each equipped with a unique antigen recognition receptor. The major effector cells of the adaptive immune system are T and B lymphocytes, initiating cellular (cytotoxic T cells) and/or humoral (B cells/plasma cells) responses in an antigen-specific manner [Medzhitov R, Seminar Immunol 1998].

B cells can take up antigens directly via cell-surface bound immunoglobulin molecules (the B cell receptor). After uptake, B cells also process and present antigens on MHC-II molecules. MHC-II-peptide complexes presented by B cells can be recognized by antigen specific T helper cells, which in turn provide a co-stimulatory signal to B cells via CD40-CD40L interaction. This T

cell feedback is necessary for the efficient activation of naïve B cells leading to clonal proliferation and further differentiation into effector plasma cells or long-lived memory B cells. A characteristic B cell response results in the production of antibodies by plasma cells recognizing specifically the pathogen-derived structures. Binding of the antigen by an antibody may result in opsonization and neutralization of toxins and pathogens or in the activation of the complement cascade. Remaining memory B cells as well as persisting antibodies in the serum are part of the immunological memory. These factors provide an immediate and strong response against the same antigen upon new encounter and due to somatic mutation usually demonstrate higher affinities after repeated infections.

Whereas B cells are able to sense native antigen via the B cell receptor, T cells can recognize only short peptides in the context of MHC molecules on specialized antigen-presenting cells (APC) [Romani N, Res Immunol 1989; Germain RN, Cell 1994; Brown MG, JI 1993; Carbone FR, Cold. Spring Harb. Symp. Quant Biol 1989]. APCs comprise of macrophages, monocytes, B cells and Dendritic Cells (DCs). These cell types and in particular the DCs are characterized by a continuous uptake and processing of antigens from the environment. Peptides originating from endogenous proteins (e.g after virus infection) are loaded onto MHC class I molecules and presented to CD8⁺ T cells. Endocytosed antigens are primarily loaded onto MHC II molecules to be presented to CD4⁺ T cells [Janeway C, Cold Spring Harb Symp Quant Biol 1989; Wang RF, Trends Immunol 2001].

The activation of T lymphocytes is a complex process. The T cell receptor (TCR) recognizes a distinct antigenic peptide in the context of MHC molecules on the surface of an APC. For sufficient activation, naïve T cells further need an additional activation signal, provided by co-stimulatory molecules (e.g. CD80, CD86) highly upregulated on activated DCs. When activated, CD8⁺ T cells differentiate into cytotoxic T cells (CTLs) that lyse tumor or virus-infected target cells [Barry M and Bleackley RC, Nat Rev Immunol 2002]. On the other hand, differentiated CD4⁺ T_H cells support and influence the development of other lymphocytes (such as B cells and CD8⁺ T cells) towards effector cells through the secretion of certain sets of cytokines. Beside the presentation of immunogenic peptides and T cell activation, DCs are important to mediate a “third signal”. Depending on the stimulus provided by the pathogen, DCs secrete distinct cytokines, which in turn influence the type of T cell response, the so-called “T helper cell polarization” [O'Garra A, Curr Opin Immunol 1994; Kalinski P, Immunol Today 1999a]. In analogy to B cells, also T cells develop a memory compartment.

The benefit of adaptive immunity lies in the large diversity of antigen-specific responses. By combinatory diversity and junctional recombination processes the B cell receptor repertoire can generate theoretically up to 10¹¹ different immunoglobulins and this number is further expanded by somatic hypermutation [Weigert M, Nature 1980]. The variability of the TCR repertoire is also created by gene rearrangements and different combinatory recombination whereas no somatic hypermutation occurred [Zheng B, Nature 1994]. Another advantage is based on the generation of an immunological memory, which provides a faster and more effective response in case of a

secondary exposure to the pathogen. For the optimal induction of adaptive immune response, APCs, and in particular DCs, have an important function. These cells not only sense, take up, and process microbial structures, but also activate T cells and induce the differentiation of naïve lymphocytes to effector cells [Guermontez P, *Annu Rev Immunol* 2002; Banchereau J and Steinman RM, *Nature* 1998]. Finally, they recruit other cells of both the innate and adaptive immune system to the site of infection and thus are crucial for the induction of immunity. Depending on the origin and status of the cells as well as on the type of pathogen either cellular or humoral immunity but also anergy (tolerance) can be initiated.

1.2 Dendritic Cells

Dendritic cells have been first described in the early 1970s by Ralph Steinman and Zanvil Cohn. These BM-derived immune cells showed a dendritic morphology characterized by protrusions of the plasma membrane, and were able to activate naïve T cells [Steinman RM + Cohn ZA, *JEM* 1973]. DCs represent not a homogeneous population but rather consist of different subsets, which develop continuously from CD34⁺ hematopoietic stem cells and migrate through the circulation into peripheral tissues. DC subpopulations differ in phenotype, life span, tissue localization, and immunological function [Shortman K and Liu YJ, *Nat Rev Immunol* 2002; Naik SH, *Nat Immunol* 2007; Shortman K, *Nat Rev Immunol* 2007].

Resident DCs from peripheral tissues typically demonstrate an immature phenotype, characterized by low expression of MHC and co-stimulatory molecules. In this immature stage DCs show a high endocytotic activity, and constantly scan their environment by taking up antigens via different mechanisms, including macropinocytosis and phagocytosis (nonspecific uptake of extracellular fluid and particles, respectively) or receptor-mediated endocytosis. DCs express a variety of receptors, which have been shown to be involved in antigen uptake, such as Calcium-dependent lectin receptors (CLRs) [Brown GD, *Nat Rev Immunol*, 2006], Toll-like receptors (TLRs) or Fc receptors [Figdor CG, *Nat. Rev. Immunol* 2002]. CLRs and TLRs belong to the family of pathogen-recognition receptors (PRRs), which recognize highly conserved pathogenic structures on Gram-positive and negative bacteria, viruses, fungi or protozoan parasites that are naturally absent in the host [Akira S, *Nat Rev Immunol* 2004; Matzinger P, *Science* 2002; Janeway CA, Jr. *Cold Spring Harb Symp Quant Biol.* 1989; Galiana-Arnoux D, *Tissue Antigens* 2006]. These receptors enable DCs to identify Danger- and Pathogen associated molecular patterns (DAMPs and PAMPs). Ligation of PRRs not only leads to the uptake of the given antigen, but also can induce maturation processes. Once maturation has been initiated DCs stop the antigen uptake and migrate to secondary lymphoid organs (draining lymph nodes (LNs) or spleen) [Banchereau J and Steinman RM, *Nature* 1998; Janeway C and Travers P, *Garland Publishing* 2001]. During this passage, activated DCs undergo a number of phenotypical and functional changes including the loss of their endocytic/phagocytic capacity, the up-regulation of cell-adhesion and co-stimulatory molecules as well as an increase of the processing and presentation activity. The latter is mainly mediated by the recruitment of MHC

molecules to the antigen processing compartments (lysosomes) and a significant increase of the half-life of peptide-MHC complexes on the cell surface. [Banchereau J, Nature 1998]. Thus, upon activation, DCs are phenotypically characterized by high expression level of MHC, cell adhesion and co-stimulatory molecules (e.g. ICAM1, LFA3, CD40, and in particular the B7 family). These molecules mediate the so-called immunological synapse between DCs and T cells, which is necessary for the efficient activation of the latter [Cella M, JEM 1996]. The activation of naïve T cells depends on - at least - two signals: a first signal is provided by the recognition of the specific MHC/peptide complex via the TCR, the second signal is mediated through the interaction of co-stimulatory receptors (CD80 and CD86) on the APC side with the appropriate ligand (CD28) on T cells. Without the co-stimulatory signal the response of naïve T cells results in anergy or apoptosis [Kuwana M, Hum Immunol 2002]. Since immature APCs continuously present autoantigens in the periphery, this mechanism prevents the activation of autoreactive T cells and the development of autoimmune responses.

For loading of MHC-I and -II molecules different processing pathways are known. After uptake, exogenous proteins are transported to endosomes and later to lysosomes. Upon acidification, lysosomal proteases degrade the proteins to smaller peptides. MHC II molecules, which are exclusively present on APCs [Wang RF, Trends Immunol 2001], are produced in the Endoplasmatic reticulum (ER) and transported to MHC-II-rich compartments (MIIC), which fuse with lysosomes upon activation. Within this fusion compartment the loading of MHC-II molecules with appropriate, so-called immunocompetent peptides takes place [Wang RF, Trends Immunol 2001].

In contrast, endogenous proteins are ubiquitinated and degraded into peptides within the proteasome. Generated peptides are then transported to the ER via TAP proteins and loaded onto MHC-I molecules for transport to the cell surface via the Golgi apparatus [York IA, Annul Rev Immunol 1996; Tong JC, Protein Science 2004]. While immature dendritic cells and other APCs express the classical proteasome and also a special “immuno-proteasome”, mature dendritic cells express the latter one, which might be more competent for antigen presentation since its cleavage patterns yield in peptides that bind efficiently to MHC-I molecules [Macagno A, EJI 1999; Van den Eynde BJ, Curr Opin Immunol 2001].

Beside the classical route describing, that peptides from exogenous proteins are presented on MHC class II molecules, several reports demonstrated that they could also be presented by MHC-I molecules [Brode S, Immunology 2004]. This mechanism is referred to as “cross-presentation” [Amigorena S, Nat Immunol 2003; Roy CR, Nature 2003; Heath WR, Nat Rev Immunol 2001; Groothuis TA, JEM 2005] and may play an important role in the priming of virus- and tumor-specific CD8⁺ T cells.

An overview of the processing pathway of both endogenous and antigens is given in Fig.1.1.

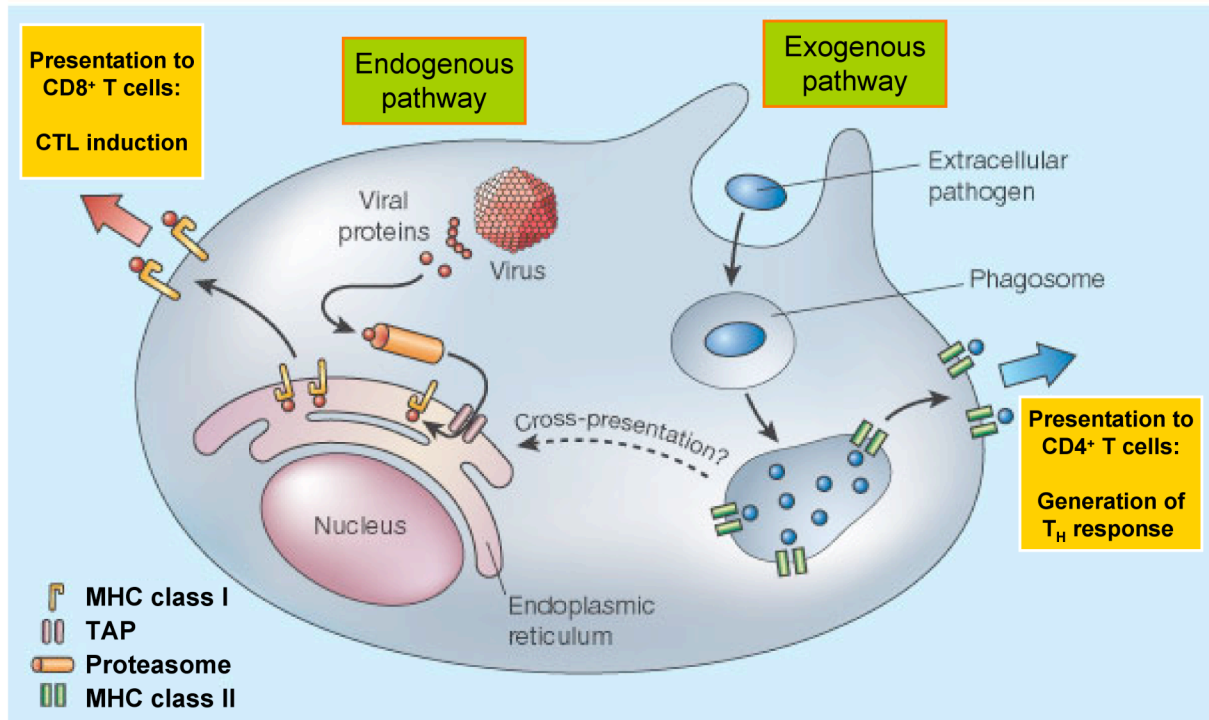


Fig.1.1 Professional antigen-presenting cells process intracellular and extracellular pathogens differently.
 Modified after Roy CR, *Nature* 2003.

The mechanism of cross-presentation is poorly understood and can be explained by several models. By the “canonical model” exogenous proteins “escape” or are translocated from the endosome and are proteasomally degraded. Resulting peptides gain access to the endoplasmic reticulum (ER) via the TAP complex and MHC molecules are loaded and transported to the cell surface [Lin ML, *Immunol Cell Biol* 2008]. In a revised model it has been demonstrated that phagosomes in particular in APCs fuse with the ER membrane. Here, specialized transporter proteins translocated the phagocytosed antigen into the cytosol for degradation. There the ubiquitination and degradation takes place, and in turn the peptides are transported to the lumen of the phagosome via TAP for MHC I loading. This mechanism differs from the first pathway described above since MHC loading occurs in the phagosome and not in the ER. A third mechanism proposed that proteins endocytosed by specific receptors (e.g. the Mannose receptor) are targeted to stable early endosomes for cross-presentation [Burgdorf S, *Science* 2007; Trombetta ES and Mellman I, *Annu Rev Immunol* 2005; Ramirez MC and Sigal LJ, *Trends Microbiol* 2004; *reviewed in* Kasturi SP, *Nat Immunol* 2008].

Based on their capacity to process and present exogenous antigens, DCs play a central role in the activation of antigen-specific responses. DCs contribute to the induction of adaptive immunity not only by their APC function but produce a variety of cytokines [Steinman RM *Annu Rev Immunol* 1991; Banchereau J, *Annu Rev Immunol* 2000]. Hereby the kind of pathogen or stimulus influences the DC and balances the cytokine production towards a cellular or humoral response. Pro-inflammatory cytokines such as IL-12, which induce a strong cellular (T_H1) response, are mainly induced after contact with viruses or intracellular bacteria [Hochrein H, *Jl* 2001; Cella M, *JEM* 1996; Koch F, *JEM* 1996]. The absence of IL-12 as well as the presence of

anti-inflammatory molecules such as IL-10, TGF- β , PGE-2, corticosteroids and also IL-4 favorite a humoral (T_H2) immune reaction [Liu Y-J, Cell 2001; Kapsenberg ML, Nat Rev Immunol 2003]. DCs seem to play also a role in the induction of regulatory T cells and so-called T_H17 cells. T_H17 cells are critical for local inflammation and amplification of inflammatory responses and mediating autoimmune diseases in mice. The commitment of these T_H subsets is induced by cytokines like TGF β and IL-10 (Tregs), or Treg-derived TGF β and DC-derived IL-6, whereas IL-23 is important for the expansion and maintenance of T_H17 cells [Reiner SL, Science 2007; reviewed by Afzali B, Clin Exp Immunol. 2007; Steinman L, Nat Med 2007]. Interestingly, naïve T cells develop into Tregs or T_H17 cells in a mutually exclusive process. The relative flexibility of DC subpopulations in their cytokine production might be based on the differential expression of PRRs by different DC subsets [Backer R, EJI 2008; Iwasaki A, Nat Immunol 2004; Schnorrer P, PNAS 2006; Dudziak D, Science 2007; den Haan JM, JEM 2000]. DC-secreted cytokines influence not only the polarization of T helper cells, but also B cells, macrophages, and NK cells, thereby mainly determining the type of immune response.

As mentioned before, DCs are not a homogeneous population and in the human and murine system several subsets are described that share the ability to process and present antigens to naïve T cells for the initiation of an adaptive immune response. Depending on their differential expression of several cell surface receptors (e.g. TLRs, CLR) each DC subtype is specialized to respond to certain pathogens and induce distinct immune responses [Steinman RM, Annu Rev Immunol, 1991; Shortman K and YJ Liu, Nat Rev Immunol, 2002].

In the human system different types of DCs can be classified according to origin, function or anatomical localization. Most DC research in humans was focused on blood-derived DCs. These cells are characterized by the expression of MHC-II and the absence of lineage markers such as CD3, CD14, CD19, and CD56. Phenotypical analysis has demonstrated that human DCs can be further divided into three subpopulations: CD11c⁺ CD1c⁺ CD123^{low} myeloid DCs, a minor CD11c^{dim} CD1c⁻ CD123⁻ CD141⁺ (BDCA-3⁺) myeloid population, and the lymphoid or Plasmacytoid DCs (PDCs). The latter are CD11c⁻ CD1c⁻ CD123⁺ (IL-3R α) and specifically express CD303 (BDCA-2) and CD304 (BDCA-4/Neuropilin-1) [Dzionek A, JI 2000; Liu Y-J, Cell 2001; Banchereau J, Annu Rev Immunol 2000].

In mice, several DC subsets are described in the steady-state, which all have been identified by the expression of the CD11c antigen (integrin α_x chain) [Shortman K, Nat Rev Immunol 2002]. Beside DCs localized in the periphery such as dermal DCs, the epidermis-resident Langerhans' cells [Romani N, J Inv Dermatol 1989], or interstitial DCs of non-lymphoid organs, the main focus has been made on DC subsets in lymphoid organs. In spleen "conventional" dendritic cells (cDCs) [Henri S, JI 2001] and PDCs have been found. The conventional DCs are subdivided according to their expression pattern of the CD11b antigen (integrin α_M), the co-receptors CD4 and CD8, as well as the C-type lectin receptor DEC205 (CD205). By doing so three cDC subpopulations can be identified: CD8 α ⁺ CD11b⁻ DEC205⁺ DCs (25%) and CD8 α ⁻ CD11b⁺ DEC205⁻ (75%), with the latter further divided into a CD4⁻ and CD4⁺ subset [Shortman

K, Immunol Cell Biol 2000]. Some reports demonstrated that the single DC subsets develop from both common lymphoid and myeloid progenitors [Wu L, Blood 2001; Karsunky H, Exp Hematol 2005; del Hoyo GM, Nature 2002]. Historically, the CD8 α^+ DCs were supposed to be of lymphoid origin, whereas the CD8 α^- subset was described to be of myeloid origin [Liu YJ, Cell 2001]. Compared to conventional DCs, the phenotype of PDCs is clearly different as this cell type is characterized by high expression of B220 but only intermediate levels of CD11c and the absence of CD11b. Compared to human PDCs, the murine counterpart does not express the IL-3R α chain. A known functional difference to other DC subsets is the lower antigen uptake and presentation activity of PDCs.

PDCs secrete less IL-12 compared to other DC subsets but produce extraordinary amounts of type I interferons (IFN-I). Based on this main characteristic, PDCs are also named Interferon producing cells (IPCs) and are supposed to play a central role in the induction of anti-viral or anti-microbial immune responses [Kadowaki N, JEM 2000; Krug A, EJI 2001a+b]. INF-Is can be produced by a multitude of cell types upon viral infection, for example monocytes, macrophages, NK cells, fibroblasts, dendritic cells, and in particular PDCs [De Maeyer E, Int Rev Immunol 1998; Siegal FP, Science 1999]. This specialized DC subset can produce up to 1,000-fold more IFN-I [as much as 3-10 pg of IFN α per cell] upon viral or microbial stimulation [De Maeyer E, Int Rev Immunol 1998; Cella M, Nat Med 1999; Asselin-Paturel C, Nat Immunol 2001; Siegal FP, Science 1999; Pestka S, Annu Rev Biochem 1987; Samuel CE, Clin Microbiol Rev 2001; Fitzgerald-Bocarsly P, Cytokine Growth Factor Rev]. Therefore, they are regarded as the major producers of these cytokines. By the secretion of IFN-Is, PDCs inhibit the virus replication and induce the apoptosis of virus-infected cells [Pestka S, Immunol Rev 2004] but can also initiate immune responses by orchestration of other leukocytes. IFN-I production by PDCs is typically induced in response to infectious agents, including viruses, bacteria, protozoa, or different mitogens. The response can be mimicked by synthetic TLR agonist, e.g. double-stranded RNA (TLR7) or unmethylated, CpG-containing DNA motifs (TLR9) both *in vitro* and *in vivo* [De Maeyer E, Int Rev Immunol 1998].

1.3 Plasmacytoid Dendritic Cells

In lymphoid organs of mice or humans PDCs represent approximately 0.1% to 1.5% of mononuclear cells. PDCs were originally described as “T cell-associated plasma cells” or “plasmacytoid T cells” [Lennert K, Acta Haematol 1958; Lennert K, Lancet 1975], because of their close proximity to T cells and their plasma-cell like morphology. Their interferon production capacity has been reported later as well as their DC characteristic [Trinchieri G, JEM 1978a+b; Grouard G, JEM 1997]. In 1999, human PDCs have been phenotypically characterized as CD11c $^-$ CD123 $^+$ (IL-3R α) CD4 $^+$ CD45RA $^+$ ILT3 $^+$ cells with an immature phenotype [Siegal FP, Science 1999; Cella M, Nat Med 1999]. It was demonstrated that the maturation of PDCs and the formation of the classical dendrite-like morphology could be induced by CD40 triggering [Grouard G, JEM 1997; O’Doherty U, Immunology 1994]. BDCA-2 and BDCA-4 were identified as specific cell surface receptors for PDCs [Dzionek A, JI 2000]. Recently it has been

demonstrated that the Immunoglobulin-like transcript (ILT) 7 is also selectively expressed in human PDCs [Cao W, JEM 2006].

The murine counterpart of PDCs has been searched for a long time; finally in 2001, three independent groups identified (natural) interferon-producing cells in several lymphoid organs of mice, which showed similar phenotype, function, and morphology [Nakano H, JEM 2001; Asselin-Paturel C, Nat Immunol 2001; Björck P, Blood 2001]. In contrast to human PDCs, murine PDCs are defined by the simultaneous expression of B220 (CD45R), Ly-6C, and CD11c, whereas BDCA-2 and -4 were not expressed. The intermediate expression level of CD11c and lack of CD11b further distinguishes them from cDCs. Also the expression level and recycling pattern of MHC-II is differentially regulated, as PDCs use a different promoter (C2ta pIII) for the transcription of the MHC class II transactivator (CIITA) compared to cDCs [LeibundGut-Landmann S, Nat Immunol 2004]. A different equipment of PRRs further reflects the functional differences to conventional DCs. Whereas cDCs express TLRs 2, 3, 4, 7, and 9, PDCs only express TLRs 7 and 9, underlining their strong responsiveness to viral or bacterial derived nucleic acids [Iwasaki A, Nat Immunol 2004; Takeda K, Annu Rev Immunol 2003; Edwards AD, EJI 2003; Krug A, Blood 2004; Heil F, Science 2004; Diebold SS Science 2004; Lund JM, PNAS 2004]. PDCs also lack characteristic CLRs, such as CD205 (DEC205), CD209 (DC-SIGN/CIRE), or Dectin-1 and -2, which are expressed on conventional DCs [Figdor CG, Nat Rev Immunol 2002; Proietto AI, Immunobiology 2004; Meyer-Wentrup F, Blood 2008; Caminischi I, Mol. Immunol 2001].

It has been shown that PDCs like other DCs develop from BM progenitors and continuously migrate to lymphoid organs via the blood stream [O’Keeffe M, JEM 2003] residing there at an immature stage. Several growth or transcription factors are crucial for the development of PDCs. FLT-3L, the Interferon α/β consensus sequence-binding protein (ICSBP) and IKAROS are involved in the regulation of PDC development [Chen W, Blood 2004; Gilliet M, JEM 2002; Brawand P, JI 2002; Schiavoni G, JEM 2002; Allman D, Blood 2006]. Although, it has been hypothesized that PDCs can originate from both common lymphoid and myeloid progenitors [Yang GX, JI 2005; D’Amico A, JEM 2003; Shigematsu H, Immunity 2004; Karsunky H, Exp. Hematol 2005; Naik SH, Immunol Cell Biol. 2005], the direct progenitor for mouse PDCs has been identified very recently. CD31^{high} Ly6C⁻ BM cells were found to develop into cells that show the typical plasmacytoid morphology, express a PDC-characteristic phenotype and produce high IFN-I amounts after TLR stimulation [Kreisel FH, Cell Immunol 2006].

In steady state PDCs circulate in low numbers in the blood stream or in lymphoid tissues [Nakano H, JEM 2001; Asselin-Paturel C, JI 2003]. PDCs migrate constantly from the blood and entry LNs via High Endothelial Venues (HEV) in a CXCL9- and L-selectin-dependent mechanism [Yoneyama H, Int Immunol 2004; Nakano H, JEM 2001]. In secondary lymphoid organs, PDCs are found in the marginal zone (spleen) or paracortex (LNs) as well as the T cell area [Asselin-Paturel C, Nat Immunol 2003; Blasius A, Blood 2004; Nakano H, JEM 2001].

Upon sensing pathogens peripheral PDCs upregulate co-stimulatory and MHC molecules. They accumulate in inflamed tissues and in particular in LNs draining the sites of inflammation where they orchestrate other leukocytes [Cella M, Nat Med 1999; Blasius AL, Blood 2004; Dicaovo TG, JEM 2005; Yoneyama H, Int Immunol 2004; Palamara F, JI 2004; Liu C, Journal Clin Inv 2008].

The role of PDCs in viral or microbial infections and other diseases such as melanoma cancer has been excessively investigated. It has been demonstrated that PDCs are required for protection against lethal herpes-simplex virus (HSV) infection [Shen H, J Clin Invest. 2006] and enhances antiviral responses against respiratory-syncytial virus (RSV) [Smit JJ, PLoS ONE 2008], mainly by IFN-I production. Although the PDC population expands after viral infections and they are the major producers of anti-replicative IFN-I, their numbers are often decreased in peripheral blood, e.g. in human immunodeficiency virus (HIV) and Hepatitis infection [Duan XZ, J Clin Immunol 2004; Soumelis V, Blood 2001; Ulsenheimer A, Hepatology 2005]. As this effect is accompanied with an increased viral load, these reduced PDCs frequencies correlate with a poor prognosis for the patients. An explanation for these decreased frequencies of PDCs in peripheral blood might be the extravasation into inflamed tissues such as lung e.g. during a respiratory infection. In case of AIDS/HIV, PDC numbers are reduced as these cells obviously reflect a target of the virus. Not only in viral infections but also in autoimmune diseases, such as systemic lupus erythematosus (SLE) or psoriasis, the decrease of blood PDCs is associated with the progression of the disease. The reduced PDC numbers in the blood of SLE or psoriasis patients correlate with the accumulation of these cells in inflamed tissues and the skin [Cederblad B, J. Autoimmun 1998; Farkas L, Am J Pathol 2001; Blomberg S, Lupus 2001].

PDCs are also linked with the outcome of further pathological situations and in particular with the outcome of tumors as PDCs and IFN-I have an important but ambiguous function [Dunn GP, Nat Rev Immunol 2006]. In the absence of an appropriate stimulus PDCs may promote regulatory T cells and contribute to an impaired T-cell-mediated immune response against tumors correlating with worse outcome of the disease [Hartmann E, Cancer Res 2003; Vermi W, J Pathol 2003]. In breast cancer and ovarian epithelial cell carcinoma, large numbers of infiltrating PDCs have been detected, but they rather induced regulatory T cells than immunity [Treilleux I, Clin Cancer Res. 2004; Zou W Nat Med 2001; Munn DH, J Clin Invest 2004]. Thus, the presence of these tolerogenic PDCs correlates with a negative prognosis. On the other hand, activated PDCs are promoting and supporting anti-tumor responses and are currently investigated in therapeutical approaches. It has been mentioned before that PDCs infiltrate inflamed tissues and tumors. Upon TLR7 activation, both human and mouse PDCs have been shown to massively infiltrate skin melanomas resulting in efficient tumor reduction [Palamara F, JI 2004; Stary G, JEM 2007]. TLR9-activated murine PDCs have been shown to have a beneficial impact for the treatment of cancer [Krieg AM, Oncogene 2008; Liu C, J Clin Inv 2008] as they synergistically act with other DCs or NK cells to induce anti-tumor responses as mentioned above. This and above studies suggest PDCs as an attractive target for cell-based

vaccination and immunotherapy against virus infections and tumor treatment.

PDCs are also associated with the emergence of autoimmune diseases and tolerance. It has been shown that e.g. DNA immune-complexes can trigger PDCs resulting in highly elevated IFN-I levels in sera of SLE patients. High IFN-I levels lead to the establishment of a pro-inflammatory environment and the differentiation and activation of cDCs or autoreactive B cells, which secrete auto-(dsDNA) antibodies [Rönnblom L, *Arthritis Res Ther* 2003]. Beside their role in SLE, PDC-mediated IFN-I production is also relevant for other autoimmune disorders including psoriasis, rheumatic arthritis (RA) or the Sjögren's syndrome [Nestle FO, *JEM* 2005; Banchereau J, *Immunity* 2006; Christensen SR, *Immunity* 2006; Farkas L, *Am J Pathol* 2001; Blanco P, *Science* 2001; Cavanagh LL, *Arthritis Res Ther* 2005; Lande R, *J Immunol* 2004]. The abrogation of PDC-produced IFN-I might result in the attenuation of autoimmune reactions/symptoms and is currently investigated as therapeutical target.

On the other hand PDCs show a tolerogenic role, suggesting a beneficial impact of these cells in transplantations [Ochando JC, *Nat Immunol* 2006; Abe M, *Am J Transplant* 2005]. PDCs also prevent inflammatory reactions against harmless antigens by suppression of effector T cells induced by cDCs. Their ablation could result in the development of other autoimmune diseases such as asthma [De Heer H, *JEM* 2004].

PDCs have an essential function in the interaction with several cell types from both the innate and adaptive immune system. Mainly by their production of IFN-I, but also of IL-12, they directly activate NK cells, shown by increased proliferation, IFN γ secretion, and cytotoxicity [Krug A, *Immunity* 2004; Biron CA, *Annu Rev Immunol* 1999; Dalod M, *JEM* 2003]. This IFN-I production also results in the activation and maturation of DCs and other APCs [Honda K, *PNAS* 2003]. In particular, IFN-I "licenses" APCs for the cross-presentation of exogenous antigens and the induction of antigen-specific CD8⁺ CTLs [Le Bon A, *Nat Immunol* 2003]. Furthermore, PDCs influence the differentiation and immuno-stimulatory functions of other DC subtypes by secretion of cytokines such as IL-6, -8, -12, and TNF α [Poeck H, *Blood* 2004; Decalf J, *JEM* 2007]. The secretion of IL-6 and IFN-I sequentially influences the development of CD40L-activated B cells towards plasma cells, as IFN-I leads to the generation of plasma blasts and IL-6 subsequently triggers the differentiation into Ig-secreting plasma cells [Poeck H, *Blood* 2004; Jego G, *Immunity* 2003]. For example in SLE, high levels of PDC-derived IFN-I promotes the differentiation and activation of cDCs that capture and present antigens (e.g. from apoptotic cells) to autoreactive B cells resulting in the generation of autoantibody-producing plasma cells [Vallin H, *Jl* 1999]. PDCs have a eminent impact on T cells as PDC-derived IFN-I can induce the activation and survival but also the polarization of naïve T cells [Agnello D, *J Clin Immunol* 2003]. The influence of PDCs on T cells is based mainly on their interaction with conventional DCs that subsequently activates the T cells, but PDCs also influence T cells directly by the secretion of pro-inflammatory cytokines: Virus-infected PDCs are found to promote a strong IFN γ production in CD4⁺ T cells, suggesting their pivotal role in the induction of T_H1 responses

[Kadowaki N, JEM 2000], but there are other reports of a PDC-triggered T_H2 polarization depending on the antigen dose and activation status of the cells (in case PDCs received not an appropriate TLR activation [Cella M, Nat Immunol 2000; Kadowaki N, JEM 2000; Boonstra A, JEM 2003; Ito T, JI 2004]. Recently, there is increasing evidence for a tolerogenic function of PDCs if PDCs are not triggered to respond in an anti-viral manner, e.g. in the absence of high IFN-I production. These inhibitory effects are either mediated via the PD-1:PD-1L pathway or induced by the tolerogenic enzyme Indoleamine 2,3-dioxygenase (IDO), which is expressed on PDCs under certain, inducible conditions. For example stimulation of PDCs with the tolerogenic ligands CTLA-4-immunoglobulin (CTLA-4-Ig), CD200-Ig or soluble GITR initiate the immunoregulatory pathway of tryptophan catabolism and the induction of IDO expression [Ito T, JEM 2007; Gilliet M, JEM 2002; Kuwana M, Hum Immunol 2002; Fallarino F, JI 2004; De Heer H, JEM 2004; Sharma MD J Clin Inv 2007; Abe M, Amerc J of Transplant 2005]. An illustration of the differential functions of PDCs and their role at the interface of innate and adaptive immunity is given in Fig 1.2.

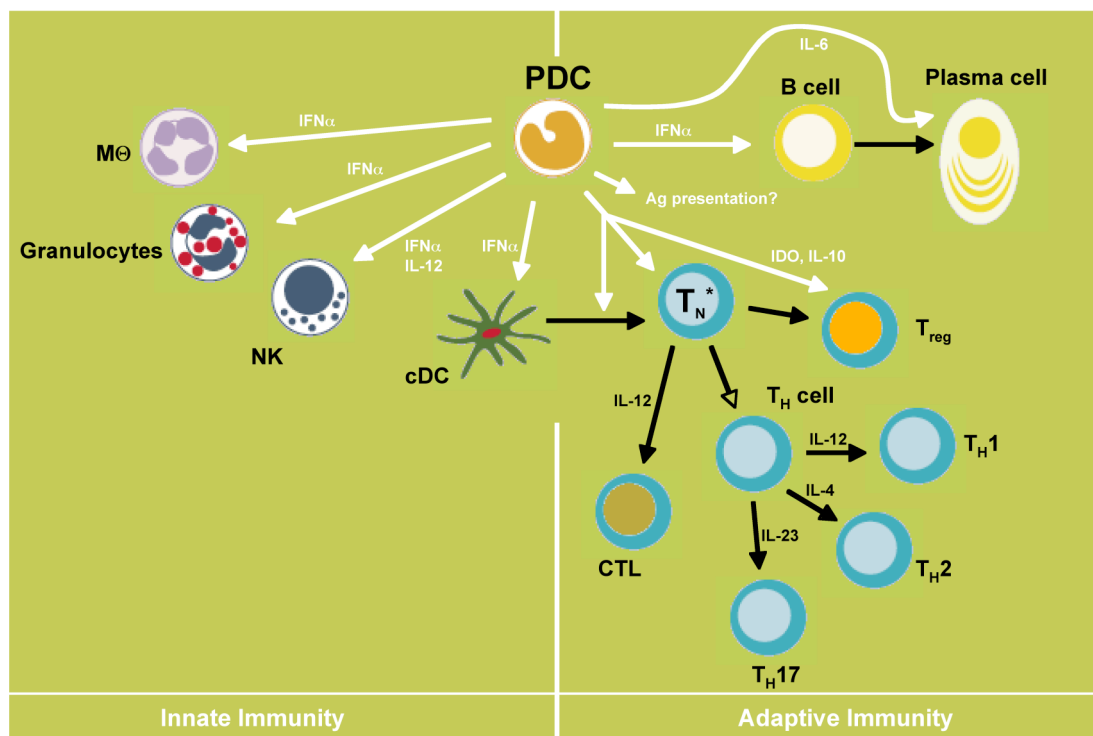


Fig. 1.2. The role of PDCs bridging innate and adaptive immune responses.

For a more detailed explanation please refer to the text.

It remains elusive whether PDCs have only an accessory function by their cytokine secretion [Yoneyama H, JEM 2005] or are directly acting as antigen-presenting cells, e.g. to prime naïve T cells, is still controversially discussed. *In vitro* generated PDCs promote *in vitro* the expansion of naïve $CD4^+$ and $CD8^+$ T cells [Boonstra A, JEM 2003; Brawand P, JI 2002]. *In vivo* experiments with peptide-pulsed and CpG-matured PDCs show that PDCs can induce naïve $CD8^+$ T cell responses to endogenous, but not exogenous, antigens [Salio M, JEM 2004]. And it has been shown that virus-activated but not CpG-activated PDCs can differentiate into APCs

and induce an effector/memory CD8⁺ T cell response *in vivo* [Schlecht G, Blood 2004]. In contrast, PDCs are considered to be poor T cell stimulators, as immature and virus-activated PDCs failed to prime naïve CD4⁺ and CD8⁺ T cells [Krug A, JEM 2003]. Recently, it has been shown that only peptide-pulsed PDCs have the capacity to activate naïve CD8⁺ T cells [Lou Y, JI 2007], whereas their ability to process soluble antigens is questionable. In a different experiment only CD8⁺ cDCs but not PDCs activate naïve CD8⁺ T cells *in vivo* [Belz GT, JI 2005]. The qualitatively different capacities between PDCs and cDCs to prime naïve CD8⁺ T cells were further underlined as BM-derived and peptide-pulsed PDCs only induced minor CD8⁺ T cell responses without significant memory CD8⁺ T cell differentiation *in vivo* [Angelov GS, JI 2005]. Thus, PDCs might have only a synergistic but important effect on cDCs to induce an antigen-specific immune response [Kadowaki N, Hum Immunol 2002; Lou Y, JO 2007; Liu C, J Clin Inv 2008]. These conflicting results are likely caused by either the different source of antigens (peptide vs. protein), the kind of PDC preparation or their activation status as freshly isolated or TLR-activated PDCs have been used in the studies. Although some experiments show the APC-function of PDC, this reaction was less efficient as compared to cDCs. Based on these reports further investigations on the antigen-presenting and -processing capacity of PDCs were necessary. A receptor-based strategy might be a promising approach, as the nature of the antigen-uptake receptor often has a critical influence on the direction and sorting of the endocytosed antigen [Burgdorf S, Science 2007]. At the beginning of this study no marker was known that allowed a specific targeting of antigens to murine PDCs in opposite to other APCs. Conventional DCs express the lectin receptors DC-SIGN, DCIR2 and in particular DEC-205. Antigens targeted to these receptors were efficiently internalized and processed resulting in efficient priming of naïve CD4⁺ or CD8⁺ T cells *in vivo* [Engering A, JI 2002; Bonifaz L, JEM 2002 and 2004; Dudziak D, Science 2007]. Thus, the identification of a novel PDC-expressed receptor might help to discover the APC function of these cells.

2. OBJECTIVES OF THE WORK

The central function of dendritic cells (DCs) is the uptake and presentation of antigens for the induction of adaptive immune responses. Several DC subpopulations have been described, differing in phenotype, morphology, tissue localization, and function. Since all cells interact with their environment via cell surface receptors, the characteristic function of the particular subpopulation is often defined by its phenotype. Thus, further exploration of specifically expressed molecules is crucial to understand the immunological role and to disclose functional differences between different DC subsets.

The aim of this work was the identification of a cell surface receptor specifically expressed on mouse PDCs. In the first part of this work a PDC-specific monoclonal antibody should be generated by contralateral footpad immunization procedure. Next, the antigen recognized by the generated mAb should be identified and functionally characterized. The results might provide further evidence for the role of PDCs in the immune system. In particular, the ability of PDCs to act as professional APCs in the induction of T cell responses is currently controversially discussed and further insights would be beneficial.

3. MATERIALS AND METHODS

3.1 Mice

In this work female wild-type Balb/c and C57BL/6 mice were used, all purchased from Harlan Winkelmann, Borchon, Germany.

To detect strain-specific differences in the expression of mPDCA-1 and/or Sca-1, additionally, AKR/J, CD1, DBA/1, FVB, HM1, and SV129 mice were used (Harlan Winkelmann, Borchon, Germany, and Charles River Laboratories, Sulzfeld, Germany).

For studies describing the interaction of PDCs and naïve T cells, the following mouse models were used:

OT-I (C57BL/6) TCR transgenic mice harboring OVA-specific CD8⁺ T cells, carrying a V α 2/V β 5 TCR specific for the OVA₂₅₇₋₂₆₄ peptide presented in the context of MHC class I H2-K^b [Hogquist KA, Cell 1994], and OT-II (C57BL/6) TCR transgenic mice harboring OVA-specific CD4⁺ T cells, carrying a TCR specific for the OVA₃₂₃₋₃₂₉ peptide [Robertson JM, JI 2000] were a kind gift of Professor Stefan Grabbe, University of Mainz, Germany.

DO11.10 (BALB/c) TCR transgenic mice harboring OVA-specific CD4⁺ T cells, carrying a TCR specific for the OVA₃₂₃₋₃₂₉ peptide [Robertson JM, JI 2000], were purchased from Charles River Laboratories.

All mice were used at the age of 6 to 15 weeks, maintained under pathogen-free conditions and handled in accordance to protocols approved by local authority guidelines. Experiments were partly performed in collaboration with the Weizmann Institute of Science, Rehovot, Israel (group of Dr. S. Jung), at the DRFZ Berlin (group of Dr. A. Scheffold), at the Albert-Ludwigs-Universität Freiburg (group of Professor C. Bogdan) or at the Washington University in St. Louis (group of Professor M. Colonna).

3.2 Reagents

3.2.1 Antibodies

3.2.1.1 Antibodies for flow cytometry

In this study the following Fluorescein Isothiocyanate (FITC), Allophycocyanin (APC), R-Phycoerythrin (PE) or Biotin-coupled rat anti-mouse monoclonal antibodies (mAb) were used to analyse cell surface markers:

CD3 ϵ (clone 145-2C11), CD4 (clone GK1.5), CD8 α (clone 53-6.7), CD11b (clone M1/70.15.11.5), hamster anti-mouse CD11c (clone N418), CD16/32 (clone 93), CD19 (clone 6D5), CD40 (clone FGK45.5), CD45R (B220, clone RA3-6B2), CD49b (clone DX5), CD90 (Clone 30-H12), CD154 (CD40-L, clone MR1), CD205 (DEC205, clone NLDC-145), MHC-II (clone M5/114.15.2), Gr-1 (Ly-6C/G, clone RB6-8C5), Ly-6C (clone 1G7.G10), mPDCA-1 (unless indicated otherwise, clone JF-05-1C2.4.1 was used), Sca-1 (clones D7, CT-6A/6E, and E13-161.7), Ter-119 (clone Ter-119), and H-2k^b:SIINFEKL (25-D1.16) were all obtained from Miltenyi Biotec. 4-1BBL (clone TKS-1), CD40 (clone3/23), CD80 (clone 16-10A1), CD86 (clone GL1), CD138 (Syndecan), CD274 (B7-H1, PD-L1 (clone MIH5), and TCRv β 5.1 (clone MR9-4), B220 (clone RA3-6B2), and MHC-I (H-2k^b; clone AF6-88.5) were all purchased from BD

Pharmingen. CD69 (Clone H1.2F3), CD209 (DC-SIGN, clone 5H10), TCR β (clone H57-597), and KJ1-26 (DO11.10 clonotype) were purchased from Natutec (eBioscience), Frankfurt, Germany. Siglec-H (clones 440c or 551-3D3) was a kind gift of M. Colonna, St-Louis, USA. SA-PE-conjugated H-2Kb-OVA (SIINFEKL) iTag™ MHC Class I murine tetramer was purchased from Immunomics [Beckman Coulter] (San Diego, CA). Anti-rat MPG1 pAb was purchased from Cell Sciences, Canton, USA. HRP-conjugated polyclonal rabbit anti-rat Ig (H+L) (Jackson Immuno Research Laboratories) and HRP-labeled rabbit anti-Ovalbumin (hen egg white) antibody (Research Diagnostics Inc., Concord, USA) were used for immunoblotting and ELISA, respectively.

The following mAbs were used to detect intracellular cytokines: mAbs against IFN- γ (clone AN18.17.24), IL-2 (clone JES6-5H4), IL-4 (clone BVD4-1D11), IL-10 (clone JES5-16E3), IL-17 (clone TC11-18H10), TNF α (clone MP6-XT22) (all MB); IFN α (clone F18) (HyCult Biotechnologies b.V., Uden, The Netherlands); PE-conjugated IL-12p40/70 (clone C15.6) (BD Pharmingen).

Secondary antibodies were anti-Biotin mAb (Bio3-18E7.2) obtained from Miltenyi as well as FITC/PE-conjugated mouse anti-rat Kappa (clone MRK-1), anti-rat IgG₁ (clone RG11/39.4), anti-rat IgG_{2a} (clone B46-79, or anti-rat IgG_{2b} (cloneRG7/11.1) that had been purchased from BD Pharmingen.

3.2.1.2 Antibodies for ELISA

Anti-IFN α mAb (clone F18) was purchased from HyCult Biotechnologies (HBT), Uden, The Netherlands. HRP-coupled anti-OVA mAb was obtained from Research Diagnostics Inc., Concord, USA.

3.2.1.3 Antibodies for Immunoblotting

HRP-conjugated anti-phosphotyrosine mAb (clone Py-20) was obtained from BD Pharmingen, whereas HRP-coupled anti-OVA mAb was purchased from Research Diagnostics Inc., Concord, USA. Rabbit anti-rat-IgG(H+L) was purchased from Jackson Immuno Research Laboratories Inc. (distributed via Dianova, Hamburg).

3.2.2 Chemicals

3.2.2.1 General reagents

Carboxy-fluorescein diacetate succinimidyl ester (CFDA-SE/CFSE) was obtained from Molecular Probes [Invitrogen], Karlsruhe, Germany.

Bio-Safe colloid Coomassie staining reagent was purchased from Bio-Rad Laboratories, München, Germany.

3.2.2.2 Proteins and peptides

Imject OVA[®] protein was obtained from Perbio, Bonn, Germany, whereas OVA peptides OVA₃₂₃₋₃₃₉ (ISQAVHAAHAEINEAGR) and OVA₂₅₇₋₂₆₄ (SIINFEKL) were synthesized by O. Braun,

Apharesis 2 Unit, Miltenyi Biotec.

3.2.2.3 Stimulatory sequences

Phorbol-12-Myristate-13-Acetate (PMA), Ionomycin Calcium salt from streptomyces conglobatus (min. 98% TLC), and the TLR7 agonist Loxoribine (7-allyl-7,8-dihydro-8-guanosine) were purchased from Sigma. CpG ODNs 1668, 1826, 2006, and 2216 were all synthesized by Metabion, München, Germany.

Heat-inactivated Influenza virus (A/FPV/H7N7; Bratislava strain 79) was a kind gift of Dr. I. Johnston (Miltenyi).

3.2.3 Buffers

Staining and separation buffer:

Antibody stainings for subsequent FACS analysis as well as MACS-based cell isolations were standardly performed in staining buffer based on phosphate-buffered saline containing 2 mM EDTA and 0.5% BSA. For stability reasons, optionally 0.05% NaN₃ was added.

Red blood cell lysis buffer:

15.5 mM NH₄CL, 1 mM KHCO₃, 0.01 mM EDTA

Cell lysis buffer for immunoprecipitation or western blot:

100 mM Tris-HCl, 150 mM NaCl, 5 mM EDTA, supplemented with detergents (1% NP-40, Triton-X100 or other) and complete EDTA-free protease inhibitor cocktail (Roche). Low salt buffer used for washing before SDS-PAGE or elution contained 10 mM Tris HCl and 15 mM NaCl.

5x sample (Laemmli) buffer:

According to the protocol of Laemmli et al. 1970, 63 mM Tris-HCl (pH 6.8), 2% SDS, 0.025% 3',3'',5',5''-tetrabromophenolsulfonphthalein, and 10% glycerol were mixed and scaled up with distilled water to 10 ml volume. Optionally, DTT or β-mercapto ethanol was added for reducing conditions [Laemmli UK, Nature 1970].

10x SDS running buffer:

25 mM Tris-Base, 192 mM Glycine, 0.1 % SDS

Transfer buffer:

48 mM Tris-Base, 39 mM Glycin, 1.3 mM SDS, 10% methanol

3.2.4 Instruments and miscellaneous

NanoDrop	NanoDrop Technologies/Thermo Scientific, Wilmington, USA
Agilent 2100 Bioanalyzer	Agilent Technologies, Böblingen
Trans-Blot SD SemiDry Transfer Cell	BioRad, München
Gene Pulser II	BioRad
Flow cytometers FACScalibur and FACSvantageSE	BD Biosciences, Heidelberg
MACS-Separators and Stand	Miltenyi Biotec, Bergisch Gladbach
Cell culture hood <i>Hera Safe</i>	Heraeus Instruments, Osterode
Incubator <i>Hera Cell</i>	Heraeus
Waterbath	Julabo, Seelbach
Centrifuge Eppendorf 5415D	Eppendorf, Hamburg
Centrifuge Megafuge 1.0	Heraeus
Thermocycler: PTC-225	MJ Research, Ramsey, USA
Multiplate reader Genios	Tecan, Crailsheim
Cryostat CM3050	Leica, Wetzlar

Chemicals were purchased at Merck Chemicals KGaA (Darmstadt) or Sigma-Aldrich Chemie GmbH (Munich; also: Fluka and Riedel-de-Haën), unless otherwise specified in the text.

10-20% Tris/Glycine-gels	Anamed, Groß-Bieberau
1 kb-PLUS-DNA-Ladder	Invitrogen
PAGE-Ruler Prestained Protein Ladder	MBI Fermentas, St. Leon-Rot
Blot Paper (Mini Blot size)	BioRad
Cell strainer (40, 70, 100 μ)	Falcon (BD Biosciences)
Conical and Round Bottom Tubes	Falcon (BD Biosciences)
Cy3/5-dCTP	GE Healthcare, Munich
Hybond-P PVDF and Hybond-XL Nylon Membranes	GE Healthcares
Electroporation Cuvette (Type 165-2107)	BioRad
NAP-5 and -10 columns	GE Healthcare
PD-10 column	GE Healthcare
Superdex 200 16/60 column	GE Helathcare
Neubauer chamber	Brand, Wertheim
MACS Separation columns (μ , MS, LS, LD)	Miltenyi Biotec
Pre-Separation filter	Miltenyi Biotec
Syringe needle 26G 1/2", short	Braun, Melsungen
CpG ODNs	Metabion, Munich
PHA-Lectin	Sigma
Azaserine	Sigma
Polyethylenglycol	Roche, Mannheim

3.3 Cell culture

3.3.1 Standard cell culture methods

All cell types were cultured in a humidified incubator with a 5-9% CO₂ atmosphere at 37°C. Murine primary cells were isolated directly from indicated tissues (as described below in the FACS section). RPMI 1640 (Miltenyi Biotec, Bergisch Gladbach, Germany; Invitrogen, Karlsruhe, Germany), supplemented with 10% FCS (PAA Laboratories, Pasching, Austria), 15 mM HEPES buffer, 1 mM Sodium pyruvate, 50 µM β-mercaptoethanol, 2 mM L-Glutamine, 100 U/ml Penicillin and 10 µg/ml Streptomycin (all medium supplements were obtained from Invitrogen) was used as culture medium for all *in vitro* experiments with primary cells.

Human HEK 293T cells, murine 1881, EL-4, SP2/0, and Raw 264 cells as well as rat RBL-1 cells were purchased from ATCC/LGC Promochem GmbH, Wesel, Germany. Cell lines were either cultured in RPMI or in Dulbeccos modified Eagles medium (DMEM; Miltenyi Biotec and Invitrogen), supplemented in analogy to RPMI.

3.3.2 Generation of FLT-3L-derived BM-PDCs

It has been shown that treatment of mice with FLT-3L resulted in increased numbers of DCs in different lymphoid organs including the bone marrow [Maraskovsky E, JEM 1996] leading to the development of several protocols to generate DCs and PDCs *in vitro*.

Total BM cells were prepared by rinsing femurs and tibiae of one mouse. Red blood cells were lysed for 10 min at room temperature in lysis buffer. After sterile washing, cells were seeded at a final cell concentration of 2×10^6 cells/ml in complete medium, additionally containing 15% FCS (Biochrome) and 1% non-essential amino acids. Recombinant murine growth factors were added for the generation of PDCs: 100 ng/ml Flt-3 Ligand (R&D Systems) and 10 µg/ml Thrombopoietin (TPO; Biosource [Invitrogen]). At days 4 and 7, 50% of the medium was replaced by fresh medium supplemented with 50 ng/ml Flt-3L. *In vitro* generated PDCs were standardly harvested between days 7 and 10.

3.4 Generation of monoclonal antibodies

3.4.1 Contralateral (footpad) immunization and fusion

For all immunization approaches PDCs were isolated from spleen of wild type (wt) BALB/c mice and subcutaneously (s.c.) immunized into the hind footpad of Lewis and LOU rats, respectively. In different immunization attempts, murine Sp2/0 myeloma or freshly isolated murine NK cells were used as decoy and subjected to the corresponding, contralateral foot pad [as described before by Brooks PC, Journal of Cell Biology, 1993; Yin AH, Blood 1997]. After several rounds of immunization, cells from the popliteal LNs of the one hind footpad were used for the fusion with a murine myeloma partner (Sp2/0 cells) based on the HAT system originally described by Köhler and Milstein [Köhler G & Milstein C: "Continuous cultures of fused cells secreting antibody of predetermined specificity", Nature 256, 495–497 (1975); Cotton RGH & Milstein C: "Fusion of two immunoglobulin-producing myeloma cells" Nature 244, 42–43 (1973)].

3.4.2 Screening of hybridoma clones

To assess the specificity of the generated hybridoma clones and to select only PDC-specific clones, the following screening strategy was performed. Spleen single cell suspensions were incubated with hybridoma supernatant for 10-15 min at room temperature. After washing, the cell suspension was incubated via PE-conjugated marker mAb (10 min at 4°C) followed by a second washing step. PDCs were subsequently identified by staining with APC-conjugated hamster anti-mouse CD11c or rat anti-mouse B220 or Gr-1 mAbs (10 min at 4°C). In case rat anti-mouse mAbs were used to detect PDCs, an intermediate blocking step (30 min at room temperature) with irrelevant rat IgG mAb was applied (100 µg/ml) before anti-B220 and Gr-1 mAbs were added directly into the staining suspension. In all these stainings blocking of Fc receptors was omitted, as the anti-CD16/32 mAb would be detected by the marker mAb.

3.4.3 Isotype determination of generated mAbs

The isotype of the generated PDC-specific antibodies was assessed either by flow cytometric analysis (intracellular staining with secondary mouse anti-rat Kappa, IgG₁, IgG_{2a}, or IgG_{2b}) or was determined using the anti-rat monoclonal antibody isotyping test kit (RMT1; AbD Serotec/Morphosys, Düsseldorf, Germany).

3.4.4 Competitive inhibition experiments with the generated mAbs

Epitope recognition of the four PDC-specific mAbs was determined by cross-blocking experiments. Spleen single cell suspensions were first incubated with 100 µg/ml unconjugated mAb for 10 min at 4°C. Next, cells were stained with fluorochrome-conjugated mAbs of indicated clones. Impact of blocking was revealed by flow cytometric analysis (by change of the mean fluorescence intensity).

3.5 Biochemical methods

3.5.1 SDS-PAGE and Western blotting:

Size fractionation of protein suspensions was performed by sodium dodecyl sulfate polyacrylamide gel electrophoresis (SDS-PAGE). 1-10⁶ cells were washed with ice-cold phosphate buffered saline and sedimented before resuspension in sample buffer. Samples were then sonicated and boiled at 95°C for 5 min. For assessing the integrity of the targeting construct proteins were also resuspended in sample buffer. Samples (5-25 µl) were then loaded onto 4-20% Tris-glycin gels that have been obtained from Invitrogen (Novex gels) or Anamed and gel electrophoresis was performed on a X-cell Sure Lock Novex Mini cell System (Invitrogen) according to the manufacturers instructions.

Protein markers of 20–150 kDa size were obtained from MBI Fermentas (Prestained Protein Ladder) or Bio-Rad (Prestained Ladder). After electrophoresis, gels were equilibrated with distilled water whereas PVDF membrane (Hybond-P, Amersham Biosciences) was activated with methanol and equilibrated with transfer buffer. Proteins were transferred onto the PVDF membrane via a semi-dry or semi-wet process in a Trans Blot SD semi dry transfer cell (Bio-

Rad). Membranes were washed and blocked with FCS, BSA, or milk powder-containing phosphate buffered saline and subjected to antibody-detection, e.g. anti-OVA, anti-rat IgG(H+L), or anti-Py-20 antibodies were used. Finally, HRP-mediated signals were analyzed via the ECL detection kit (Amersham Pharmacia Biotech, Uppsala, Sweden).

3.5.2 Induction and analysis of tyrosine phosphorylation

PDCs were untouched isolated by MACS technology (see below) and pre-incubated for 30 minutes in supplemented RPMI medium at 37°C. Anti-mPDCA-1 mAb or anti-Ter119 mAb (rat IgG_{2b} isotype control) were added at a final concentration of 10 µg/ml. Five minutes later cells were wash in ice cold PBS buffer and lysed in Laemmli protein sample buffer. Cell lysates were sonicated, boiled, separated by sodium dodecyl sulfate-polyacrylamide gel electrophoresis (SDS-PAGE), and transferred to PVDF membranes. After blocking with 5% BSA, membranes were probed with HRP-coupled anti-phosphotyrosine mAb Py-20 (BD Pharmingen). Immunoblotted proteins were visualized by chemiluminescence using enhanced chemiluminescence detection reagents (Amersham).

3.5.3 Immunoprecipitation

5×10^6 cells were resuspended in 1 ml lysis buffer and incubated for 30 min on ice. Optionally, cells were additionally sonicated. After lysis nuclei and debris were removed by centrifugation (13,000 rpm for 5 min). For “preclearing”, irrelevant antibody was added to the supernatant and incubated for 1 h at 4°C. 100 µl protein-G sepharose was washed with lysis buffer and added to the lysates. After overnight incubation anti-mPDCA-1 mAb was added to the precleared supernatant (after sepharose-bound irrelevant antibody was removed by centrifugation) and incubated for 2-4 hrs. Anti-mPDCA-1 mAb was detected by fresh sepharose (incubation for 2 hrs) and washed with lysis buffer as well as low salt buffer before resuspension in SDS sample (Laemmli) buffer. Samples were stored at -20°C until SDS-PAGE or Western blot analysis.

3.5.4 Immunoprecipitation after metabolic labeling

To identify IFN α -induced and PDC-specific proteins cells were metabolically labeled with ³⁵S-Methionine before subsequent immunoprecipitation was performed: A 10 µCi/ml ³⁵S-methionine working solution was prepared in pre-warmed (37°) long-term labeling medium lacking methionine. 5×10^6 cells were resuspended in 5-10 ml of the indicated medium and transferred to a 25 cm² tissue culture flask and cultured for 16 hrs in the presence or absence of 10² U/ml recombinant murine IFN α . After washing, cells were lysed and subjected to immunoprecipitation as described above. Radioactive signaling of samples was visualized on x-ray films.

3.5.5 Generation of antibody conjugates and fragments

Anti-mPDCA-1 mAb or ChromePure rat IgG (Jackson Immuno Research Lab. Inc., West Grove, PA, USA) F(ab')₂ fragments were conjugated to OVA protein that had been activated with succinimidyl-4-(N-maleimidomethyl) cyclohexane-1-carboxylate (SMCC, Perbio) according to

the manufacturer's protocol as described elsewhere [Sapozhnikov A, JEM 2007]. The F(ab')₂-OVA conjugates were size fractionated to remove unconjugated OVA. For *in vivo* application the reagents were sterile filtrated (Millex GV filter unit 0.22 µm; Millipore, Carrigtwohill, Ireland). Construct integrity was evaluated by SDS-PAGE and Western blot analysis, and fragments were detected with HRP-conjugated polyclonal rabbit anti-rat Ig (H+L) (Jackson Immuno Research Laboratories) and HRP-coupled rabbit anti-OVA antibody (Research Diagnostics Inc., Concord, MA, USA), respectively. To assess specific *in vivo* targeting of PDCs, mice were subcutaneously (10 µg) or intraperitoneally (50 µg) injected once with Alexa488-conjugated anti-mPDCA-1-F(ab')₂. Two hours after subcutaneous injection and 15 hours after intraperitoneal injection single cell suspensions were prepared from the popliteal LN and spleen, respectively, and were analyzed for specific *in vivo* labeling of PDCs, counter-stained against B220, Ly-6C or CD11c.

To deliver model antigens to PDCs *in vitro*, spleen single-cell suspensions were incubated with OVA protein covalently coupled to FITC-conjugated anti-mPDCA-1-F(ab')₂ antibody fragment. For detection of PDC-specific targeting, cells were stained with Siglec-H.

3.5.6 Enzyme-Linked Immunosorbent Assay (ELISA)

ELISA readout was generally performed by measurement of the absorbance at 450 nm using a Microplate ELISA reader (MWG-Biotech, High Point, USA) via Softmax Pro v5.0.1 software (Molecular Devices, Sunnyvale, USA).

3.5.6.1 Anti-IFN α -ELISA

The capacity of PDCs to produce IFN-I and the impact of mPDCA-1 triggering was analyzed both *in vivo* and *in vitro*. Animals received a dose of PDC-depleting anti-mPDCA-1 mAb and were infected with MCMV. Blood was collected by retro-orbital puncture at the indicated time points after treatment. Serum was prepared from whole blood by coagulation for 30 min at 37°C and centrifugation. Collected sera were analyzed with a Mouse IFN alpha Colorimetric ELISA Kit (PBL Biomedical Laboratories, USA).

Alternatively, mice received 10 µg CpG ODN 2216 in combination with DOTAP (Roche Diagnostics), and serum IFN α was analyzed 6 hrs later.

In vitro IFN α production by PDCs was assessed as follows: 10⁵ isolated or enriched mouse PDCs were cultured in a 96-well plate in the absence or presence of a TLR9 stimulus (5 µg/ml CpG ODN) for 24 hrs. Subsequently, supernatant was analyzed by IFN α -specific ELISA (PBL).

3.5.6.2 Anti-OVA-ELISA

To determine the OVA content on generated mPDCA-1 and isotype targeting constructs, an OVA-specific ELISA was performed. Soluble OVA and different OVA-antibody fragments were coated for 60 min at 37°C onto high-binding capacity 96-well polystyrene microtiter plates (Greiner bio-one) in PBS. After washing (PBS, 0.1% Tween-20), the plate was incubated with

blocking buffer (PBS, 0,1% Tween-20, 5% BSA) at 4°C. After 12 hrs, the plate was washed and incubated with horseradish peroxidase (HRP-) coupled rabbit anti-OVA antibody (Research Diagnostics Inc., Concord, USA) for 1h at 37°C. After repeated washing, 100 µl tetramethyl benzidine substrate (TMB; Pierce) was added to the wells and incubated for 10 min. Reaction was stopped with 100 µl sulfuric acid (10%). OVA content of the conjugates was quantified by a standard curve, which was based on soluble OVA protein.

3.6. Flow cytometric analysis

The flow cytometric analysis of cells or particles is based on their physical and immunological characteristics. Beside their scatter properties, cells were investigated by fluorochrome-conjugated antibodies within a fluid stream. The combination of scattered and fluorescent light emissions was detected and analyzed to define information about the physical structure and expression pattern of different molecules for each single cell.

3.6.1 Tissue preparation

Mice were either euthanatized by isoflurane inhalation or sacrificed by cervical dislocation. Peripheral blood was obtained from retro-orbital puncture or tail bleeding. Organs collected for different experiments included spleen, bone marrow, liver, thymus, lung, mesenterial and peripheral lymph nodes (popliteal, inguinal, cervical, brachial and axillary) as well as Peyer's Patches. If indicated, spleen, liver, and lungs were subjected to Collagenase D (Roche Diagnostics) treatment in AnnexinV buffer for 35 min at 37°C.

For single cell suspensions, collected organs were mechanically disrupted by passing through a cell strainer (40-100 µm nylon mesh; BD Biosciences, Franklin Lakes, USA). After centrifugation at 300xg for 10 min, cells were resuspended in staining buffer in case not otherwise indicated.

3.6.2 General staining procedure for CDs and other cell surface molecules

For standard flow cytometric analysis, 2×10^6 cells were resuspended in ice-cold staining buffer. Cells were stained with designated antibodies for 10 min according to manufacturer's instructions, whereas Fc-receptors were blocked by simultaneous incubation with unlabeled anti-CD16/CD32 mAb. Cells were then analyzed on FACS Calibur or FACS Scan Flow cytometers (Becton-Dickinson, Heidelberg, Germany) using CellQuest software (Becton-Dickinson) or FlowJo (TriStar, San Carlos, CA, USA). Cell debris and dead cells were excluded from the analysis based on scatter signals and PI fluorescence [Flow cytometry and cell sorting; A. Radbruch, editor. Berlin; New York: Springer-Verlag 1992].

3.6.3 Intracellular cytokine staining (ICS)

3.6.3.1 Detection of IL-12, TNF α and IFN α production in PDCs

PDCs were activated *in vitro* with different TLR agonists. Four hours before ending of the culture Brefeldin A (10 µg/ml; Calbiochem) was added to prevent cytokine secretion. Subsequently, PDCs were fixed and permeabilized (Inside Stain Kit, Miltenyi Biotec) and intracellularly stained

for indicated cytokines (IL-12, IFN α , and TNF α) before flow cytometric analysis.

3.6.3.2 Cytokine staining of IL-2, IL-4, IL-10, IL-17, IFN γ , and TNF α produced by T cells

PDC-primed CD4⁺ T cells were expanded for eight days until restimulation with PMA [20 ng/ml] and Ionomycin [1 μ g/ml] for 6 hours *in vitro*. In the last four hours the medium was supplemented with Brefeldin A as described before. Cells were fixed and permeabilized (Inside Stain Kit, Miltenyi Biotec) and stained for intracellular cytokines (IL-2, IL-4, IL-10, IL-17, IFN γ , and TNF α) before flow cytometric analysis.

3.6.4 Internalization experiments

For internalization of the mPDCA-1 antibody-receptor complex *in vitro*, FL or BM PDCs were isolated and stained with FITC-conjugated anti-mPDCA-1 mAb on ice. After washing cells were resuspended in medium and incubated at 37 °C for 0-120 min. To detect cell surface-bound antibody, cells were then labeled with biotinylated anti-FITC mAb followed by counterstaining with PE-conjugated anti-Biotin mAb. Mean fluorescence intensities of both FL-1 and FL-2 signals were normalized (the starting MFI values were set to 100%).

To demonstrate *in vivo* internalization of mPDCA-1, Alexa488-conjugated anti-mPDCA-1(Fab2) mAb was administrated intraperitoneally. Next, spleen PDCs were isolated, fixed in 1.8% formaldehyde at room temperature and additionally stained for surface-bound mPDCA-1 with anti-mPDCA-1-Biotin followed by Alexa633-conjugated anti-Biotin mAb. Confocal laser scanning microscopy (CLSM) analysis showed either signals derived from *in vivo* administrated Alexa488-conjugated anti-mPDCA-1-F(ab')₂ or cell surface located, *in vitro* stained mPDCA-1 or merged pictures.

3.6.5 Induction and analysis of intracellular calcium flux

To detect Ca²⁺ released from intracellular compartments upon receptor triggering, 1-5x10⁶/ml PDCs were loaded with a fluorochrome, which exhibited different extinction stages in the free and Ca²⁺-bound conformation (5 mM Indo-1; Molecular Probes). After washing with medium supplemented with FCS, cells were incubated for 45 min at 37°C before washing with PBS and kept on ice until analysis on a FACS Vantage Flow Cytometer Cell Sorter (BD; operated by C. Göttlinger, Institute of Genetics, University of Cologne). To define PDCs, cells were optionally stained with PE and APC-conjugated anti-B220 and anti-CD11c mAbs, respectively. The filter set-up of the FACS Vantage for Indo-1 (UV excitation only) was either a FL-5 424/44 nm BF filter (calcium bound Indo-1) or a FL-4 530/30nm BF filter (unbound Indo-1). Calcium flux was measured as a ratio between calcium bound and unbound Indo-1 (FL-5/FL-4) versus time.

To assess background signal intensity, ice-cold and Indo-1 loaded PDCs were first analyzed in the untriggered status. After signal detection of untreated PDCs, an aliquot of unconjugated anti-mPDCA-1 mAb was injected into the reaction tube and the modulation of the indo ratio was analyzed. Complete deflection of the calcium flux was measured by the addition of ionomycin (1 mg/ml).

3.7 Biomolecular methods and gene expression analysis

3.7.1 Standard biomolecular techniques:

Standard methods were based on protocols as described in “Molecular Cloning. A Laboratory Manual. 2nd edition” [Eds. Sambrook J, Fritsch EF, Maniatis T, Cold Spring Harbor Laboratory Press, Cold Spring Harbour 1989].

3.7.1.1 Isolation of nucleic acids

3.7.1.1.1 RNA isolation

Total RNA was isolated using the NucleoSpin[®] RNA II Kit (Macherey-Nagel, #740955.x) according to the manufacturers protocol.

Messenger RNA was isolated using the μ MACS mRNA Isolation Kit (Miltenyi, #130-075-201, 130-090-276) according to the manufacturers protocol. Recombinant RNase-free DNase I was obtained from Roche (#04716728001).

3.7.1.1.2 DNA isolation

Plasmid DNA was prepared from *E. coli* cultures using the NucleoSpin[®] Plasmid Kit (Macherey-Nagel) according to the manufacturers protocol.

DNA was isolated from agarose gels using either the Gel extraction kit (Macherey-Nagel) or the Agarose Gel DNA Extraction Kit (Roche, # 1 696 505).

3.7.1.2 cDNA synthesis

cDNA was synthesized from mRNA or total RNA by reverse transcription. A reaction mix of 10 μ l total volume was prepared:

- 7 μ l (total) RNA
- 2 μ l Oligo(dT) primer (920 pmol)
- 1 μ l random hexamers (100 pmol) were mixed and incubated for 10 min at 70°C. This first reaction mix was then stored on ice.

On ice, a second reaction mix was prepared by adding

- 16.5 μ l RT buffer (Miltenyi)
- 0.6 μ l dNTP mix (25 mM each)
- 3 μ l Reverse transcriptase (RT, MACS-Script, Miltenyi).

Both mixes were combined and incubated at 42°C. After 1 h another 1.5 μ l RT were added to the reaction mix and incubated for an additional 1 h at 42°C. To digest contaminating RNA, two units of RNaseH were added and incubated for 20 min at 37°C.

Alternatively, cDNA was directly synthesized “in column” via the μ MACS[™] One-step cDNA Kit (Miltenyi; #130-091-902). In this protocol cell lysates were mixed with poly(A) microbeads, applied to a MACS column, and reversely transcribed.

3.7.1.3 Polymerase chain reaction (PCR)

Standard PCR was performed using the PicoMaxx High Fidelity PCR System (Stratagene, #600420) or according to the following protocol:

- 1-100 ng template DNA
- 200 μ M dNTPs
- forward and reverse primer (250 nM each)
- 2 mM $MgCl_2$ (only supplemented if Tag polymerase was used)
- 1x PCR buffer
- 1-5 U Tag (Pfu) polymerase /100 μ l reaction volume
- Deionized H_2O (ad 50 μ l)

Table 3.1 Cycler settings for standard PCR

Nr.	Step	Temperature	Time
1	Denaturation	95°C	5 min
2	Annealing	54-62°C	30 sec
3	Primer extension	72°C	1 min
4	Denaturation	94°C	30 sec
5	Cycles (repeat Step 2-4)	15-35x	
6	Annealing	54-62°C	30 sec
7	Final extension	72°C	5 min
8	Store	10°C	∞

Amplified PCR products were purified with either the QIAquick PCR Purification Kit (Qiagen), the NucleoSpin[®] Extract II kit (Macherey-Nagel, #740609) or the High Pure PCR Product Purification Kit (Roche, #1 732 668).

Reverse transcriptase (RT)-PCR was performed either via the Titan One Tube RT-PCR System (Roche, #11 855 476 001) or – for subsequent LightCycler analysis – via the LightCycler[®] RNA Master SYBR Green I kit (Roche; see 3.7.3).

3.7.1.4 Primer design

Homologous oligonucleotide sequences were generated based on sequence information deposited in the databases GeneBank or Nucleotide (NCBI). Primer sequences were chosen on criteria defined by Innis and Gelfand [Innis MA and Gelfand DH, Academic Press 1990]. The melting temperature was calculated according to the Wallace rule: T_m (°C) = $2 \times \sum (A + T) + 4 \times \sum (G + C)$ [Wallace R, Nucleic Acids Res. 1979; Sambrook J and Russell DW, Cold Spring Harbor Laboratory Press 2001]. The following software simulated primer integrity and annealing: Amplify v1.2b (Bill Engels, University of Wisconsin, USA) and Sequencher 4.1 (Genes Codes Corporation, Ann Arbor, USA).

3.7.1.5 DNA modification

3.7.1.5.1 Restriction digestion:

Qualitative restriction digest of DNA templates was performed by incubation for 1-2 hrs with appropriate restriction enzymes at a final concentration of 1 Unit/ μ g DNA according to the manufacturers protocols (NEB and MBI Fermentas). For preparative hydrolysis, DNA sequences were digested o/n. Resulting DNA fragments were isolated using the NucleoSpin[®] Extract II Kit (Macherey-Nagel) after agarose gel electrophoresis (see 3.7.1.1.2 *DNA isolation*).

3.7.1.5.2 Dephosphorylation of vector DNA:

Vector DNA was dephosphorylated at the 5' end prior to ligation with insert fragments. Thus, DNA was subjected to Shrimp Alkaline Phosphatase (SAP) treatment according the manufacturers protocol (Roche, #11 758 250 001).

3.7.1.5.3 DNA ligation

For DNA ligation a commercial available kit was used (Rapid DNA Ligation Kit from Roche [#11 635 379 001]) or the following ligation protocol was performed:

- Vector and insert DNA were mixed in 10 μ l volume with dH₂O (at varying ratios of 1:1 to 1:5).
- 2 μ l 10x ligation buffer,
- 2 μ l PEG 4000 (50%),
- 1-2 Units T4-Ligase for sticky ends or 5 Units T4-Ligase for blunt ends were added and filled up with dH₂O ad 20 μ l.
- An incubation for 1 h at 22°C or o/n at 16°C was followed by a heat inactivation of the T4-Ligase for 10 min at 65°C.

3.7.1.6 *E. coli* transformation

Transformation of plasmid DNA into competent *E. coli* bacteria was performed using the heat shock method.

- Reaction tubes were pre-cooled on ice.
- 2-5 μ l plasmid DNA were mixed with 25-50 μ l competent *E. coli* and incubated for 30 min on ice.
- Transformation was performed for 40-60 sec at 42°C (water bath).
- Reaction mix was instantly incubated for 2 min on ice before adding 200-700 μ l of pre-warmed S.O.C or LB medium.
- Bacteria were agitated for at least 1 h at 37°C (300 rpm) before plating and o/n incubation at 37°C.

E. coli strains *One shot Top-10* or *DH5 α* (both Invitrogen) or *XL-1.blue* (Stratagene) were used for transformation.

3.7.2 Gene chip microarrays

For differential gene expression analysis RNA from PDCs, T cells, NKs, B cells, cDCs, macrophages, and cells lines, as well as sorted Sca-1⁺ and Sca-1⁻ PDCs was compared. Amplification of RNA samples for microarray and quantitative real-time PCR (qPCR) experiments was performed by in vitro transcription (IVT) based on modified linear T7 amplification [Eberwine J, Biotechniques 1996; Van Gelder RN, PNAS 1990].

3.7.2.1 Identification of mPDCA-1 candidate genes (Agilent microarray)

The Whole Mouse Genome Oligo Microarray Kit (Agilent Technologies, Waldbronn, Germany) was used to identify the antigen specifically expressed on PDCs and recognized by the anti-mPDCA-1 mAb. Therefore, the differential gene expression profile of mPDCA-1-expressing and not expressing cells was compared.

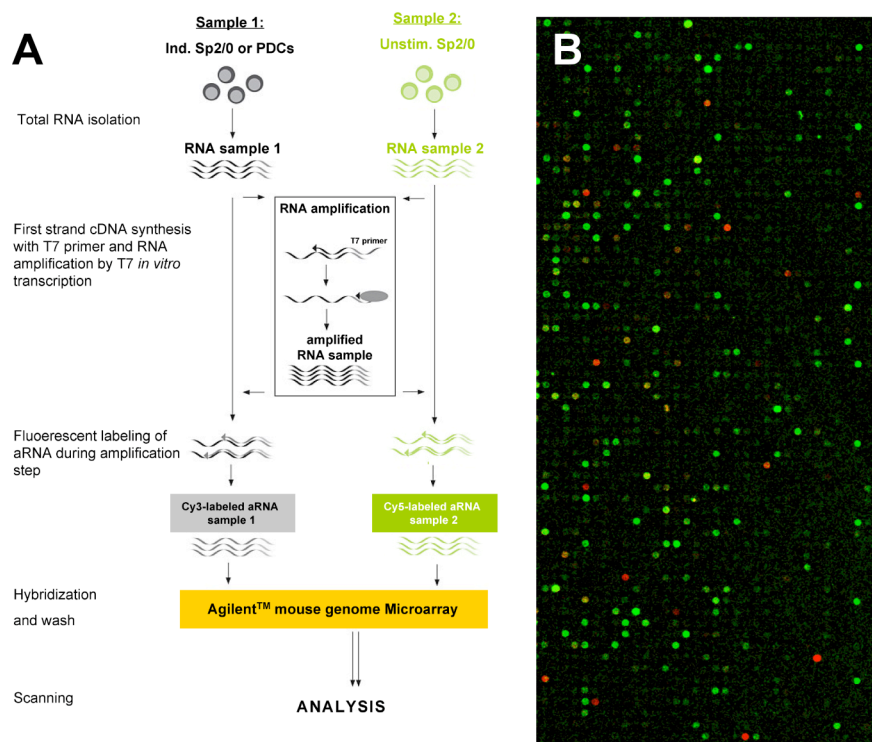


Fig. 3.1 Differential gene expression analysis on Agilent microarrays.

(A) Schematic principle of sample processing and hybridization for differential gene expression analysis of mPDCA-1⁺ and mPDCA-1⁻ cells. (B) An impression of the signal distribution of a representative microarray is demonstrated. The regulation of each gene is displayed by Cy3 (red) and Cy5 signal (green).

Total RNA was isolated via the Nucleospin RNA II RNA Extraction Kit (MACHEREY-NAGEL, Düren, Germany). After confirmation of the RNA integrity (2100 Bioanalyzer platform, Agilent), the target RNA was amplified and converted to Cyanine 3- or Cyanine 5- labeled cRNA. A mixture of differentially labeled target RNAs was hybridized to the Agilent oligo microarray. Hybridized microarrays were scanned with the ScanArray Lite (Packard Bioscience, Dreieich) and analyzed using the Imagen software version 4.1 (Bio-Discovery, Los Angeles, USA). The signal of each spot was measured in a fixed circle of 350 μm diameters and the background outside the circle within rings 40 μm distant to the signal and 40 μm wide. Local background was subtracted from the signal to obtain the net signal intensity and the ratio of Cy5/Cy3. The

ratios were normalized to the median of all ratios using only those spots for which the fluorescent intensity in one of the two channels was two-fold higher than the negative control. The microarray procedure is illustrated in Fig. 3.1.

An overview of the differentially hybridized microarrays using different mRNA samples is given in Table 3.2:

Table 3.2 Overview of the hybridization scheme and setup for the gene expression analysis on Agilent microarrays.

Mouse genome microarrays (Agilent Technologies) consisting of about 22,500 mouse transcripts were used to identify the antigen recognized by the anti-mPDCA-1 mAb. In four different sets (chip I-IV) Sp2/0 cells, either untreated or cultured in the presence of IFN α , or after downregulation of mPDCA-1 were compared against each other. Set V consisted of PDCs vs. untreated Sp2/0 cells, demonstrating PDC-presence of regulated gene candidates.

Sets VI+VII were reproductions with the same samples described for set I+II using whole-genome mouse chips (Agilent Technologies) consisting about 40,000 transcripts.

Chip	Sample A	vs.	Sample B	mPDCA-1 expression	Micro array
I	Sp2/0+IFN α (Cy3)	vs.	Sp2/0 unst. (Cy5)	+/-	Half genome
II	Sp2/0 unst. (Cy3)	vs.	Sp2/0+IFN α (Cy5)	-/+	"
III	Sp2/0+IFN α (Cy3)	vs.	Sp2/0+IFN α wash (Cy5)	+/-	"
IV	Sp2/0+IFN α wash (Cy3)	vs.	Sp2/0+IFN α (Cy5)	-/+	"
V	PDCs (Cy3)	vs.	Sp2/0 unst. (Cy5)	+/-	"
VI	Sp2/0+IFN α (Cy3)	vs.	Sp2/0 unst. (Cy5)	+/-	Whole genome
VII	Sp2/0 unst. (Cy3)	vs.	Sp2/0+IFN α (Cy5)	-/+	"

3.7.2.2 Parallel identification and quantification of RNA (PIQOR microarray)

PIQOR cDNA microarrays (Miltenyi Biotec) were used to compare gene expression profiles of FACS-sorted Sca-1⁺ and Sca-1⁻ PDCs.

About sorted 10⁴ cells were resuspended in SuperAmp lysis buffer (Miltenyi) to enable mRNA isolation and amplification. Isolation was performed with the Nucleospin RNA II RNA Extraction Kit (MACHEREY-NAGEL, Düren, Germany). Due to limited starting material the μ MACS One-step T7 Template Kit (Miltenyi) was used to extract total RNA, followed by poly-A⁺ RNA enrichment and IVT based on T7 primers. Amplified RNA (aRNA) samples were again photometrically quantified (NanoDrop) and quality was confirmed by the Agilent BioAnalyzer. First strand cDNA was incubated for 60 min at 37°C with Terminal deoxynucleotidyl transferase followed by heat inactivation of the enzyme at 70°C. 5'-tagged cDNA was amplified and PCR products were purified using the NucleoSpin Extract II Kit (Macherey Nagel). Yield of cDNA was quantified by NanoDrop analysis and by capillary electrophoresis (Bioanalyzer). At last 250 ng of purified PCR product was labeled with either Cy3- or Cy5-dCTPs in a Klenow Fragment reaction (10 Units per sample) for 2 hrs at 37°C followed by heat inactivation at 70°C. Cy3/5-labeled cDNA samples from either Sca-1⁺ or Sca-1⁻ PDCs were combined and purified using the

CyScribe GFX Purification Kit (GE Healthcare) before hybridization to PIQOR mouse immunology microarrays, which contain cDNAs of 1,076 genes, spotted as four-fold replicates on different positions of the array. After 18 hrs of incubation, hybridized microarrays were washed with washing buffer, scanned and analyzed as described above. The mean of four spots representing the same cDNA was determined. As a qualitative measurement for the validity of the data and to check for the uniformity of the hybridization process, the coefficient of variation (cv) of the four ratios for the respective gene was calculated. Hybridization, scanning and data analysis were performed as described [Bosio A, Carcinogenesis 2002]. Image capturing and signal quantification of hybridized PIQOR microarrays were performed with the ScanArrayLite4000 Microarray Scanner and ImaGene software Version 5.0 (BioDiscovery, Los Angeles, USA).

3.7.2.3 Microarray data mining

Scanned images were analyzed using the Agilent Feature Extraction software (Version 9.1) by which the local background was subtracted from the signal to obtain the net signal intensity and the ratio of Cy5/Cy3. A rank consistency based probe selection for Lowess normalization was done. After filtering the data with respect to signal significance a two-tailed t test was used to determine signal versus background significance. Only those spots were used for which the fluorescent intensity in one of the two channels was twice the mean background of all “unflagged” spots. Only genes displaying net signal intensity 2-fold higher than the mean background were used for further analysis. Spots with p-values >0.01 were omitted.

For analysis of PIQOR data, the normalized mean ratio of four corresponding spots, representing the same cDNA, was computed. After log₂-transformation of the ratios, data were imported in TIGR MeV Version TM4 [Saeed AI, Biotechniques 2003]. Average linkage clustering of genes was done using Euclidean Distance [Eisen MB, PNAS 1998]. Gene ontology analysis, “clustering”, was carried out after gene annotation to verified pathways (Annotate, Miltenyi Biotec, unpublished).

3.7.3 Quantitative real time RT-PCR (LightCycler)

All oligonucleotide primers used in this work were purchased from Metabion GmbH (Martinsried, Germany).

A real-time RT-PCR was performed to compare transcript levels of PDC-specific (mPDCA-1) gene candidates obtained from the microarray analysis. The LightCycler[®] RNA Master SYBR Green I kit (Roche Diagnostics GmbH/Roche Applied Science, Mannheim, Germany) was used for the amplification and detection of selected RNA targets, analyzed on the LightCycler platform. All assays were performed at least in duplicates. In principle, this method is based on the intercalation of an unspecific fluorochrome (SYBR green) during the DNA syntheses process of the PCR, which is measured after each cycle. The cycle number is determined at which the SYBR green emission increased above threshold level. From this signal an

exponential curve is calculated and compared to a standard curve for each primer pair, which demonstrated the amount of amplified DNA (LightCycler Software 3.5, Roche).

Messenger RNA was prepared from MACS-isolated hematopoietic cell populations (e.g. PDCs, NK cells, B cells, or T cells) using the RNeasy Mini Kit (Qiagen, Hilden). After quantification, an equal amount of mRNA was used for the real time RT-PCR reaction. Messenger RNA amount was normalized by the expression of house keeping genes (murine β -actin, PPIA, Hprt-1, and GAPDH). For each candidate primer pairs were designed using the Primer3 software (Whitehead Institute for Biomedical Research; Rozen S, Bioinformatics Methods and Protocols: Methods in Molecular Biology 2000) and a standard curve with titrated amounts of mRNA was performed to confirm primer integrity and to determine the optimal reaction conditions. Melting curve analysis of amplified samples was performed to assess the specificity of the amplified PCR product by discrimination between primer-dimers, side reaction products, and specific PCR product.

3.7.4 Generation of transfectants

3.7.4.1 Cloning strategies

The open reading frame of selected gene candidates were cloned in different vectors providing selection resistance, a HA-tag as well as the bi-cistronic expression of a truncated human CD4 antigen for direct separation. The cloning strategies for two genes of interest, MPG1 and BST2, is demonstrated in Fig. 3.2.

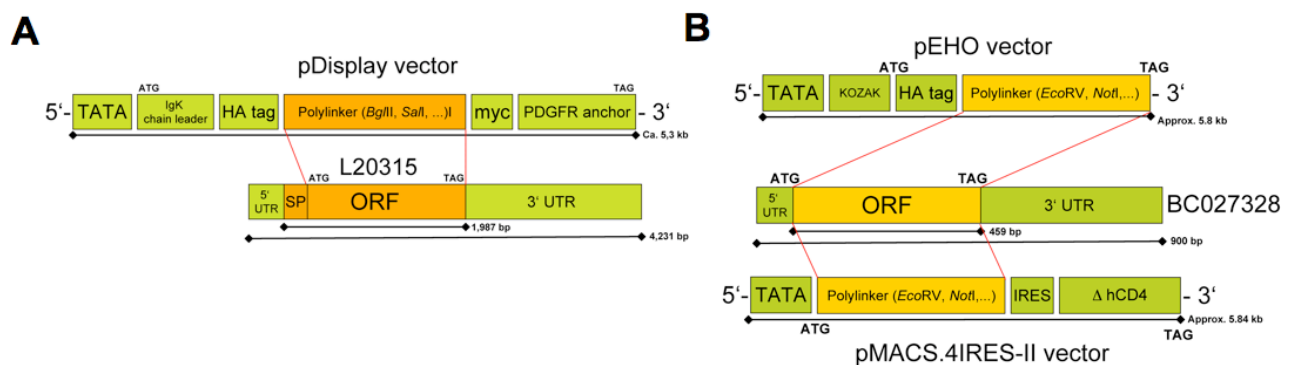


Fig. 3.2 Cloning strategies for L20315 (MPG1) and BST2 (BC027328) as well as generation of a full-length transfectants.

(A) Cloning strategy of L20315 full length ORF without signal peptide into pDisplay vector is demonstrated. Abbreviations are explained in the result text.

(B) Cloning strategy of BC027328 full length ORF into two vectors (pEHO and pMACS.4IRES-II) via EcoRV and NotI is demonstrated.

Briefly, the complete coding sequence of MPG1 was amplified by PCR from genomic murine DNA. Primer pairs used also provided a BglII restriction site (5') as well as a SalI restriction site (3') for the subsequent ligation into the L20315 vector backbone. The coding sequence of BST2 was cloned without the start signal (ATG), which was provided by the pEHO and pMACS.4IRES-II vectors. BST2 was cloned via EcoRV (5') and NotI (3') and primer pairs were equipped with these restriction sites.

3.7.4.2 Transfection of eukaryotic cell lines

Depending on culture conditions, two different transfection protocols (electroporation or lipofection) were performed for suspension or adhesively growing cells. During the exponential proliferation phase suspension cells were harvested and resuspended in fresh medium without FCS. After transfer into a sterile electroporation cuvette (Bio-Rad), $1-5 \times 10^6$ cells were mixed with 10-50 μg pre-diluted DNA and incubated for 15 min. Electroporation was performed using the Bio-Rad Gene Pulser II instrument with the following settings: 210-270 V, 0.975 μF , time constant 15-25 ms. After the pulse, cells were kept for 10 min at 37°C before subsequent culture in standard medium.

Alternatively, adhesive cells were transfected using the FuGENE[®] 6 lipofection reagent (Roche). Standardly, a monolayer of 50-70% confluent cells was transfected with a mixture of DNA and FuGENE at different ratios. Normally, 2 μg DNA plasmid in 100 μl serum-free medium was premixed with 3-6 μl FuGENE, gently mixed and incubated for 30-45 min at room temperature to allow complex generation. Then the mixture was transferred onto the cells, which were cultured in standard (serum-containing) medium. After 12-36 hrs, culture dishes were supplemented with fresh media.

3.7.4.3 Selection and enrichment of transfected cells

MPG1- and BST2-transfected cells were selected via Neomic/Geneticin resistance provided by the vectors pDisplay and pEHO. In addition, the pMACS vector enabled the selection of CD4^+ transfectants using anti-hCD4 mAb-conjugated microbeads to magnetically enrich cells that could be stained positive for CD4 and the wanted antigen. As the HA-tag was expressed intracellularly, it served only as control to confirm the successful cloning. Anti-mPDCA-1-conjugated microbeads (clone JF-3D5) were used for magnetic separation of mPDCA-1⁺ cells.

3.8 Microscopic and histological analyses

3.8.1 Immuno-histochemistry of cryo sections

Isolated and acetone-fixed peripheral lymph nodes were embedded in Tissue-Tec OCT compound (Miles Inc., Elkhart, USA) and stored at -80°C . 5 μm thick sections were placed onto microscope slides and stained in Tris-buffered saline (containing 2% FCS) with different antibodies for 1 h at RT: biotinylated anti-mPDCA-1, FITC-conjugated Ly-6C and APC-conjugated anti-CD11c, followed by secondary incubation with Cy3-conjugated Streptavidin. Stained cryosections were sealed with Vectrashield (Vector, Burlingame, USA).

3.8.2 Confocal laser scanning microscopy (CLSM) of single cell suspensions

Mice received i.p. administration of Alexa488-conjugated anti-mPDCA-1-F(ab')₂ (50 $\mu\text{g}/\text{ml}$). After isolation of spleen PDCs, cells were centrifuged onto coverslips, fixed in PBS containing 3,7% paraformaldehyde for 15 minutes before additional washing. Cells were then incubated for 1 hour with Alexa633-conjugated anti-mPDCA-1 antibody and washed three times with PBS. For microscopic analysis, cells were covered and sealed as described above.

All cells were immediately analyzed by CLSM using the Axioskop 2 plus microscope (Zeiss, Göttingen). The following objectives were utilized: Plan-Neofluar 2,5x/0,075; Ph2 Plan-Neofluar 20x/0,50; Plan-Neofluar 40x/0,75; Plan-Neofluar 63x/1,25 Oil (Zeiss). Filter set 15 (excitation BP546/12, beamsplitter FT 580, emission LP590) was used for fluorescent microscopy (488015-000, Zeiss).

Microscopic pictures (transmitted light bright field) were taken using the digital camera AxioCam HR (Zeiss).

3.9 Cell separation

3.9.1 Principle of Magnetic Cell Separation (MACS)

The MACS[®] technology allows the fast and reliable separation of cells according to specific cell surface markers [Miltenyi S, Cytometry 1990; Radbruch A, Methods Cell Biol. 1994; Abts H, J Immunol Methods. 1989]. In brief, monoclonal antibodies were covalently linked to superparamagnetic microbeads. Next, single cell suspensions were magnetically labeled by incubation with these beads. After extensive washing, cell suspensions were separated on high gradient magnetic columns. Cells labeled with the microbeads were retained on the column whereas unlabeled cells passed through and were collected as the untouched fraction. In general, this technology allows either depletion of unwanted cells and collection of the eluted, unlabeled fraction or direct enrichment of magnetical positive cells. After magnetic separation, purity of isolated cell subsets was analyzed by flow cytometry. Usually, more than 90% purity was obtained.

3.9.2 PDC isolation

PDCs were isolated via two kits:

The “Mouse PDC isolation kit” is based on a depletion of unwanted cells (B cells, T cells, NK cells, myeloid cells, and erythrocytes) followed by an enrichment of B220⁺ cells, thus PDCs.

The “Mouse PDC isolation kit II” enables an “untouched” isolation of PDCs by stringent removal of non-PDCs without the need for further enrichment.

3.9.3 Isolation of T cells

For isolation of splenic T cells in context of the microarray analysis, the “pan T cell isolation Kit, mouse” (Miltenyi) was used.

For the isolation of OVA TCR transgenic T cells, spleen and LNs were collected and pooled. Single cell suspensions were depleted of CD11c⁺ and B220⁺ cells by magnetic sorting. Then either CD4⁺ (DO11.10 and OT-II mice) or CD8 α ⁺ (OT-I mice) cells were enriched with corresponding MicroBeads.

3.9.4 Isolation of other hematopoietic cells

For semi-quantitative analyses of the mRNA expression of different mPDCA-1 candidate genes,

several hematopoietic populations were isolated from spleen:

- B cells via the mouse B Cell Isolation Kit,
- NK cells via the mouse NK Cell Isolation Kit
- Conventional DCs by enrichment via anti-CD11c MicroBeads
- Macrophages (and other cells) was obtained by peritoneal lavage

3.9.5 Principle of Fluorescence-Activated Cell Sorting (FACS)

Flow cytometry is not only an excellent tool for the analysis of cells according to their cell surface properties, but also allows the separation of a heterogeneous mixture of cells [Cantor H, Herzenberg LA, Cell Immunol. 1975]. The so-called Fluorescence-activated cell sorting (FACS) is based on the same flow cytometric principle as mentioned in chapter 3.6. Here, cells become electrically charged after measuring the fluorescence characteristics and are deflected into reaction tubes based upon their charge.

To obtain highly pure PDCs for T cell priming experiments, PDCs were magnetically separated via the Mouse PDC isolation kit II. Then the PDC-enriched fraction was labeled with FITC-conjugated anti-B220 mAb and either PE-conjugated anti-Ly-6C or biotinylated anti-Siglec-H mAbs followed by PE-conjugated anti-Biotin mAb. B220⁺, Siglec-H⁺ or Ly-6C⁺ PDCs were isolated on a FACS Vantage Flow Cytometer Cell Sorter (BD; operated by C. Göttlinger, Institute for Genetics, University of Cologne). Purity of sorted PDCs was again checked by three-color FACS analysis (mPDCA-1, CD11c, and B220 expression), demonstrating an average purity between 97% to more than 99%. The positive fraction of PDCs contained less than 0.5% contaminating CD11c^{high} cDCs or CD11c⁻ B220⁺ B cells.

3.10 Biological assays

3.10.1 Culture and *in vitro* maturation of PDCs

Murine PDCs were isolated as described above and stimulated in the presence of Loxoribine [50 µM] as synthetic TLR7 ligand or the following CpG ODNs (5 µg/ml; Metabion) as synthetic TLR9 ligands. ODN sequences were: ODN-1668 (5'-tccatgacgttctgatgct-3'), ODN-1826 (5'-tccatgacgttctgacgtt-3'), ODN-2006 (5'-tcgtcgttttgtcgttttgtcggtt-3), ODN-2216 (5'-ggGGGACGATCGTCgggggg-3'), and ODN-2395 (5'-tcgtcgttttcggcgcgccg-3'). Capital letters indicate phosphodiester bases, whereas lower case designate phosphorothioate bases, which are nuclease resistant. Functional grade anti-CD40 mAb (clone FGK45.5) was used at a final concentration of 50 µg/ml for *in vitro* activation.

3.10.2 *In vivo* maturation of PDCs

Several TLR agonists were used to activate PDCs *in vivo*. 25 µg Poly-I:C [Bochtler P, JI 2008], 5 µg Loxoribine [Asselin-Paturel C, JEM 2005], or different CpG ODNs (50-100 µg) were administrated i.v. 24 and 48 hrs later, the expression of co-stimulatory molecules (CD40, CD80, and CD86) and other molecules (e.g. MHC-I, -II, CD274 [PD-1L], 4-1BBL [CD137L]) was evaluated on PDCs by flow cytometry.

3.10.3 Analysis of PDC-T cell interactions („priming“)

3.10.3.1 CFSE-labeling

Isolated cells were washed with sterile PBS. 10^7 cells were resuspended in 1ml protein-free PBS and incubated with CFSE for 3 min at a final concentration of 1-5 μ M at room temperature. CFSE loading was stopped by addition of an excess of FCS-supplemented medium. After extensive washing with FCS-containing medium, CFSE-labeling was confirmed by flow cytometric analysis (FL-1 channel).

3.10.3.2 Priming of naïve CD4⁺ and CD8⁺ T cells in vitro

Highly pure PDCs were either isolated from wild type BALB/c or C57BL/6 mice (as described before) depending on background of OVA-TCR^{tg} T cells used. 10^5 PDCs were pre-cultured without antigen or in the presence of different OVA antigens (100 ng/ml SIINFEKL; 5 μ g/ml OVA₃₂₃₋₃₃₉ peptide; OVA-conjugated to anti-mPDCA-1-Fab2, isotype control-Fab2 or soluble OVA in equal concentrations). Where indicated an additional stimulus (5 μ g/ml CpG ODN) was administered.

On the next day PDCs were co-cultured with 2×10^5 CFSE-labeled OVA-specific CD4⁺ or CD8⁺ T cells isolated from DO11.10 or OT-I or OT-II mice for further 72 hrs. Naïve T cells (from pooled LNs and spleen) were thereby depleted for B220⁺ and CD11c⁺ cells (anti-B220 and anti-CD11c Microbeads, Miltenyi Biotec) and subsequently enriched for CD4⁺ or CD8⁺ T cells, respectively (anti-CD4 or anti-CD8a Microbeads, Miltenyi Biotec).

T cell proliferation was measured by loss of CFSE intensity of either gated CD4⁺ KJ-26.1⁺ B220⁻ cells or CD8a⁺ TCR ν β 5.1/2⁺ B220⁻ cells.

To show the specificity of T cell priming by mPDCA-1-OVA targeted and stimulated PDCs, antigen-presenting cells were incubated with unconjugated anti-mPDCA-1 at saturating concentrations before co-culture with both CD4⁺ and CD8⁺ T cells.

3.10.3.3 Analysis of T helper cell polarization

CD4⁺ T cells isolated from DO11.10 mice were primed for three days in co-culture with total splenocytes, purified cDCs or PDCs from Balb/c mice in the absence or presence of a CpG stimulus, as described before. The OVA antigen was either OVA₃₂₃₋₃₃₉ peptide or soluble OVA protein or OVA conjugated to the anti-mPDCA-1 mAb targeting construct and was supplied at the beginning of the culture.

After initial priming, T cells were expanded in the presence of recombinant human IL-2 (R&D Systems, 20 U/ml) for seven days until cytokine was removed. On the next day, CD4⁺ T cells (purity >99%) were restimulated with PMA [20 ng/ml] and Ionomycin [1 μ g/ml] for 6 hours *in vitro* whereas medium was supplemented in the last four hours with 1 μ g/ml Brefeldin A (Calbiochem) to prevent cytokine secretion. Cells were fixed and permeabilized (Inside Stain Kit, Miltenyi Biotec) and intracellularly stained for indicated cytokines (IL-2, IL-4, IL-10, IL-17, IFN γ , and TNF α).

3.10.4 Proliferation assay

To assess the proliferative capacity of different PDC subsets, mice initially received a single dose of BrdU (1 mg i.p. in PBS) to ensure immediate availability of the precursors. In parallel, BrdU was provided continuously in sterile drinking water (0.8 mg/ml), which was changed every second day [O’Keeffe M, JEM 2002; Kamath AT, JI 2000]. Mice were sacrificed at indicated time points (day 0-20) and single cell suspensions of different lymphoid organs were prepared as described above.

For the pulse/chase experiment, mice received BrdU as described above for five days. BrdU was then removed from the drinking water. Mice were sacrificed at indicated time points (day [5+] 0-20) and single cell suspensions were analyzed for BrdU incorporation.

Incorporated BrdU was detected via the APC BrdU Flow Kit (BD Pharmingen). Briefly, cells were stained with FITC-conjugated anti-Sca-1 and PE-conjugated anti-mPDCA-1 mAbs in standard staining buffer. Then cells were fixed and permeabilized, followed by treatment with DNase to expose incorporated BrdU, which was finally detected by an APC-conjugated anti-BrdU mAb.

3.10.5 Endocytosis of DQ-OVA to demonstrate the antigen-uptake capacity

To measure the OVA uptake and processing, mice were immunized with DQ-OVA (Invitrogen) (10 µg s.c. or 50 µg i.v.) and different cell populations were isolated from spleen or draining LNs. After extensive washing, cells were stained with indicated cell surface markers and analyzed by flow cytometry. Amount of OVA internalized and processed by the different DC populations was quantified as the mean fluorescence intensity within the FL1 (FITC) channel.

Alternatively, cells were pulsed with 10 µg/ml DQ-OVA and cultured for 24 hrs before flow cytometric analysis.

3.10.6 *In vivo* PDC depletion using the anti-mPDCA-1 mAb

For specific PDCs depletion mice received a (single) administration of 500 µg anti-mPDCA-1 mAb. Clone JF05-1C2 was used standardly, either i.p., i.v. or s.c. administrated.

3.10.7 Transfer of PDCs and T cells

3.10.7.1 Transfer of PKH67-labeled PDCs

Isolated and sorted Sca-1^{+/-} PDCs were labeled using the PKH67 Green Fluorescent Cell Linker Kit (Sigma). Briefly, PDCs were washed with PBS and $\leq 5 \times 10^6$ were resuspended in diluent buffer. 2 µl PKH67 reagent was prepared in 500 µl diluent buffer, before combining both mixes. After incubation for 3 min, unspecific labeling was blocked with excess of FCS. Cells were extensively washed before i.v. transfer into a syngenic host mouse. 24 hrs after transfer, grafted PDCs, identified by mPDCA-1 expression and PKH67 labeling, were analyzed in different lymphoid organs (spleen and liver) and assessed for their Sca-1 expression.

3.10.7.2 Transfer of CFSE-labeled OVA-transgenic T cells

CFSE-labeling of isolated CD4⁺ or CD8⁺ T cells was performed as described above. About 2x10⁶ labeled T cells were administrated i.v. into a recipient mouse. 15 to 24 hrs later antigen-targeted PDCs were inoculated s.c. or i.v. T cell proliferation was then measured 72 hrs later in draining LNs or spleen.

3.11 Statistical analysis

Statistical analyses were performed using the Prism software (GraphPad Software, San Diego, USA). Standardly mean or median ± SEM was used to analyze the results presented in the result chapter. If indicated the 2-tailed unpaired t test was used. Significance of the results was demonstrated as indicated.

4. RESULTS

Plasmacytoid Dendritic Cells have a key function in the linkage of innate and adaptive immunity, and are involved in a variety of diseases and immunological disorders [Dalod M, JEM 2003; Rönnblom L, Arthritis Res Ther 2003; Nestle FO, JEM 2005]. Therefore their phenotypical and functional characterization is of particular importance. In contrast to their human counterpart, murine PDCs had been only marginally described. The lack of a specific marker further hampered the functional characterization of mouse PDCs and the disclosure of their immunological role.

The first aim of this work was the identification of a novel receptor, which is only expressed on PDCs. Thus, at the beginning a specific mAb against PDCs should be generated, which also could serve as an appropriate tool for further studies of this cell type. Next, the molecular nature and functional characterization of the specific antigen was the main focus of this work as specifically expressed molecules are often connected to a unique function of the cell type. After the identification, further functional characteristics of this molecule were investigated; particularly with regard to the uptake and processing of antigens and the interaction with naïve T cells. Interestingly, by antibody-based characterization of PDCs, a heterogenic phenotype of PDCs was detected, which was further analyzed.

Therefore, four distinct aims were addressed and structured as follows:

- Generation of a mAb against a novel cell surface receptor specifically expressed by mouse PDCs.
- Identification and molecular characterization of the unknown molecule.
- Functional implications of mPDCA-1 as antigen-uptake receptor of murine PDCs for efficient priming of naïve T cells.
- Differential Sca-1 expression defines functional heterogeneity of mouse PDCs.

4.1 Generation of monoclonal antibodies for the detection of PDC-specific cell surface receptors

4.1.1 Contralateral footpad immunization

For all immunization approaches PDCs were isolated from spleen of wild type (wt) BALB/c mice and subcutaneously (s.c.) inoculated into the hind footpad of Lewis or LOU rats. In different immunization attempts, murine Sp2/0 myeloma or freshly isolated murine NK cells were used as decoy and subjected to the corresponding, contralateral footpad as mentioned in Materials & Methods. After several rounds of immunization, cells from the popliteal LNs of the hind footpad that had been injected with PDCs were used for the fusion with a murine myeloma partner (Sp2/0 cells).

To assess the specificity of the generated hybridomas several screening strategies (e.g. using with mouse anti-rat (mar) kappa (κ) mAb coated latex beads) were applied, from which the following strategy is described in detail: (1) Spleen single cell suspensions were incubated with hybridoma supernatant. (2) After washing, bound rat IgG was then detected via R-phycoerythrin (PE)-conjugated mar κ mAb. Lambda light chain positive clones were anticipated only in a minor

percentage rate for murine and rat IgGs and therefore ignored or excluded from this screening system. (3) PDCs were counterstained either with Allophycocyanin (APC)-conjugated hamster anti-mouse CD11c or rat anti-mouse B220 or Gr-1 mAbs. In case rat anti-mouse mAbs were used to identify PDCs, an intermediate blocking step with excess of irrelevant rat IgG mAb was applied to avoid (“block”) any interaction of the mark secondary mAb with B220 and Gr-1 mAbs. The screening strategy to detect PDC-specific/recognizing clones is depicted schematically in Fig 4.1.1. Hereby, the signal derived from the mark staining had to be reviewed in the context of the PDC phenotype, thus on $CD11c^{int}$, $B220^+$ or $Gr-1^+$ cells.



Fig 4.1.1 Screening strategy to detect PDC-specific hybridoma clones.

Balb/c splenocytes were incubated with hybridoma supernatants (1), followed by detection of bound rat Ig with PE-conjugated mouse anti-rat mAb (2). Next, PDCs were counterstained with APC-conjugated hamster anti-mouse CD11c mAb (3), which also detects other dendritic cells, whereas PDCs show only an intermediate expression of this molecule. In the end, hybridoma clones that detect only $CD11c^{int}$ cells were regarded as potential candidates for a PDC-specific antibody.

4.1.2 Antibodies that identify murine PDCs

The majority of the screened clones were not specific for PDCs but recognized epitopes expressed also on other leukocytes. For further characterization of potential PDC-specific hybridoma clones the antibodies were small-scale purified and fluorochrome conjugates were produced. Via these conjugates the staining pattern of each candidate clone on splenic leukocytes was flow cytometrically analyzed. Based on these experiments two different groups of PDC-recognizing clones were charted.

- (1) The first set of clones, although recognizing mouse PDCs, in fact also showed staining of other leukocytes, e.g. B cells and cDCs (Data not shown). Potential candidates were for example the clones 7H9 and 9B8 generated in the second fusion (JF02, Lewis rat). Because the aim of the project was the identification of a molecule specifically expressed on PDCs, both clones were stored but within this work not further characterized. Their potential might be evaluated in further experiments.
- (2) The next cluster of clones was comprised only of PDC-specific antibodies and multi-color FACS revealed that they bind only e.g. $CD11c^{int}$ $B220^+$ cells. An impression of a typical screening result of a negative clone (JF05-1D6; top) and a positive clone (JF05-1C2; bottom) is given in the dotplots shown in Fig. 4.1.2: Whereas with clone 1D6 almost no visible staining on spleen cells was detected, clone 1C2 nicely stained $CD11c^{int}$

B220⁺ cells, thus PDCs. The minor background staining might be FcR-dependent. A FcR β blocking (with anti-CD16/32 mAbs) was not applicable because of the secondary staining system, as the mark mAb would also detect the anti-CD16/32 mAbs. Taken together, this group comprised of four clones with similar staining pattern, originating from different fusions (JF05, Lewis rat; JF07, LOU rat) and recognizing cells with a PDC phenotype: JF05-1C2; JF07-3D5, -7B3, and -12A5.

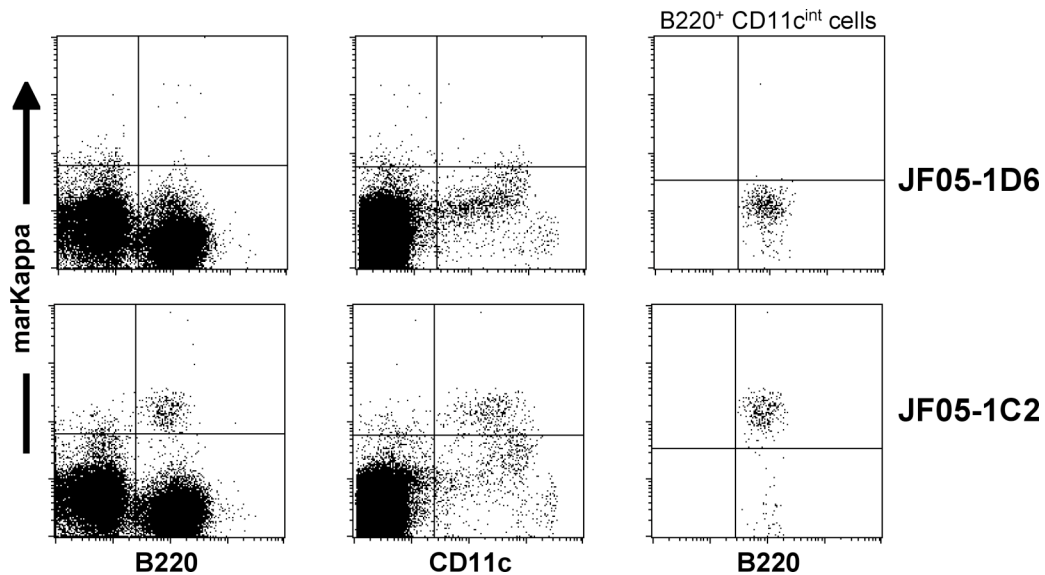


Fig 4.1.2 Staining of spleen cells with the PDC-specific clone JF05-1C2.

Balb/c splenocytes were incubated with supernatant from hybridoma 1D6 (upper lane) or 1C2 (lower lane), followed by detection with PE-conjugated mouse anti-rat κ mAb. PDCs were counterstained with FITC-conjugated B220 (left dotplot) and APC-conjugated hamster anti-mouse CD11c mAb (middle). The right dotplots showed mark staining of gated B220⁺ CD11c^{int} PDCs.

4.1.3 Isotype designation and epitope determination (blocking experiments)

The isotype of the resulting PDC-recognizing hybridoma clones was assessed in two experiments. Hybridoma supernatant or purified mAb was tested either by flow cytometric analysis (intracellular staining with secondary mouse anti-rat Kappa, IgG1, IgG2a, or IgG2b antibodies) or was analyzed with anti-rat IgG/M isotype strips (AbD Serotec, Düsseldorf, Germany), which gave a specific determination of both the light and heavy chain isotype (data not shown).

Next, the epitope recognition of the four PDC-specific mAbs was determined by cross-blocking experiments. All four clones recognized the same antigen, which was termed “mouse Plasmacytoid Dendritic Cell Antigen 1” (mPDCA-1). To evaluate whether two antibodies detect the same epitope, spleen cells were pre-incubated with an excess of the one antibody followed by staining with fluorochrome-conjugated other antibody and vice versa. These blocking experiments demonstrated whether both clones recognized the same epitope (blocking), partial overlapping epitopes (fractional blocking) or different, non-overlapping epitopes (no interference with the staining). The results and the isotype information are shown in Table 4.1.1A+B.

A Table 4.1.1A Overview of the outcome of the cross-blocking experiments

Staining	Blocking (with 100 µg/ml):			
	1C2	3D5	7B3	12A5
1C2	-	+	-	+
3D5	+	-	-*	-
7B3	+	-	-	-
12A5	+	-	-	-

"-": blocking; "+": staining; "-*": partial blocking

B Table 4.1.1B Isotype and recognized epitopes of different anti-mPDCA-1 clones

Antigen	Clone	Epitope	Host	Isotype
mPDCA-1	JF05-1C2	1A	rat (Lewis)	IgG _{2b} , κ
mPDCA-1	JF07-3D5	2A	rat (LOU)	IgG ₁ , κ
mPDCA-1	JF07-7B3	1B	rat (LOU)	IgG ₁ , κ
mPDCA-1	JF07-12A5	2A	rat (LOU)	IgG ₁ , κ

4.1.4 Flow cytometric analysis of mPDCA-1⁺ cells in lymphoid organs

In the past, murine PDCs were characterized by the simultaneous expression of B220, CD11c, and Ly-6C. To confirm the specificity of the four generated mAbs against mouse PDCs, spleen cell suspensions from naïve Balb/c mice were stained with mAbs against mPDCA-1 and other markers and subjected to FACS analysis. Flow cytometric analysis revealed that mPDCA-1 is not expressed on lineage marker positive cells representing T (CD3, TCR α/β), B (CD19), NK (CD49b), or myeloid (CD11b) cells (Figure 4.1.3A). In contrast, mPDCA-1⁺ cells expressed B220⁺, CD11c^{int}, and Ly-6C⁺, which is consistent with the PDC phenotype (Figure 4.1.3B). Furthermore, using four-color-FACS analysis it could be shown, that all B220⁺, CD11c^{int}, and Ly-6C⁺ cells are mPDCA-1⁺ and that there are no further mPDCA-1⁺ cells showing a different phenotype (Figure 4.1.3C). These data clearly showed the PDC-specificity of the anti-mPDCA-1 mAb. Additionally, counterstaining with other markers also showed a staining pattern characteristic for PDCs. mPDCA-1⁺ cells showed no expression of CD40, expressed only low levels of CD8a, CD86, and CD90, but intermediate levels of MHC-II (Fig. 4.1.3D).

Altogether these data demonstrate that the anti-mPDCA-1 mAb is a useful and a specific instrument to investigate PDCs in mice. Furthermore, the identification and molecular characterization of the novel antigen is an important point of this work.

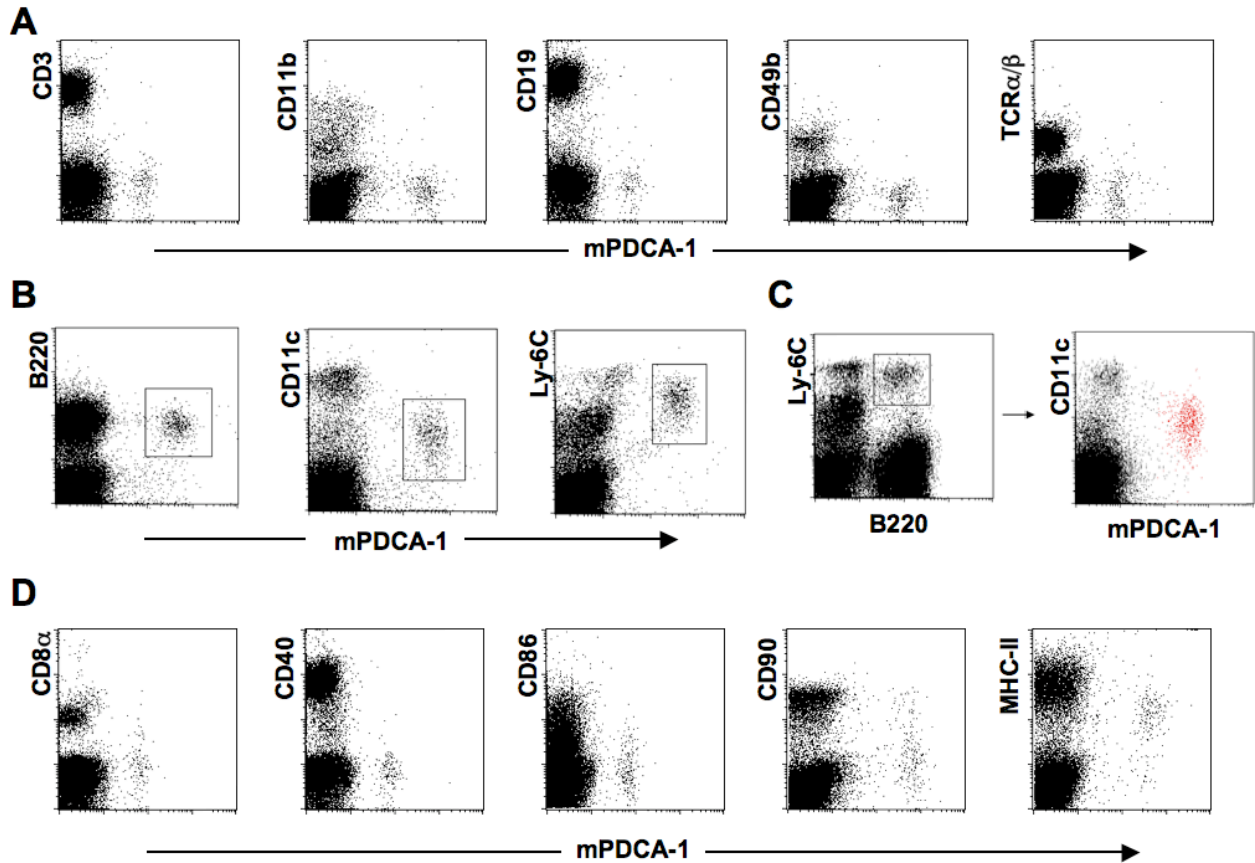


Fig 4.1.3 Determination of the specificity of the generated anti-mPDCA-1 mAbs on Balb/c spleen cells.

(A) FACS analysis of mPDCA-1 expression on spleen cells stained with mAbs against lineage markers representing T cells, myeloid cells, B cells, or NK cells. (B, C) Multicolor analysis of mPDCA-1 expression vs. PDC markers Ly-6C, B220, CD11c. Expression of mPDCA-1 is shown either directly against the indicated markers (B) or on gated B220+ Ly-6C+ cells (C). (D) Further phenotypic characterization of mPDCA-1⁺ cells.

The flow cytometric analysis of splenocytes from naïve Balb/c mice revealed that mPDCA-1 is only expressed on cells that showed the PDC-specific phenotype (B220⁺ CD11c⁺ Ly-6C⁺). However, it has been demonstrated that PDCs from different lymphoid origins vary in their phenotype (expression of maturation markers, adhesion molecules) and also their frequency is different [O’Keeffe M, Blood 2003; Asselin-Paturel C, JI 2003; Kamogawa-Schifter Y, Blood 2005]. Hence, the expression of mPDCA-1 on other lymphoid tissues, such as BM, LNs, lung, liver, thymus, Peyer’s Patches (PP) and others, was investigated. Analog to spleen cells, mPDCA-1 is also only expressed on cells showing PDC-specific phenotype (Fig. 4.1.4). The expression level of mPDCA-1 is comparable in all organs tested except of BM in which mPDCA-1 was expressed at a lower level (data not shown).

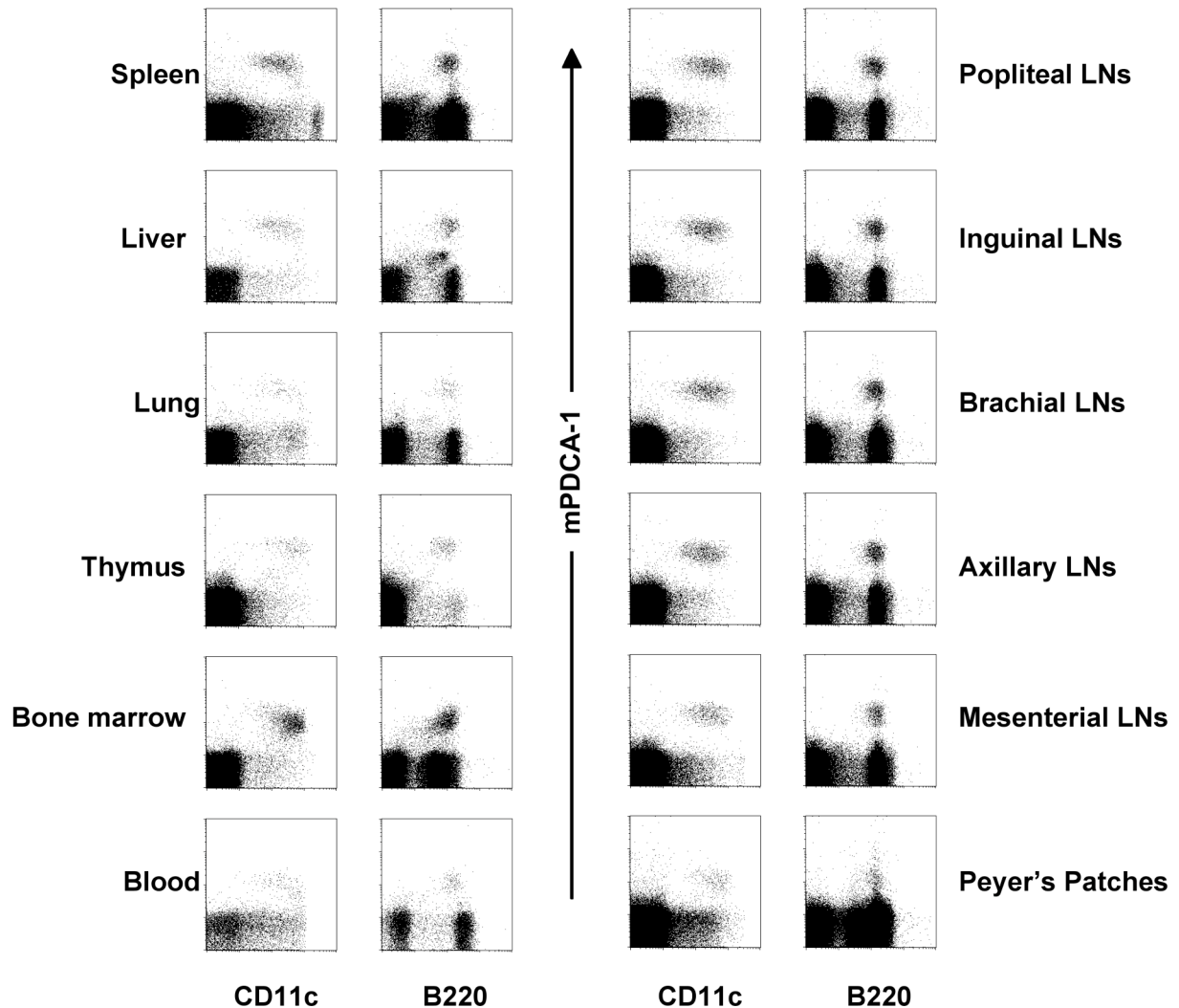


Fig 4.1.4 Expression of mPDCA-1 on PDCs in different lymphoid organs.

Shown is a multi-color flow cytometric analysis of mPDCA-1 expression on PDCs from different lymphoid organs. Single-cell suspensions of different organs were stained with mAbs against B220 and CD11c as well as mPDCA-1.

The investigation of mouse PDCs is often hampered by the low frequency and viability of primary cells. To overcome these limitations PDCs can also be generated *in vitro* from BM precursors by culturing in the presence of FMS-related tyrosine kinase 3 ligand (Flt-3L). Hence, these *in vitro* generated PDCs were termed Flt-3L- or FL-PDCs. As shown in Fig. 4.1.5 mPDCA-1⁺ cells among cultured cells display a typical PDC-phenotype, which is B220⁺ CD11c⁺ Ly-6C⁺. The expression level of mPDCA-1 on *in vitro* generated PDCs is comparable to that of freshly isolated BM-PDCs as demonstrated in Fig. 4.1.4. Thus, among BM cells cultured in the presence of Flt-3L mPDCA-1 shows a PDC-restricted expression pattern.

Previously, the specific expression of mPDCA-1 on PDCs has been shown only for Balb/c mice. In this experiment the expression of mPDCA-1 was evaluated in different mouse strains. Therefore spleen cells were prepared from different mouse strains, and counterstained with mPDCA-1 and B220 for FACS analysis. It could be demonstrated that although PDC frequencies varied between different mouse strains (0.5-2.0%; Fig. 4.1.6A), mPDCA-1 was expressed only on PDCs and there were no significant, strain-specific differences in the expression pattern regarding specificity or expression level (Fig. 4.1.6B). Therefore mPDCA-1

can be considered as selective marker for PDCs, regardless of the mouse strain.

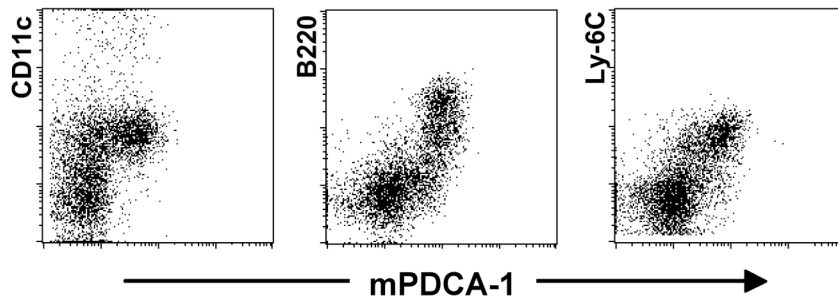


Fig 4.1.5 Expression of mPDCA-1 on *in vitro*-generated PDCs.

The dotplots demonstrate a flow cytometric analysis of Flt-3L treated BM cultures (day 10). Shown is the mPDCA-1 expression on *in vitro* generated PDCs against characteristic PDC markers (CD11c, B220, and Ly-6C).

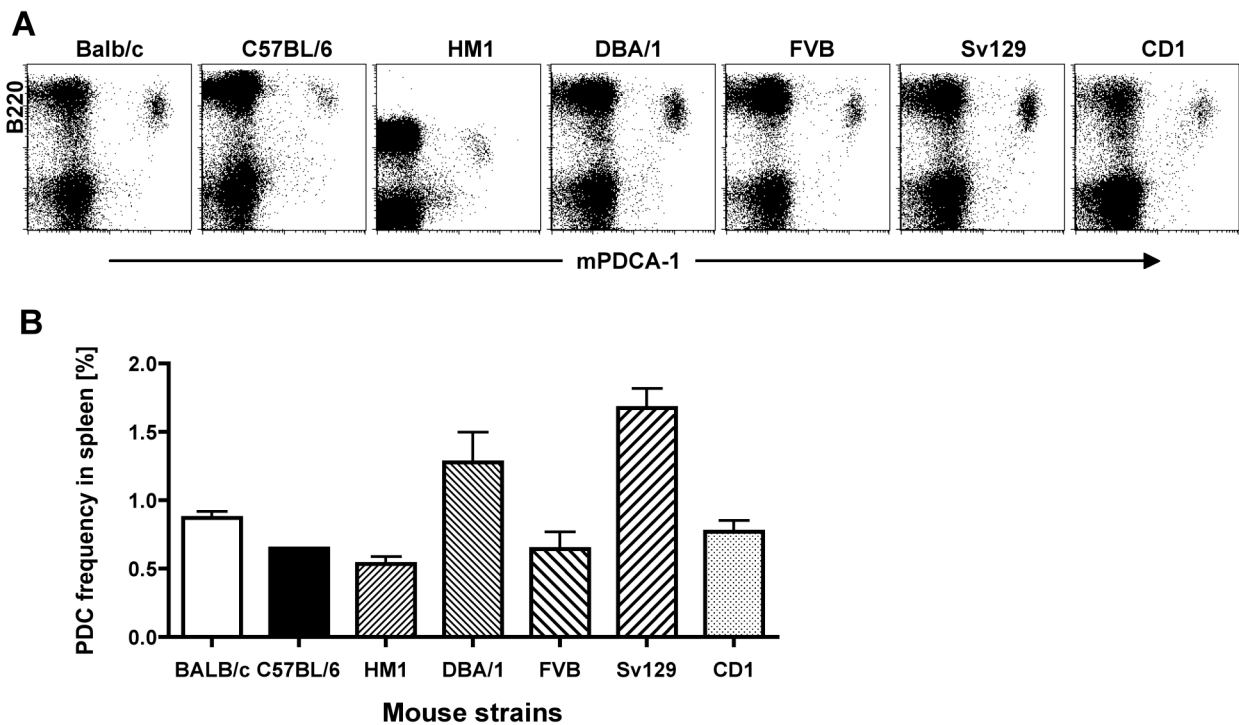


Fig 4.1.6 Expression of mPDCA-1 on PDCs from different mouse strains.

(A) Flow cytometric analysis of spleen single cells suspensions after staining with mAbs against B220 and mPDCA-1. Representative dotplots for each mouse strains are shown. (B) Bar diagram demonstrates the frequency of spleen PDCs of different mouse strains, based on the calculation of B220⁺ mPDCA-1⁺ cells (mean +/- SEM of n=1-3).

4.1.5 Immuno-histochemical staining of mPDCA-1 (performed by Lars Ohl, Hannover Medical School)

Beside flow cytometric application, the generated antibodies were also tested for their immuno-histochemical usage. The anti-mPDCA-1 antibodies seemed to be sensitive to paraffin-embedding as no viable signals were obtained on Paraffin-sections of mouse lymphoid organs (data not shown). In contrast the distribution of PDCs could be analyzed on acetone-fixed cryosections of lymph nodes and spleens (C57BL/6 mice). Fig. 4.1.7 showed the localization of PDCs in peripheral lymph nodes that had been stained with anti-mPDCA-1 (red), Ly-6C (green), and CD11c (blue). In summary the *in situ* distribution of PDCs in LN sections based on the

mPDCA-1 staining demonstrated a similar distribution compared to conventional DCs but not direct co-localization.

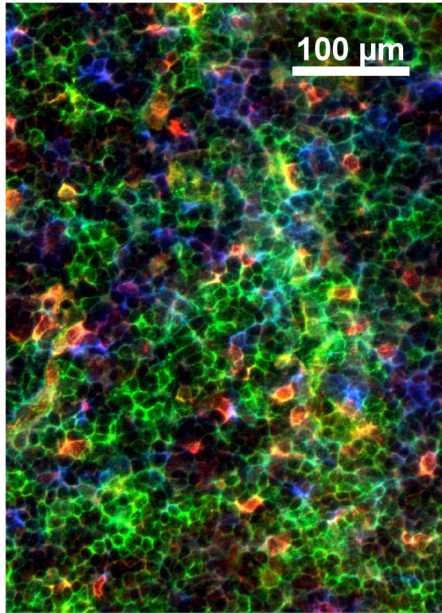


Fig 4.1.7 Immuno-histochemical staining of mPDCA-1 on lymph node cryosections.

Acetone-fixed cryosections of peripheral lymph nodes from C57BL/6 mice were stained with anti mPDCA-1-Biotin, followed by counterstainings with Streptavidin-Cy3 (red), anti Ly-6C-FITC (green), and anti CD11c-APC (blue). Bar represents 100 μ m. Shown is a representative picture from confocal laser scanning analysis.

4.1.6 Effects of mPDCA-1 cross-linking on maturation and IFN α production of PDCs

Next, the effect of mPDCA-1 ligation on the maturation status of PDCs was investigated. Triggering PDCs with anti-mPDCA-1 mAb neither led to an activation (upregulation of co-stimulatory molecules CD40/80/86) of the cells nor had an effect on their viability (data not shown).

As PDCs are regarded as the major type I interferon producing cells, it was essential to show whether triggering with mAbs against mPDCA-1 had an impact on the production of IFN- α . Triggering of mPDCA-1 *in vitro* with different clones led to a significant abrogation of interferon- α secretion by PDCs after stimulation with CpG ODN 2216 (Fig. 4.1.8A). The inhibitory capacity of the four described anti-mPDCA-1 mAb clones was comparable to anti-Siglec-H, another PDC-specific mAb (e.g. clone 551.3D3), which has been previously described to block the IFN α production in PDCs and served as high control in this experiment [Blasius A, Blood 2004].

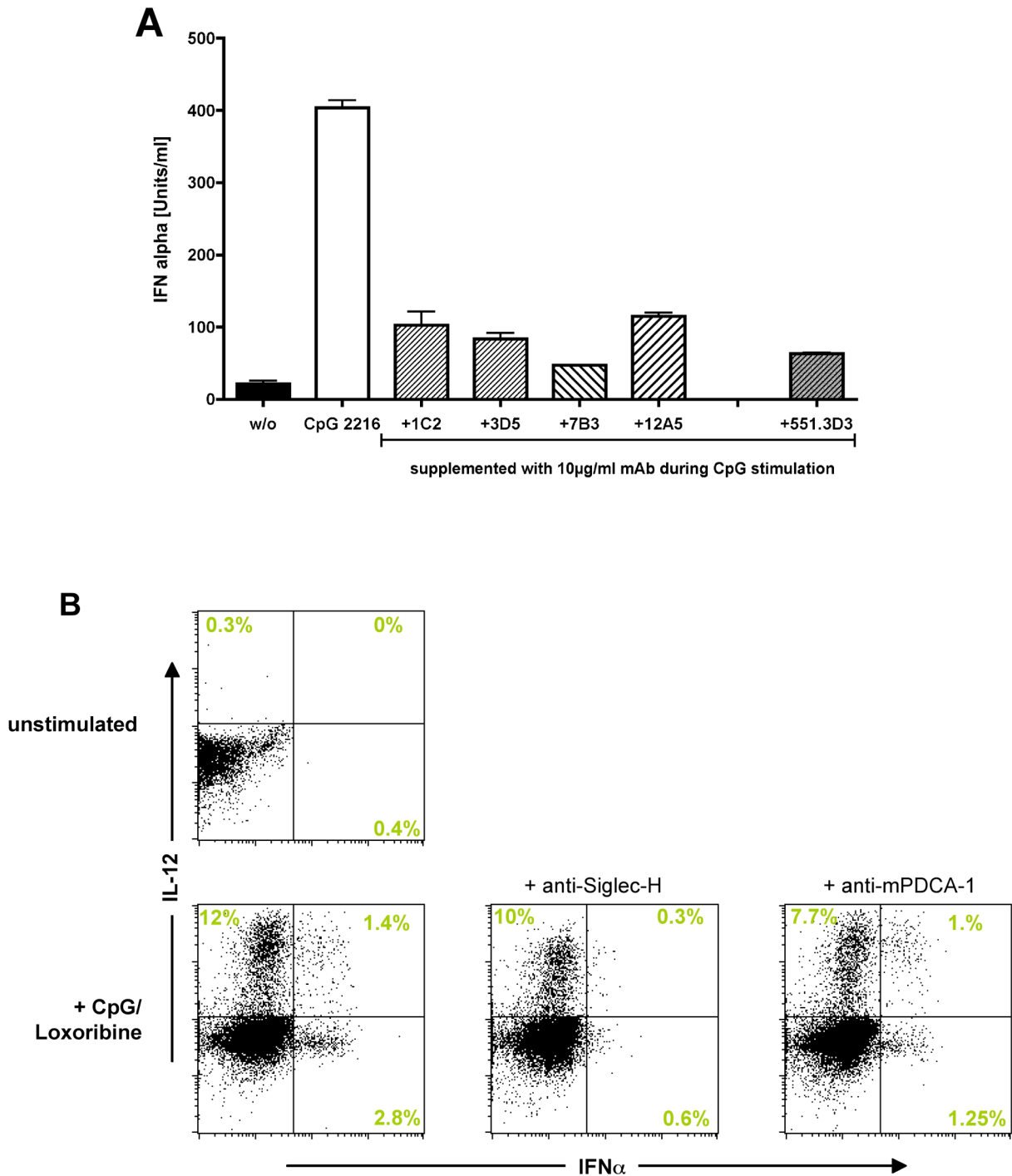


Fig 4.1.8 Effect of mPDCA-1 cross-linking on the *in vitro* cytokine production of PDCs.

(A) Inhibition of the IFN α production in PDCs after mPDCA-1 cross-linking.

Isolated PDCs were cultured in the absence or presence of 5 μ g/ml CpG 2216 for 24hrs. Additionally, 10 μ g/ml of different anti-PDC mAbs was supplemented: anti-mPDCA-1 (clones 1C2, 3D5, 7B3, and 12A5) or anti-Siglec-H mAbs (clone 551.3D3) were used. Interferon alpha secretion was measured in the supernatant via ELISA. The data shown represent the mean \pm SEM of three experiments.

(B) Effect of mPDCA-1 and Siglec-H cross-linking on IFN α and IL-12 production by PDCs.

BM-PDCs were cultured in the absence or presence of TLR7 and 9 agonists (Loxoribine and CpG ODN 2216, respectively) for 6hrs. If indicated, anti-mPDCA-1 clone JF05-1C2 or anti-Siglec-H clone 440c were supplemented. Dotplots show intracellular staining of Interferon alpha and IL-12 production.

Beside IFN α , further pro-inflammatory cytokines like IL-12 and TNF α play a pivotal role in the initiation of immunological responses. Although cDCs were regarded as main IL-12 producers,

also murine, but not human PDCs are able to produce IL-12 upon TLR stimulation [Liu YJ, *Annu Rev Immunol* 2005; Dalod M, *JEM* 2002; Ito T, *Blood* 2006]. Here on the one hand the capacity of PDCs to produce IL-12 but also a possible effect of mPDCA-1 ligation on the cytokine secretion was investigated. As expected, TLR7 and 9 stimulation led to significant IL-12 production by PDCs as demonstrated in intracellular stainings of CpG and Loxoribine-activated cells (Fig. 4.1.8B), whereas unstimulated PDCs produced neither IL-12 nor IFN α . Interestingly, beside single IFN α or IL-12 producers (3-6% IFN α ⁺; 8-12% IL-12⁺ PDCs) also double-producing cells were detected (1.5-2%). Surprisingly, incubation of PDCs with antibodies against mPDCA-1 and Siglec-H *in vitro* resulted in a (50-80%) reduction of IFN α secretion whereas the IL-12 production was less affected.

In summary, mPDCA-1 cross-linkage clearly demonstrated an inhibitory effect on the IFN α production of TLR-stimulated PDCs *in vitro*. Whereas the results obtained by ELISA showed a significant reduction, the intracellular cytokine stainings, which have been performed over a shorter time period (6 hrs vs. 24 hrs), indicated less apparent results.

4.1.7 *In vivo* PDC depletion

4.1.7.1 Depletion of PDCs after anti-mPDCA-1 administration

Previously, the function of PDCs (in particularly during microbial or viral infections) was demonstrated by depleting them by the means of anti-Gr-1 mAb. Due to the promiscuous expression of Ly6G/C not only PDCs were depleted but also neutrophils, macrophages or activated T cells. The application of a PDC-specific mAb to deplete only PDCs might be more suitable for *in vivo* studies of this cell type.

Based on other studies, in a preliminary experiment 500 μ g of purified and unconjugated anti-mPDCA-1 mAb (clone 1C2) was administrated. Interestingly, the majority of PDCs had been depleted 24 hrs later. To exclude the possibility that the disappearance of PDCs was based on a blocking effect of the antigen, the cells were subjected to multicolor FACS analysis by counterstaining with both a non-blocking anti-mPDCA-1 mAb (data not shown) and further PDC markers (B220 and Ly-6C; Fig. 4.1.9). This analysis demonstrated that PDCs were in fact specifically depleted (without affecting other cell populations, like T cells or cDCs; data not shown).

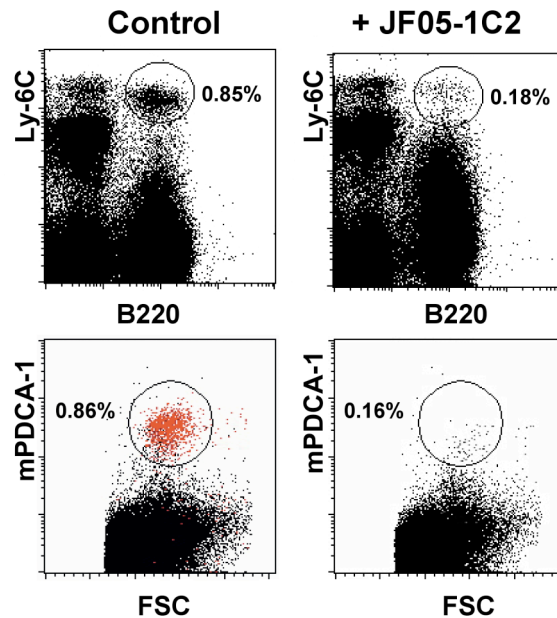


Fig 4.1.9 *In vivo* depletion of PDCs.

BALB/c mice were treated with PBS only or with 500 μ g anti-mPDCA-1 mAb (Clone JF05-1C2; i.p.). 24 hrs later, PDC frequency was assessed in spleen by FACS analysis after staining with PDC-markers B220, Ly-6C, and mPDCA-1. Shown is a representative experiment (n=5).

All tested clones exhibited a significant and comparable PDC depletion capacity (Fig. 4.1.10). The depletion efficiency between the four clones varied in the organs analyzed: in general, clone 1C2 showed the highest depletion in spleen, liver, BM or PPs, and has been used for the depletion of PDCs to assess their role in MCMV infection (Krug A, Immunity 2004). For all following experiments it has been used at a dose of 500 μ g as reported in 4.1.9.

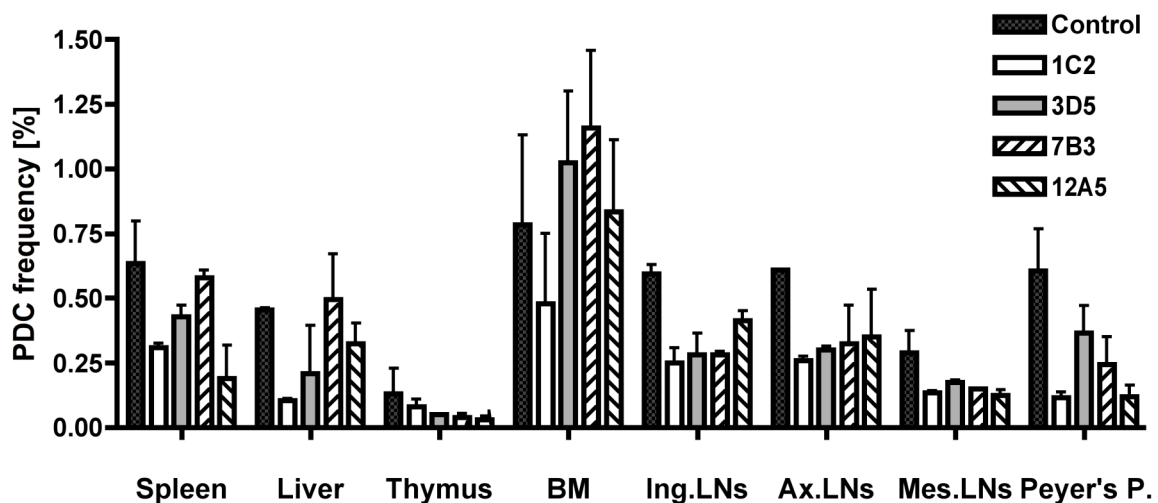


Fig 4.1.10 Comparison of the depletion efficiency of four different anti-mPDCA-1 clones.

Mice were treated with different anti-mPDCA-1 clones: JF05-1C2; JF07-3D5, -7B3, and -12A5 (500 μ g each). 24 hrs after i.p. administration, PDC frequency in spleen was assessed by FACS analysis. The data shown represent the mean \pm SEM of two experiments.

To have a proper information of the quantity of antibody needed for an effective PDC depletion, the amount was titrated: 100, 200, and 500 μ g anti-mPDCA-1 mAb (clone 1C2) was injected and the depletion was assed 24 hrs later. In spleen and liver, more than 75% of PDCs were depleted, whereas only diminishing effects were detected in BM. It was evident that already a low dose (100 μ g) resulted in significant and efficient PDC depletion. However higher dosages of 200 and 500 μ g led to higher depletion of the cells in BM or PPs and LNs (Fig. 4.1.11).

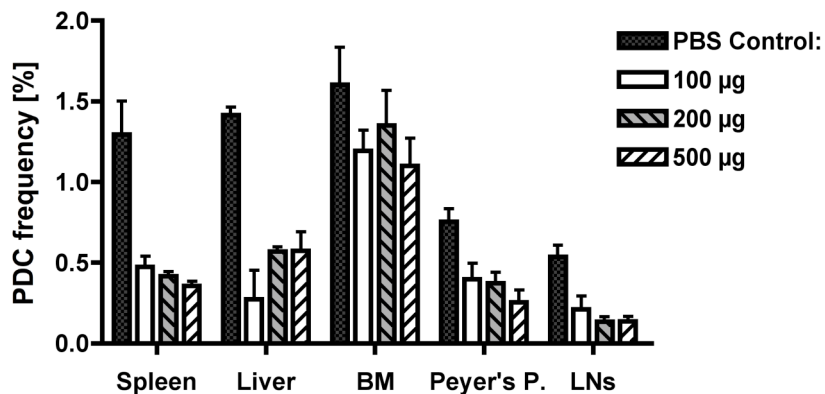


Fig 4.1.11 Titration of the anti-mPDCA-1 mAb effector dose for *in vivo* PDC depletion.

Mice were treated with different doses of anti-mPDCA-1 mAb. 24hrs after i.p. administration, PDC frequency was assessed by FACS analysis (B220⁺ Ly-6C⁺ mPDCA-1⁺ cells) in different lymphoid organs. The data shown represent the mean \pm SEM of three experiments.

To further test the impact of PDC depletion in different organs, several lymphoid tissues were investigated for PDC frequencies after intraperitoneal anti-mPDCA-1 administration. The results demonstrated that in spleen up to 80% of PDCs were specifically depleted, whereas in BM a reduction of maximally 50% could be detected. LNs displayed a heterogeneous effect: In some LNs (cervical + mesenteric LNs) an efficient depletion was observed, however other (peripheral) LNs demonstrated no depletion as Figs. 4.1.10-12 revealed. To improve the effect of the PDC depletion especially for *in vivo* studies a special protocol was developed (see Krug A, Immunity 2004; Barchet W, EJI 2005): repeated antibody application at different time points led to significant and efficient (approx. 90%) PDC reduction in tested lymphoid organs, in particular in LNs (data not shown).

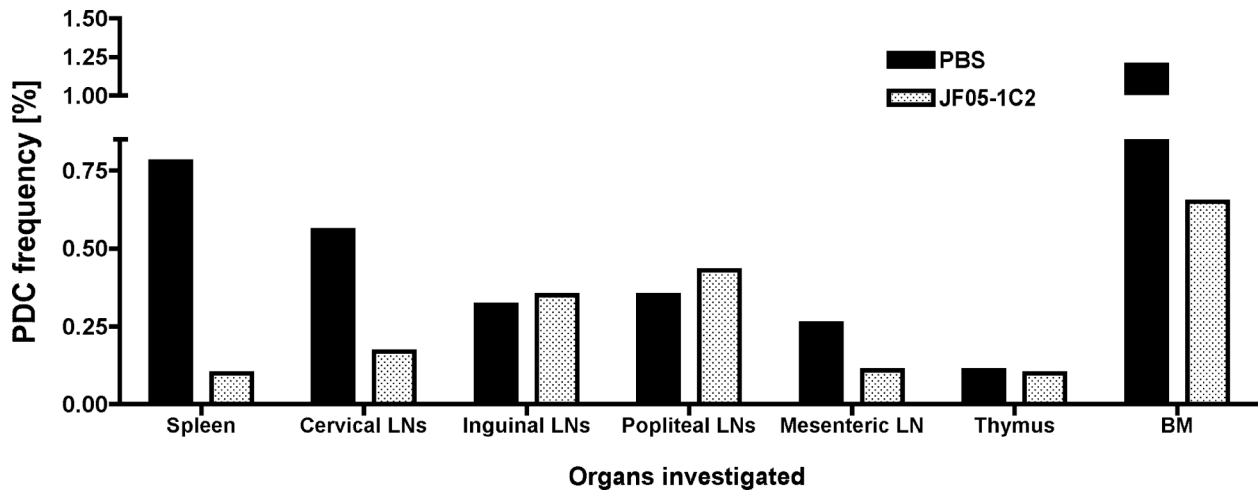


Fig 4.1.12 Depletion efficiency in different lymphoid organs after anti-mPDCA-1 mAb administration.

As described above mice were treated with 500 μ g anti-mPDCA-1 clone JF05-1C2, (i.p.) and PDC frequency was assed 24hrs later in different lymphoid organs by FACS analysis. Bar diagram shows PDC frequencies of control mice (black) or anti-mPDAC-1 treated mice (dotted bars). Shown is one representative experiment out of 5.

In the previously described experiments PDC depletion was achieved by intraperitoneal administration of anti-mPDCA-1 mAb. However, to evaluate the role of PDCs in inflamed skin e.g. in a psoriasis model (collaboration with A. Stratis, University of Cologne) a different application route should be more reasonable and was tested in this experiment. Mice received same amount of anti-mPDCA-1 mAb via i.p., i.v., and s.c. administration and PDC depletion was assessed 24 hrs later. The results suggested that in all cases PDCs were depleted significantly and to a comparable level as demonstrated previously only for i.p. administration (Fig. 4.1.13). In summary, PDC depletion reached 85-90% and could be achieved independently of the route of administration.

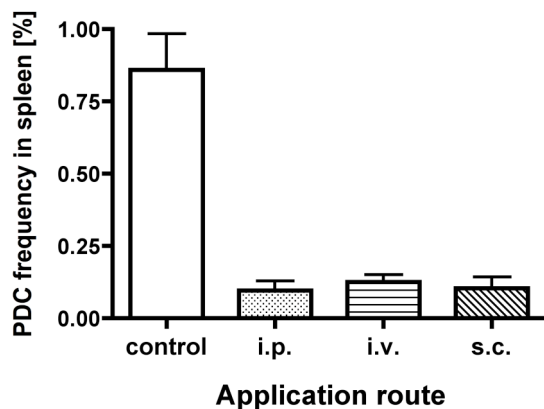


Fig 4.1.13 Impact of the application route on PDC depletion efficiency.

Mice were treated with 500 μ g anti-mPDCA-1 clone JF05-1C2, and PDC frequency in spleen was assessed after 24 hrs. Control represents untreated animals. The administration was performed either i.p., i.v. or s.c. The data shown represent the mean \pm SEM of 2 (i.v.) - 3 experiments.

Next the mPDCA-1-mediated *in vivo* depletion kinetic was analyzed, as there were no reports about the duration of this effect. After a single anti-mPDCA-1 administration PDC frequency (or repopulation) was assessed. A significant effect could be observed within the first day (up to 70% reduction), whereas the maximum depletion was detected on day two, lasting until day four as illustrated in Fig. 4.1.14 (>90% depletion, depending on the lymphoid organ). Between days four and seven PDC frequencies increased again and reached base level after two to three

weeks later. In principle this effect was valid for all organs tested, except of minor differences, e.g. in BM. In this organ the depletion was not that effective (see Figs. 4.1.10-12) and PDCs repopulated earlier.

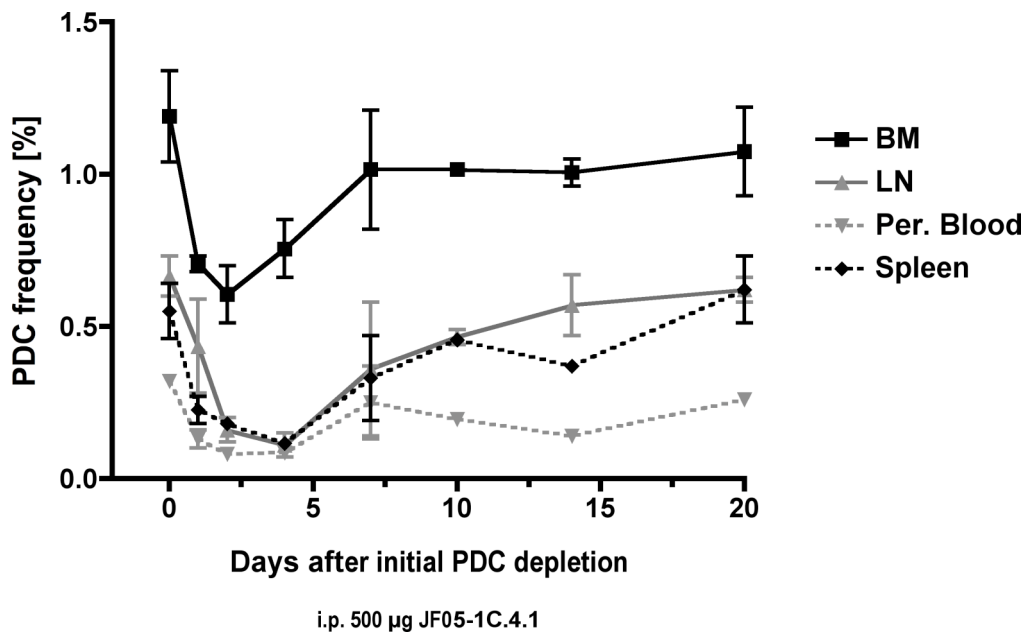


Fig 4.1.14 PDC depletion and repopulation kinetics.

After administration of 500 µg anti-mPDCA-1 mAb (i.p.), PDC frequency was monitored 1-20 days later in different lymphoid organs by FACS analysis. Graph represents mean \pm SEM of two mice per time point.

4.1.7.2 PDC depletion capacity of complete or F(ab')₂ anti-mPDCA-1 antibodies

The anti-mPDCA-1 mAb was shown to be an effective tool for *in vivo* PDC depletion to investigate their function but the precise mechanism of this depletion remained unclear. It had been hypothesized that the PDC ablation could be induced by an intrinsic effect of the mPDCA-1 molecule, although triggering with the mAb did not influence their viability *in vitro* (data not shown). Another mechanism might be due to complement-dependent lysis. Therefore a Fc-part lacking F(ab')₂ fragment of the antibody was generated by Pepsin A digestion. Resulting F(ab')₂ fragments were purified by size-fractionation to remove the degraded Fc part or remaining complete mAb and Fab fragments, which were generated as side products. A typical impression of the size-fractionation and the subsequent SDS-PAGE is shown in the appendix (see Fig.7.1A+B+C).

As expected, administration of complete anti-mPDCA-1- mAb resulted in efficient PDC depletion (approx. 75%) compared to PBS-treated mice. In contrast, the administration of 500 µg anti-mPDCA-1 F(ab')₂ did not lead to a PDC-specific depletion *in vivo* as B220⁺ CD11c^{int} mPDCA-1⁺ cells were still present (Fig. 4.1.15). Thus the mPDCA-1 F(ab')₂ fragment provided an eminent tool to investigate the function of the mPDCA-1 molecule *in vivo*.

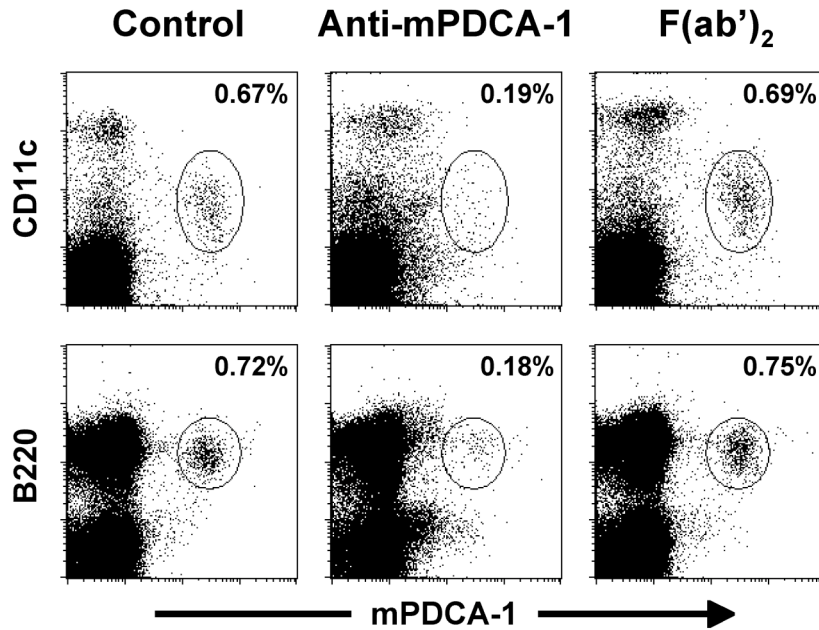


Fig 4.1.15 PDC depletion capacity of complete or F(ab')₂ anti-mPDCA-1 mAb.

24 hrs after i.p. administration of 500µg either complete anti-mPDCA-1 mAb (middle) or its Fab2 fragment (right dotplots), PDC frequency was assessed in spleen by FACS analysis of B220⁺ CD11c⁺ mPDCA-1⁺ cells. In the left dotplots, mice received only PBS diluent. One representative experiment of two is shown.

4.1.7.3 Effect of PDC depletion on *in vivo* cytokine production after viral challenge or CpG stimulation (viral infection experiments conducted by Anne Krug, St. Louis, USA)

To assess the effect of PDC depletion on the cytokine production *in vivo*, C57BL/6 mice were infected with murine cytomegalovirus (MCMV). Mice previously treated with anti-mPDCA-1 mAb showed a markedly impaired IFN-α response in blood serum 36 hrs after MCMV infection compared to the control group as demonstrated in Fig. 4.1.16A. In contrast, serum levels of IL-12p70 and IFNγ were significantly higher in PDC-depleted than in isotype control mAb-treated mice [Krug A, Immunity 2004, and data not shown].

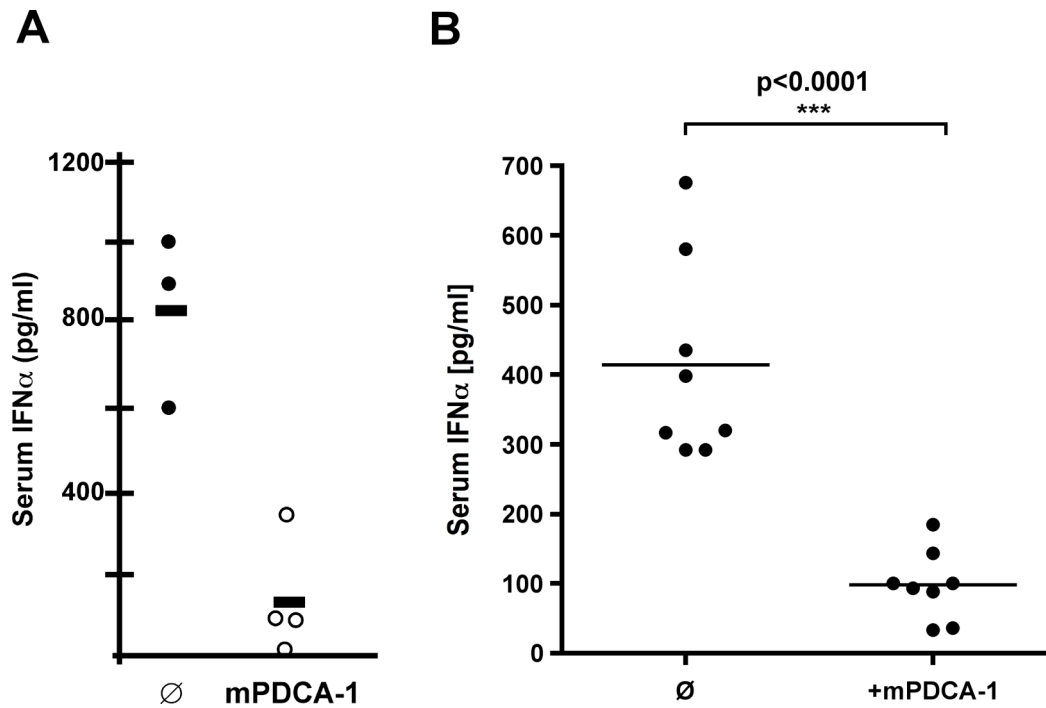


Fig 4.1.16 Abrogation of IFN α production after *in vivo* PDC depletion.

(A) **MCMV infection following the depletion of PDCs *in vivo* shows an impaired IFN α response.** C57BL/6 mice were either injected three times i.v. with 500 μ g anti-mPDCA-1 mAb at time points 24 hr, 4 hr before, and 20 hr after infection (white circles, n = 4) or were left untreated (filled circles, n = 3). Blood sera were collected 36 hr after the i.p. infection with 5×10^4 PFU and serum IFN- α ELISA was determined by ELISA. (see Krug et al., Immunity 2004).

(B) **Inhibition of CpG-induced IFN α production after mPDCA-1-mediated *in vivo* PDC depletion.** Mice were depleted of PDCs via i.p. administration of 500 μ g anti-mPDCA-1 mAb. On the next day mice received i.v. 5 μ g CpG ODN 2216 complexed with 30 μ l of a cationic liposome preparation (DOTAP; Boehringer Mannheim). 6 hrs later, serum was collected and analyzed by IFN α -specific ELISA (PBL). Shown is the serum IFN α level of CpG-activated and additionally PDC-depleted mice (n=4 per group, samples were analyzed in duplicates). Mean \pm SEM were 413.7 \pm 50.83 (\emptyset) vs. 97.55 \pm 17.77 (+mPDCA-1) as assessed by unpaired t test. Experiment was performed in collaboration with Stefanie Kurig (Miltényi).

In a different experiment the *in vivo* IFN α production after CpG activation was assessed. Mice received an administration of anti-mPDCA-1 mAb (i.p.; d-1) before challenge with CpG ODN 2216. The scatter diagram demonstrated strong IFN α levels in the serum in contrast to significantly reduced IFN α amounts in PDC-depleted mice (mean reduction of approx. 75%; Fig. 4.1.16B). Compared to viral challenge, CpG stimulation resulted in strong but less intensive IFN α production *in vivo*.

These data clearly demonstrated the PDC-dependent IFN α secretion upon viral or microbial challenge *in vivo*.

4.1.8 Signal transduction via mPDCA-1

Since mPDCA-1 triggering abrogated the IFN α production in stimulated PDCs, the possibility of mPDCA-1 signaling was next investigated. In two experiments potential signal transduction cascades initiated by cross-linking of this receptor was analyzed as it was already shown for other human PDC antigens ILT-7 and BDCA-2 [Cao W, JEM 2006, Röck J, EJI 2007; Dzionek A, JEM 2001].

Cytosolic calcium concentrations ($[Ca^{2+}]_i$) in PDCs were measured before and after anti-mPDCA-1 mAb cross-linking to address whether mPDCA-1 mAb triggering leads to signal transduction. As shown in Fig. 4.1.17A, ligation of surface mPDCA-1 with a specific mAb elicited a rapid and transient rise in $[Ca^{2+}]_i$ in PDCs (red arrows), irrespective if isolated PDCs or spleen cells were used. Treatment with Ionomycin, a calcium ionophore that facilitated the sustained entry of extracellular calcium, induced the maximal effect of a global increase in $[Ca^{2+}]_i$, as indicated by arrow heads.

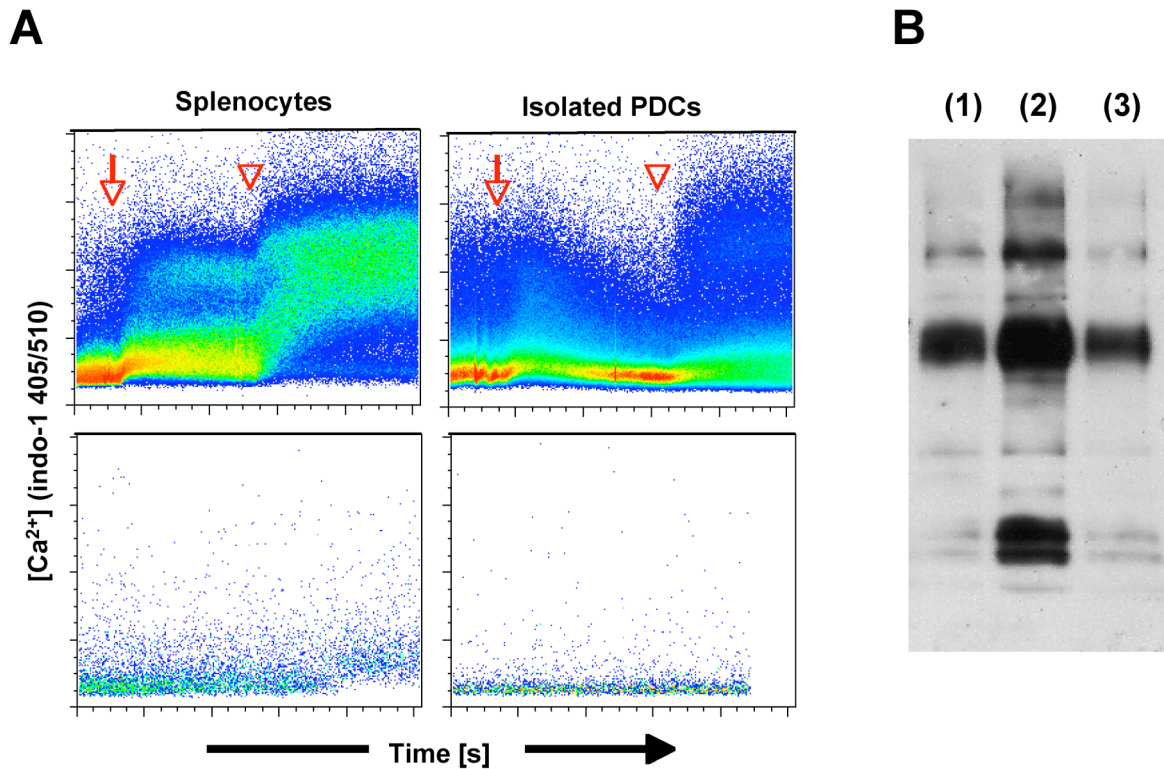


Fig 4.1.17 Cross-linking of mPDCA-1 on PDCs results in calcium flux and overall protein-tyrosine phosphorylation *in vitro*.

(A) PDCs, either within splenocytes suspension (left) or isolated (right) were loaded with Indo-1. In the pseudo-color density plots (FlowJo) is shown the increase of intracellular calcium (as demonstrated by alteration of the indo-1 405/510 ratio after triggering with anti-mPDCA-1 mAb (Clone JF05-1C2) (arrow; upper lane)). Arrowheads indicate application of Ionomycin as high control. In the lower lane unstimulated spleen cells and PDCs, respectively, are plotted.

(B) Triggering of mPDCA-1 induces protein tyrosine phosphorylation in isolated PDCs (90-96% purity). Cells were incubated with medium alone (1), with anti-mPDCA-1 mAb (JF5-1C2, IgG_{2b}) (2), or with isotype antibody (3) for 5 min at 37°C. After washing, cells were resuspended in Laemmli buffer, sonicated, boiled, size-fractionated by SDS-PAGE, transferred to PVDF membranes, and probed with horseradish peroxidase-coupled anti-phosphotyrosine mAb PY20. One representative experiment of three is shown.

Next it was tested whether intracellular calcium mobilization was correlated with protein-tyrosine phosphorylation. Therefore an anti-phosphotyrosine immunoblotting on whole cell lysates of isolated PDCs was performed before and after incubation with anti-mPDCA-1 mAb. As shown in Fig. 4.1.17B, PDCs triggered via mPDCA-1 exhibited a significant increase in overall protein-tyrosine phosphorylation, as compared with unstimulated or isotype control-treated PDCs.

The results of these two experiments suggested a principle involvement of mPDCA-1 in signal

transduction. Further signaling and the disclosure of involved downstream pathways in PDCs should be analyzed in other experimental settings after disclosure of the molecular nature of mPDAC-1, e.g. by means of mPDCA-1 transfectants.

4.1.9 *In vitro* and *in vivo* internalization of mPDCA-1 receptor-antibody complex

It has been shown that mPDCA-1 triggering influenced the IFN-I production and was further involved in signal transduction. These characteristics were also reported for other PDC-specific antigens, such as BDCA-2, ILT7 or Siglec-H [Blasius A, Blood 2006; Cao W, JEM 2006, Röck J, EJI 2007; Dzionek A, JEM 2001]. At least BDCA-2 and Siglec-H were further shown to internalize upon antibody ligation. To test whether mPDCA-1 is also an endocytic receptor specifically expressed on mouse PDCs, the ability of mPDCA-1 to be internalized from the cell surface was analyzed.

Therefore PDCs were isolated either from Flt-3L-treated BM-cultures or *ex vivo* from spleen. Cells were labeled with FITC-conjugated anti-mPDCA-1 mAb and cultured at 37°C for different lengths of time ranging from 5 min to 2 hrs. For detection of surface-bound antibody, a secondary staining was performed consisting of biotinylated anti-FITC mAb, followed by counterstaining with PE-conjugated anti-Biotin mAb. The constant FITC intensity in Fig. 4.1.18A demonstrated that the mPDCA-1 mAb was not sheared but was still present on the cell surface or intracellularly. In contrast, the secondary signal for surface-bound antibody rapidly decreased (up to 40% within the first 5 min and up to 80% after 30 min). This demonstrated that mPDCA-1 is internalized *in vitro* upon mPDCA-1 mAb labeling through receptor-mediated endocytosis.

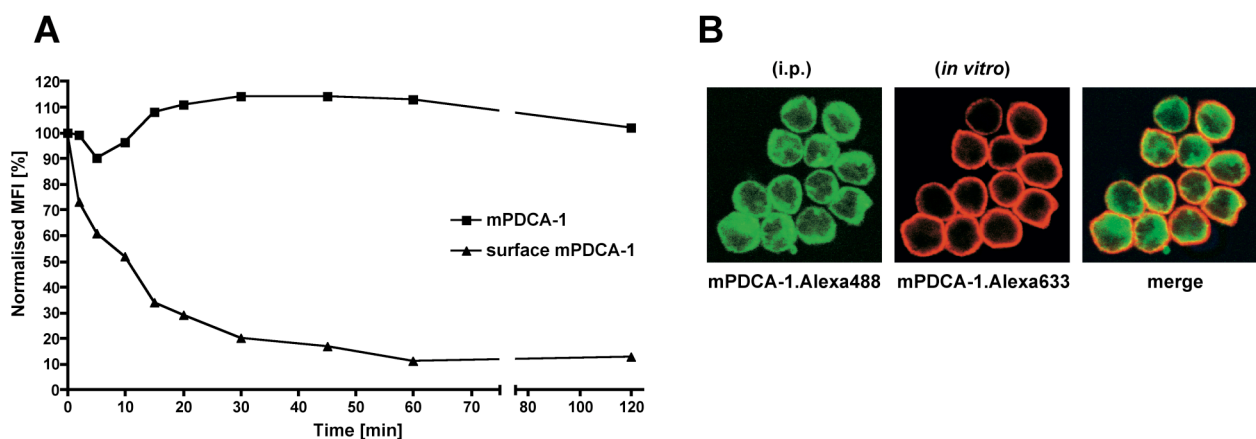


Fig 4.1.18 Internalization of the mPDCA-1 mAb:receptor complex *in vitro* and *in vivo*.

(A) Flt-3L-generated (FL) bone marrow (BM) PDCs were isolated and stained with FITC-conjugated anti-mPDCA-1 mAb on ice. Cells were then incubated at 37 °C for the indicated time, followed by counterstaining with anti-FITC secondary system to detect cell surface-bound antibody (consisting of biotinylated anti-FITC and PE-conjugated anti-Biotin mAbs).

(B) Alexa488-conjugated anti-mPDCA-1-F(ab')₂ was administrated intraperitoneally. 15 hrs later spleen PDCs were isolated, fixed with formaldehyde, and additionally stained for surface mPDCA-1 with anti-mPDCA-1-Biotin and Alexa633-conjugated anti-biotin mAb (red). Alexa488-conjugated anti-mPDCA-1 (green), was internalized as shown by merged confocal scan laser microscopy pictures.

In addition, *in vivo* internalization of mPDCA-1 was assessed after i.p. administration of anti-mPDCA-1-F(ab')₂ antibody conjugated to Alexa488 fluorochrome. After 15 hrs, spleen PDCs

were isolated, fixed and stained with PE-conjugated anti-mPDCA-1 mAb at the cell surface. Confocal analyses of isolated PDCs revealed the presence of administrated Alexa488-conjugated mPDCA-1 (green signal) in intracellular compartments (Fig. 4.1.18B). The internalized mPDCA-1 mAb clearly contrasted to *in vitro* counterstained mPDCA-1 (red) that was only observed at the cell surface. These internalization results suggested that mPDCA-1 could mediate delivery of bound mAb to endocytic pathways both *in vitro* and *in vivo* implying a function in antigen-uptake.

Taken together, by contra-lateral immunization a panel of mAbs was generated, each specifically detecting mouse PDCs in all lymphoid organs tested. All mAbs recognized the same, presumably novel antigen, which has been termed mouse PDC antigen-1 (mPDCA-1). These PDC-specific mAbs provided the opportunity for exact identification and isolation of this DC subpopulation (e.g. via anti-mPDCA-1 fluorochrome conjugates or Microbeads; data not shown).

Interestingly, mPDCA-1 cross-linking resulted in signal transduction as was evident by an increase in overall protein-tyrosine phosphorylation and calcium release. Preliminary data also demonstrated that binding the receptor induced an inhibition of IFN α production in activated PDCs. The shown results further indicated that triggering the mPDCA-1 via the mAbs resulted in rapid and efficient internalization of the receptor:antibody complex, both *in vitro* and *in vivo*, further underlining a potential role of this receptor in antigen uptake.

A very promising feature of the anti-mPDCA-1 mAb was the opportunity to deplete PDCs specifically *in vivo*. Therefore the anti-mPDCA-1 mAbs were not only useful for single-color identification of PDCs by flow cytometry, but also of great value for advanced studies to disclose the function and biological role of PDCs both *in vitro* and *in vivo*.

4.2 Identification and molecular characterization of mPDCA-1

4.2.1 Biochemical approaches to identify the mPDCA-1 antigen

Peptide Mass Fingerprint (PMF) analysis after immuno-precipitation or immuno-blotting is a standard method for the identification of unknown antigens. Therefore anti-mPDCA-1 immuno-blotting was performed on whole cell lysates of isolated PDCs. Unfortunately, no PDC-specific bands could be detected compared to cell lysates of others cells (data not shown). This might be due to the disintegration of the recognized mPDCA-1 epitope. For example a linear epitope recognized by the anti-mPDCA-1 mAb might be denaturalized in the conditions of this experiment, and precluded the detection via the antibody.

In another approach the unknown antigen should be identified by immuno-precipitation, but no reliable results were obtained by precipitating the mPDCA-1 molecule out of whole PDC lysates or prepared membrane fractions. In analogy to the above description, the parameters were modified regarding cell source and preparation method and further protocols were applied. For example, immuno-precipitation was performed after biotinylation of the cell surface of PDCs, thereby labeling the unknown antigen before immuno-precipitation via anti-mPDCA-1 mAb and

providing subsequent detection via the Biotin signal. Also for these experiments no molecule resembling mPDCA-1 could be demonstrated.

It could be demonstrated that the expression of mPDCA-1 was inducible on certain cell lines after IFN α treatment (*see below, chapter 4.2.2*). Therefore metabolic labeling and immunoprecipitation from ^{35}S -cultured cells were performed after induction of the mPDCA-1 expression. Methionine and Cysteine-free medium was supplemented with radiolabeled, sulfur-containing amino acids at the beginning of the experiments to enable the incorporation of ^{35}S -methionine or -cysteine during the *de novo* protein synthesis. 18 hrs after IFN α treatment, cell lysates were prepared and subjected to immunoprecipitation using the anti-mPDCA-1 mAb. As for the above-described methods, no PDC-specific molecule was obtained by this procedure.

4.2.2 Induction of mPDCA-1 expression *in vivo* and *in vitro*

The above described biochemical methods did not lead to reliable results for the identification of the novel antigen, but in the meantime a promising observation has been made. It has been demonstrated that mPDCA-1 was expressed specifically on PDCs from naïve mice, but infected or otherwise stimulated animals often showed an increased “background staining” for mPDCA-1. This observation was consistent with data for another recently described PDC-specific antigen [Asselin-Paturel C, JI 2003]. Thus, it was investigated, whether the antigen could be detected also on other cells upon activation with CpG and further stimuli. Injection of viral or microbial compounds (e.g. Influenza virus and CpG ODNs) or recombinant IFN α resulted in a significant upregulation of mPDCA-1 on cells different to PDCs. In contrast to naïve mice, upon poly-I:C (Fig. 4.2.1A, B) or CpG treatment (Fig. 4.2.1C) this molecule was upregulated on e.g. B cells, NK cells or T cells, and other cDCs *in vivo*. Interestingly, among cDCs the highest upregulation was found within the CD8 α^+ compartment. This effect could be also shown *in vitro* in activated spleen cell cultures (data not shown).

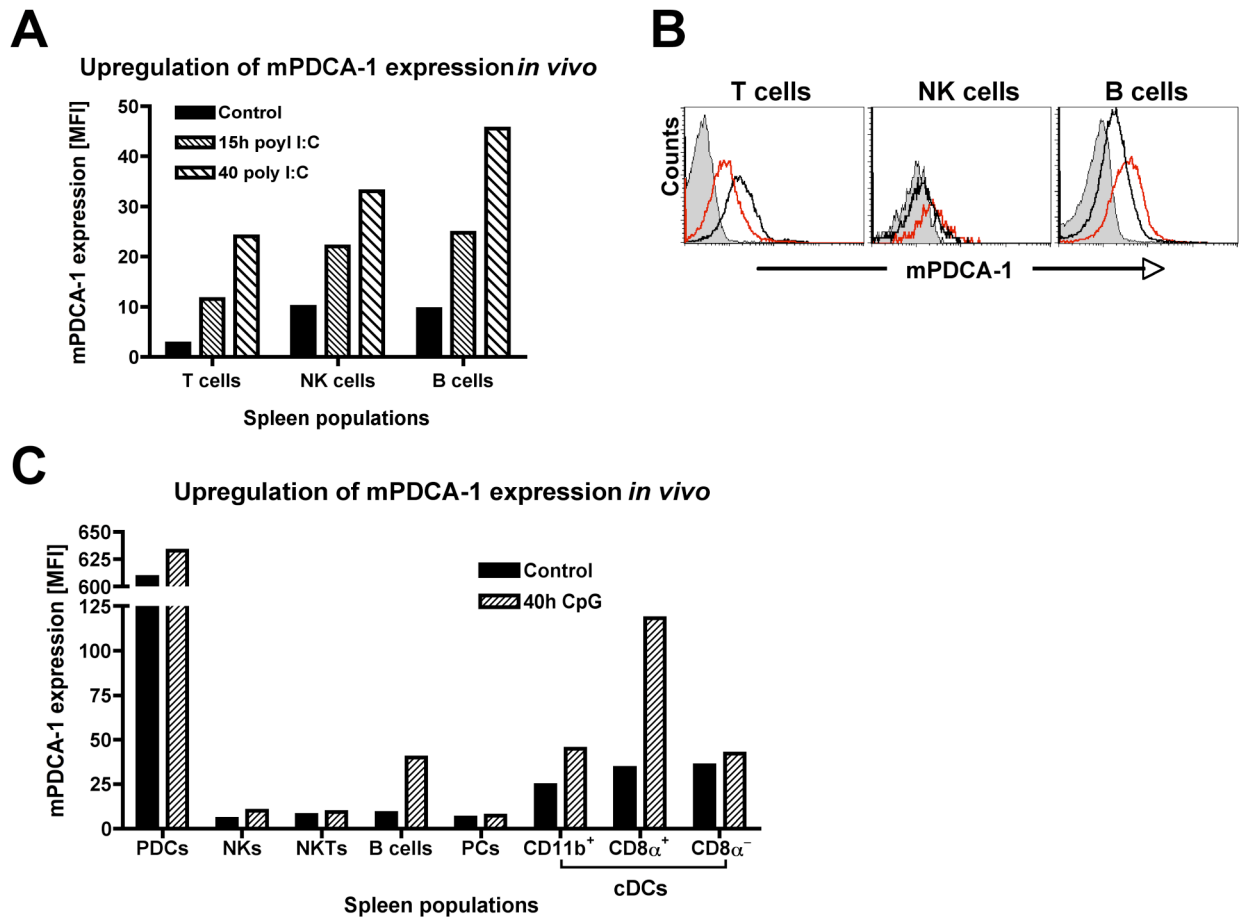


Fig 4.2.1 Upregulation of mPDCA-1 expression *in vivo*.

Balb/c mice were either left untreated (control) or activated with 25 μ g poly I:C (A; B) or 50 μ g CpG ODN 2216 (C). 15 and 40 hrs later, spleen single cell suspension were prepared and mPDCA-1 expression on different cell populations was examined by flow cytometric analysis. Distinct cells were defined as follows: B cells (CD19⁺), NK cells (CD49b⁺ CD3⁻), NKT cells (CD49b⁺ CD3⁺), T cells (CD3⁺ TCR α/β ⁺), PDCs (mPDCA-1^{high} Siglec-H⁺), and Plasma cells (PC; CD19⁺ CD138⁺). cDCs were additionally divided into “myeloid” CD11c^{high} CD11b⁺, “lymphoid” CD11c^{high} CD8 α ⁺ or CD11c^{high} CD8 α ⁻ subsets. In B the histogram analysis of the upregulation of mPDCA-1 expression in different hematopoietic cell types is shown (as described in (A)): Cells were isolated from control mice (filled grey) or 15 hrs (red line) and 40 hrs (black line) after poly-I:C treatment, respectively.

Screening of several cell lines revealed that upon IFN α induction a variety of murine cell lines upregulated mPDCA-1 on the cell surface as could be detected by flow cytometric analysis, e.g. 1881 pro-B cells, Sp2/0 cells, Raw cells (data not shown). In contrast to IFN α -inducing reagents, other stimuli did not led to an upregulation of this marker on Sp2/0 cells, as was evident in Fig. 4.2.2.

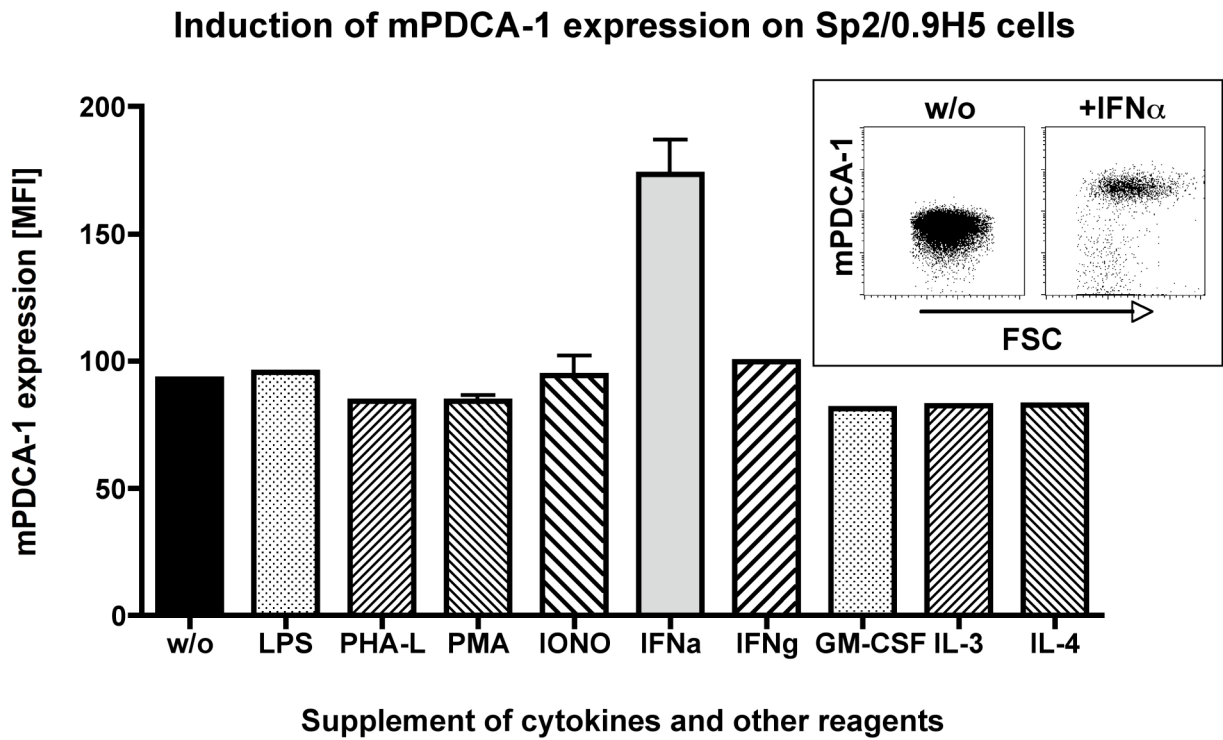


Fig 4.2.2 Upregulation of mPDCA-1 expression on Sp2/0 cells.

Sp2/0 cells were cultured for 24 hrs in medium or in the presence of different stimuli. Bar diagram shows the fluorescence intensity of mPDCA-1 expression as detected by flow cytometric analysis of these cells. Shown is the mean and SEM of 1-3 experiments. Insert demonstrates upregulation of mPDCA-1 expression 24 hrs after IFN α treatment (10^2 U/ml).

The kinetics shown in Fig. 4.2.3 demonstrated a transient upregulation of the mPDCA-1 expression in these cells after IFN α induction. Eight hours after IFN α -treatment, Sp2/0 cells showed a slight increase in mPDCA-1 expression, reaching a maximum after 1-2 days. A typical impression of the upregulation is shown in the insert, comparing untreated and IFN α -stimulated cells. This expression rapidly decreased after removal of IFN α in the cultures, reaching basal level within four days.

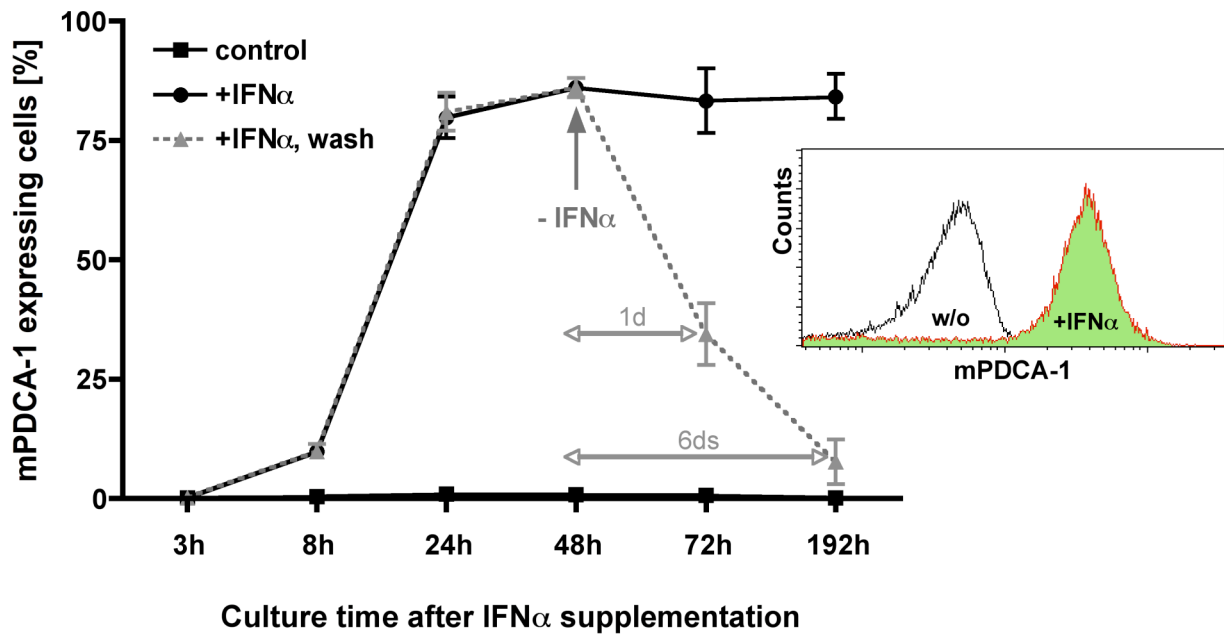


Fig 4.2.3 Kinetic of IFN α -induced upregulation of mPDCA-1 expression on Sp2/0 cells.

Sp2/0 cells were left untreated (square symbols) or cultured in the presence of 10^2 U/ml recombinant IFN α (circles and triangles). 48 hrs after induction the cytokine was washed out (only triangles/grey line). The data shown represent mean \pm SEM of 2-8 experiments per time point and setting. The histogram shown in the insert exemplarily demonstrates the upregulation of mPDCA-1 expression after IFN α treatment (flow cytometric analysis).

In summary, the results presented in these two chapters revealed that the expression of mPDCA-1 is inducible via IFN α .

4.2.3 Identification of mPDCA-1 by differential gene expression analysis

In this experiment the unknown antigen recognized by the anti-mPDCA-1 mAb should be identified by comparing the gene expression profile of cells expressing or not expressing mPDCA-1 as demonstrated previously by flow cytometric analysis. A detailed overview of the experimental settings (Sp2/0 cells, cultured with or without recombinant IFN α or after IFN α removal, and from freshly isolated spleen PDCs) is given in Fig. 3.1 of the Materials & Methods section. RNA was isolated from mPDCA-1 expressing or not expressing Sp2/0 cells as well as from freshly isolated spleen PDCs, converted into cDNA and thereby differentially labeled with Cy3 and Cy5 fluorochromes before hybridization on an Agilent mouse genome microarray. All hybridizations were performed as technical replicates ("dye switch"). After hybridization, fluorescence signals were scanned (Agilent Micro-array Scanner GB2505GB) and quantified (ImaGene, BioDiscovery). In Fig. 3.1 the procedure is shown schematically and a representative microarray picture is also given, demonstrating the regulation of each single gene on the basis of Cy5 (green) and Cy3 (red) signal distribution.

Significantly regulated genes (two-fold background intensity) were included into subsequent analyses, where candidates had to fulfill the following criteria: (1) beside reproducible regulation upon IFN α stimulation, genes must be present on PDCs (shown by chip V); (2) the genes should not be expressed on other cells than macrophages or DCs); (3) a cell surface-bound

molecule was expected due to the cell surface staining with the specific anti-mPDCA-1 mAb. Thus, the gene should contain at least one trans-membrane domain (TMD). With these criteria the multiplicity of regulated genes should be limited to find the candidate for mPDCA-1.

In the initial experiments a microarray from Agilent Technologies was used consisting of about 22,500 mouse transcripts. In four different experimental settings (microarrays I-IV; see Materials and Methods, Table 3.2) Sp2/0 cells, either untreated or cultured in the presence of IFN α , or after downregulation of mPDCA-1 were compared against each other. On microarray V the differential gene expression of freshly isolated PDCs was compared to untreated Sp2/0 cells, demonstrating the PDC-presence of regulated gene candidates. Furthermore, Agilent Technologies provided a “whole-genome mouse chip”, consisting about 40,000 transcripts at a later time point. By the means of this extended microarray the gene expression profile of untreated and IFN α -stimulated Sp2/0 cells was reproduced as described for microarrays I+II (microarrays VI+VII).

Upon the multiplicity of significantly regulated genes, the above-mentioned criteria were applied to shorten this list. In Table 4.2.1 a schematic overview of regulated genes within the separate chips is demonstrated, giving a summary of (1) the number and percentage of all present genes on each single chip, (2) the number of up/downregulated genes, and (3) the number of significantly upregulated genes.

Table 4.2.1 Schematic overview of regulated genes within the seven separate chip hybridizations

Micro-array	Genes present on respective microarray	Genes up-regulated	Genes down-regulated	Upregulated candidates
I	~ 6,500 (28.88%)	564	128	184
II	~ 8,550 (38.00%)	500	579	94
III	~ 7,100 (31.55%)	558	220	125
IV	~ 9,860 (43.82%)	349	939	55
V	~ 7,260 (32.26%)	1,955	1,834	
VI	~ 11,160 (26.19%)	418	198	129
VII	~ 15,880 (35.85%)	351	32	

Within the upregulated candidates, subsets were assembled from the different microarrays. In general, a final intersection was generated, which was listed in Table 4.2.2. Hereby, only genes were displayed that were upregulated on all chips. The differential gene expression analysis demonstrated the significant upregulation of more than 50 candidates. In a second screening step, the PDC-specific expression of regulated candidates should be evaluated by quantitative RT-PCR, comparing mRNA from PDCs and other hematopoietic cell types. The final proof should be given by staining with anti-mPDCA-1 mAb and flow cytometric analysis of transfected cell lines generated using cDNAs of selected candidates.

Table 4.2.2 Differentially regulated gene candidates after extensive Agilent microarray analysis.

Genes are listed in alphabetical order according to their GeneBank Accession nomenclature. Demonstrated is the regulation on the different Agilent microarrays (\emptyset : mean ratio of chip I-IV). TMD: Trans-membrane domain: (-) n.d.; (+) 1 TMD; (++) more than 1 TMD. Reference.: K. Hofmann & W. Stoffel (1993) Biol. Chem. Hoppe-Seyler 374,166 "Tmdbase - A database of membrane spanning proteins segments & TMpred - Prediction of Transmembrane Regions and Orientation". (http://www.ch.embnet.org/software/TMPRED_form.html)

No.	GenBank Acc.No.	Gene Name	I	II	III	IV	\emptyset	V	TMD
1	AK010014	similar to Alpha-interferon inducible protein	16.14	13.16	3.52	7.06	9.97	24.23	-
2	AK030414	similar to Guanylate binding protein	5.64	4.75	2.61	3.43	4.1	7.06	++
3	AK035479	cDNA FLJ31952 FIS, CLONE "Schlafen-4"	8.71	7.64	7.87	4.01	7.06	1.40	++
4	AK037025	similar to 2.5-OLIGOADENYLATE SYNTHETASE-LIKE 5 (Oas1f)	23.99	22.89	7.9	10.48	16.32	2.34	+
5	AK046674	Interferon inducible GTPase 1	3.69	5.60	2.92	7.62	4.95	6.32	++
6	AK054410	9130002C22RIK PROTEIN homolog similar to UBIQUITIN-ACTIVATING ENZYME E1	18.88	8.02	4.72	11.53	10.8	16.46	++
7	AK077176	PHD finger protein 11 (Phf11) similar to PUTATIVE ZINC FINGER PROTEIN NY-REN-34 ANTIGEN	18.88	8.02	4.72	11.53	10.79	16.46	n/a
8	AK077641	Tudor domain containing 7; Tudor repeat associator with PCTAIRE 2 homolog	15.04	17.33	4.19	4.95	10.4	9.62	-
9	AK077880	D11Erd759e DNA segment Chr 11 similar to THYRO1000270 PROTEIN	17.01	30.96	15.51	24.13	21.9	4.47	+
10	AK080076	RIKEN clone A530058D14; unknown EST	22.24	16.86	6.77	11.85	14.43	4.33	n/a
11	AK083376	similar to H-2 CLASS I HISTOCOMPATIBILITY ANTIGEN, D-37 ALPHA CHAIN PRECURSOR	3.78	4.07	2.76	4.93	3.7	12.25	-
12	BB684123	Poly ADP-ribose polymerase family member 14 similar to hypothetical protein, MGC: 7868	16.45	17.16	15.51	12.39	15.3	4.89	-
13	BC006779	Mus musculus, clone IMAGE:3589116	4.43	10.99	4.21	9.11	7.18	3.72	++
14	BC010238	Scotin	4.93	6.44	3.63	4.99	5	4.89	++
15	BC021821	Mus musculus, RIKEN cDNA 5033415K03 gene, clone MGC:7873 IMAGE:3581940,	15	6.9	9.6	10.85	10.59	3.47	n/a
16	BC025170	Mus musculus, clone IMAGE:4013674, mRNA RIKEN cDNA 0610037M15 gene	3.42	4.03	3.72	3.81	3.7	12.91	-
17	BC027328	Similar to bone marrow stromal cell antigen 2	5.24	6.33	3.93	5.34	5.21	15.66	++
18	BY549658	Mus musculus RIKEN cDNA 2610510B01 gene	19.2	5.92	3.09	3.58	7.95	1.97	+
19	ENSMUST0000016427	H-2 CLASS I HISTOCOMPATIBILITY ANTIGEN, TLA(B) ALPHA CHAIN PRECURSOR (MHC THYMUS LEUKEMIA ANTIGEN)	3.89	5.05	2.83	5.05	4.02	16.05	n/a
20	L20315	MPS1 gene = Macrophage expressed gene 1 (MPG1)	5.95	7.30	4.87	4.70	5.7	31.21	++
21	M55219	Mouse HSR, clone pMmHSRc-[1,3,3E,10 + 10E]	32.64	8.29	7.48	6.27	13.67	2.1	+
22	NM_008326	Interferon inducible protein 1 (Ifi1)	18.19	12.14	16.34	9.06	13.9	13.5	++
23	NM_008327	Interferon activated gene 202A (Ifi202a)	22.27	9.31	48.12	24.25	25.99	1.38	+
24	NM_008329	Interferon activated gene 204 (Ifi204)	35.07	11.27	10.36	10.09	16.7	32.02	+
25	NM_008330	Interferon gamma inducible protein 47 kDa (Ifi47)	4	10.46	8.34	5.54	7.08	2.60	++
26	NM_008331/P09914	Interferon-induced protein with tetra-icopeptide repeats 1 (Ifi1)	119.2	141.5	36.52	110.6	102	-	n/a
27	NM_008332	Interferon-induced protein with tetra-icopeptide repeats 2 (Ifi2)	30.37	68.17	181.0	44.86	81.1	-	-
28	NM_009099	Tripartite motif protein 30 (Trim30)	29.32	22.24	13.57	18.21	2.8	34.68	1/-
29	NM_010259	Guanylate nucleotide binding protein 1 (Gbp1)	6.39	6.87	6.32	5.7	6.32	1.6	++
30	NM_010260	Guanylate nucleotide binding protein 2 (Gbp2)	23.23	4.22	13.34	4.01	11.2	-	++
31	NM_010392.1	Histocompatibility 2, Q region locus 2 (H2-Q2)	5.12	2.34	3.59	3.08	3.5	7.00	++
32	NM_010393	Histocompatibility 2, Q region locus 5 (H2-Q5)	2.83	3.11	2.85	2.96	2.94	11.5	n/a
33	NM_010394	Histocompatibility 2, Q region locus 7 (H2-Q7)	2.51	3.21	3.04	4.06	3.30	12.41	n/a
34	NM_010397	Histocompatibility 2, T region locus 22 (H2-T22)	3.31	2.80	3.65	3.44	3.3	37.65	n/a
35	NM_010398	Histocompatibility 2, T region locus 22 (H2-T23)	3.7	3.68	4.14	3.75	3.82	9.45	n/a
36	NM_010501	interferon-induced protein with tetra-icopeptide repeats 3 (Ifi3)	4.95	3.68	4.14	3.75	4.13	-	n/a
37	NM_010741	Lymphocyte antigen 6 complex, locus C (Ly6c)	9.29	9.63	9.86	5.38	8.5	32.40	+
38	NM_010846	Myxovirus (influenza virus) resistance 1 (Mx1)	15.43	3.8	18.1	8.51	11.46	-	n/a
39	NM_011150	Peptidylprolyl isomerase C-associated protein (Ppicap)	10.11	10.58	6.2	6.88	8.44	-	+
40	NM_011637	Three prime repair exonuclease 1 (Trex1)	7.09	8.77	5.55	7.10	7.1	6.62	+
41	NM_011854	2-5 oligoadenylate synthetase-like 2 (Oas2)	5.87	10.44	6.55	16.53	9.85	-	+
42	NM_011909	Ubiquitin specific protease 18 (Usp18)	18.93	30.92	14.47	18.2	20.66	-	++
43	NM_013606	Myxovirus (influenza virus) resistance 2 (Mx2)	25.81	35.53	16.36	22.73	25.11	2.18	n/a
44	NM_019665	Adenosine deaminase, RNA-specific (Adar)	8.06	5.60	6.72	2.01	5.60	1.59	+
45	NM_019963	STA2 Signal transducer and activator of transcription 2	93.51	6.93	8.41	7.24	29.02	3.01	++
46	NM_020583	Interferon-stimulated protein (20kd) lsg20	7.79	18.76	14.26	14.74	13.89	2.91	n/a
47	NM_021274	Small inducible cytokine B subfamily (Cys-X-Cys), member 10 (Scyb10)	55.84	28.75	16.15	13.26	28.5	-	+
48	NM_021430	Mus musculus RIKEN cDNA 2900002H16 gene	42.31	4.76	4.60	3.67	13.84	-	n/a
49	NM_021792	Interferon-inducible GTPase (ligp-pending)	165.2	18.88	5.44	21.72	52.81	4.19	+
50	NM_023141	Torsin family 3, member A (Tor3a)	11.47	19.11	9.89	12.60	13.27	1.62	++
51	NM_023386	ATP-dependant interferon responsive (Adir)	73.41	66	47.13	28.05	53.64	1.71	+
52	NM_030253	Mus musculus RIKEN cDNA 5830458K16 gene	13.64	5.41	7.88	2.49	7.35	2.14	++
53	NM_031367	Mus musculus hypothetical protein, MGC: 7868 (BC003281)	505.5	78.06	159.5	22.23	191	9.84	+
54	NM_133871	Histocompatibility 28 (H28) Interferon-induced protein 44	78.62	171.8	29.11	38.97	79.5	6.11	+
55	NM_146114.1	Mus musculus expressed sequence AW261460 SNM1-like (Snm1)	4.26	2.20	3.55	2.05	3.02	8.88	-/1

4.2.4 Validation of mPDCA-1 candidates for PDC-specific expression by quantitative real time RT-PCR

The expression in PDCs and selected hematopoietic cell populations of each regulated gene candidate that have passed all screening criteria was assessed by quantitative RT-PCR, performed on a LightCycler system (Roche). Messenger RNA of PDCs was amplified using primers specific for the investigated genes and was compared to mRNA of other hematopoietic cell types, e.g. T cells, NK cells, B cells, CD11c^{high} cDCs, macrophages or other cell lines. Before starting the analysis, for all mRNA sources a standard curve for selected housekeeping genes (β -actin, PPIA, GAPDH, and Hprt-1) was established to determine the absolute mRNA

level (see appendix, Fig. 7.2). Additionally, the integrity of each primer set was tested (data not shown). A list of all primers used in this work is also deposited in the appendix (Tab. 7.1A+B+C).

Table 4.2.3 Validation of candidates by quantitative real time RT-PCR analysis.

The regulation of 45 genes was compared according to their mRNA expression in PDCs and T cell, normalized to β -actin.

Shown is the mean of the respective crossing-points of the LightCycler runs (n=2) and the difference between PDC and T cell mRNA. A negative numerical value represents a higher expression in PDCs. Highlighted in green are genes demonstrating a predominate expression in PDCs.

#	Gene Acc.	Mean Crossing-points		
		PDC	T cell	Difference
1	AF017175	27,79	26,61	1,18
2	AK010014	21,215	22,345	-1,13
3	AK030414	25,535	25,935	-0,4
4	AK037025	34,315	32,23	2,085
5	AK046674	24,28	23,235	1,045
6	AK050122	26,335	25,695	0,64
7	AK054410	22,84	23,695	-0,855
8	AK077641	26,44	26,975	-0,535
9	AK077880	24,99	24,665	0,325
10	AK079685	-	-	-
11	AK080076	28,545	26,75	1,795
12	AK083376	21,825	22,925	-1,1
13	BB684123	23,115	22,66	0,455
14	BC021340	24,855	24,885	-0,03
15	BC021821	25,32	24,325	0,995
16	BC025170	23,145	23,135	0,01
17	BC027328	19,865	25,36	-5,495
18	BC029209	26,49	27,3	-0,81
19	BC052532	24,725	24,325	0,4
20	L20315	18,54	25,455	-6,915
21	M55219	23,515	24,38	-0,865
22	NM_008326	28,95	28,175	0,775
23	NM_008331	24,08	23,85	0,23
24	NM_008332	26,07	25,205	0,865
25	NM_008452	-	-	-
26	NM_009099	23,25	25,855	-2,605
27	NM_010255	27,97	27,29	0,68
28	NM_010260	26,545	25,16	1,385
29	NM_010392	17,46	18,33	-0,87
30	NM_010393-E	19,14	19,35	-0,21
31	NM_010394-E	24,82	27,89	-3,07
32	NM_010397	24,145	23,665	0,48
33	NM_010398	22	23,13	-1,13
34	NM_010501	21,875	21,78	0,095
35	NM_010741 (Ly6C)	25,085	25,475	-0,39
36	NM_011637	26,92	31,085	-4,165
37	NM_011909	24,48	29,03	-4,55
38	NM_021430	25,615	30,56	-4,945
39	NM_023386	24,105	25,03	-0,925
40	NM_025821	-	-	-
41	NM_029803	23,785	24,75	-0,965
42	NM_031367	23,145	27,25	-4,105
43	NM_133871	28,61	31,835	-3,225
44	NM_146114	29,29	28,745	0,545
45	NM_199146	25,33	25,86	-0,53

The results of 45 from 55 candidates that could be tested successfully by quantitative RT-PCR analysis are listed in Table 4.2.3. Here, the mean crossing-points of distinct gene candidates were compared between mRNA of PDCs or T cells, as the latter were negative for mPDCA-1. The crossing-point itself defined the cyclus in which the fluorescence started to increase linearly as measured in a LC run. In principle, the lower the value for a crossing-point the more nucleic acid has been detected. As an approximate value, a difference in the crossing-points (Δ CP) of “3” represents a nearly 10-fold upregulation. From these 45 candidates nine genes were significantly upregulated in PDCs compared to T cells (Δ CP=2-5), representing a 6->20-fold regulation. These candidates were depicted in green. Exemplary LightCycler runs are given in Fig. 4.2.4. For housekeeping genes β -actin and PPIA there were almost no differences in their crossing points between mRNA isolated from T cells and PDCs (A) as well as for NM_008331 (Ifit1) (B). In contrast, the LightCycler analysis for L20315 (MPG1) demonstrated an enormous difference in the crossing points if mRNA from T cells or PDCs was used (C). As shown in the representative LightCycler analysis, for PDC mRNA L20315 reached the crossing point after about 18 cycles compared to more than 24 cycles if T cell mRNA was used.

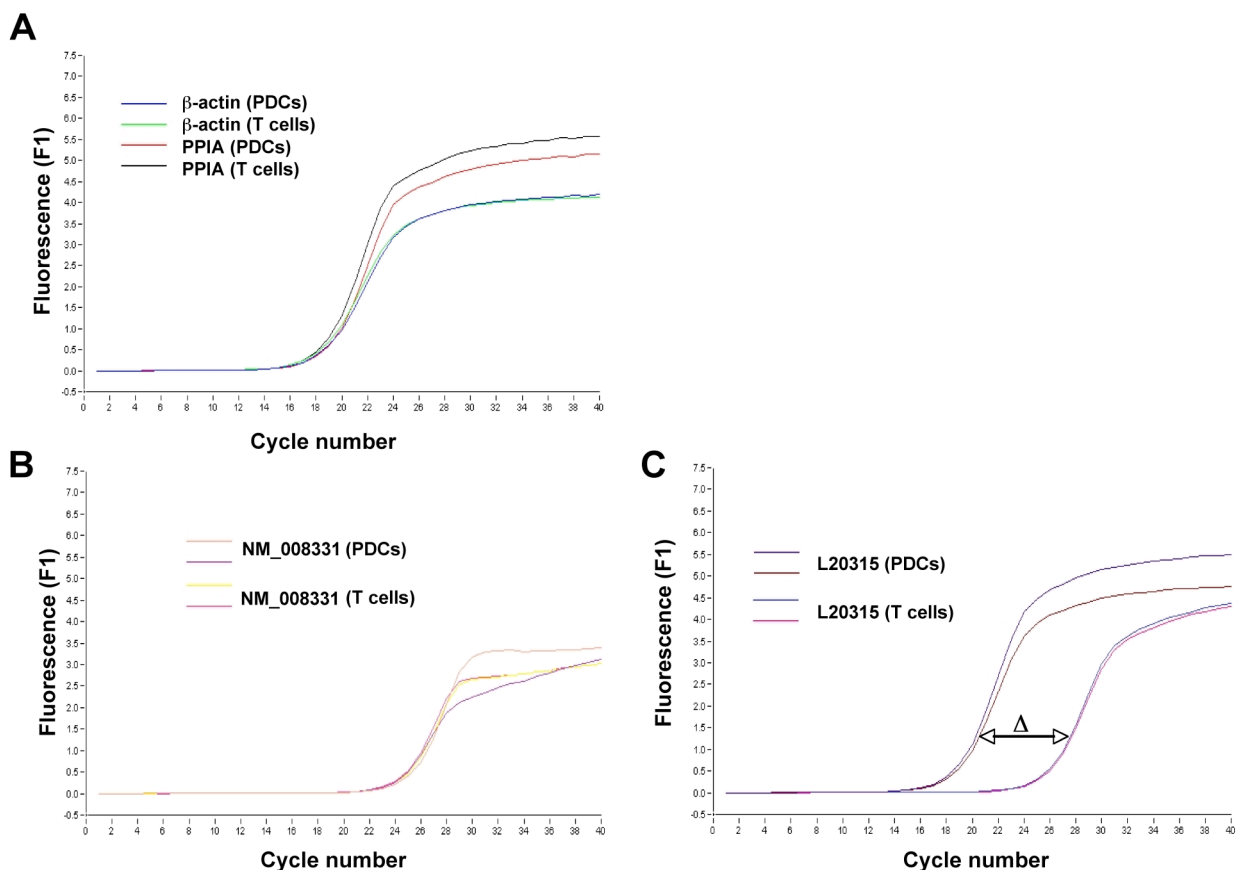


Fig. 4.2.4 LightCycler curves indicating crossing points for L20315 and NM_008331 performed on different mRNA templates.

Isolated mRNA of purified spleen PDCs or T cells was used as template for quantitative real time PCR analysis. RT-PCR was performed using the LightCycler[®] RNA Master SYBR Green I kit (Roche Diagnostics). All assays were performed at least in duplicates. Messenger RNA amount was normalized by the expression of house keeping genes (murine β -actin, PPIA, Hprt-1, and GAPDH) (A). Differential transcript levels of two exemplary genes, NM_008331 and L20315, are shown. Significant difference in the cycle numbers between PDCs and T cells were observed for L20315(C) in contrast to NM_008331 (B).

The performed real time PCR analysis could shorten the number of regulated genes, leading to a final list of nine genes that passed all criteria and demonstrated on the one hand high regulation in the Agilent analysis as well as predominant expression in PDCs compared to T cells (Table 4.2.4).

Table 4.2.4 Final list of mPDCA-1 candidates after microarray and RT-PCR analysis.

Regulated gene candidates from the Agilent microarrays were validated by LightCycler analysis of PDC and T cell mRNA. Prediction of trans-membrane regions and orientation (TMD) was evaluated as described before. Values in parentheses showed scores of the TMD prediction, whereas only scores above 500 were considered significant.

#	Gene ID	Name	PDCs vs. T cells		Agilent regulation	TMD
			Δ CP	Regulation		
1	L20315 (E3)	Macrophage-specific gene 1 (Mpg-1, MPS1)	-6.915	"23fold"	4.7-31fold	5 (2>1000)
2	BC027328	Mus musculus bone marrow stromal cell antigen 2	-5.495	"18fold"	3.9-15.7fold	2 (2>1000)
3	NM_021430	Mus musculus RIKEN cDNA 2900002H16 gene	-4.945	"16fold"	3.7-42fold	0
4	NM_011909	Mus musculus ubiquitin specific peptidase 18 (Usp18)	-4.55	"15fold"	14.5-30fold	3 (1>score)
5	NM_011637	Mus musculus three prime repair exonuclease 1 (Trex1)	-4.165	"14fold"	5.6-7.1fold	1 (2000)
6	NM_031367	Mus musculus histocompatibility 28 (H28)	-4.105	"13fold"	9.8-505fold	1 (>score)
7	NM_133871	Mus musculus interferon-induced protein 44 (Ifi44)	-3.225	"10fold"	6.1-170fold	2 (1>1000)
8	NM_009099	Mus musculus tripartite motif protein 30 (Trim30)	-2.605	"8fold"	13.6-35fold	(1<score)
9	NM_010741	Mus musculus lymphocyte antigen 6 complex, locus C	-0.39	"1.2fold"	5.4-32fold	2 (1>1000)

4.2.5 Cloning and generation of transfectants of potential mPDCA-1 candidates

To identify the molecule recognized by the anti-mPDCA-1 mAb, genes that are present on the final candidate list have been cloned and full-length transfectants have been generated. According to their higher expression in PDCs compared to T cell mRNA, a more detailed expression analysis was performed for two examples (L20315 and BC027328), comparing their mRNA content in PDCs to a variety of other leukocyte cell types (Fig. 4.2.5A+B; representative LC runs for BC027328 and L20315 are attached in the appendix). It was demonstrated that both genes were predominantly expressed in PDCs in contrast to cells or cell lines from the lymphoid or myeloid lineage. The mean of the relative expression, normalized via β -actin content, is displayed below the bar diagrams. Interestingly, after IFN α -induction, only Sp2/0 cells showed high expression of BC027328 but not L20315 mRNA, which was comparable to native PDCs.

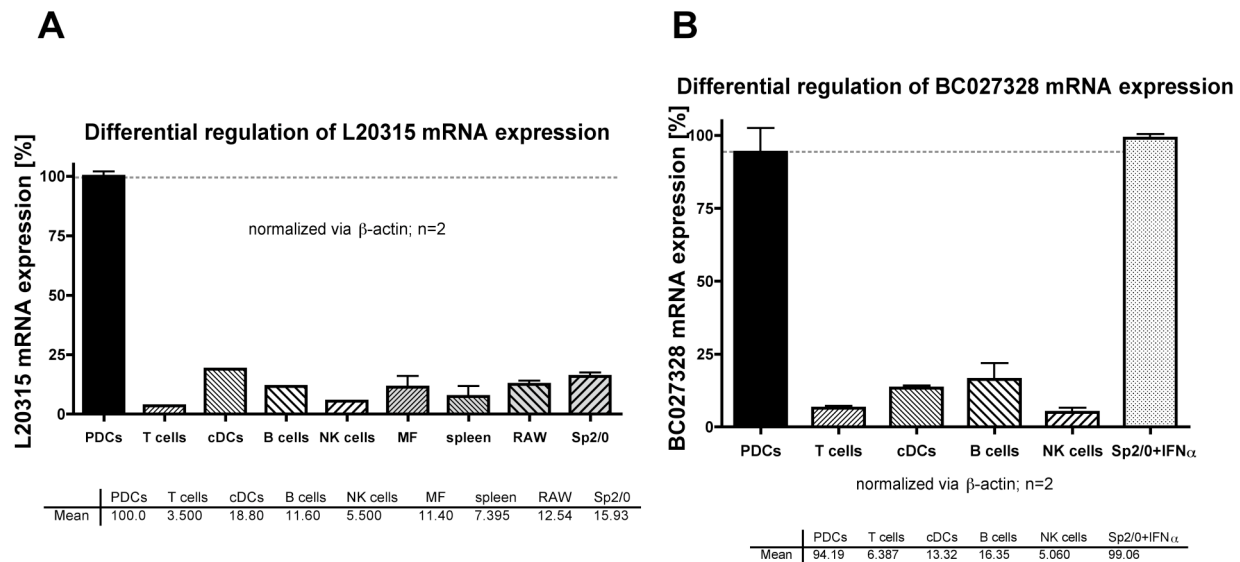


Fig 4.2.5 Differential expression of L20315 (MPG1) and BC027328 (BST2) mRNA.

mRNA was prepared from indicated cell types and real-time RT-PCR was performed with primers for L20315 (A) and BC027328 (B) (n=2). Values were normalized for β -actin expression. Shown is the relative mRNA amount of indicated genes in different cell types (PDCs expression was set to 100%).

Taken together, these two candidates showed promising results and the cloning and generation of transfectants are demonstrated in detail in the following.

4.2.5.1 The macrophage-specific gene 1

The L20315 gene coding for the macrophage-specific gene 1 (MPG1) was the first one cloned, because this candidate was both highly regulated in the differential gene analysis and also showed a predominant mRNA expression in spleen PDCs compared to all other cells tested as validated by quantitative real time PCR.

The complete open reading frame (ORF) of MPG1 was inserted into the pDisplay vector without the leader sequence and start codon (ATG) that was provided by the vector backbone (see Materials and Methods). Sequence information of primers used for gene amplification is deposited in the appendix (Table 7.1D).

After transfection of HEK293T cells, the construct was easily detected intracellularly via N-terminal HA-tag of pDisplay-Vector as flow cytometrical analysis of intracellular HA staining revealed (Fig. 4.2.6). Using a commercial rabbit anti-rat MPG1 mAb (described to be also cross-reactive with murine MPG1) staining of MPG1- but not MOCK-transfected HEK293T cells could be demonstrated. In contrast, detection with anti-mPDCA-1 mAbs showed no significant signal of this transfected cell line (compared to the isotype control or MOCK-transfected cells).

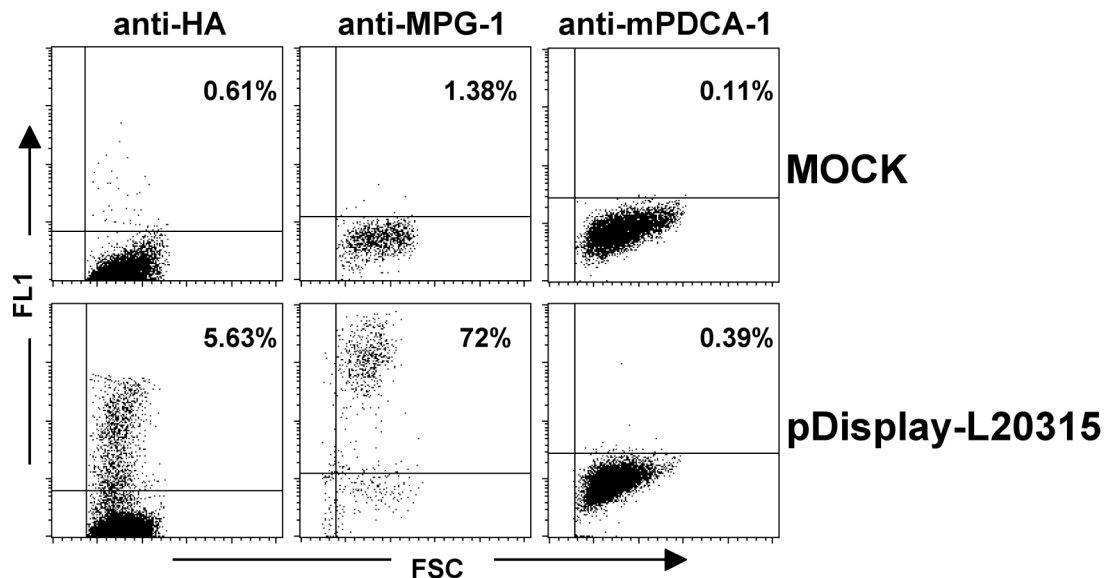


Fig 4.2.6 Cloning of L20315 (MPG1) and generation of a full-length transfectant.

HEK293T cells were either transfected with the empty vector (MOCK) or with the pDisplay vector containing the L20315 sequence. Representative flow cytometric analysis of anti-HA, anti-MPG-1, and anti-mPDCA-1 stainings are shown.

In general, several transfections with other cell lines were performed to avoid cell type-specific modulations: e.g. human HEK293T cells, rat RBL-1 cells, and mouse RAW cells were tested. The results demonstrated that at least RAW cells upregulated mPDCA-1 upon transfection with the MOCK vector (data not shown). Therefore, to exclude an unspecific induction of the mPDCA-1 only human and rat cell lines, but not mouse cells (such as RAW) were used from this point on.

Taken together the positive staining both for HA and MPG1 showed the integrity of the construct; on the other hand, these results led to the suggestion that MPG1 was not identical to the mPDCA-1 antigen, although it was predominantly expressed on PDCs (at least on mRNA level). Nevertheless, future investigations might show further implications of this molecule and its role for PDCs.

4.2.5.2 The Bone marrow stromal antigen 2

Above-described results demonstrated that MPG1 was not detected by the anti-mPDCA-1 mAb. Hence, the next gene on the final list of regulated and validated gene candidates was cloned and transfectants were generated. BC027328, coding for the Bone marrow stromal antigen 2 (BST2), was another highly regulated candidate that also showed a predominant PDC expression (see above).

The gene organization (900 bp in length, CDS of 45-563 base pairs) led to the cloning strategy into two vectors as described in detailed in the Materials & Methods section. BST2 was cloned in either a pEHO or a pMACS.4IRES-II vector. While the first vector involved a Blasticidin resistance and a HA tag, the latter one vector did not provide a resistance gene, but enables bicistronic expression of BST2 together with a truncated human CD4 surface. As for BST2, the

N-Terminus was proposed to be located intracellular (based on a TMD prediction), the HA-tag should be detected by intracellular staining in pEHO-BST2 transfectants. In pMACS.4IRES-II-BST2 transfectants the human CD4 protein should be co-expressed on the cell surface enabling effective enrichment of positively transfected cells via anti-CD4 microbeads.

Cells transfected with the above-mentioned pEHO-BST2 vector or with the MOCK control could be both specifically detected via the HA-TAG (only intracellularly; data not shown), demonstrating the integrity of the vector. In contrast, with the anti-mPDCA-1 but not with the isotype control (rat IgG_{2b}) mAb a significant staining was detected on the BST2 transfectants (Fig. 4.2.7A). The MOCK control did not show a significant staining. As for MPG1, transfectants were generated also for BST2 in several cell lines (HEK293T, 1881; and EL4.2), which gave similar results. To avoid any unspecific signals induced by unwanted activation of these cells (as shown in chapter 4.2.5.1), transfectants were not generated in RAW cells.

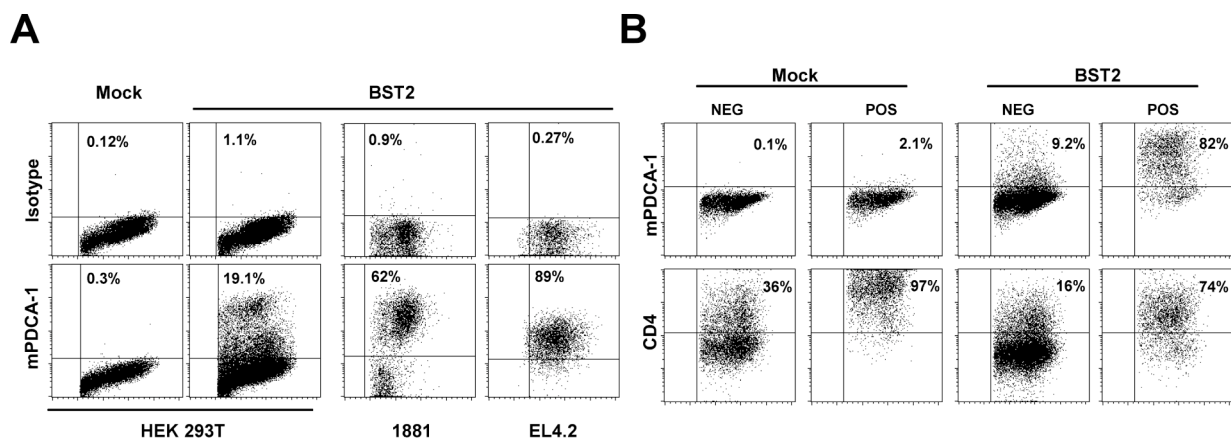


Fig 4.2.7 Cloning of BC027328 (BST2) and generation of full-length transfectants.

(A) HEK293T, 1881, and EL4.2 cells were transfected with the pEHO vector, either empty (MOCK) or containing the BC027328 sequence. Flow cytometric analysis of the mPDCA-1 expression is performed 24 hrs after electroporation (HEK293T) or after limited dilution (1881 and EL4.2; Mock control not shown).

(B) Representative flow cytometric analysis of HEK2932T cells transfected with the pMACS.4IRES-II vector. Anti-mPDCA-1 and anti-human CD4 stainings are shown after enrichment with anti-hCD4 microbeads (NEG/POS = magnetical negative/positive fraction).

The pMACS.4IRES-II vector provided the opportunity to enrich transfected cells via the expression of human CD4. Fig. 4.2.7B demonstrated representative results of CD4 microbead-enriched HEK293T cells after transfection. Whereas the Mock-transfected cells only showed an enrichment of CD4⁺ cells, BST2-transfected cells displayed both accumulations of mPDCA-1⁺ and CD4⁺ cells. Similar results were obtained by using anti-mPDCA-1 microbeads (clone JF07-3D5; data not shown).

In summary, all transfectants of the above constructs showed comparable and specific mPDCA-1/BST2 expression as was evident by anti-mPDCA-1 FACS staining.

In this second chapter, the molecular nature of mPDCA-1 was successfully revealed by a strategy based on the combination of differential gene analysis followed by the validation of potential candidates by quantitative RT-PCR and FACS analysis of generated transfectants.

Furthermore, a variety of PDC-regulated genes were found, either already known (e.g. Ly-6C (NM_010741) or other, IFN-I-inducible genes) or hitherto unknown molecules. In addition, the BST2 transfectant could be used for further experiments including internalization and signal transduction studies, and to analyze the function of the molecule and its immunological role, in particular in the modulation of IFN α production (as demonstrated in previous experiments) and for the uptake of antigens.

4.3 Characterization of mPDCA-1 as novel antigen-uptake receptor on PDCs enabling priming and cross-priming of naïve T cells

The immune system consists of specialized cell types for the recognition and the elimination of pathogens. On the effector side T lymphocytes play a pivotal role in adaptive immunity. Naïve T cells do not recognize native antigens, but only respond to antigenic peptides presented on major histocompatibility complex (MHC) molecules of so-called antigen-presenting cells (APCs) comprised of B cells, macrophages and mainly dendritic cells (DC) [Romani N, Res Immunol 1989; Romani N, JEM 1994; Germain RN, Cell 1994; Brown MG, JI 1993; Carbone FR, Cold. Spring Harb. Symp. Quant. Biol. 1989]. The T cell population can be principally divided into cytotoxic CD8⁺ T cells (CTLs) that recognize antigenic peptides in the context of MHC class I, and CD4⁺ helper T cells, which respond to peptides loaded onto MHC class II complexes. The DC family comprises of at least five different subsets, suggesting the potential to initiate distinct responses to diverse challenges. PDCs were regarded as a distinct subset of Dendritic cells, which have a critical role both in the innate and adaptive immune defense against bacterial and viral infection [Liu YJ, Ann Rev Immunol 2005], by sensing viral or microbial structures through engagement of Toll-like-receptors (TLR) 7 and TLR 9 [Kadowaki N, JEM 2001] and (Myd88/IRF7-dependent) secretion of massive amounts of type I interferons (IFN α , β , ω , τ) [Kawai T, Nat. Immunol 2004]. PDCs have also been proposed to play a direct role as APCs in the initiation of T cell responses by their constitutive presence in lymphoid organs, by expression of MHC molecules and by acquisition of DC morphology upon activation. Nevertheless, their DC characteristic relied on their capacity to prime naïve T cells, and in fact this is controversially discussed: Freshly isolated PDCs are poor T cell stimulators as human blood-derived PDCs did not stimulate naïve CD4⁺ T cells in a Mixed Leukocyte Reaction (MLR) unless cultured in the presence of virus (HSV) [Kadowaki N, Hum Immunol 2002]. On the other hand murine splenic PDCs failed to induce naïve CD4⁺ and CD8⁺ T cell proliferation to endogenous antigens even after virus exposure [Krug A, JEM 2003]. In contrast, peptide-pulsed PDC derived from Flt-3-driven BM culture or spleen can promote the *in vitro* expansion of CD4⁺ T cells and T_H polarization [Boonstra A, JEM 2003]. Adoptive transfer experiments showed that splenic and BM culture-derived PDC are capable to elicit responses of naïve CD8⁺ T cells to endogenous, but not exogenous antigens after CpG activation [Salio M, JEM 2004]. These conflicting results are likely due to the different source of PDCs used in the reports as well as their activation status. Recently, PDCs have been shown to play a critical role in the control of airway inflammation [de Heer HJ, JEM 2004; Smit JJ, JEM 2006] and regulation of alloimmune

reactivity and tolerance [Abe M, *Transplant. Proc.* 2005; Ochando JC, *Nat Immunol* 2006]. Additionally, we showed a direct interaction of PDCs with naïve CD4⁺ T cells in an antigen-specific manner *in vivo* [Sapozhnikov A, *JEM* 2007] characterizing PDCs as "bona fide" DC that can initiate adaptive immune responses.

The aim of this project was to disclose the function of the recently described mPDCA-1 molecule for antigen delivery and processing. Additionally, mPDCA-1-targeted delivery of antigens was utilized to analyze PDC-induced primary CD4⁺ and CD8⁺ T cell responses, which allows a better understanding of the principle role of PDCs in adaptive immunity. Although PDCs express MHC-II molecules and display further DC-features, including upregulation of co-stimulatory molecules upon maturation and displaying a dendrite-like morphology, they were still not regarded as professional DCs [Kadowaki N, *Hum. Immunol* 2002]. Thus, it was of particular interest to show whether PDCs were acting as competent APCs.

4.3.1 Endocytosis of DQ-OVA demonstrated the antigen-uptake capacity of PDCs

A unique hallmark of DCs is the uptake of exogenous, soluble antigens for subsequent presentation to naïve T cells. PDCs were characterized to take up soluble antigens poorly [Grouard GM, *JEM* 1997; Dzionek A, *Ji* 2000]. To investigate their *in vivo* endocytosis capacity the uptake of the model antigen DQ-OVA was investigated. DQ-OVA is a fluorogenic reagent that is invisible in its unprocessed form due to auto-quenching, but shows fluorescence upon entry into the endosomal cellular compartment. 24 hrs after s.c. and i.v. administration of DQ-OVA only PDCs but not myeloid DCs or T cells were able to take up and proceed DQ-OVA into the endosomal/lysosomal pathways as was revealed by the FACS analyses (Fig. 4.3.1): approximately 15% of PDCs in contrasts to less than 0.5% of other cell types showed a positive signal. Interestingly, simultaneous activation via TLR9 signaling resulted in weaker signal intensities. In addition, only LN-PDCs but not cells from spleen could be stained for processed antigen (data not shown). The two murine cell lines 1881 (murine pre-B cells) and RAW 264.7 (macrophage/monocyte-derived cells) ingested this antigen efficiently *in vitro*. Again, addition of CpG did not lead to increased uptake of DQ-OVA. Other experiments also showed an increased uptake of FITC-labeled Dextran at 37°C compared to 4°C, further underlining the capacity of PDCs to ingest exogenous antigens (data not shown).

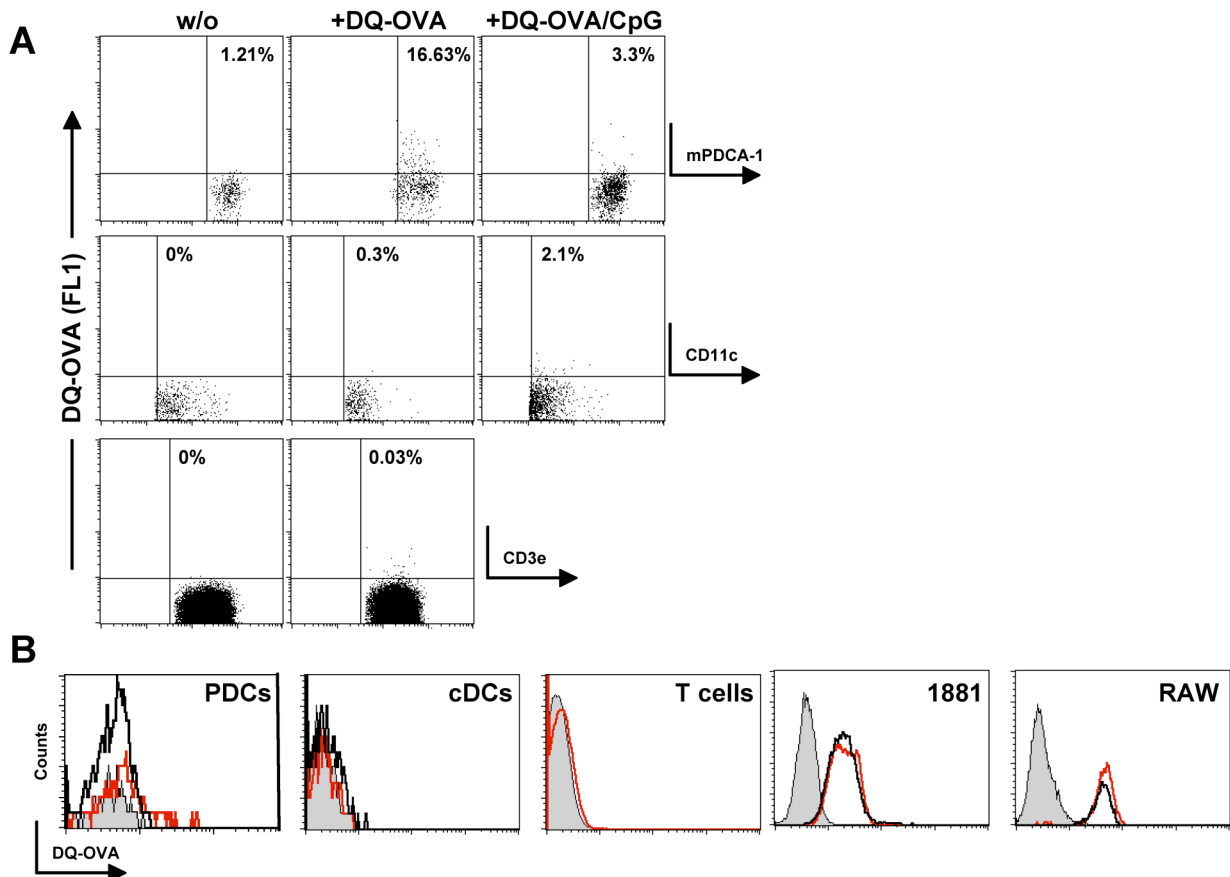


Fig 4.3.1 Uptake and processing of DQ-OVA by PDCs *in vivo*.

(A) To determine the endocytotic capacity of PDCs, mice received 20 μ g DQ-OVA. 24 hrs after s.c. administration the antigen uptake and processing was evaluated by FACS analysis of cells isolated from draining LNs. If indicated, mice received additionally 10 μ g CpG ODN 1668. The dotplots show FL1 signal derived from processed DQ-OVA on mPDCA-1⁺ CD11c^{int} PDCs, mPDCA-1⁻ CD11c^{high} cDCs, and CD3e⁺ T cells.

(B) Flow cytometric analysis of DQ-OVA uptake by PDCs, cDCs, T cells (*in vivo*) and 1881 and RAW cell lines (*in vitro*). The histograms display overlays of FL1 intensities of cells in the absence (grey filled lines) or presence of DQ-OVA (red lines) or optionally of DQ-OVA in combination with CpG (black lines) as demonstrated in (A). The *in vitro* endocytosis capacity of 1881 and RAW cells is shown after culture for 24 hrs in the absence or presence of DQ-OVA.

4.3.2 Generation of a PDC-specific *in vitro* and *in vivo* antigen delivery strategy

Administration of the anti-mPDCA-1 mAb led to specific and efficient depletion of PDCs *in vivo*. It has been shown in chapter 4.1.7 that about 80-90% of PDCs in spleen were depleted after anti-mPDCA-1 mAb application in contrast to diluent or isotype control antibody. This efficient PDC depletion was also detected in other lymphoid organs, whereas administration of anti-mPDCA-1-F(ab')₂ showed that in contrast to the complete mAb the F(ab')₂ fragment did not deplete PDCs (Fig. 4.1.15). These data suggest a complement-dependent lysis or an induction of antibody-dependent cell-mediated cytotoxicity (ADCC) of the complete anti-mPDCA-1 mAb. Thus, immunizing mice with a fluorochrome-conjugated F(ab')₂ fragment resulted in specific targeting of PDCs *in vivo*, as indicated by flow cytometric analysis of isolated spleen and LN cells (Fig. 4.3.2). These data demonstrate that anti-mPDCA-1-F(ab')₂ fragments allowed a specific *in vivo* targeting of PDCs without killing the cells.

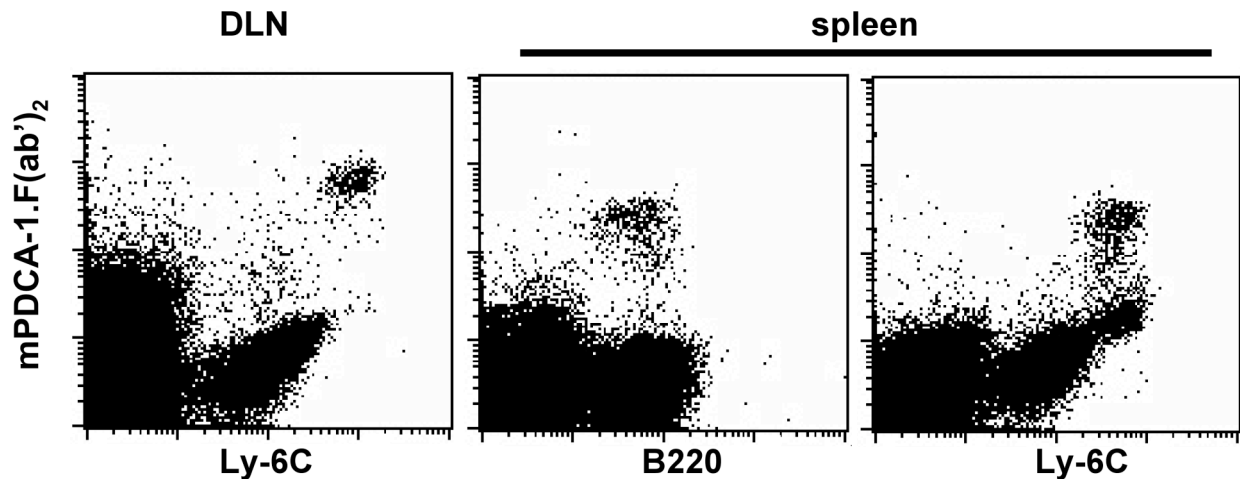


Fig 4.3.2 *In vivo* PDC targeting via anti-mPDCA-1-F(ab')₂ antibody fragment.

To demonstrate the *in vivo* specificity, mice received either a s.c. or i.v. administration of anti-mPDCA-1-F(ab')₂ conjugated to Alexa488. Spleen and draining LNs (DLN) were isolated 2 and 15 hrs later, respectively. Dotplots show Ly-6C and B220 staining that had been performed on single cell suspensions. Hereby the mPDCA-1 staining (as demonstrated on the y-axis) is derived from administrated anti-mPDCA-1-F(ab')₂ fragment.

After demonstration that the antibody-receptor-complex was internalized upon cross-linking (see Fig. 4.1.18), targeting OVA protein to PDCs was in the focus of the next experiments. As described elsewhere, full-length OVA protein was conjugated to the anti-mPDCA-1-F(ab')₂ mAb [Sapoznikov A, JEM 2007]. Purified fragments of the non-depleting anti-mPDCA-1-F(ab')₂ fragments were covalently conjugated with OVA protein. Generated anti-mPDCA-1-F(ab')₂-OVA was purified by size exclusion chromatography as shown in the appendix (see Fig.7.1). Functional integrity of the construct was tested by Western blotting. As depicted in Fig. 4.3.3A, the conjugates were readily detected both via the kappa light chain and the OVA-fraction, whereas free OVA or unconjugated anti-mPDCA-1-F(ab')₂ fragments were only detected with an anti-rat IgG or anti-OVA antibody, respectively. Fig. 4.3.3C revealed that a FITC-labeled targeting construct was only detected on Siglec-H⁺ PDCs within a spleen single cell suspension, underlining that the targeting construct was delivered specifically to PDCs *in vitro*. The specificity of the antigen delivery had also been shown *in vivo*: i.v. and s.c. injection of the anti-mPDCA-1-F(ab')₂-OVA construct resulted in specific labeling of CD11c^{int} PDCs from spleen and DLNs as demonstrated by flow cytometric staining in Fig. 4.3.3B. Therefore targeting mPDCA-1 might be a valuable approach for specific delivery of antigens to PDCs for presentation via MHC-I and -II molecules both *in vitro* and *in vivo*.

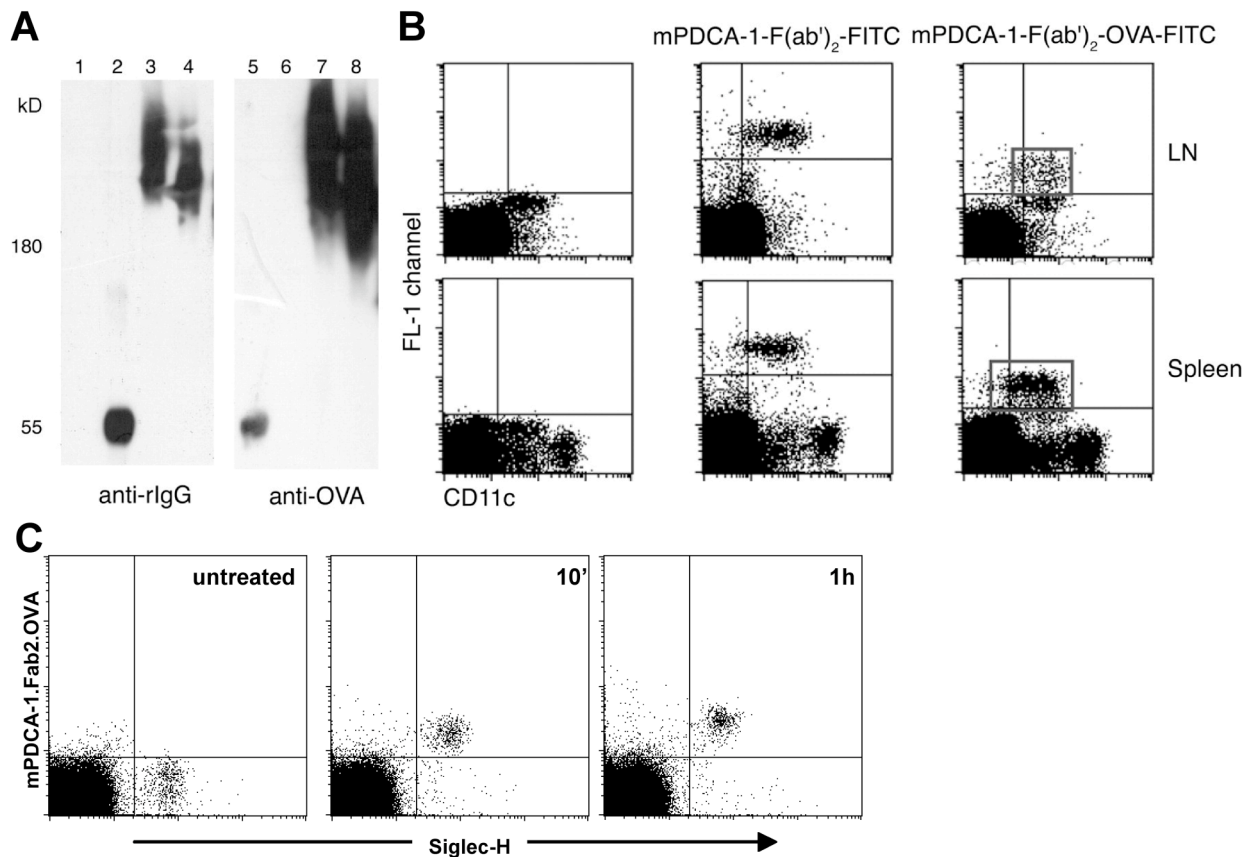


Fig 4.3.3 Characterization of selective PDC targeting and antigen delivery.

(A) Western blot analysis of the generated OVA-conjugated antibody construct. Free OVA and unconjugated or OVA-conjugated anti-mPDCA-1-F(ab')₂ antibody constructs were resolved by SDS-PAGE (4-12% gradient Tris-glycine gel) and, after immunoblotting, detected with anti-ratκ and anti-OVA antibody, respectively. Lanes 1 and 5 contain free OVA, lanes 2 and 6 contain the unconjugated anti-mPDCA-1-F(ab')₂ antibody fragment, and lanes 3 and 4 as well as 7 and 8 contain two fractions of the anti-mPDCA-1-F(ab')₂-OVA conjugate.

(B) Specific *in vivo* targeting of PDCs with FITC-labeled anti-mPDCA-1-F(ab')₂-OVA. Conjugates were injected i.v. or s.c. and, after 3 h, spleens and popliteal LNs were isolated. Dotplots demonstrate counterstaining with CD11c that has been performed on single-cell preparations from untreated (left dot plots) or *in vivo*-targeted cells (middle and right dot plots). The staining in the FL-1 channel is based on the *in vivo*-injected, FITC-coupled mPDCA-1-F(ab')₂-OVA construct.

(C) Dotplots show spleen single cell suspensions of untreated mice that have been incubated for indicated times with anti-mPDCA-1-Fab₂-OVA (conjugated to FITC fluorochrome). OVA-conjugated targeting construct is specifically directed to PDCs *in vitro*, as counterstaining with further PDC-specific marker Siglec-H revealed.

4.3.3 Capacity of murine PDCs to prime antigen-specific CD4⁺ T cells *in vitro*

4.3.3.1 Peptide-pulsed PDCs are able to induce naïve CD4⁺ T cell proliferation

To confirm their general stimulatory capacity, PDCs from Balb/c were first co-cultured with CFSE-labeled CD4⁺ T cells from DO11.10 mice in the presence of an OVA peptide that could be loaded onto MHC-II molecules. As expected, T cells responded in a vigorous expansion (<1% vs. average 85-95%) if PDCs were loaded with peptide (Fig. 4.3.4B). The same results were obtained in the C57BL/6 background with CD4⁺ T cells from OT-II mice (data not shown).

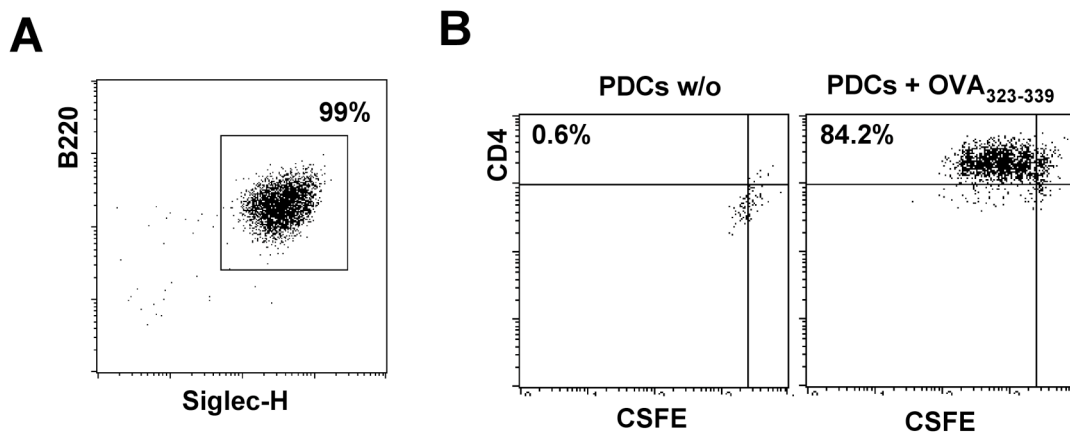


Fig 4.3.4 Capacity of murine PDCs to present antigen to naïve CD4⁺ T cells.

(A) PDCs were untouched isolated from several lymphoid organs by MACS technology and then sorted into B220⁺ Siglec-H⁺ or Ly-6C⁺ cells (FACS Vantage). Representative dotplot demonstrates the purity of isolated PDCs as revealed by subsequent flow cytometric analysis of B220 and Siglec-H expression.

(B) Highly pure PDCs (97-99%) were isolated from Balb/c mice and cultured in the absence or presence of OVA peptide (OVA₃₂₃₋₃₃₉; 5 µg/ml). Thereafter, PDCs (1×10^5 cells) were co-cultured with 2×10^5 purified and CFSE-labeled CD4⁺ T cells isolated from DO11.10 mice. Dotplots show the proliferation of CD4⁺ T cells (gated on viable KJ-26.1⁺ B220⁻ cells) after 72 hrs.

4.3.3.2 Activated PDCs prime naïve CD4⁺ T cells after antigen-uptake via mPDCA-1

After demonstrating that PDCs *per se* were able to stimulate T cells, it was next investigated whether PDCs are able to efficiently process and present exogenous antigen (OVA protein) after antigen-uptake via the mPDCA-1 receptor. Therefore highly pure PDCs were enriched from spleen by MACS technology and subsequently sorted by FACS into B220⁺ and Siglec-H⁺ or Ly-6C⁺ cells. As shown in Fig. 4.3.4A, PDC purity normally reached over 97-99%, whereas cross-contamination of cDCs as determined by CD11c⁺ cell phenotyping was below 0.5% (data not shown). Isolated PDCs were incubated with anti-mPDCA-1-F(ab)₂-OVA targeting construct or OVA-conjugated to isotype-matched irrelevant rat IgG F(ab)₂ fragment - thereafter named control OVA construct - in the presence or absence of a CpG stimulus for 15 hours. CFSE-labeled CD4⁺ T cells from OT-II mice (>95% purity) were then added to PDCs at a T cell:PDC ratio of 2:1 and subsequently co-cultured for additional 72 hours. T cell proliferation was examined by flow cytometry. PDCs targeted via mPDCA-1 were able to induce a strong antigen-specific CD4⁺ T cell response (Fig. 4.3.5A). In contrast, PDCs incubated with equal amounts of either soluble OVA (data not shown) or OVA control construct or in the absence of antigen did not result in visible T cell priming. Interestingly, only (CpG-) activated but not immature PDCs were able to prime naïve antigen-specific T cells. Stimulation with other reagents, e.g. the TLR7 agonist Loxoribine or different CpG ODNs also led to efficient T cell priming (Fig. 4.3.5B). The substantial T cell proliferation after mPDCA-1-mediated OVA uptake was comparable to OVA peptide (Fig. 4.3.5C). The titration of the antigen amount revealed that the mPDCA-1 targeting construct turned out to be an efficient vector to induce a T cell response. In a further experiment the efficiency of the antigen-uptake was investigated. To evaluate the required duration of antigen presence, the anti-mPDCA-1-F(ab)₂-OVA targeting

construct was washed out from the co-culture after different time points. We found that the antigen had to be present at least for more than 15 hrs to elicit an efficient CD4⁺ T cell priming (Fig.4.3.5D). The maximum T cell response was induced if the antigen was present more than 36 hrs.

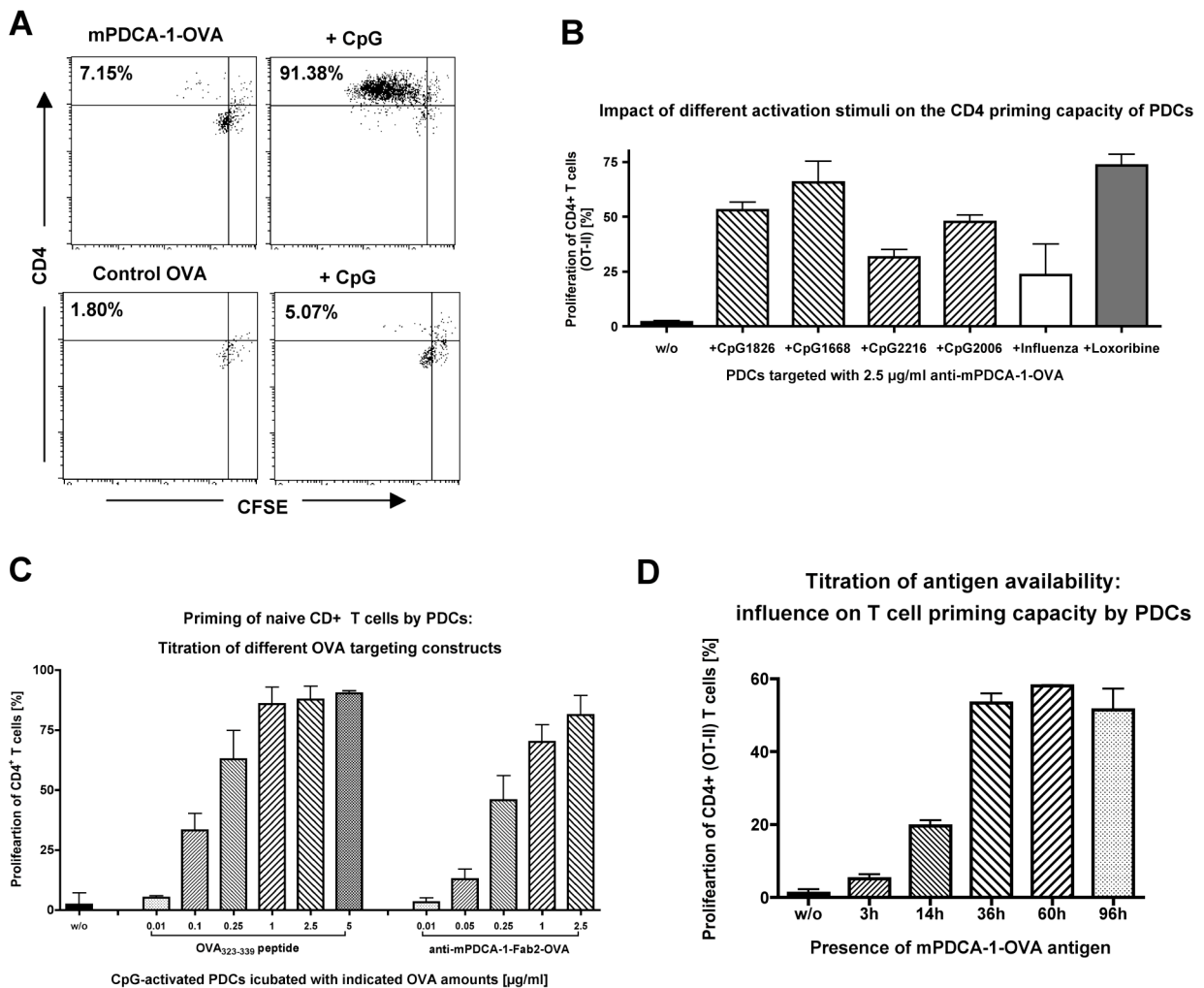


Fig 4.3.5 Murine PDCs targeted with OVA antigen via mPDCA-1 prime antigen-specific CD4⁺ T cells.

(A) To show PDC-induced T cell priming, PDCs were targeted with anti-mPDCA-1-F(ab')₂-OVA or isotype matched control F(ab')₂-OVA (2.5 µg/ml OVA each). Cells were cultured in the absence or presence of CpG (5 µg/ml). 15 hrs later PDCs were co-cultured with CFSE-labeled CD4⁺ T cells from OT-II mice (in a PDC:T cell ratio of 1:2). Shown in the dotplots is the proliferation of CD4⁺ T cells after 72 hrs, thereby gated on viable TCR⁺ B220⁻ CD4⁺ cells.

(B) **Impact of different activation stimuli on the CD4⁺ T cell priming capacity of PDCs.** PDC:T cell co-culture was performed as described before with targeting OVA via mPDCA-1. Bar diagram indicates the influence of additional stimuli on PDC-induced T cell proliferation.

(C) **Bar diagram compares the efficiency of different OVA targeting constructs.** PDCs were incubated with titrated amounts of OVA peptide or mPDCA-1 targeting construct and activated with CpG before co-culture with naive T cells. Shown is the median T cell proliferation and range after 72 hrs co-culture (n=2-4).

(D) **Influence of the antigen availability on the T cell priming capacity of PDCs.** PDC:T cell co-culture was performed as described before modifying the time of antigen presence: anti-mPDCA-1-F(ab')₂-OVA was washed out after indicated times or not. Shown in the bar diagram is the proliferation of naive CD4⁺ T cells after 72 hrs.

These results were generated not only in C57BL/6 background but also PDCs isolated from Balb/c mice were able to efficiently prime OVA-specific CD4⁺ T cells from DO11.10 mice (data not shown).

4.3.3.3 Priming capacity of PDCs from different lymphoid organs

To analyze the priming capacity of PDCs from different lymphatic tissues, PDCs were isolated from lymph nodes, spleen, and bone marrow or were generated *in vitro* from FL cultures. PDCs were targeted with anti-mPDCA-1-F(ab')₂-OVA targeting construct and co-cultured with antigen-specific T cells in the presence of a CpG stimulus as described above. In Fig. 4.3.6A the proliferation of CFSE-labeled OT-II CD4⁺ T cells is shown. Representative dotplots of PDCs from different lymphoid origins are depicted, demonstrating the proliferation of CD4⁺ T cells. The T cell proliferation initiated by PDCs isolated from LNs ranged from 58% to 78%. Spleen PDCs induce between 48% and 82% T cell proliferation, BM-PDCs between 47% and 91%, and finally *in vitro* generated PDCs 40% to 97% proliferation (Fig.4.3.6B). The overall mean proliferation ranged from 72% to 82%. These results indicated that activated PDCs from all lymphoid origins tested have a similar stimulatory capacity and were able to efficiently prime CD4⁺ T cells.

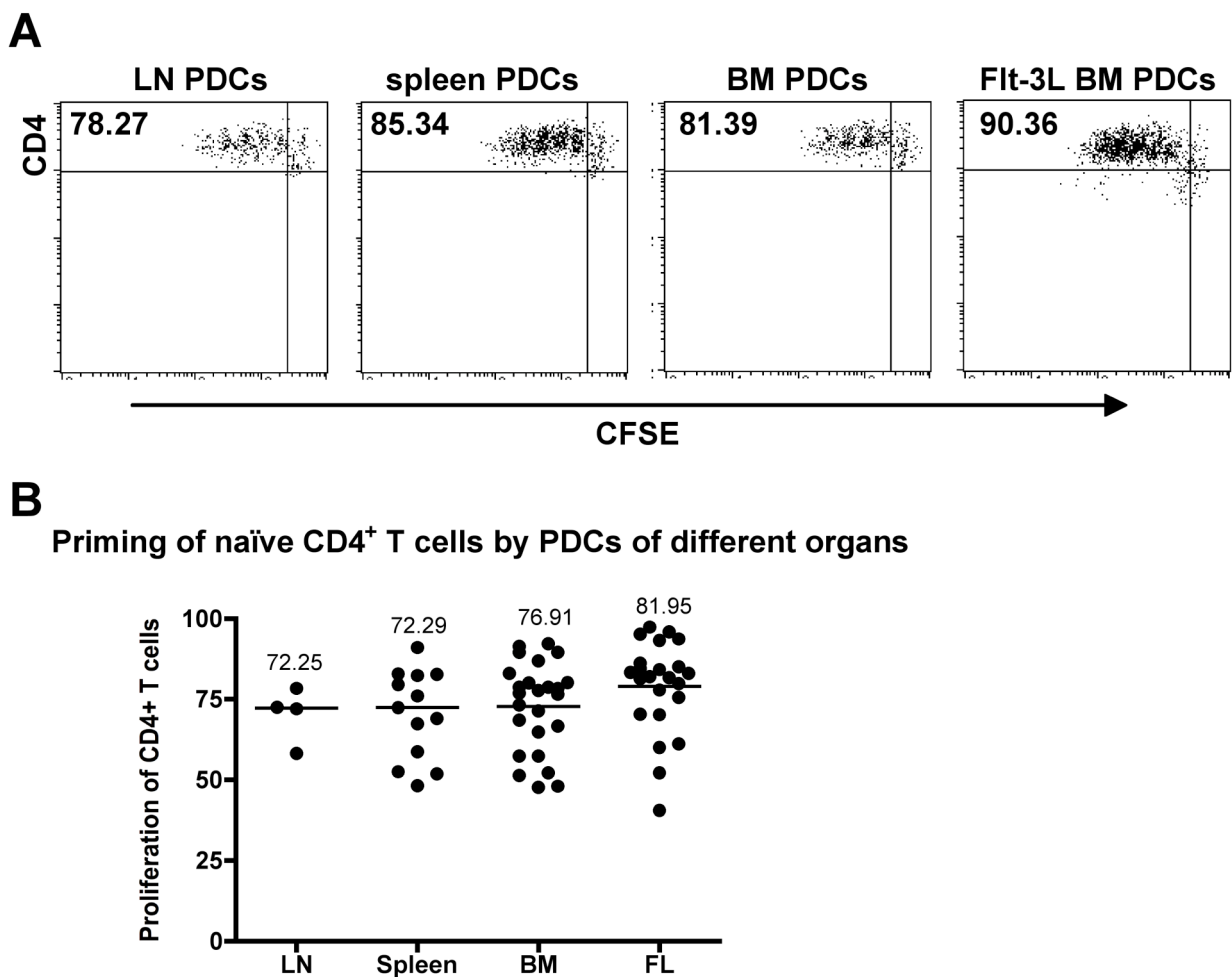


Figure 4.3.6 PDCs from different lymphoid organs have similar capacities to prime naïve CD4⁺ T cells *in vitro*.

(A) PDC:T cell co-culture was performed as described before. In contrast to previous experiments, here PDCs were isolated from different lymphoid organs. Shown is the proliferation of naïve CD4⁺ T cells after 72 hrs of co-culture with mPDCA-1-OVA targeted and CpG-activated PDCs.

(B) Scatter diagrams summarize the priming capacities of PDCs derived from several lymphoid organs. Values represent mean proliferation of OVA-TCR^{tg} CD4⁺ T cells from (A).

4.3.4 PDC-induced (cross-) priming of CD8⁺ T cells *in vitro*

4.3.4.1 Cross-presentation and –priming capacity of mouse PDCs

PDCs were often regarded to support CD8⁺ T cell priming by secretion of type I interferons [Yoneyama H, JEM 2005; Le Bon A, Nat Immunol 2003], which further activates/sharpens the cross-priming machinery of bystander APCs [Lapenta C, EJI 2006]. However, there were reports showing that only SIINFEKL-loaded PDCs are able to stimulate CTLs via peptide:MHC-I complexes, but not OVA protein loaded PDCs. Thus, a direct evidence of the cross-priming capacity remains controversial [Lou Y, JI 2007; Liu C, J Clin Invest. 2008; Schlecht G, Blood 2004].

Here, isolated spleen PDCs were loaded with antigen and co-cultured with isolated and CFSE-labeled CD8⁺ T cells from OT-I mice (as described in analogy to the CD4⁺ T cell experiments). Based on the previous experiments, PDCs were either left unstimulated or were activated with CpG. As shown in Fig. 4.3.7A, in the absence of antigen PDCs did not induce a T cell response, also upon CpG-activation. In contrast, SIINFEKL peptide-loaded PDCs were strongly stimulating CD8⁺ T cells. In this case, an additional stimulus showed no effect as also unstimulated PDCs presented the (exogenously loaded) peptide for efficient T cell priming. But if antigen was taken up via mPDCA-1, only activated PDCs efficiently cross-prime T cells, whereas soluble OVA [data not shown] or OVA conjugated to isotype-matched control antibody were unable to induce a significant T cell proliferation. At least higher concentrations were needed to induce similar responses (Fig. 4.3.7A+B). In all experiments in which PDCs had been incubated with OVA protein and had to process the antigen, a stimulus was required for optimal cross-presentation and T cell priming.

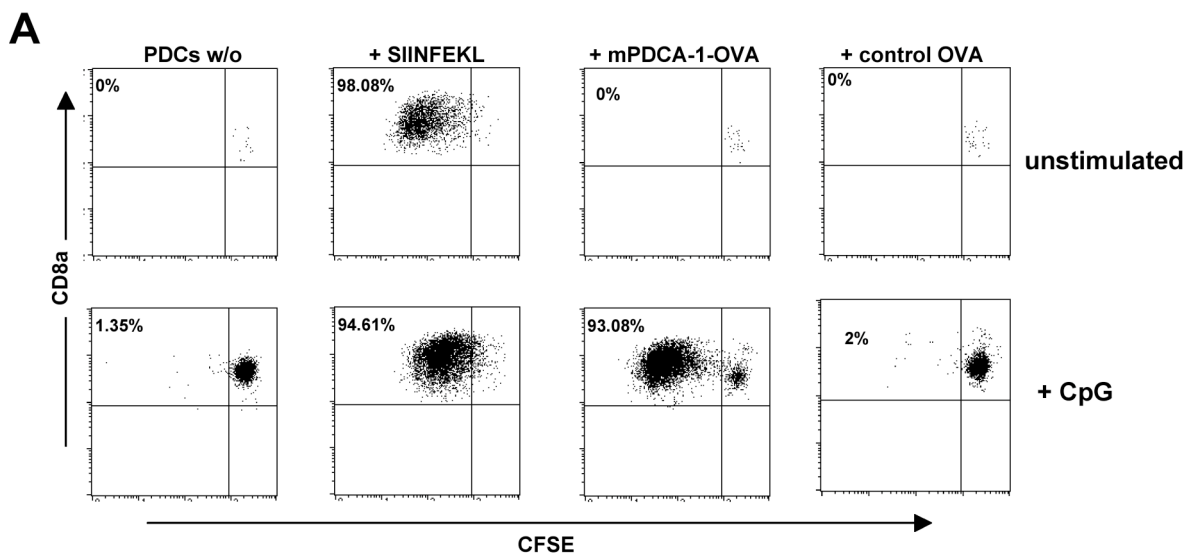


Figure 4.3.7. CD8⁺ T cell proliferation showing the cross-priming capacity of murine PDCs.

(A) *In vitro* cross-priming of naive CD8⁺ T cells by PDCs. Shown in the dotplots is a representative overview of the CD8⁺ T cell proliferation (OT-I) after 72 hrs co-culture with isolated spleen PDCs. PDCs were either left untreated or incubated in the presence of SIINFEKL peptide, anti-mPDCA-1-F(ab')₂-OVA or OVA-conjugated to irrelevant rat F(ab')₂ for 15 hrs. If indicated PDCs receive an additional CpG stimulus (5 µg/ml CpG 1826). After this time period, highly pure (>95%) CFSE-labeled CD8⁺ T cells from OT-I mice were added to PDCs and co-cultured for additional 72 hours. T cell proliferation was examined by flow cytometry. Dotplots show a representative overview of CD8⁺ T cell proliferation induced by spleen PDCs.

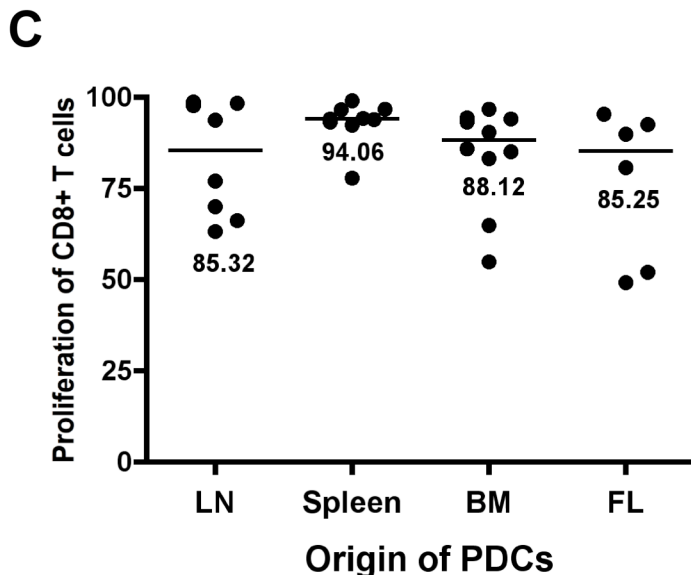
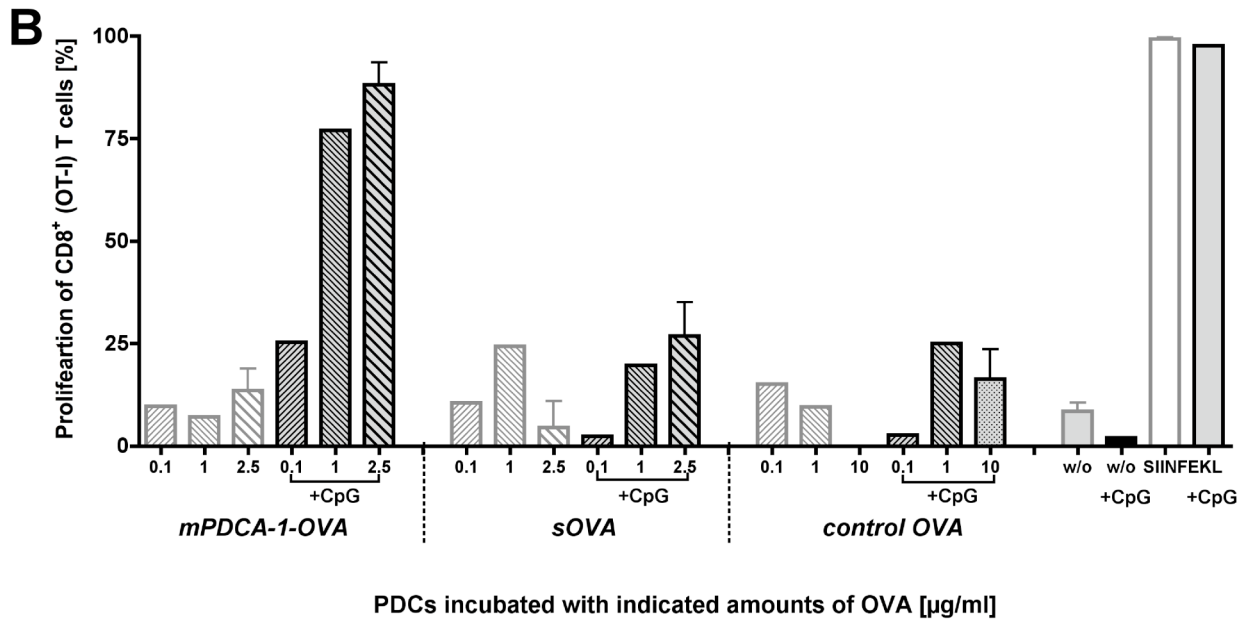


Figure 4.3.7. CD8⁺ T cell proliferation showing the cross-priming capacity of murine PDCs.

(B) Priming of naive CD8⁺ T cells by PDCs after targeting with different OVA constructs. To compare the efficiency of different OVA targeting constructs PDCs were incubated with titrated amounts of soluble OVA, anti-mPDCA-1-F(ab')₂-OVA, and isotype control F(ab')₂-OVA before co-culture with CFSE-labeled OVA-transgenic CD8⁺ T cells. Shown is the proliferation after 72h hrs of co-culture (mean and standard deviation of n=1-4).

(C) Cross-priming capacities of PDCs from different lymphoid organs. PDCs from different lymphoid organs or generated *in vitro* were isolated and incubated in the presence of anti-mPDCA-1-F(ab')₂-OVA and CpG stimulus. PDCs were then co-cultured with CD8⁺ T cells to compare their cross-priming capacities. Scatter diagram shows the T cell proliferation after 72 hrs (n=6-9). Values represent mean proliferation of CD8⁺ T cells after co-culture.

4.3.4.2 Cross-priming capacity of PDC from different lymphoid organs

By comparing the cross-priming efficiency of PDCs from different lymphoid tissues, Fig. 4.3.7C indicates that there were no considerable differences in the capacity of PDCs to induce proliferation of naive CD8⁺ T cells: LN-PDCs induced 63-98% proliferation, PDCs from spleen demonstrated 78-99%, PDCs isolated from BM or generated *in vitro* (FL-PDCs) induced 55-97% and 52-95% proliferation, respectively. The mean proliferation ranged between approximately 85-95%.

4.3.5 Receptor blocking elucidates specificity of mPDCA-1-mediated antigen delivery for priming of CD4⁺ and CD8⁺ T cells

To show the specificity of antigen-uptake and processing via mPDCA-1, the receptor was blocked with excess of unconjugated anti-mPDCA-1 mAb during incubation with anti-mPDCA-1-F(ab')₂-OVA. CpG-stimulated PDCs were then co-cultured with either CD4⁺ or CD8⁺ T cells as mentioned before. Fig. 4.3.8A+B shows that blocking the receptor almost abolished the CD4⁺ T cell priming. The mean proliferation was reduced from 71.01% (+/-5.33) to 2.43% (+/-0.51). In addition, proliferation of CD8⁺ T cells induced by anti-mPDCA-1-F(ab')₂-OVA-targeted PDCs was markedly inhibited (up to 95%) by blocking the receptor: 83.55% (+/-6.37) vs. 9.43% (+/-3.16) (Fig. 4.3.8A+B). On the other hand, mPDCA-1 blocking had no effect on the uptake and processing of (high doses of) soluble OVA or the presentation of OVA peptide (data not shown), indicating that the inhibition of T cell priming after blocking the mPDCA-1 receptor did not influence other pathways involved in antigen presentation.

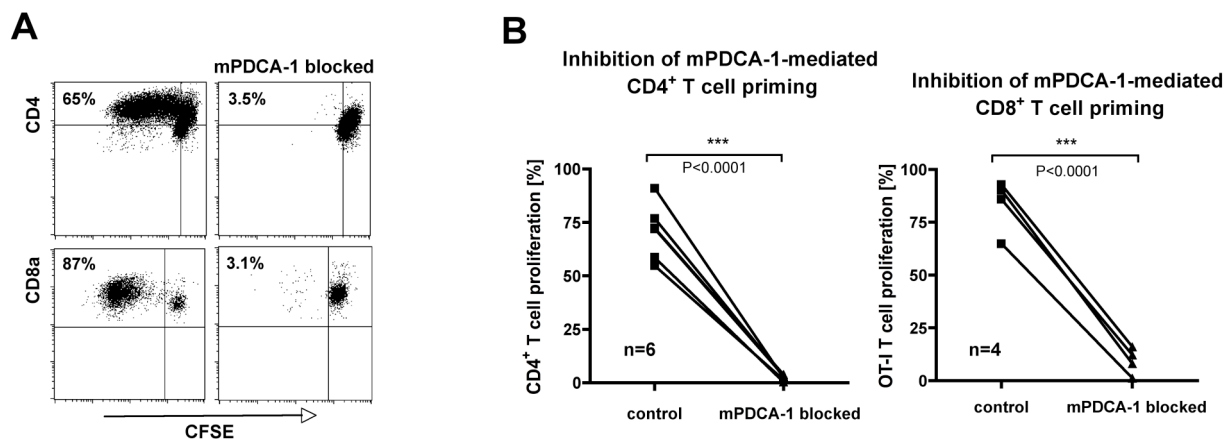


Figure 4.3.8 Receptor blocking abolishes mPDCA-1-mediated priming of both CD4⁺ and CD8⁺ T cells.

PDCs were loaded with anti-mPDCA-1-F(ab')₂-OVA and activated with CpG ODN 1826 before co-culture with OVA-specific, CFSE-labeled CD4⁺ or CD8⁺ T cells as described earlier. To block the receptor, PDCs were incubated with excess of unconjugated anti-mPDCA-1 mAb (100 µg/ml) before adding the antigen.

(A) Representative dotplots give an impression of T cell proliferation after mPDCA-1 mediated antigen-uptake (*left dotplots*) or after blocking the receptor (*right dotplots*).

(B) Scatter diagrams summarize the effect of mPDCA-1 receptor blocking on antigen-specific CD4⁺ or CD8⁺ T cell proliferation. Here, unblocked priming experiments were compared to experiments in which mPDCA-1 was blocked. Shown is the relative T cell proliferation.

In summary, these results indicated that mPDCA-1 might serve as a specific antigen uptake receptor for PDCs delivering its ligands for both MHC-I and MHC-II presentation.

4.3.6 PDC activation: Up-regulation of co-stimulatory and MHC molecules (maturation)

The experiments above demonstrated a strong effect of CpG and other TLR agonists on the priming capacities of PDCs. The influence of TLR7 and TLR9 triggering on the activation of these cells was of particular interest. Therefore, murine PDCs were activated with TLR ligands (Loxoribine or numerous CpG oligonucleotides) *in vitro*. After 24 and 48 hours, respectively, CD80 and CD86 expression on PDCs was determined by flow cytometry. Although there were

differences in the kinetics, Fig. 4.3.9A demonstrated a strong upregulation of the co-stimulatory molecules CD80 and CD86 upon activation *in vitro* with all CpG ODNs or Loxoribine. Administration of anti-CD40 mAb (clone FGK45.5) did not show significant effects *in vitro*. Interestingly, mouse (B type) CpG ODNs 1826 and 1668 as well as Loxoribine gave a slightly better impact compared to human CpG ODNs 2006 (B type) and 2216 (A type). In contrast, the amount of secreted interferon alpha was comparable between all CpG types (data not shown). This activation pattern was also observed by evaluation of further activation indicators (CD69), the co-inhibitory marker PD-L1 (also known as B7-H1 or CD274) as well as MHC-I and -II molecules, as was evident by Fig. 4.3.9B.

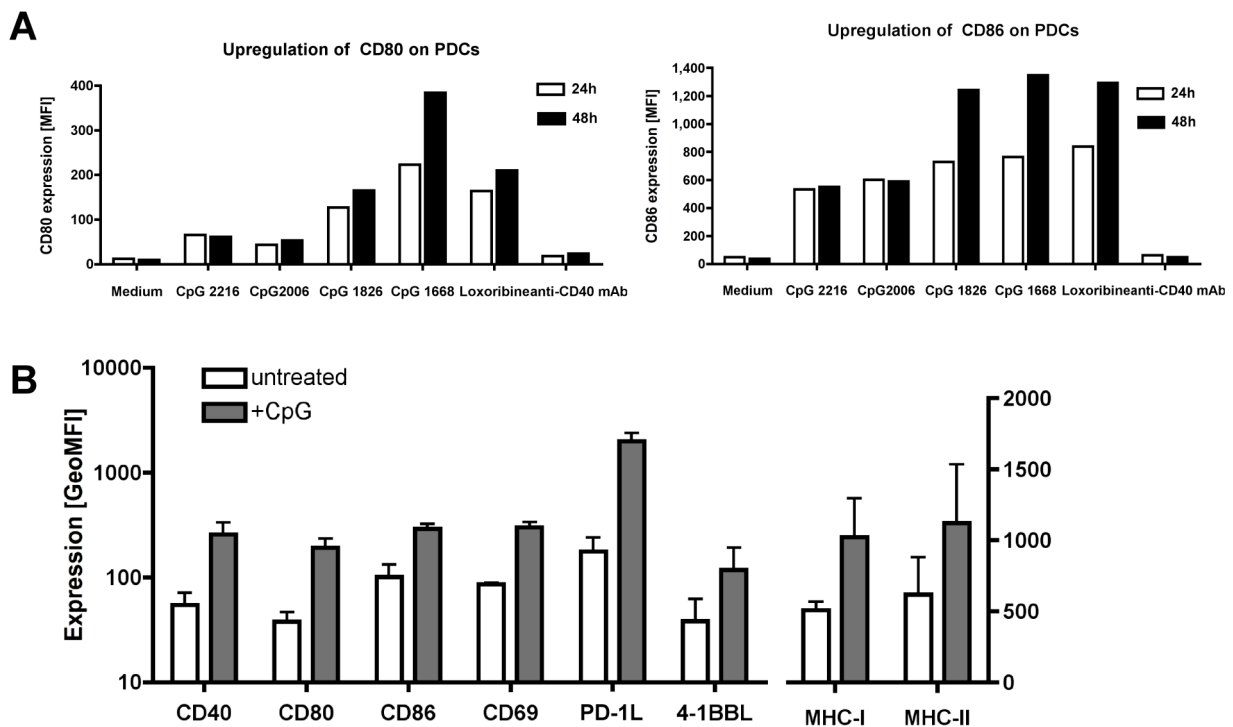


Figure 4.3.9 *In vitro* activation and maturation of PDCs.

(A) **Effect of different stimuli on the expression of CD80 and CD86 on PDCs.** BM-PDCs were cultured in medium alone or in the presence of different stimuli (5 $\mu\text{g}/\text{ml}$ CpG, 20 mM Loxoribine, and 25 $\mu\text{g}/\text{ml}$ anti-CD40 mAb). Flow cytometric analysis was performed 24 and 48 hrs later, respectively. Bar diagram shows the mean fluorescence intensity of CD80 and CD86 expression on PDCs, respectively (n=2).

(B) **TLR9 triggering resulted in upregulation of activation markers.** Effect of *in vitro* CpG stimulation on the expression of CD40, CD80, CD86, CD69, CD274 (PD-L1), 4-1BBL, as well as MHC class I and II molecules on PDCs. Bar diagram demonstrates the relative expression [mean fluorescence intensity] of indicated markers of either medium-cultured or CpG-activated PDCs after 24 hrs as obtained by flow cytometric analysis. For co-stimulatory molecules and activation markers the y-axis is drawn is logarithmic scale, whereas the expression of MHC molecules is displayed linearly. Shown is the mean \pm SEM of n=4.

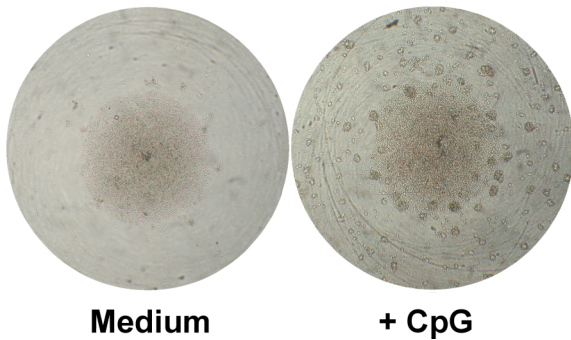
C

Figure 4.3.9 *In vitro* activation and maturation of PDCs.

(C) Purified PDCs are cultured in the absence or presence of a stimulus (5 $\mu\text{g/ml}$ CpG). 10^5 PDCs/ $100\mu\text{l}$ are seeded into 96-well culture plates and cultured for 24 hrs. Shown is a representative microscopic survey of untreated PDCs and activated PDCs demonstrating cluster formation.

Taken together the stimulation of PDCs with TLR7 and TLR9 ligands resulted in an efficient upregulation of common co-stimulatory or co-inhibitory molecules, activation markers and MHC molecules, representing an activated state of PDCs. Beside these phenotypical changes also morphological modifications were apparent *in vitro*. In particular, CpG-activation of PDCs resulted in a typical “cluster formation” as shown in Fig. 4.3.9C. This phenomenon had also been described by Carine Asselin-Paturel for PDCs under inflammatory conditions (unpublished observations).

4.3.7 PDC activation: Impact on antigen processing capacity?

The above data demonstrate that PDCs loaded with OVA peptide or protein can prime naïve CD4^+ and CD8^+ T cells. Referring to the basic necessity of an additional PDC stimulation for efficient T cell priming it was still unclear to which degree this activation influenced only the upregulation of co-stimulatory molecules (see chapter 4.3.6) or led to an onset of the antigen processing and presentation machinery. Surprisingly, if PDCs were loaded exogenously with OVA peptide, an extra stimulation had no effect on the presentation capacity of PDCs, as demonstrated by identical CD4^+ (Fig. 4.3.10A) or CD8^+ T cell proliferation (Fig. 4.3.7A+B). A possible explanation could be that in this case the upregulation of co-stimulatory molecules was irrelevant and the activation influenced (only) the processing pathway.

Expecting that an additional stimulus would have a significant effect on the priming capacity of PDCs at lower peptide concentrations, the following experiment was performed. PDCs were loaded with titrated amounts of OVA peptide in the presence or absence of a stimulus before co-culture with naïve CD4^+ T cells. The results of the T cell proliferation showed that also at lower peptide concentrations no differing priming capacity was observed for activated or unstimulated PDCs. In general, below a certain threshold of the antigen dose no visible T cell proliferation was detected (Fig. 4.3.10B). Thus, the above hypothesis could not be confirmed and the impact of an additional PDC stimulation on the antigen processing and presentation or T cell priming capacity was still not resolved.

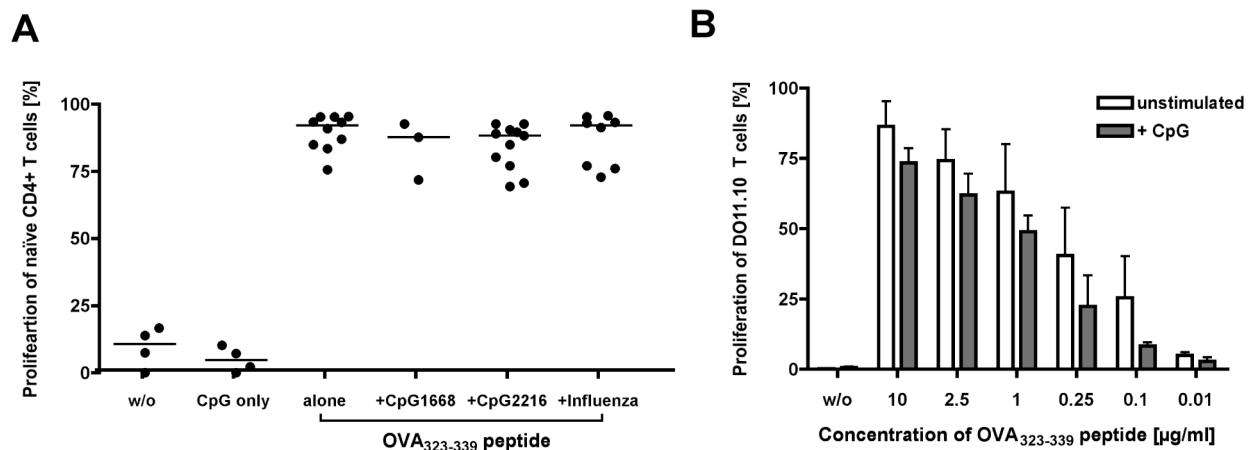


Figure 4.3.10 Influence of PDC activation on the T cell priming capacity.

(A) **Influence of additional activation on the peptide presentation of PDCs.** Where indicated, isolated PDCs were loaded with 5 µg/ml OVA₃₂₃₋₃₃₉ peptide and optionally received an additional stimulus, as described before. The scatter diagram shows T cell proliferation after 72 hrs co-culture with OVA-specific CD4⁺ T cells. Displayed line represents median of T cell proliferation.

(B) **Impact of PDC activation on the peptide presentation capacity as demonstrated by CD4⁺ T cell priming.** To analyze if an additional stimulus is required for the presentation of peptides in lower concentrations, PDCs were incubated with titrated amounts of OVA₃₂₃₋₃₃₉ peptide and then co-cultured with naive CD4⁺ T cells in the absence or presence of a CpG stimulus (5 µg/ml). Bar diagram shows the resulting T cell proliferation after 72 hrs. Demonstrated is the mean and range of n=3.

At this point the following assumptions were hypothesized: In principle, PDCs were able to efficiently present exogenously loaded OVA peptide to T cells, independently of their activation status but this activation influenced the processing/presentation of OVA protein. To confirm this hypothesis processed OVA should be detected on MHC-I molecules via an anti-H-2k^b:SIINFEKL specific mAb only if PDCs were activated. This mAb adequately stained SIINFEKL-loaded PDCs as shown by FACS analysis in Fig. 4.3.11A (and other dendritic cells; data not shown). Interestingly, additional CpG-activation further increased the signal intensity for peptide-loaded MHC-I molecules (Fig. 4.3.11B), possibly by upregulation of the MHC expression (Fig. 4.3.9B). Further experiments revealed the specificity of the antibody by blocking the staining, and demonstrated the detection limit of the antibody, which was about 5-50 ng/ml (Fig. 4.3.11C). In contrast, processed OVA was never detected on MHC-I molecules of PDCs and other professional APCs, although high (unphysiological) OVA concentrations were used. This may reflected the limited sensitivity of the antibody or the low amount of processed SIINFEKL sequences (Fig. 4.3.11D and data not shown).

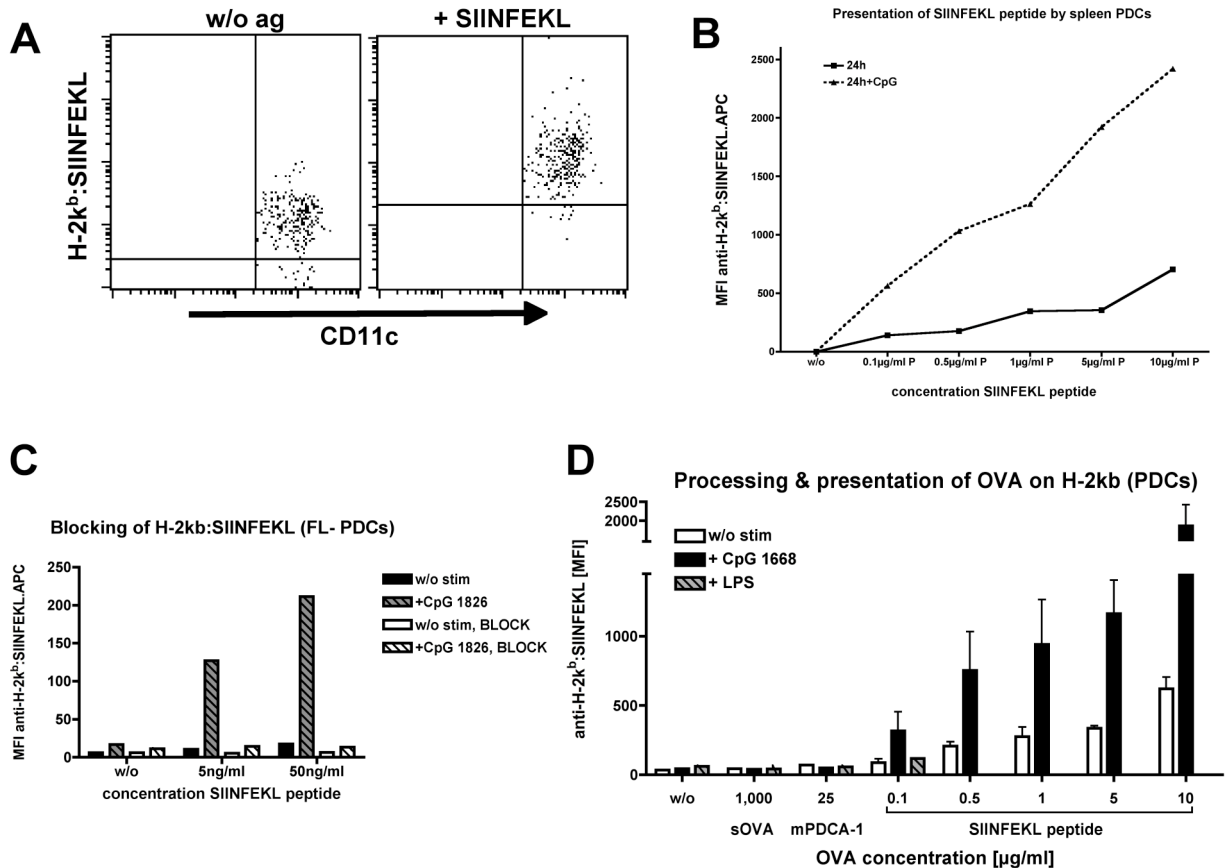


Figure 4.3.11 Detection of processed OVA antigen in the context of MHC-I on PDCs.

(A) Flow cytometric analysis of anti-H-2k^b:SIINFEKL mAb staining (clone 25D1). Isolated PDCs from C57BL/6 mice were cultured in the presence or absence of SIINFEKL peptide (100 ng/ml) and were stained for CD11c expression and SIINFEKL peptide in the context of MHC-I molecules on the next day.

(B) CpG effect on SIINFEKL-MHC-I loading. PDCs were loaded with titrated amounts of SIINFEKL peptide in the absence or presence of CpG ODN 1826 [5 μg/ml]. Anti-H-2k^b:SIINFEKL staining was performed 24 hrs after loading. Graph shows the mean fluorescence intensity of anti-H-2k^b:SIINFEKL staining as assessed by flow cytometric analysis.

(C) Blocking of H-2kb:SIINFEKL staining. SIINFEKL-loaded PDCs were stained with anti-H-2k^b:SIINFEKL mAb in the presence or absence of excess of unconjugated anti-H-2kb:SIINFEKL mAb (c_{fin} =100μg/ml) before flow cytometric analysis.

(D) MHC-I presentation of processed OVA antigen on PDCs. PDCs were cultured for 24 hrs with titrated amounts of SIINFEKL peptide, soluble OVA or OVA conjugated to anti-mPDCA-1-F(ab')₂ targeting construct in the presence or absence of different stimuli. Bar diagram demonstrates flow cytometric analysis of anti-H-2k^b:SIINFEKL stainings on PDCs as described before.

Thus, these experiments did not resolved the influence of an additional activation on PDC-induced T cell priming, and both hypotheses (the requirement of a second signal by co-stimulatory molecules and the effect on the antigen processing and presentation machinery) were still questionable.

4.3.8 Cytokine production of expanded CD4⁺ T cells after PDC-mediated priming

Conventional and plasmacytoid DCs differed in their role to initiate adaptive T cell responses. It has been shown that PDCs were able to induce proliferation of antigen-specific, naïve CD4⁺ T cells after mPDCA-1 targeting [Sapoznikov A, JEM 2007]. Hereby the T cell priming was

associated with generation of cytokine-producing effector (memory) T cells, whereas also abortive T cell responses or anergy had been reported [Hawiger D, JEM 2001; Itano AA, Nat Immunol 2003; Sporri R, Nat Immunol 2005]. Therefore the cytokine production and polarization pattern was investigated after restimulation of effector-memory CD4⁺ T cells that had been initially primed with mPDCA-1-OVA-targeted, CpG-activated PDCs *in vitro*. T_H1-polarized CD4⁺ T helper cells were characterized by the production of TNF α and IFN γ whereas the presence of IL-4, IL-5, IL-10, and IL-13-producing cells would suggest a T_H2 polarization.

The appearance of T cells producing IL-2, TNF α , and IFN γ demonstrated that under these circumstances mainly a T_H1-polarization occurred. The secretion of this characteristic cytokines was shown by representative intracellular stainings in Fig. 4.3.12A. No difference between PDCs that were loaded with OVA peptide or targeted with anti-mPDCA-1-OVA or isotype control mAb conjugated to OVA protein could be detected.

Few IL-4 producing T cells (T_H2) were detected (Fig. 4.3.12B) only if peptide-loaded PDCs (but not spleen cells) were used. In contrast, PDCs incubated with the mPDCA-1 targeting construct did not induce the generation of IL-4 producing T cells.

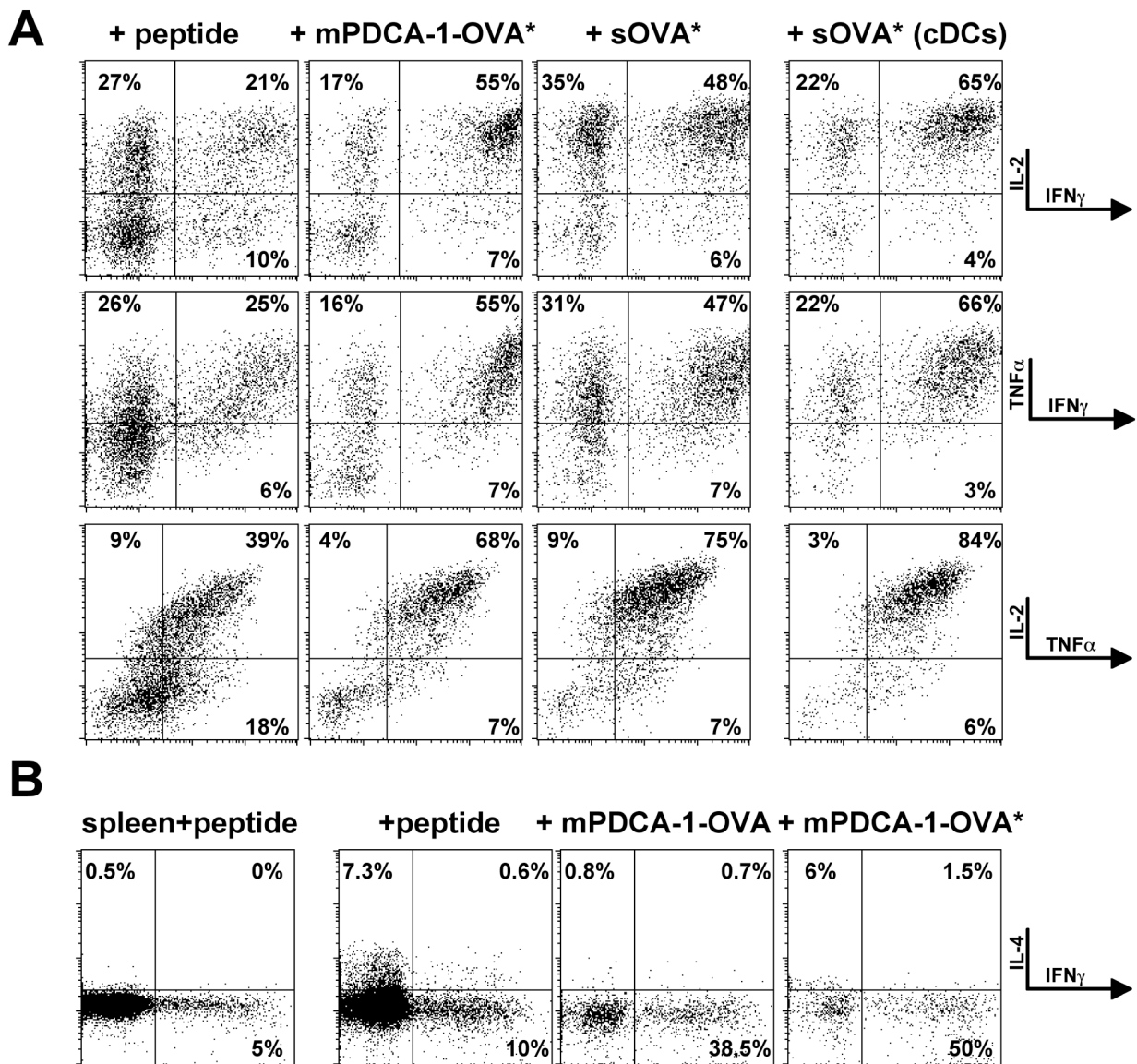


Figure 4.3.12 Cytokine profile of restimulated CD4⁺ T cells after PDC-mediated priming.

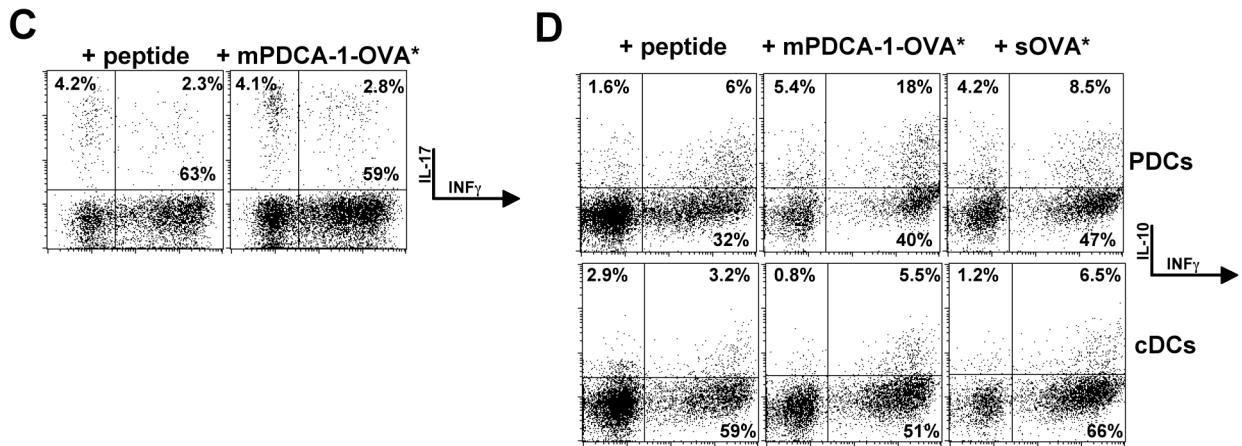


Figure 4.3.12 Cytokine profile of restimulated CD4⁺ T cells after PDC-mediated priming.

CSFE-labeled CD4⁺ T cells (isolated from OT-II or DO11.10) were primed with (CpG-activated) syngenic PDCs after targeting OVA via mPDCA-1 as described earlier. 72 hrs after initial proliferation, T cells were expanded for additional seven days in the presence of recombinant human IL-2. One day after removal of IL-2, T cells were restimulated with PMA/Ionomycin for 6 hrs prior to assessment of intracellular cytokine production by flow cytometric analysis. Resulting cytokine profiles are representatives of at least three independent experiments. Asterisks indicate that priming occurred in the presence of CpG.

(A) T_H1 cytokine profile of PDC- and cDC-primed T cells shown by intracellular staining of IL-2, IFN γ , and TNF α .

(B) T_H2 cytokine profile evaluated by intracellular staining of IL-4 vs. IFN γ after initial priming by PDCs and splenocytes.

(C) Secretion of IL-17 and IFN γ (shown are intracellular stainings) upon PDC-induced priming.

(D) IL-10 and IFN γ -producing CD4⁺ T cells were assessed comparing the outcome after PDC- and cDC-induced priming. cDCs are represented by CD11c^{high} cells isolated from spleen.

Among the classical T_H1/T_H2 polarization, T cells were recently classified into other subsets according to the cytokine production and their function. Here, also the presence of IL-17-producing T cells was evaluated (~7%; see Fig. 4.3.12C), demonstrating the induction of so-called T_H17 cells [Harrington LE, *Curr Opin Immunol* 2006]. In general, after PDC-initiated priming the majority of resulting CD4⁺ T cells (50-75%) secrete IFN γ upon restimulation. Interestingly, about 10-20% of all CD4⁺ T cells were IFN γ IL-10 double-positive (Fig. 4.3.12D). The generation of these IFN γ ⁺ IL-10⁺ T cells was preferably induced by PDCs but not cDCs. These cells might have a regulatory function. The production of the anti-inflammatory cytokine IL-10 is normally restricted to the T_H2 lineage, but can also be secreted by regulatory T cells (such as Treg and Tr1) [Groux H, *Jl* 1997; Asseman C, *JEM* 1999; de la Rosa M, *EJI* 2004].

In summary, these data revealed that after targeting OVA antigen to mPDCA-1, PDCs initiated a functional CD4⁺ T cell immune response dominated by a T_H1 phenotype. Beside the classical polarization and independent of the route they had acquired the antigen, PDC-mediated T cell priming also led to the generation of recently reported T_H17 and IL-10⁺ IFN γ ⁺ cells, which might support the role of PDCs in tolerance as well autoimmune diseases.

4.3.9 Conclusion

Although PDCs were believed to link innate and adaptive immune responses by production of type I interferon, it remained controversial whether PDCs were in fact able to prime naïve T cells. Here the function of the recently described PDC-specific receptor mPDCA-1 investigated as well as the potential of PDCs to induce naïve CD4⁺ and CD8⁺ T cell responses after targeting a model antigen (Ovalbumin) to mPDCA-1.

Targeting of PDC with OVA-conjugated anti-mPDCA-1 mAb, but not with an equivalent amount of soluble OVA or OVA conjugated to isotype control antibody, resulted in strong proliferation of OVA-specific naïve CD4⁺ T cells. The same was observed for OVA-specific naïve CD8⁺ T cells showing that PDCs were capable of cross-priming exogenous antigens. Blocking the receptor with excess of unconjugated anti-mPDCA-1 mAb inhibited priming of CD4⁺ and CD8⁺ T cells. These results indicated that mPDCA-1 might serve as an antigen uptake receptor delivering its ligands for MHC-I and MHC-II presentation. Interestingly, processing and presentation of antigens taken up via mPDCA-1 were strongly dependent on stimulation, since only activated but not immature PDC were able to prime naïve antigen-specific T cells. In contrast, antigen uptake was independent of activation as unstimulated PDC also internalized the mAb-receptor complex.

These results demonstrated that PDC could take up and process antigens for efficient priming of naïve T cells and thus combined innate and adaptive functions. Hereby mPDCA-1 served as beneficial antigen-uptake receptor for efficient antigen delivery.

4.4 Heterogeneous Sca-1 expression defines two functional different PDC subsets

4.4.1 Sca-1 is differentially expressed on PDCs

Recently it has been reported that PDCs express Sca-1 [O’Keeffe M, JEM 2002]. But neither its function in these cells nor any differential expression could be demonstrated. Here it was shown that splenic PDCs from BALB/c mice as well as other strains display a heterogeneous expression of Sca-1. About 50% of mPDCA-1⁺ PDCs expressed Sca-1 at a very high level, whereas the other PDCs failed to express or expressed intermediate levels of this molecule (Fig. 4.4.1A, middle dotplot).

Also in other lymphoid organs a differential expression of Sca-1 within the PDC population could be observed. Interestingly, the proportion of the Sca-1⁺ subsets showed an organ specific variation Fig. 4.4.1A. The frequencies of Sca-1-expressing PDCs in different lymphoid organs are summarized in Fig. 4.4.1B. Among organs tested the percentage of Sca-1⁺ PDCs was lowest in BM (10-20%) and increased through peripheral blood (20-25%) and spleen (50%) reaching its maximum in LN (70-85%), which could indicate a correlation between Sca-1 expression and the maturation/activation status of PDCs. Additionally, as shown in Fig. 4.4.1A, PDCs expressed Sca-1 at the highest level in all organs tested, when compared to other cells analyzed.

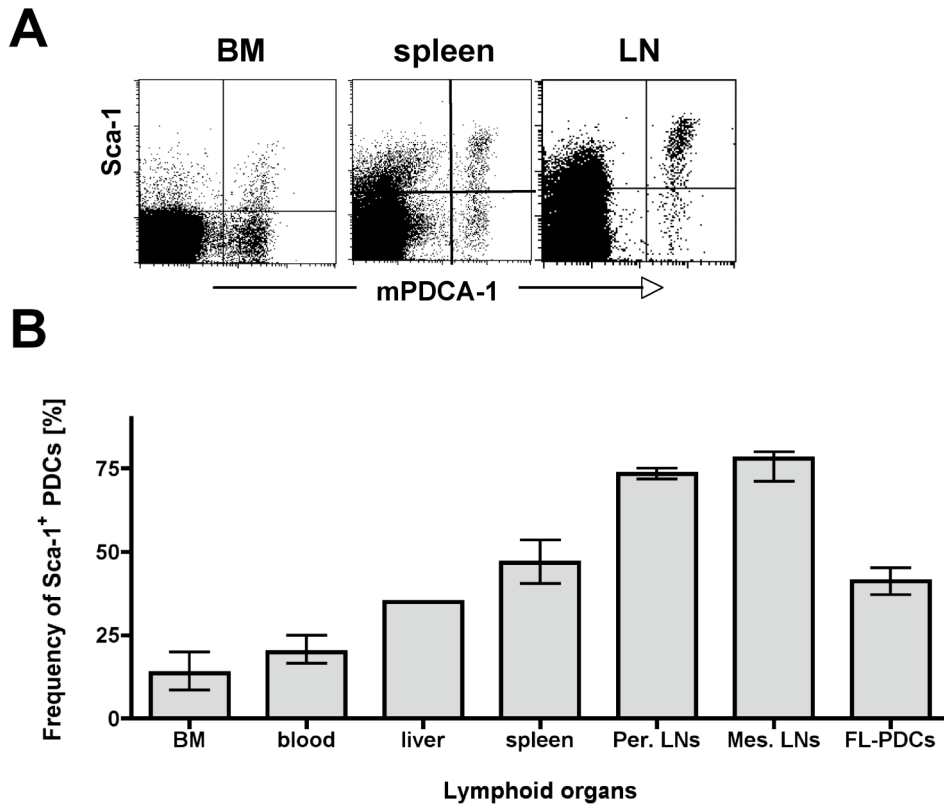


Fig 4.4.1 Heterogeneous expression of Sca-1 on PDCs.

(A) PDCs from different lymphoid organs of Balb/c mice were stained for mPDCA-1 and Sca-1. Dotplots demonstrate a representative flow cytometric analysis of the differential Sca-1 expression on PDCs within a single cell suspension from BM, spleen, and LNs.

(B) The differential Sca-1 expression on PDCs from different lymphoid organs was further analyzed by flow cytometry. The bar diagram demonstrates the percentage of Sca-1⁺ PDCs within PDCs from different lymphoid organs. Shown is the mean and SEM ($n \geq 2$, with exception of liver [$n=1$]).

In current literature there are reports showing homogeneous Sca-1 expression on PDCs [O’Keeffe M, JEM 2002]. This could be due to the fact that these studies were performed using C57BL/6 mice that are of the Ly-6.2 haplotype. Non-activated splenocytes from Ly-6.2 strains including C57BL/6, SJL, Sv129, AKR, and others show higher frequency of Sca-1⁺ cells compared to the Ly-6.1 strains such as BALB/c, C3H, NZB, and DBA [Yang L, JI 2005; Malek TR, JEM 1986; Ortega G, JI 1986; Codias EK, Immunogenetics 1989]. The high percentage of Sca-1⁺ PDCs in Ly-6.2⁺ C57BL/6 mice could induce the authors to the conclusion that the Sca-1 expression on PDCs in this strain is homogenous. Consequently, the Sca-1 expression pattern was investigated in several Ly-6.1 and Ly-6.2 mouse strains. As shown in Fig. 4.4.2, a heterogeneous expression of Sca-1 on splenic PDCs was observed in all strains tested. In mouse strains that belong to the Ly-6.2 haplotype (AKR/J, C57BL/6 or SV129 mice), the majority (75-90%) of PDCs were Sca-1⁺. In contrast, in several other strains, such as Balb/c and FVB a more balanced ratio between Sca-1⁺ and Sca-1⁻ PDCs (45-65%) was observed. In the Ly-6.1⁺ DBA/1 mice actually the majority of PDCs (~80%) failed to express Sca-1.

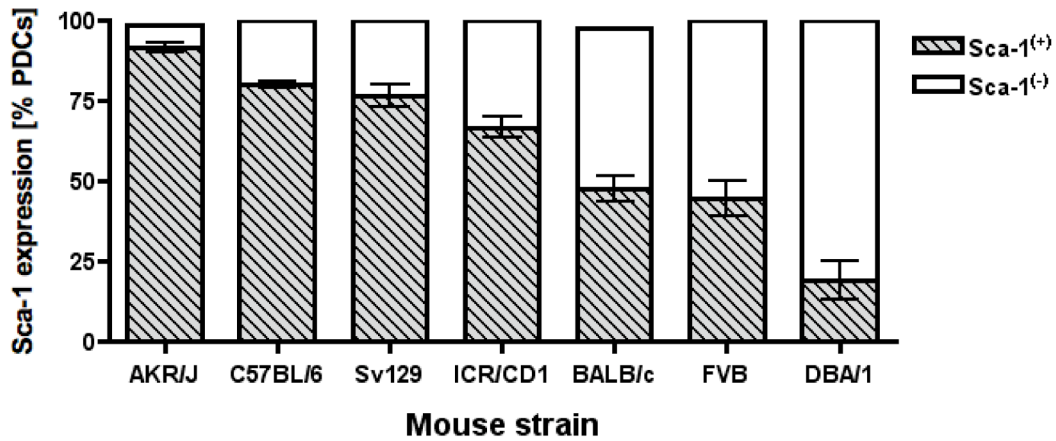


Fig 4.4.2 Strain-specific expression of Sca-1 on spleen PDCs.

Spleen PDCs were isolated from different mouse strains and stained for the expression of Sca-1. The bar diagram displays the distribution of the Sca-1 expression on PDCs as evaluated by FACS analysis. Shown are mean and SEM (n=1-5).

4.4.2 The expression of Sca-1 correlates with the developmental stage of PDCs

Sca-1 has been previously described as an important indicator for stem cell/progenitor cells and is involved in T cell differentiation and proliferation. The initial results indicated that the expression of Sca-1 on PDCs could correlate with the maturation status of PDCs, since the proportion of Sca-1⁺ PDCs was lowest in BM and increased in the peripheral tissues reaching its maximum in secondary lymphoid organs (see chapter 4.4.1).

To investigate the regulation of Sca-1 during PDC development, the incorporation of BrdU in developing PDCs was tested *in vivo*. Since PDCs in the periphery are regarded as non-dividing, resting cells [O’Keeffe M, JEM 2002], BrdU incorporation was only expected in PDCs newly developing from BM progenitors. Mice received intraperitoneal BrdU injections and four days later, BM and spleen cells were isolated and intracellular BrdU stainings were performed. Within the BrdU⁻ PDCs an equal distribution of Sca-1⁺ and Sca-1⁻ could be observed. In contrast, within the BrdU⁺ compartment the majority of PDCs (90%) failed to express Sca-1 (Fig. 4.4.3A). For BM-PDCs the majority of BrdU⁺ cells were within the Sca-1⁻ compartment.

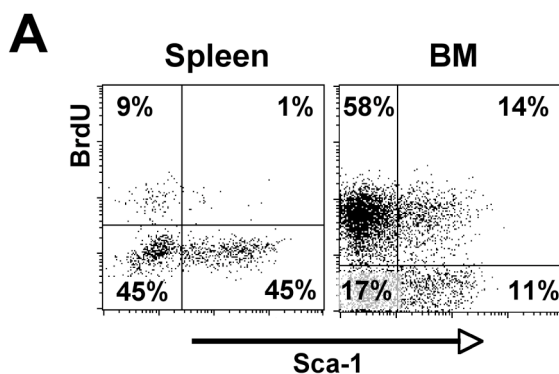
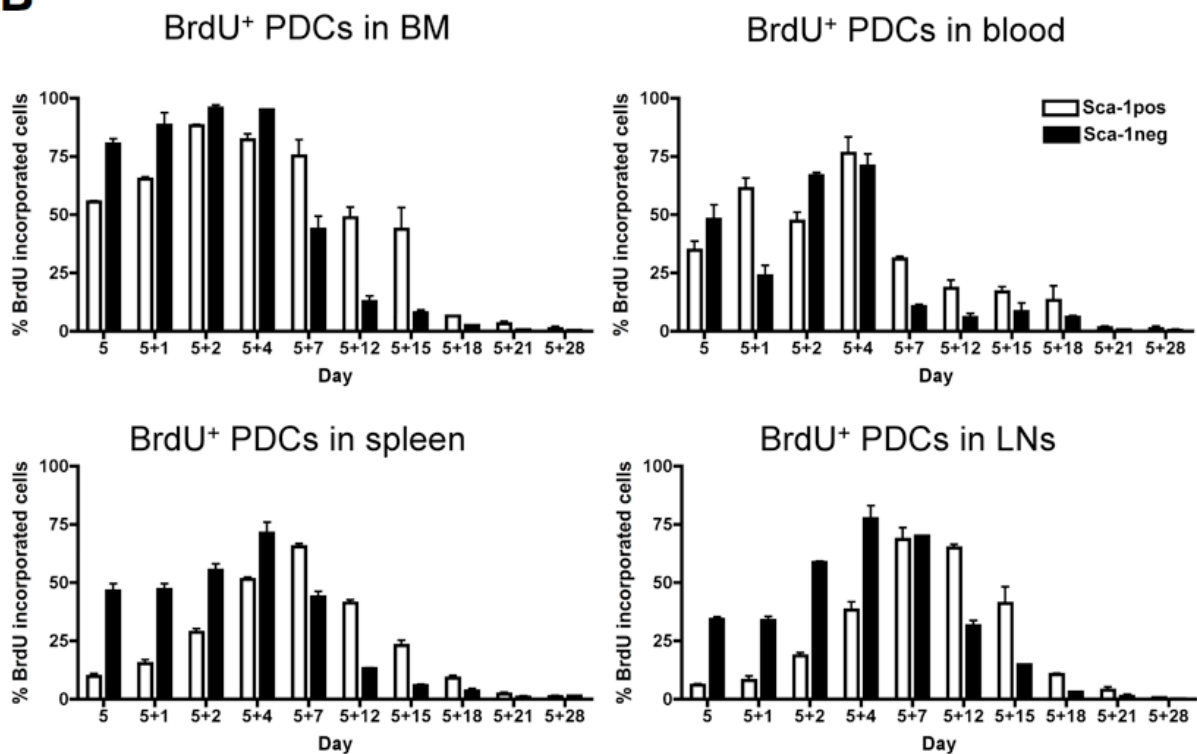


Fig 4.4.3 Correlation of Sca-1 expression and PDC proliferation.

(A). Mice received i.p. BrdU injection. Four days later single cell suspensions of spleens (left dotplot) and BM (right dotplot) were analyzed for BrdU incorporation in PDCs (gated on mPDCA-1⁺ Sca-1^{+/+}) as revealed by intracellular FACS staining. Dotplot gives a representative impression on the distribution of BrdU incorporation and Sca-1 expression in spleen PDCs.

B**Fig 4.4.3 Correlation of Sca-1 expression and PDC proliferation.**

(B) Mice received a single i.p. BrdU injection (1 mg at day 0) and BrdU was then provided in drinking water until day 5. From this day on until days 28, PDCs were isolated from indicated lymphoid organs, stained for PDC-specific marker mPDCA-1 and Sca-1 as well as intracellular BrdU to determine the BrdU incorporation. Bar diagrams represent the percentage of BrdU⁺ PDCs within both Sca-1^{+/+} subsets, showing the mean and SEM from one experiment with two animals per time point based on data from the flow cytometric analysis.

This preliminary experiment indicated that Sca-1⁻ PDCs appear earlier in the development of PDCs than the Sca-1⁺ PDCs. These data also suggested a “developmental transition” of Sca-1⁻ PDCs to Sca-1⁺ PDCs. To verify this hypothesis and to gain more data about the developmental processes and the Sca-1 expression a pulse/chase experiment was performed and the incorporation of BrdU both within the Sca-1⁻ and Sca-1⁺ compartment of PDCs was analyzed in several lymphoid organs. For this, mice received an initial i.p. administration of BrdU and this thymidine analogue was also provided in the drinking water. Five days later, BrdU was removed from the drinking water and its incorporation was flow cytometrically assessed in both Sca-1⁺ and Sca-1⁻ PDC subsets.

As expected, a higher incorporation of BrdU was detected in the Sca-1⁻ PDCs of all organs (except blood) in the first phase after removal of BrdU (Fig. 4.4.3B). In particular between days 0 and 4 after removal, in spleen and LNs the discrepancy of incorporated BrdU between Sca-1⁺ and Sca-1⁻ PDCs was biggest. Here, significantly more Sca-1⁻ than Sca-1⁺ cells were found in BrdU⁺ PDC compartment. Further differences were observed in the BM, although in this organ the BrdU incorporation should be assessed earlier. For blood PDCs an inconsistent, not-significant effect was detected. In contrast, at later times (between 7 and 15 days after BrdU removal) a shift in the proportion for BrdU⁺ between Sca-1⁺ and Sca-1⁻ PDCs was detected:

Here, the highest BrdU contingent was found in Sca-1⁺ PDCs. In general, this shift was first observed in BM, followed by spleen and LNs suggesting a transition of Sca-1⁻ to Sca-1⁺ PDCs by upregulation of this marker during their post-proliferation phase or at a more mature stage. Finally, about 15 days after BrdU removal BrdU⁺ PDCs from almost all organs disappeared, likely due to the restricted life span of PDCs of about 2-3 weeks. Another explanation might be that at this time point recently generated PDCs were excluded from the analysis as only BrdU⁺ PDCs were analyzed.

4.4.3 The expression of Sca-1 correlates with the maturation level of PDCs

The above-described results led to the suggestion that Sca-1 is differentially regulated during the life span of PDCs. In the past, Sca-1 was often described to be associated with T cell differentiation, but also cell adhesion and signaling [Codias EK, JI 1990; Flood PM, JEM 1990]. The Ly-6 family was also involved in regulation and function of T cell activation and thereby Sca-1 was expressed at high levels on T cells upon activation, regardless of the Ly-6 haplotype [Codias EK, JI 1990; Flood M, JEM 1990; Bamezai A, JI 1995]. Significantly more Sca-1⁺ PDC were detected in LNs compared to the BM, and BM-PDCs were regarded as less differentiated or activated. To test whether Sca-1 expression on PDCs correlated with the activation/maturation status, PDCs were stimulated with different TLR agonists and the expression level of Sca-1 was analyzed by flow cytometry. PDCs were isolated from spleen or BM and checked for purity and Sca-1 expression. In a first experiment, PDCs were cultured in the presence of CpG and analyzed for Sca-1 expression after 15 hrs. Comparing freshly isolated vs. CpG-stimulated PDCs, a strong upregulation of the Sca-1 expression was found after *in vitro* activation (Fig. 4.4.A). The percentage of Sca-1⁺ PDCs increased upon stimulation from 46% to 93% (spleen PDCs) and from 7% to 42% (BM-PDCs).

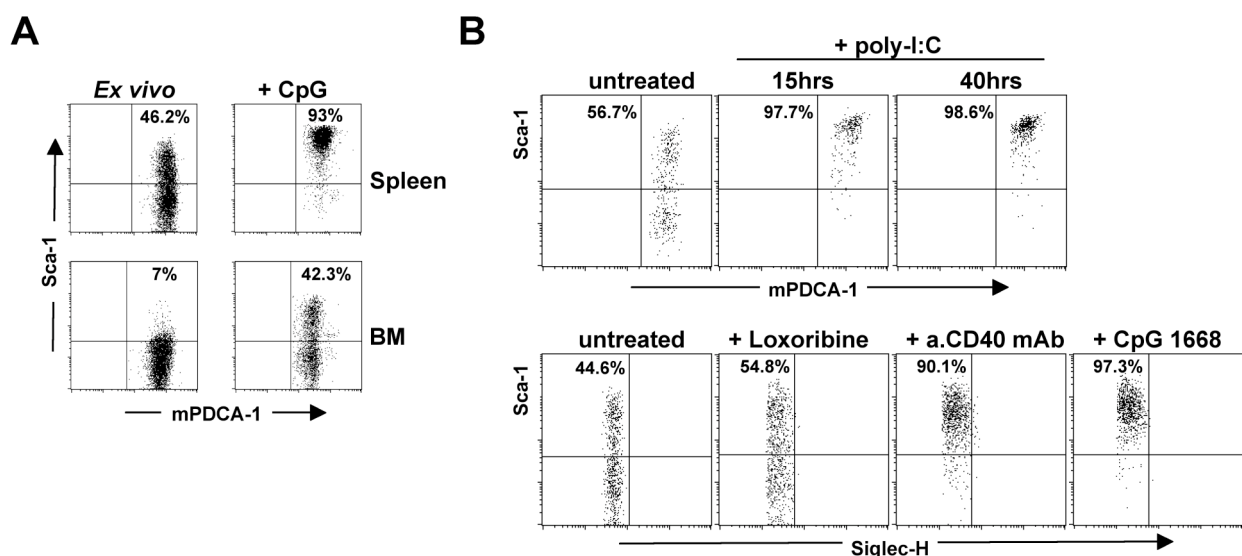


Fig 4.4.4 Sca-1 upregulation on PDCs upon TLR-mediated activation.

(A) Sca-1 upregulation *in vitro*. PDCs were isolated from spleen (upper dotplots) or BM (lower dotplots) and checked for purity and Sca-1 expression. PDCs were then cultured for 15 hrs in the presence of 5 µg/ml CpG and analyzed again. Shown is a representative flow cytometric analysis of the Sca-1 expression on PDCs, gated on mPDCA-1⁺ cells.

(B) Sca-1 expression on PDCs after *in vivo* activation with synthetic TLR agonists and CD40 ligation.

Shown in the upper dotplots is the Sca-1 distribution on B220⁺ mPDCA-1⁺ spleen PDCs before and 15 and 40 hrs after i.v. administration of 50 µg poly-I:C. In the lower dotplots spleen PDCs were cultured in the absence or presence of additional TLR stimuli. 24 hrs after activation with Loxoribine, CpG ODN 1668, or after treatment with 50 µg anti-CD40 mAb (clone FKG45.5; rat IgG_{2a}). PDCs were isolated, stained with Siglec-H and analyzed for Sca-1 expression.

Additional *in vivo* activation by i.v. administration of TLR3 ligand poly-I:C led to a significant upregulation of this marker within 15-40 hrs (Fig. 4.4.4B). After activation, almost all spleen PDCs were positive for Sca-1 and also the absolute expression level increased (indicated by staining intensity, Fig. 4.4.4B). This effect was also consistent in other organs tested, like BM, LNs, and liver (data not shown).

When activated with anti-CD40 mAb or other types of CpG ODNs an upregulation of Sca-1 expression could be observed as well (>90% of all spleen PDCs expressed Sca-1). Of all stimuli tested, only the TLR7 agonist Loxoribine showed a poor capacity to induce upregulation of Sca-1 expression on PDCs (Fig. 4.4.4B). In general, these *in vitro* and *in vivo* results clearly demonstrated that PDCs upregulate the expression of Sca-1 upon activation and this molecule could serve as a sensitive marker for the activation status of murine PDCs.

In a transfer experiment it was investigated whether Sca-1⁺ PDCs develop directly from the Sca-1⁻ subset. For this, Sca-1⁻ PDCs isolated from spleen or BM were administered i.v. into a second mouse. Transferred spleen PDCs that were detected 24 hrs later in both spleen and liver, predominantly upregulated this marker (approx. 75-90% of grafted PDCs were Sca-1⁺; Fig. 4.4.5A+B). Not only the frequencies of Sca-1⁺ PDCs increased (Fig. 4.4.5B, left bar diagram), also the expression level of Sca-1 on grafted PDCs was upregulated in contrast to host PDCs (Fig. 4.4.5B, right bar diagram, and data not shown). Although there were no differences in the frequency, a significant dissimilarity in the expression level between grafted PDCs found in spleen or liver was demonstrated, possibly suggesting an influence of the organ environment. No variation was found comparing the origin of transferred PDCs, either derived from spleen or BM.

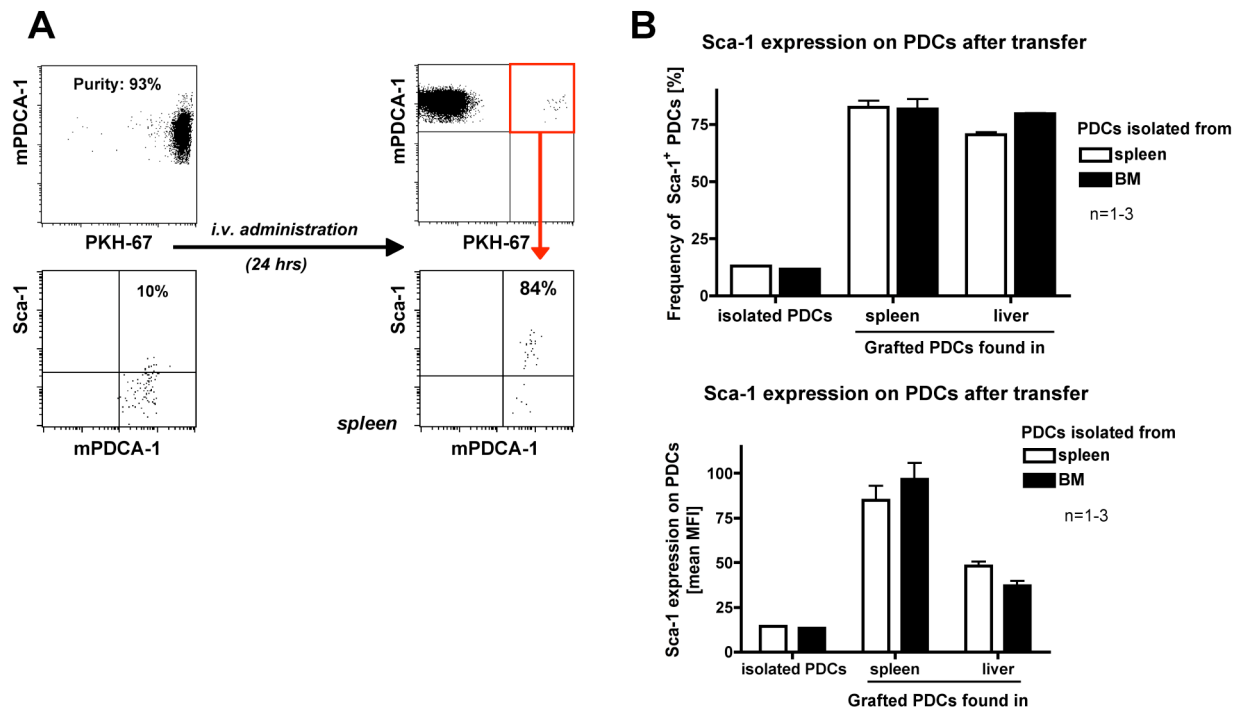


Fig 4.4.5 Upregulation of Sca-1 expression on transferred PDCs.

(A) The dotplots give an impression of the isolation, labeling, and transfer process of PDCs within this experiment. PDCs were untouched isolated from spleen (93% purity) and subsequently labeled with a cell tracker (PKH67, Sigma). Flow cytometric analysis reveals the Sca-1 distribution before and 24 hrs after i.v. administration. The Sca-1 distribution was then assessed only on transferred mPDCA-1⁺ pKH67⁺ PDCs (red gate). One representative experiment out of two is shown.

(B) Bar diagram demonstrates expression of Sca-1 on PDCs before and 24 hrs after transfer as revealed by flow cytometric analysis. Shown is the mean frequency of Sca-1⁺ PDCs +/- SD of n=1-3 and the mean fluorescence intensity of Sca-1 expression.

In summary these results demonstrated an evidence for the development of Sca-1⁺ PDCs from the Sca-1⁻ type.

Sca-1 was also described as an activation marker for T cells. Thus, a possible co-expression of Sca-1 and co-stimulatory molecules was investigated on PDCs in steady state or after activation. As demonstrated in Fig. 4.4.6, about 50% of spleen PDCs expressed Sca-1 but were negative for CD40, CD80 and CD86. A correlation of the few PDCs stained positive for the co-stimulatory molecules (<5%) with Sca-1 expression was not observed in inactivated PDCs. After CpG activation only Sca-1⁺ PDCs were detected and almost all cells were also positive for CD40 and CD86. The majority of PDCs (>80%) also expressed CD80. The co-expression of Sca-1 with these common maturation markers implicated that the differential Sca-1 expression may describe two activation or developmental stages of PDCs. Whether the heterogeneous Sca-1 expression further represent functional differences of the subpopulations, e.g. by differential cytokine secretion, will be tested later on.

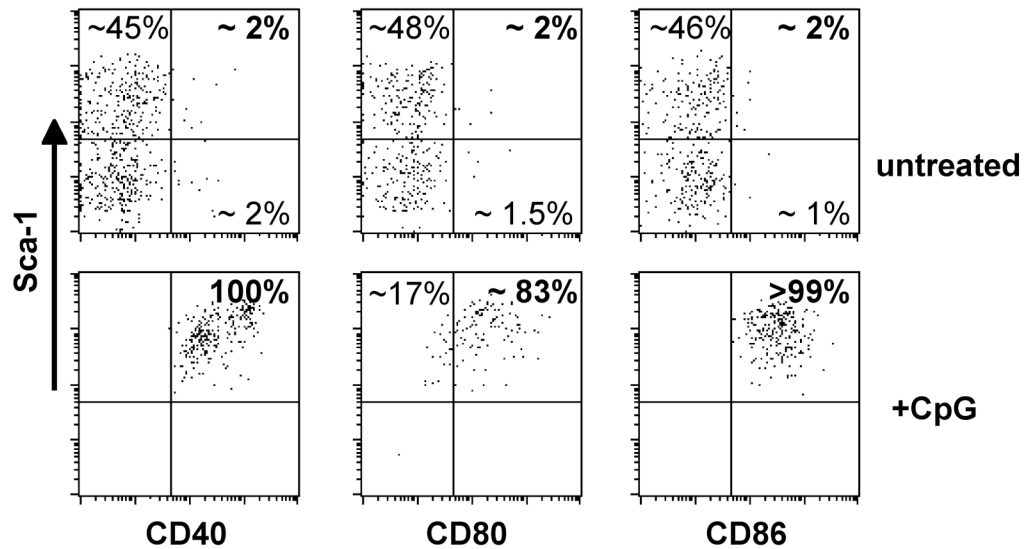


Fig 4.4.6 Expression of co-stimulatory molecules in correlation with Sca-1 expression in both steady state and after CpG-activation. Isolated spleen PDCs were gated on the basis of Siglec-H expression and analyzed for Sca-1 expression in correlation with indicated markers. Shown are representative dotplots from the flow cytometric analysis of freshly isolated PDCs or 24 hrs after culture in the presence of 5 $\mu\text{g/ml}$ CpG 1668.

To gain further insights into the transcriptional profile of these PDC subsets, FACS-sorted Sca-1⁻ and Sca-1⁺ PDCs (Fig. 4.4.7A) were compared on PIQOR microarray chips. To this end mRNA was isolated from both PDC subsets (both from LNs and spleen), amplified, and hybridized to the “PIQOR Mouse Immunology” chip, which comprises more than 1,000 immuno-relevant genes, that are spotted in quadruplicates. The microarrays were analyzed in analogy to the gene expression analysis described for the identification of mPDCA-1.

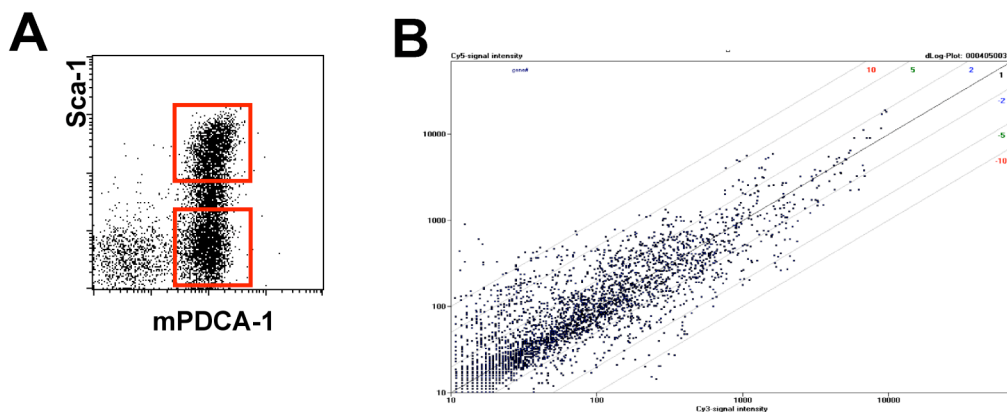


Fig 4.4.7 Differential Gene regulation of Sca-1⁺ and Sca-1⁻ PDCs.

(A) PDCs were enriched from Balb/c spleen or LNs (data not shown), sorted into mPDCA-1⁺ Sca-1⁻ and mPDCA-1⁺ Sca-1⁺ subsets (red squares; FACS Vantage) for subsequent PIQOR micro array analysis (as described in the Materials and Methods section). Amplified and labeled RNA was hybridized onto PIQOR Mouse Immunology chips (according to manufacturer's protocol).

(B) Representative double-log scatter plot of the micro array analysis of Sca-1⁺ and Sca-1⁻ PDCs (PIQOR Mouse Immunology microarray) demonstrates the signal intensities of all detected genes that pass quality control in a single spot. On the x-axis the signal intensity detected in the Cy3 channel is depicted, whereas the y-axis demonstrates Cy5 signal intensity. Diagonals define the area of x-fold differential signal intensity.

A representative distribution of the signal intensities is shown in Fig. 4.4.7B and in the following table an overview of highly upregulated genes is listed, which demonstrated a signal intensity more than 3.5-fold higher compared to the background level and was present at least on 3 of 4 micro arrays (see Table 4.4.1A+B).

Tab. 4.4.1 A: Genes that are predominantly regulated on Sca-1⁻ PDCs

No.	Gene name & description	Mean Regulation	Mean SD [%]	Arrays
1	RABGAP1: RAB6 GTPASE ACTIVATING PROTEIN	7,68	15	4
2	BCL6: B-CELL LYMPHOMA 6 PROTEIN	7,52	14	3
3	TRAIP: TRAF INTERACTING PROTEIN	7,39	7	4
4	CD22: B-CELL RECEPTOR CD22 PRECURSOR	6,95	16	4
5	ZBTB19: ZINC FINGER PROTEIN 278	6,30	34	3
6	TXLN: TAXILIN (IL14)	6,19	15	3
7	RRAS: RAS-RELATED PROTEIN R-RAS (P23)	5,15	11	4
8	IRF5: INTERFERON REGULATORY FACTOR 5	4,67	13	4
9	CD163: M130 ANTIGEN PRECURSOR	4,23	16	4
10	SODD: BAG-FAMILY MOLECULAR CHAPERONE REGULATOR-4	3,95	14	3
11	DNAJC2: ZUOTIN RELATED FACTOR-1	3,50	20	3

Tab. 4.4.1 B: Genes that are predominantly regulated on Sca-1⁺ PDCs

No.	Gene name & description	Mean Regulation	Mean SD [%]	Arrays
1	EGR1: EARLY GROWTH RESPONSE PROTEIN 1	28,89	54	4
2	OACT5: O-ACYLTRANSFERASE	23,00	16	3
3	NFX1: TRANSCRIPTIONAL REPRESSOR NF-X1 (EC 6.3.2.)	17,26	22	4
4	PROCR: (EPCR) ENDOTHELIAL PROTEIN C RECEPTOR PRECURSOR	16,79	47	3
5	IPLA2: CALCIUM-INDEPENDENT PHOSPHOLIPASE A2	11,61	15	3
6	STAM2: SIGNAL TRANSDUCING ADAPTOR MOLECULE 2	10,40	17	3
7	EDEM1: ER DEGRADATION-ENHANCING ALPHA-MANNOSIDASE-LIKE.	10,04	56	4
8	TNFR1: TNFR SUPERFAMILY MEMBER 1A PRECURSOR	8,77	38	4
9	CBLB: SIGNAL TRANSDUCTION PROTEIN CBL-B	7,32	16	4
10	DLL1: DELTA-LIKE PROTEIN 1 PRECURSOR	7,29	11	4
11	CD84: LEUKOCYTE DIFFERENTIATION ANTIGEN CD84.	7,22	55	3
12	PTPN12: PROTEIN-TYROSINE PHOSPHATASE G1	6,81	13	3
13	RLIP76: RLIP76 PROTEIN, RAL-INTERACTING PROTEIN 1	6,60	13	4
14	CD44_EX7-9_MOUSE: CD44 ANTIGEN PRECURSOR	6,17	19	3
15	BIRC2_5PRIME: BACULOVIRAL IAP REPEAT-CONTAINING PROTEIN 2	5,47	12	4
16	PCGF3: POLYCOMB GROUP RING FINGER 3.	5,21	13	3
17	ITCH: ITCHY HOMOLOG E3 UBIQUITIN PROTEIN LIGASE	5,08	29	4
18	MAPK6: (ERK3) MITOGEN-ACTIVATED PROTEIN KINASE 6	5,02	15	4
19	CD69: EARLY ACTIVATION ANTIGEN CD69	4,61	34	3
20	MAPK9: (JNK2) MITOGEN-ACTIVATED PROTEIN KINASE 9	4,32	20	3
21	TBC1D23: TBC1 DOMAIN FAMILY, MEMBER 23	4,05	15	4
22	ID1: INTEGRAL MEMBRANE PROTEIN DGCR2/IDD	4,03	26	3
23	VEGF: VASCULAR ENDOTHELIAL GROWTH FACTOR C PRECURSOR	3,67	19	4

In detail, genes significantly (> two-fold) over-represented in Sca-1⁻ PDCs were e.g. IRF-5, RABGAP1, BCL, TRAIP, but also CD22 and CD163 as cell surface markers. In total about 30 genes were preferentially expressed in this PDC subset and the distribution of the differential gene regulation in each microarray is demonstrated in Fig. 4.4.7C. On the other hand in Sca-1⁺ PDCs EGR1, OACT5, NFX1, PROCR, IPLA2, STAM2, and EDEM1 showed a more than 10-fold higher expression, and also TNFR1, CD44, CD69, CD84 and MAP kinases 6 and 9 were significantly upregulated on mRNA level. Here, almost 100 genes were significantly over-represented in Sca-1⁺ PDCs compared to Sca-1⁻ PDCs (Fig. 4.4.7D). The complete list

containing the raw data \pm SD of all 1,070 genes regulated in all four hybridization settings is shown in the appendix (Table 7.2).

C



Fig 4.4.7 Differential Gene regulation of Sca-1⁺ and Sca-1⁻ PDCs.

(C, D) The raw data of the microarray were analyzed via MEV TIGR software. The table shows an overview of the expression of genes that are predominantly regulated on Sca-1⁻ PDCs (C) or Sca-1⁺ PDCs (D). Hereby only genes are considered that are at least 2-fold regulated and are present at least on 3 of 4 microarrays. Colors represent an over-represented (increased) expression (red), repressed expression (green), unaltered gene expression (black). Gray colors are used if no signal was detected.

In Fig. 4.4.7E the regulated genes were clustered ontologically. The four bar diagrams show the over-representation of several genes belonging to different ontology clusters (GOC). In general there were more genes derived from the Sca-1⁺ PDC compartment, which in particular belonged to the Toll/cytokine receptor or NF- κ B pathways. Comparing the GOC of differentially regulated genes from both subsets directly demonstrated that significantly more regulated genes in Sca-1⁺ PDCs were represented in all pathways. Relative comparison (percentaged analysis) showed that the distribution of regulated genes was very similar but not identical between indicated GOC pathways. For example, genes belonging to cellular behavior, immunity, inflammation, Toll/cytokine receptor, NF- κ B, and other signaling pathways were more represented in Sca-1⁺ PDCs, whereas more molecules that are involved in adhesion/migration, immune reactions and in particular in metabolic pathways were enabled in the Sca-1⁻ subpopulation.

D

Fig 4.4.7 Differential Gene regulation of Sca-1⁺ and Sca-1⁻ PDCs.

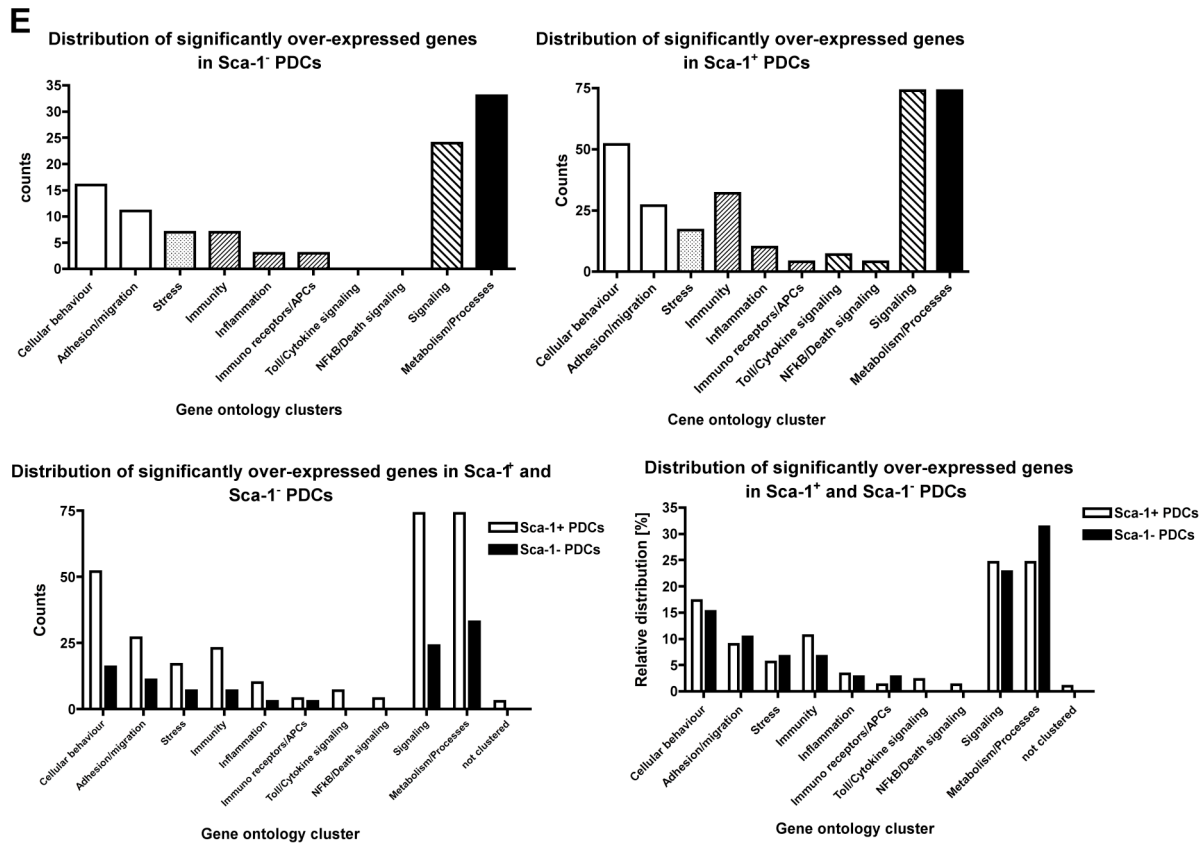


Fig 4.4.7 Differential Gene regulation of Sca-1⁺ and Sca-1⁻ PDCs.

(E) Gene ontology clustering. Gene ontology analysis was carried out after gene annotation (MIGO terms, GOA based extended) to verified pathways (Annotate, Miltenyi Biotec, unpublished).

At this point further experiments were necessary to assign the results of the differentially regulated genes in the context of developmental differences between Sca-1⁺ and Sca-1⁻ PDCs or their activation status. Additionally, these data might explain the functional properties reported in the next chapter.

4.4.4 Correlation of the different Sca-1 expression with the cytokine production capacity of PDCs

Since PDCs were regarded as the major IFN α producers, a functional correlation of the Sca-1 expression and their capacity to produce IFN α (and also other cytokines, e.g. IL-12 or TNF α) was assessed. In the past, differences in the IFN-I production of PDCs have been described. Krug et al. demonstrated that mature PDCs produced decreased amounts of IFN α after CpG induction [Krug A, EJI 2001]. In addition there were reports demonstrating that the capacity to produce IFN-I is restricted to immature PDCs and there is a functional dichotomy between IFN α -producing PDCs and PDCs inducing an adaptive immune response [Jaehn PS, EJI 2008; Iparraguirre A, J Leukoc Biol. 2008]. These data and the results obtained in the previous chapters led to the suggestion that Sca-1⁺ PDCs were more mature and were of a more differentiated stage. Thus, it was speculated that LN-resident Sca-1⁺ PDCs have a stronger T cell-stimulatory ability and produce less IFN-I compared to Sca-1⁻ PDCs from the BM and vice versa. To test this assumption, untouched isolated spleen or BM-PDCs were cultured for 6 hrs

with CpG and/or Loxoribine in order to induce IFN α production, followed by intracellular staining. Flow cytometric analysis (Fig. 4.4.8A, dotplots) revealed that the majority of IFN α -producing PDC belonged to the Sca-1⁻ compartment indicating a functional difference between both PDC subpopulations. As shown by the staining intensity, BM-PDC produced higher per cell-amounts of IFN α when compared to spleen derived PDC. LN-derived PDCs were only weak producers (data not shown). Additionally, the IFN α production was also analyzed by specific ELISA. Untouched isolated PDCs as well as PDCs, which were additionally depleted of Sca-1⁺ cells, were cultured in the presence of CpG. After 24 hrs culture supernatants were harvested and examined for IFN α . PDCs, which have been previously depleted for Sca-1⁺ cells produced 10-fold higher amounts of IFN α upon CpG stimulation, supporting flow cytometric data obtained from intracellular IFN α stainings (Fig. 4.4.8A lower bar diagram). Analysis of the IFN α secretion capacity of PDC isolated from different lymphoid organs further underlined this observation showing a clear correlation between produced IFN α amount and the percentage of Sca-1⁺ cells within the PDC compartment. BM-PDCs demonstrated a superior capacity to produce IFN α compared to PDCs from spleen, whereas LN-PDCs produce almost no visible IFN α (Fig. 4.4.8A upper bar diagram).

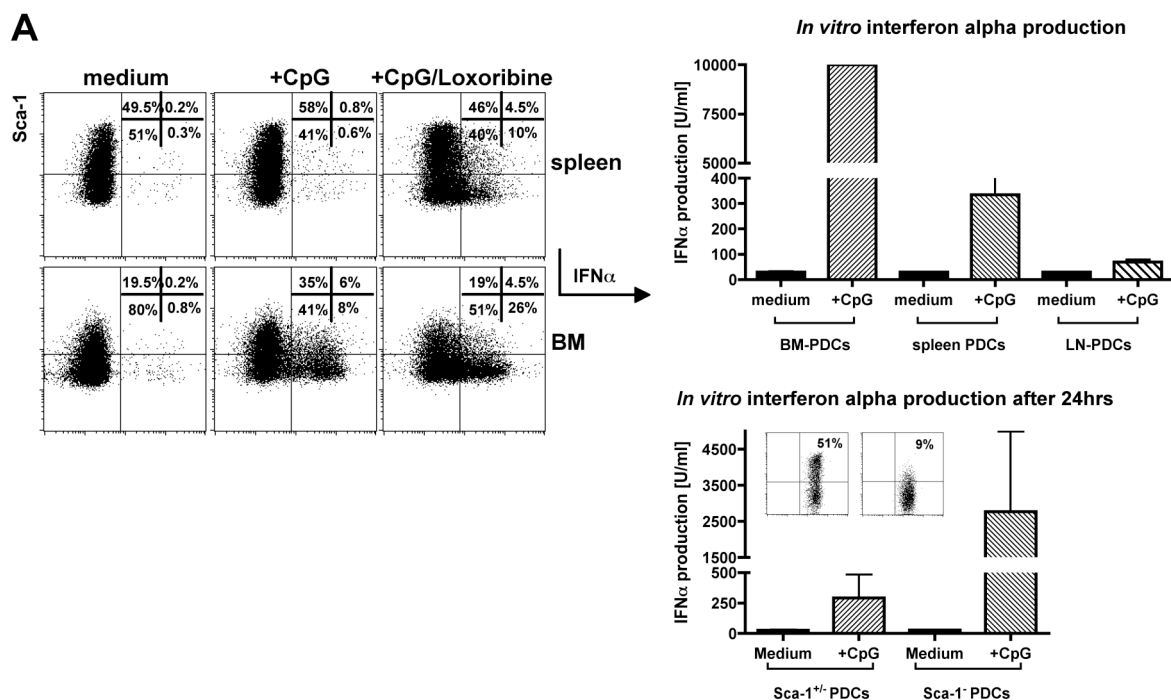


Fig 4.4.8 Functional correlation of the Sca-1 expression and cytokine production capacity of PDCs.

To assess cytokine secretion, PDCs were isolated from indicated lymphoid organs and cultured in the absence or presence of TLR agonists for 7 hrs (intracellular stainings) or 24 hrs (ELISA). CpG and Loxoribine were used at a final concentration of 5 μ g/ml and 20 mM, respectively. To prevent secretion in case of intracellular staining, BrefeldinA was added in the last 4 hrs.

(A) IFN α production was assed by intracellular staining of BM or splenic PDCs (dotplots).

For ELISA PDCs were either isolated from different lymphoid organs (upper bar diagram) or spleen PDCs were used, which were either left untreated (representing a mixed Sca-1^{+/+} populations) or were separated into Sca-1⁻ PDCs (lower bar diagram). Here, inserted dotplots demonstrate the Sca-1 expression of used PDC subsets. Supernatants of unstimulated or CpG-activated PDCs were collected after 24 hrs and analyzed by IFN α -specific ELISA (PBL).

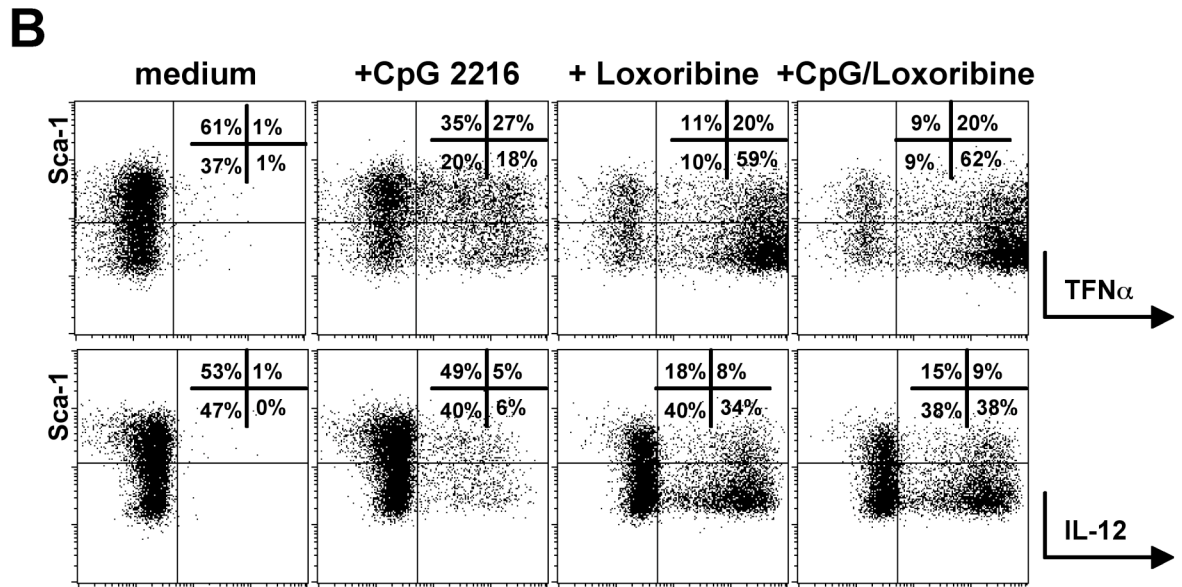


Fig 4.4.8 Functional correlation of the Sca-1 expression and cytokine production capacity of PDCs.

(B) Dotplots demonstrate cytokine production in correlation to Sca-1 expression in isolated PDCs. Shown are representative intracellular stainings for IL-12 and TNF α production in untreated or TLR-triggered PDCs.

Beside the differences in their IFN α production, the two Sca-1^{+/-} PDC subsets differed also in their capacity to produce TNF α and IL-12 when stimulated with TLR7 ligand Loxoribine (Fig. 4.4.8B). Interestingly, when stimulated with TLR9 ligand CpG, both TNF α and IL-12 were produced at significantly lower level and there was no difference between Sca-1⁺ and Sca-1⁻ subset.

In summary, the differential expression of Sca-1 on PDCs was in line with functional heterogeneity and might define two functional different subsets of PDC in mice.

5. DISCUSSION

An effective immune response is based on the co-operation of a variety of distinct cell types that are appointed with different characteristics and properties. These cell types can be assigned either to the innate or the adaptive arm of immunity, but for some cell populations a fix assignment is not suitable, as they are known to function in the linkage or synchronization of both immune responses. In this context, PDCs are regarded to bridge innate and adaptive immunity, but it still remains unclear whether PDCs are able to initiate adaptive immune responses in an antigen-specific manner.

To gain more insight into the complex interactions of PDCs a specifically expressed cell surface antigen should be identified and characterized, since molecules uniquely expressed by a single cell type often contribute to the specific function of these cells. At the beginning a panel of mAbs that all recognized murine PDCs was generated. After identification of the molecular nature of the novel antigen, further studies of the molecule were performed including the investigation of cytokine secretion or signaling. Functional characterization revealed a function of mPDCA-1 as an antigen-uptake receptor and demonstrated the role of PDCs in the interaction with naïve T cells. Finally, the heterogeneity and plasticity of PDCs are exemplified by the differential expression of Sca-1 on PDCs.

5.1 Generation of PDC-specific monoclonal antibodies and phenotyping of mPDCA-1⁺ cells

There are several techniques to identify specifically expressed genes. The generation of a mAb against PDCs provides the advantage for the identification of the detected antigen and the isolation of cells expressing this specific molecule. Furthermore, antigens could be cloned from a cDNA library followed by FACS analysis with a specific antibody [Zhang J, Blood 2006; Dzionek A, JEM 2001; Blasius A, JI 2006]. Other methods, including “Subtractive Hybridization” or “Differential Display”, only allow the identification of specifically transcribed genes but gain no information on the expression on protein level. These methods were less applicable for selectively expressed cell surface markers. Thus, the first aim of the work was the generation of a mAb against a PDC-expressed cell surface molecule. Unfortunately, the immune reaction against a specific molecule could interfere with the response against immuno-dominant antigens. In this study the recently described “contralateral footpad immunization method” was used to direct the immune reaction towards PDC-specific antigens [Brooks, PC, Journal of Cell Biology, 1993; Yin, AH, Blood 1997]. This technique is based on the fact that naïve B and T cells circulate through peripheral lymphoid organs until they detect an antigen [Breadly LM, Curr. Opin. Immunol 1996; Butcher EC, Science 1996; Picker LJ, Annu. Rev. Immunol 1992; Watson SR, Cell. Adhes. Commun 1998]. Upon recognition and additional activation these lymphocytes accumulate and arrest in the draining lymph node next to the site of infection [Jacob J, JEM 1992; Kearney ER, Immunity 1994; Ridderstad A, JI 1998; Tarlinton D, Curr. Opin. Immunol. 1998]. Thus, by the local administration of an antigen, B and T cells would be “trapped” in the draining lymph node. These specific lymphocytes were then depleted from the

periphery and a form of “local tolerance” against the administered antigen would be induced. In this work, murine Sp2/0 cells or isolated NK cells were injected as decoy into the one hind footpad before inoculation with purified PDCs into the other. These decoy cells express a variety of strongly immunogenic antigens. Highly immunogenic antigens are e.g. MHC-II molecules. Thus, Sp2/0 cells were chosen for this reason. By the spatiotemporal separation an immune reaction against non-specifically expressed antigens was restricted to the one site. The other lymph node was expected to contain lymphocytes (B cells) specific for a PDC expressed molecule and finally four specific mAbs were obtained by repetitive immunizations. The clones JF-1C2, -3D5, -7B3, and -12A5 specifically detect PDCs in single cell suspensions of spleen and other lymphoid organs. The anti-mPDCA-1 mAbs does not cross-react with human PDCs (data not shown). Thus, the unknown antigen was termed “Murine plasmacytoid Dendritic Cell Antigen 1”. In the past this technique has been used to generate mAbs specifically recognizing human DC subsets [Dzionek A, JI 2000], whereas other PDC-detecting antibodies were generated differently by intraperitoneal or subcutaneous inoculation of PDCs [Asselin-Paturel C, JI 2003; Blasius A, Blood 2004] or cloned Fc-fusion proteins [Zhang J, Blood 2006], followed by screening on spleen cells, PBMC or transfected cell lines. In contrast to the utilized method, in other strategies a decoy was not applied, possibly leading to an increased amount of unspecific mAbs.

These data demonstrate that contralateral footpad immunization is a reliable method for the generation of specific antibodies against cellular antigens without availability of the antigen. The local tolerance induced by this procedure might be beneficial for less immunogenic antigens. In contrast to other methods described above the obtained antibodies also facilitate the characterization of the novel molecule on protein level.

Flow cytometric analysis revealed that mPDCA-1⁺ cells express no markers for lineage commitment, i.e. are negative for CD11b, CD19, CD49b, and CD138, and do not express the TCR. On the other hand, these cells express B220 and Ly-6C and display intermediate expression levels of CD11c. CD4 and CD8 were moderately expressed, whereas co-stimulatory molecules CD40, CD80, and CD86 were absent. MHC-II, typically expressed by APCs and DCs, is found at intermediate levels on mPDCA-1⁺ cells. The co-expression of B220, Ly-6C, CD11c and MHC-II as well as the absence of co-stimulatory molecules and lineage markers was shown to be characteristic for murine PDCs [Nakano H, JEM 2001; Asselin-Paturel C, Nat Immunol 2001; Björck P, Blood 2001]. Thus, mPDCA-1⁺ cells are phenotypically identical to PDCs. Multi-color FACS analysis demonstrated that the anti-mPDCA-1 mAb detects PDCs but does not react with other cells. This has been shown for PDCs in spleen and also in other lymphoid organs, including BM, liver, lung, thymus, peripheral and mesenteric LNs as well as Peyer's Patches. Interestingly, the expression level of mPDCA-1 is not identical on all PDCs. It was shown to be highest on PDCs located in secondary lymphoid organs, such as spleen or LNs, but it is significantly lower expressed on BM-PDCs. This implicates that mPDCA-1 is upregulated during the development, as immature PDCs exist in the BM developing from CD34⁺

DC progenitors [Banchereau J, Nature 1998; Kreisel FH, Cell Immunol 2006; Toma-Hirano M, EJI 2007]. A similar regulation was observed for other PDC markers, including Ly-49Q, Sca-1, or Siglec-H [Toyama-Sorimachi N, JI 2005; Blasius A, Blood 04].

The frequency of mPDCA-1⁺ cells in different lymphoid organs varies between 0.2% to 0.5% in LNs, about 0.3% to 0.8% in spleen, about 0.9% to 1.5% in BM. Thereby, the frequency and phenotype of PDCs were identical using either the mPDCA-1 mAb or a characterization based on CD11c, B220, and Ly-6C. In the meantime the data presented here regarding the frequency, phenotype and characterization of PDCs had been reproduced by other groups [Wendland M, PNAS 2007; Ohbayashi M, Exp Mol Pathol. 2007; Zucchini N, Int Immunol. 2008; Sung SS, JI 2006]. Not only phenotypically but also functionally mPDCA-1⁺ cells resemble PDCs *in vitro* and *in vivo*. It was further shown that mPDCA-1⁺ cells were the main producers of type I interferon compared to mPDCA-1⁻ cDCs. In these experiments, isolated DCs were stimulated with CpG ODNs *in vitro*. IFN α -specific ELISA revealed that mPDCA-1⁺ cells but not the mPDCA-1⁻ subset produced significantly amounts of IFN α . Moreover, PDCs were also the major IFN-I producers *in vivo* as the depletion of mPDCA-1⁺ cells resulted in drastic reduction of virally or CpG-induced IFN-I production [Krug A, Immunity 2004; Barchet W, EJI 2005; Schleicher U, JEM 2007]. The administration of antibodies to deplete specific cell populations *in vivo* has been established previously [Fleming T, JI 1993]. As a F(ab')₂ fragment of the anti-mPDCA-1 mAb did not induce depletion of PDCs, the depletion by application of the complete mAb might be caused by activation of either the classical complement pathway or by antibody-dependent cell-mediated cytotoxicity (ADCC) [Tao MH, JEM 1993; Xu Y, J Biol Chem. 1994; Golay J, Blood 2000; Di Gaetano N, JI 2003].

Recently, other groups also developed antibodies that recognize PDCs specifically. In the laboratories of Marco Colonna and Paul Crocker antibodies were produced (clones "440c" and "MB15", respectively) reacting with the Sialic acid binding Ig-like lectin H (Siglec-H), which is also specifically expressed on murine PDCs [Blasius A, Blood 2004 and Blood 2006; Zhang J, Blood 2006]. Multi-color FACS analysis revealed that mPDCA-1 and Siglec-H were co-expressed on PDCs. Blocking experiments showed that mPDCA-1 is not identical to the Siglec-H antigen (data not shown). The group of Giorgio Trinchieri generated the 120G8 mAb [Asselin-Paturel C, JI 2003] also reacting with an unknown antigen expressed on PDCs. Competitive inhibition experiments revealed that the staining of 120G8 could be completely blocked by the clone JF-1C2 and *vice versa*. Interestingly, other clones, such as JF-3D5 did not inhibit this staining. These blocking data suggested that the clones 120G8 and 1C2 reacted with identical epitopes or adjacent epitopes that were blocked by steric hindrance. Cross-blocking experiments with all four clones generated in the work presented here showed the existence of at least three different epitopes of the same antigen. One epitope is detected by the 1C2 clone but not by the others, whereas clones 3D5 and 12A5 recognize the same epitope. Blocking studies with clone 7B3 at least partially inhibited the staining of the other three clones. Further studies might be necessary to resolve the exact peptide sequence or epitope formation recognized by these antibodies including epitope mapping experiments or generation of

transfected cells after identification of the antigen.

The anti-mPDCA-1 mAb was also used by our collaboration partners and other research groups for the identification of PDCs in flow cytometric analyses or immuno-histochemical stainings, and their findings supported the data reported in this work [Zucchini N, *Int Immunol* 2008; Chan CW. *Nat Med* 2006; Taieb J, *Nat Med* 2006; Vosshenrich CAJ, *JEM* 2007; Caminschi I, *JEM* 2007; Blasius AL, *JEM* 2007; Weslow-Schmidt JL, *J Virol* 2007].

In this work the generation and application of a novel antibody was described that is highly specific for murine PDCs. Using the anti-mPDCA-1 mAb, PDCs can now be identified by single parameter analysis reducing the number of required markers (B220, Ly-6C, and CD11c) from three to one [Nakano H, *JEM* 2001; Asselin-Paturel C, *Nat Immunol* 2001; Björck P, *Blood* 2001].

5.2 Identification and functional characterization of mPDCA-1

Several biochemical methods were performed to identify the molecular nature of the novel antigen. Western blotting and immune-precipitation experiments were carried out first, followed by peptide mass fingerprint analysis to discover the amino acid sequence. These techniques did not result in the identification of mPDCA-1, probably due to a lower affinity of the generated mAbs to the solubilized antigen or due to a masked epitope. Another reason might be the existence of a linear epitope, which could not be recognized by the antibody after denaturation. Limited number of PDCs further hampered these experiments. As the expression of mPDCA-1 was transiently induced by IFN α treatment on several cell lines, mPDCA-1 should be identified by differential gene expression analysis.

The main idea was that whole genome microarray analysis often resulted in a considerable quantity of regulated gene candidates. Using Agilent microarrays, mPDCA-1⁻ cell lines were compared with IFN α -induced mPDCA-1⁺ cells or isolated PDCs. It was possible that beside the mPDCA-1 candidate also other genes such as IFN-I-responsive genes or other irrelevant genes would be regulated [Der SD, *PNAS* 1998; Baechler EC, *PNAS* 2003]. To create an intersection as little as possible mPDCA-1⁺ cells were also hybridized against cells that had downregulated mPDCA-1. Resulting candidates were further investigated by comparing the mRNA transcription levels in PDCs and T cells as well as in other hematopoietic cell types. Looking for a cell surface molecule, the mPDCA-1 candidate should contain a TMD and its expression should not be described on other cells. Microarray analysis and validation by real time PCR impressively showed that several transcripts were highly upregulated in PDCs. As the specific antibody was the only tool to identify the mPDCA-1 antigen, in the next step cell lines were transfected with the cDNAs of corresponding gene candidates. Flow cytometric analysis revealed that only cell lines transfected with the coding sequence of BST2 were specifically recognized by the anti-mPDCA-1 mAb. All four anti-mPDCA-1 clones detected human and rat cell lines transfected with BST2 but not mock transfectants or cells expressing other regulated gene candidates, e.g. MPG1. The anti-mPDCA-1 mAb was also ideal for the enrichment of BST2-transfected cells.

The results of this work were supported at the same time by the group of Marco Colonna, performing gene expression cloning using a PDC-specific cDNA library [Blasius A, JI 2006]. The transfectants of both groups were specifically detected by the anti-mPDCA-1 antibody JF05-1C2, although they generated a BST2 transfectant comprised of a different ORF and Start codon, suggesting a potential splice variant with a truncated N-terminal cytoplasmatic tail [Blasius A, JI 2006]. Taken together, BST2 has been confirmed as the antigen recognized by anti-mPDCA-1 antibodies. As BST2 is not a novel molecule, different names were given to this antigen: beside mPDCA-1 and BST2, the molecule has been named DAMP-1, HM1.24 or 120G8 antigen and was designated as CD317 [Asselin-Paurel, JI 2003, Blasius A, JI 2006; Li X, Mol. Biol. Cell 2007; Vidal-Laliena A, Cellular Immunology 2005 (*submitted to the 8th HLDA workshop*)]. Since mPDCA-1 was established in PDC research, this term will be used in the following.

The mPDCA-1 transcript codes for a small type II transmembrane glycoprotein of about 25-30 kDa size, depending on the kind of glycosylation [Kupzig S, Traffic 2003; Ishikawa J, Genomics 1995; Neil SJD, Nature 2008]. These data were in line with the prediction of two TMDs for mPDCA-1, based on statistical analysis of naturally occurring transmembrane proteins using the TMPred software [Hofmann K, Biol. Chem. Hoppe-Seyler 1993]. BST2 contains a conventional TMD near the N-terminus and a C-terminal signal sequence for a GPI anchor as well as two additional N-linked glycosylation sites at the extracellular domain [Kupzig S, Traffic 2006]. The suggested GPI anchor might explain the difficulty to immuno-precipitate the mPDCA-1 molecule from PDC lysates or membrane fractions. This was supported by the observation that only a specific Phospholipase C (PI-PLC) cleavage released the molecule out of the lipid rafts of the plasma membrane. Only after this treatment BST2 could be solubilized via Triton-X detergent [Kupzig S, Traffic 2003]. Thus, for successful immuno-precipitation of mPDCA-1 from PDCs a PI-PLC treatment should be tested before the application of different. Fig. 5.1 shows a model of the structure of the mPDCA-1/BST2 protein and its topology.

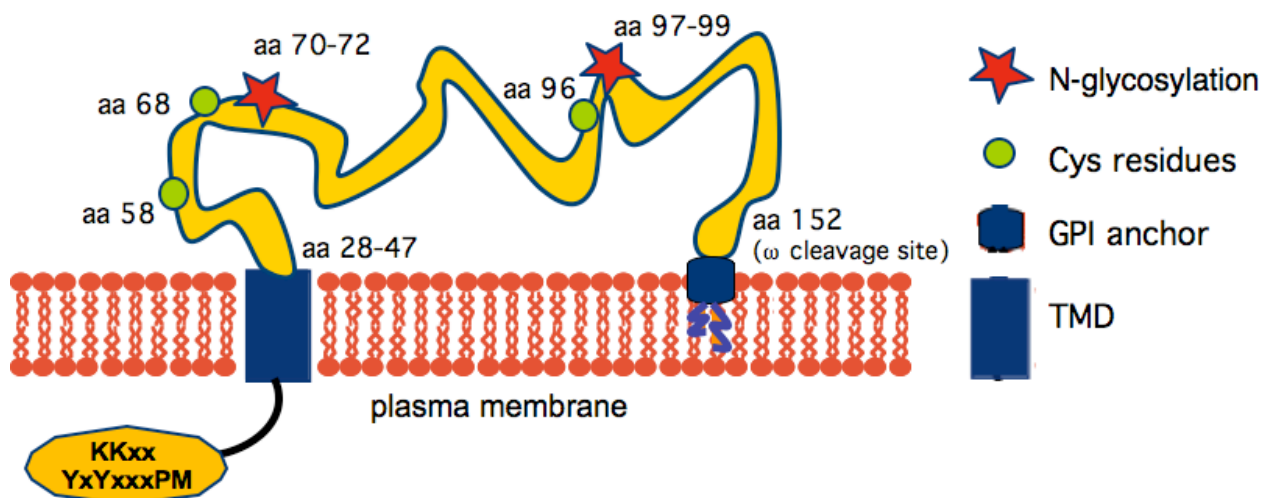


Fig. 5.1 Predicted protein structure of the mPDCA-1/BST2 molecule.

This model is based on data taken from Kupzig *et al.*, Traffic 2003; Blasius *et al.*, JI 2006; Rollason *et al.*, J Cell Sci. 2007; Ohtomo *et al.*, Biochem Biophys Res Commun 1999; Ge *et al.*, Blood 2006. Legend: Y: tyrosine; P: proline; M: methionine; K: lysine; x: any amino acid.

The remarkable topology of mPDCA-1 is similar to the neuropathologic form of the Prion protein [Hedge R, Science 1998; Hedge RS, Nature 1999], although no significant sequence homology was demonstrated. Based on the amino acid sequence mPDCA-1 shares homologies with the integral BAP31 protein of the endoplasmic reticulum, which has a chaperone-like or cargo receptor function and might regulate apoptosis [Hidvegi T, J Biol Chemistry 2007; Blasius A, JI 2006; Wang B, Molecular and Cellular Biology 2004]. mPDCA-1 contains two N-terminal transport signals, (1) "Y-x-Y-x-x-P-M" and (2) "KKxx" [Van Vliet C, Prog. Biophys. Mol. Biol. 2003]. These motifs are supposed to sort proteins into secretory and endocytic pathways. This might enable a role of mPDCA-1 in cytokine secretion (in particular of IFN-I) or a potential function in the endocytosis of antigens for processing and presentation [Kaczorowski DJ, J Leuko Biol 2008; Blasius A, JI 2006]. Additionally, it has been shown that mPDCA-1 was closely connected to the Golgi apparatus and the trans-Golgi network [Blasius A, JI 2006, Kupzig S, Traffic 2003]. This and the localization within lipid rafts of the plasma membrane may give mPDCA-1 a function both in trafficking, signaling or protein sorting [Kupzig S, Traffic 2003].

mPDCA-1 and its rat, monkey or human homologues had been already described in the past [Ohtomo T, Biochem Biophys Res Comm 1999]. It was reported that human BST2 is expressed within the B cell lineage (terminally differentiated B and plasma cells) and on several non-hematopoietic cell lines, and a function in B cell differentiation and growth of pre-B cells was speculated [Ishikawa J, Genomics 1995]. BST2 was also found on multiple myeloma cells, neoplastic B cells and on rheumatoid arthritis synovial cell lines [Goto T, Blood 1994; Ohtomo T, Biochem Biophys Res Comm 1999; Ozaki S, Blood 1999], but the function on these cells remained unknown. Currently, the therapeutic application of this antibody in order to induce an ADCC response against BST2-expressing tumors is under investigation [Ozaki S, Blood 1999].

It was demonstrated that mPDCA-1 is specifically expressed on PDCs of naïve mice. The expression was rapidly induced on other hematopoietic cells and cell lines upon TLR9 triggering or IFN α treatment as was shown by results of this work and by others [Asselin-Paturel C, JI 2003; Blasius A, JI 2006, Bochtler P, JI 2008]. The IFN α -dependent upregulation of mPDCA-1 might depend on the Interferon-stimulated response elements (ISRE) in the promoter region of BST2 as reported by Ohtomo *et al.* and Ge *et al.* Binding of IFN-I resulted in the activation of the JNK pathway. Beside three STAT3 DNA-binding sites the promoter contained further motifs, such as GATA1 binding elements, which also have an important role in BST2 transcription [Ohtomo T, Biochem Biophys Res Commun 1999; Ge Y, Blood 2006; Becker M, Mol Cancer Ther 2005; Matsuda A, Oncogene 2003]. mPDCA-1 was transiently upregulated on other hematopoietic cells and different cell lines, but the expression level was lower compared to PDCs. The data presented in this work demonstrated that PDCs showed highest expression levels of mPDCA-1, which remained unchanged under IFN-inducible conditions as reported elsewhere [Blasius A, JI 06]. It is speculative whether the strong but constant expression of mPDCA-1 on PDCs might be due to either an autocrine IFN-I secretion loop or was differently regulated in these cells. The function of upregulated mPDCA-1 on other cells than PDCs still

remains elusive, and further experiments are necessary. Very recently different groups have analyzed the role of human BST2. Cao *et al.* showed that BST2 might be the natural ligand for ILT7, another receptor expressed on human PDCs (Cao W, EB 2008, San Diego; The FASEB Journal 2008;22:1065.17; unpublished data). It might be of interest, whether mPDCA-1 also interacts with the murine ILT7 homologue. Further studies exploring the molecular nature, source or localization of a potential ligand might implicate the exact function of mPDCA-1 in PDCs. Recent data regarding the function of BST2 have been generated by studying cell lines or other BST2-expressing cells different from PDCs. In this context, the generation of a mPDCA-1 knockout mouse would be promising either to study the precise function of the molecule or the role of PDCs in general. Such a system would be superior to the existing Ikaros knockout mouse (Ik^(L/L)) [Allman D, Blood 2006]. These mice lack peripheral PDCs but not BM-PDCs. However, PDCs from these transgenic mice expressed lower levels of CD11c and were negative for B220 and Ly49Q. As these mice also showed reduced B cell numbers [Iparraguirre A, J Leukoc Biol. 2008] a system would be desirable in which only mPDCA-1 is silenced and not a transcription factor potentially affecting the lymphoid lineage [Kirstetter P, EJI 2002]. As the knockout of mPDCA-1 would probably not affect the development of PDCs, the expression of a toxin, e.g. diphtheria toxin, under the mPDCA-1 promoter would be more applicable to deplete PDCs *in vivo*. [Jung S, Immunity 2002].

IFN-I production is the prominent function of PDCs and plays a role in both viral infections and some autoimmune diseases (SLE, psoriasis). Consequently, the impact of receptor triggering on important PDC functions was investigated in this work. Cross-linking of mPDCA-1 with the four antibodies generated in this work resulted in significantly impaired IFN α production *in vitro*. The inhibitory effect of mPDCA-1 triggering was comparable to the IFN-I abrogation induced by the Siglec-H-recognizing mAb 440c [Blasius A, Blood 2004; Blasius A, JI 2006]. Thus the IFN-I inhibition seems not to be a unique function of mPDCA-1, but PDCs express several receptors with similar characteristics. Human PDCs receptors BDCA-2 and ILT7 also demonstrate IFN α -inhibiting functions [Dzionek A, JEM 2001; Cao W, JEM 2006]. They are currently discussed to have direct implications for autoimmune therapies, e.g. the abrogation of IFN α in SLE patients. The group of Patricia Fitzgerald-Bocarsly reported that cross-linking of BDCA-2 and -4, CD4, and CD123 on human PDCs led to the inhibition of IFN α production. It has been suggested that in this case IFN-I was regulated either at the level of IRF-7 translocation or by maturation of the cells [Fanning SL, JI 2006]. As mPDCA-1 triggering did not affect regulation of CD80/86 on murine PDCs (data not shown), further experiments had to be undertaken to reveal the INF-inhibition pathway of mPDCA-1. Recently, Röck *et al.* as well as Cao *et al.* showed that a B cell receptor (BCR)-like signaling might suppress IFN-I responses in human PDCs, demonstrating the involvement of PLC γ 2 or the Fc ϵ RI γ complex [Röck J, EJI 2007, Cao W, PLoS Biol. 2007; Swiecki MK, EJI 2007]. Targeting of PDC cell surface receptors PDC-TREM or DCIR with mAbs also led to impaired IFN-I production. In that case, a direct interaction with DAP-12 (PDC-TREM) or a not specified “cross-talk” with TLR9 (DCIR) might be responsible for this effect

[Watarai H, PNAS 2008; Meyer-Wentrup F, Blood 2008]. In previous reports an interaction of mPDCA-1 with the adaptor protein DAP12 was excluded [Blasius A, Blood 2006; Kupzig S, Traffic 2003].

To elucidate possible mPDCA-1 downstream signaling properties, first signal transduction experiments were performed. As the ligand for murine BST2 was elusive, the anti-mPDCA-1 mAb was used as surrogate ligand. It remained speculative whether the antibody recognizes the same epitope as the natural ligand, but in past specific antibodies were often used in similar approaches [Mahnke K, J Cell Biol 2000]. Here it was shown that ligation of the receptor resulted both in rapid and transient increase of the intracellular calcium concentration in combination with an overall protein-tyrosine phosphorylation, suggesting a signal transmission after mPDCA-1 triggering.

In contrast to other receptors expressed on DCs such as Dectin-1, DCIR, DC-SIGN, or members of the Siglec family no classical signal motifs like ITAMs or ITIMs were found for mPDCA-1 [Blasius A, Blood 2006; Meyer-Wentrup F, Blood 2008; van Kooyk Y, Nat Rev Immunol 2003]. This might indicate that the signaling of mPDCA-1 depends on intracellular adaptor molecules, shown for example for Dectin-2 that also lacks classical signal motifs [Ariizumi K, J Biol Chem. 2000]. Structural data, such as the dual-tyrosine motif in the cytosolic domain, implicated that BST2 potentially interacts with other adaptor molecules (e.g. the μ 1 and μ 2 subunit of the AP1 and AP2 adaptor molecules) [Rollason R, J Cell Sci. 2007]. Kupzig *et al.* proposed that the cytosolic domains of BST2 might create a platform for the docking of signaling complexes [Kupzig S, Traffic 2003]. The exact mechanism of the mPDCA-1-mediated signal transduction for IFN-I inhibition remains unclear and so far no downstream key molecules were described to be activated after cross-linkage of this receptor. Hence, further experiments are necessary to identify the involved pathways. The observed tyrosine phosphorylation and calcium influx were also demonstrated for the human PDC-specific receptor BDCA-2. Here, signaling was dependent on Src kinases [Dzionek A, JEM 01] resulting in Syk, Slp65 and PLC γ 2-mediated NF- κ B activation [Röck J, EJI 07; Cao W, PLoS 2007]. These molecules might be also attractive targets for mPDCA-1.

The role of the mPDCA-1 mediated IFN α -inhibition is still unclear. The function of PDC-secreted IFN-I had been described earlier. Briefly, IFN-I has potent anti-viral and anti-proliferative functions. IFN-I induces the expression of several IFN-I-responsive genes, including 2',5'-oligoadenylate synthetase and synthetase-like proteins, MX2 or members of the IFIT family, and other anti-viral proteins resulting in the inhibition of viral replication [Der SD, PNAS 1998; Baechler EC, PNAS 2003]. IFN-I also induces the production of other pro-inflammatory cytokines and thereby activates NK cells or cDCs. PDCs have a bystander function in the induction of anti-viral reactions, as PDC-secreted IFN-I for example leads to the upregulation of MHC-I molecules on cDCs. The increased MHC-I presentation of viral peptides on infected cells then enables an efficient anti-viral response by CTLs [Le Bon A, Nat Immunol 2005; Dalod M, JEM 2003; Barchet W, Semin Immunol 2005]. Thus, the inhibition of IFN-I production after

triggering mPDCA-1 could be a viral escape mechanism by attenuation of immune responses. The interaction of human BST2 with viral proteins was recently observed as well as many DC-expressed cell surface receptors, such as DC-SIGN or other lectin structures, interacted with viral proteins or glycoproteins [Neil SJD, Nature 2008; van Damme N, Cell Host Microbiol 2008; Geijtenbeek TB, J Biol Chem. 2002]. PDCs also have a regulatory function in the initiation of anti-tumor responses and are correlated with a negative outcome of cancer [Hartmann E, Cancer Res 2003; Vermi W, J Pathol 2003; Treilleux I, Clin Cancer Res. 2004; Zou W Nat Med 2001; Munn DH, J Clin Invest 2004]. Therefore, the natural ligand could be also a tumor-expressed molecule or a soluble factor, which initiates a tumor-escape mechanism by abrogation of IFN-I. This would result in reduced orchestration of DC-mediated tumor responses including less tumor-reactive CD4⁺ and CD8⁺ T cells or NK cells, finally leading to the survival of the tumor. Recently, BST2 was identified as a tetherin member involved in the interaction with the Vpu protein of maturing HIV virions *in vitro*, preventing its release and leading to the inhibition of the viral replication and spreading [Neil SJD, Nature 2008; van Damme N, Cell Host Microbiol 2008]. Thus, in addition to the anti-viral effect of secreted IFN-I and expression of anti-proliferative molecules, PDCs might be equipped with another antiviral function. In addition, the IFN-dependent induction of BST2 in other cells augmented the antiviral mechanism by further inhibition of virus spread. The interaction with the IFN-I pathway and the importance for HIV retention implicates that mPDCA-1 would be an attractive target for future immunotherapy of viral infections.

A different effect was observed in autoimmune diseases, where PDC-secreted IFN-I is a major factor for the induction and development of the disorders [Nestle FO, JEM 2005; Christensen SR, Immunity 2006; Farkas L, Am J Pathol 2001; Blanco P, Science 2001; Cavanagh LL, Arthritis Res Ther 2005; Lande R, J Immunol 2004]. For example the high concentrations of IFN α in the sera of SLE patients were found to activate auto-antigen presenting cDCs to trigger T cell-mediated autoimmunity [Rönnblom L, Arthritis Res Ther 2003; Blanco, P, Science 2001]. This process is called “break of tolerance” [Palucka AK, PNAs 2005; Banchereau J, Immunity 2006]. Other effects of IFN-I include the reduction of apoptosis of autoreactive T cells. PDC-secreted IFN α as well as IL-6 and IL-8 further lead to the differentiation of plasma cells [Jego G, Immunity 2003; Poeck H, Blood 2004], producing antibodies against auto-antigens. As a consequence, the effect of mPDCA-1 triggering could be investigated in a murine SLE model. Suitable lupus models are e.g. New Zealand Black (NZB), New Zealand White (NZW), or MRL mice [reviewed by Banchereau J, Immunity 2006; Barrat FJ, EJI 2007]. Similar to the human BDCA-2 receptor, the abrogation of IFN-I would have a beneficial impact for the treatment or functional investigation of this autoimmune disease [Dzionek A, Hum Immunol. 2002].

The most important function of DCs is the uptake, processing and presentation of exogenous antigens. For the antigen uptake DCs are equipped with a number of specific antigen uptake receptors including c-type lectins, scavenger and Fc receptors [Dzionek A, JEM 2001; Röck J, EJI 2007; Bonifaz L, JEM 2002 and JEM 2004; Dudziak D, Science 2007; Sancho D, J Clin

Invest. 2008; Zhang J, Blood 2006; Meyer-Wentrup F, Blood 2008]. Thereby, the expression-pattern of antigen uptake receptors determines the spectrum of pathogenic structures, which a particular DC population can respond to. Thus, the endocytotic capacity of mPDCA-1 was investigated. It could be demonstrated that mPDCA-1 significantly internalized *in vitro* and *in vivo* following the ligation with the specific mAb. This observation indicated a potential function of this receptor in antigen-uptake. These results were supported by other groups, showing an efficient internalization of anti-mPDCA-1 mAbs [Kupzig S, Traffic 2003; Blasius A, Blood 2006]. Zhang *et al.* demonstrated only weak internalization of mPDCA-1, which can be explained by the usage of PDCs isolated from different lymphoid tissues or other antibody clones [Zhang J, Blood 2006]. Recently, Dudziak *et al.* demonstrated that the rate of internalization not necessary correlates with the efficiency of antigen presentation [Dudziak D, Science 2007]. The four anti-mPDCA-1 mAbs generated in this study internalized with different kinetics. For example clone 3D5 showed only poor internalization, whereas clone 1C2 showed similar kinetics as the antigen uptake receptors BDCA-2 and DEC205 [Dzionek A, JEM 2001; Bonifaz L, JEM 2002 and JEM 2004]. As clone 3D5 recognizes a different epitope than clone 1C2, these data imply that 3D5 might induce another conformational change of mPDCA-1 as the other clones or bind an atypical, irrelevant domain. This might be a reason for the weaker internalization. In the opposite sense, the other clones might detect the epitope recognized by natural ligand of mPDCA-1.

Different reports demonstrated a clathrin-mediated endocytosis (CME) of rat or human BST2. Rollason *et al.* reported a sequential interaction of the intracellular domain of BST2 with the AP2 and AP1 adaptor complexes in a clathrin-mediated manner [Rollason R, J Cell Sci. 2007]. In addition, Kupzig *et al.* showed that BST2 cycled between the cell surface ("lipid rafts") and the TGN [Kupzig S, Traffic 2003]. Also co-localization with markers related to the CME pathway, such as transferrin and EEA1, had been reported. In contrast, BST2 failed to enter LAMP1/CD63⁺ late endosomes [Rollason R, J Cell Sci. 2007]. The efficient endocytosis of the receptor-antibody complex, delivery to the TGN as well as the co-localization to EEA1⁺ early endosomes were indications for a function as antigen-uptake receptor [Kupzig S, Traffic 2003; Rollason R, JCS 2008]. These implications were further underlined as many cell surface receptors on DCs are connected to the uptake of antigens. In contrast, mPDCA-1 did not co-localize with lysosomes in opposition to other antigen uptake receptors such as BDCA-2 or DEC205 [Dzionek A, JEM 2001; Jähn PS, EJI 2007; Mahnke K, J Cell Biol 2000]. These latter observations were contradictory to the molecular structure of mPDCA-1 and the rapid endocytosis, and it had to be tested, whether mPDCA-1 in fact functions as antigen-uptake receptor.

In the past PDCs were assigned only a minor role in the induction of adaptive immune responses unlike their contribution to innate immunity and tolerance induction [Yoneyama H, JEM 2005; Le Bon A, Nat Immunol 2003; Abe M, Am J Transplant. 2005; Grohmann U, Nat Med 2007; Kang H-K, JI 2007; Sharma MD, J Clin Inv 2007; Fallarino F, Curr Drug Metab.

2007; Lou Y, *J Clin Invest.* 2008]. In these studies PDCs were not targeted via specific antigen-uptake receptors and their poor T cell stimulation might be due to the fact that PDCs were not able to take up the antigens. Receptor-mediated endocytosis of antigens is more efficient and several molecules were shown to function as specialized antigen-uptake receptors such as BDCA-2, DCIR, DEC-205, or DC-SIGN [Dzionek A, *J Clin Invest.* 2000; Bonifaz L, *JEM* 2002; Wang J, *Immunology* 2007; Aarnoudse CA, *Int J Cancer.* 2007]. Thus, in this work the role of mPDCA-1 as an antigen-uptake receptor and thereby the APC function of PDCs was tested. It was planned to use the anti-mPDCA-1 mAb as vector for antigen delivery to PDCs. Since PDCs are depleted rapidly and efficiently *in vivo* after administration of the mAb as described earlier, a F(ab')₂ fragment of the anti-mPDCA-1 mAb was generated, which did not induce the depletion of these cells. A model antigen was covalently conjugated to the non-depleting F(ab')₂ anti-mPDCA-1 fragment, which specifically targeted PDCs both *in vitro* and *in vivo*. In this work Ovalbumin protein was chosen as an appropriate model, as several transgenic T cell readout systems were available. This targeting construct was designed to show whether mPDCA-1 functions as antigen-uptake receptor and PDCs could prime naïve T cells. The mere endocytosis is not sufficient for this function as other internalizing cell surface molecules, such as MHC, TCR or interleukin receptors are not antigen-uptake receptors.

The general stimulatory capacity of PDCs was tested in a preliminary experiment. For this, PDCs were loaded exogenously with OVA peptide before co-culture with naïve, antigen-specific T cells. It was shown, that PDCs were able to initiate strong CD4 and CD8 T cell proliferation. These results indicated that peptide-loaded PDCs efficiently present MHC-peptide complexes and stimulate naïve T cells. As even unstimulated, peptide-loaded PDCs induce T cell priming, the basic level of co-stimulatory molecules on PDCs might be sufficient for activation of the T cells. It cannot be excluded that PDCs were artificially activated in these *in vitro* experiments, although they did not upregulate significant amounts of co-stimulatory molecules. Another explanation is that the low level of co-stimulatory molecules on immature PDCs was compensated by unphysiologic excess of MHC-peptide complexes after peptide loading. Thus, only few co-stimulatory molecules were sufficient to stimulate naïve T cells. After confirming that PDCs were generally able to prime T cells, the uptake of OVA protein conjugated to the mPDCA-1 targeting construct for delivery into processing pathways was analyzed. Recent reports demonstrated an influence of the receptor for antigen delivery into distinct processing/presentation compartments. Antigens targeted to DEC205 or the Mannose receptors were efficiently cross-presented on MHC-I molecules, whereas DCIR2-delivered antigen was presented on MHC-II molecules [Dudziak D, *Science* 07; Burgdorf S, *Science* 07]. Beside the function of mPDCA-1 as antigen-uptake receptor it was investigated in the experiments presented here, whether targeted antigens were processed for MHC I or II presentation. *In vitro* CD4 priming experiments were performed at the beginning. Unstimulated PDCs did not prime antigen-specific naïve CD4⁺ T cells, although the uptake via mPDCA-1 was stimulus-independent. In contrast, if PDCs received an additional stimulus, antigen delivery via

mPDCA-1 resulted in efficient CD4⁺ T cell priming. These differential *in vitro* results can be explained by the fact that immature DCs need an additional activation stimulus to efficiently prime naïve T cells. Bonifaz *et al.* and Steinman *et al.* demonstrated that cDCs, which were *in vivo* targeted with anti-DEC-205-OVA antibody construct, also needed a stimulus to initiate a T cell response [Bonifaz LC, JEM 2002 and 2004; Steinman RM, Ann N Y Acad Sci. 2003]. In contrast, immature cDC induced anergy or apoptosis of the T cells (“peripheral tolerance”) although they presented antigen (first signal) but did not provide a second signal via co-stimulatory molecules [Hawiger D, JEM 2001]. To induce a strong T cell response Bonifaz *et al.* used CD40L-activated cDCs. As PDCs express only low levels of CD40, in this work the TLR9 ligand CpG was used, which is an established PDC stimulus [Meyer-Wentrup F, Blood 2008]. In contrast to peptide-loaded PDCs, which stimulated naïve T cells without further stimulation, the presentation of native antigen *in vitro* clearly depended on additional activation. It is still speculative, whether in this case the activation had an impact on the upregulation of co-stimulatory molecules to produce a second signal. On the other hand it was possible that PDCs could process endocytosed antigen only after activation, underlining the affection of the processing/presentation pathway.

To assess the efficiency of mPDCA-1-mediated antigen uptake, the OVA quantities necessary for efficient CD4⁺ T cell priming were directly compared. Targeting OVA via mPDCA-1 was always and significantly superior to soluble OVA or OVA-targeted via isotype control antibody (Fig. 4.3.5A+C). The minimum concentration of mPDCA-1-OVA required for a detectable effect was about 250 ng/ml *in vitro* (Fig. 4.3.5C), which was in line with our previous results [Sapozhnikov A, JEM 2007]. In contrast, if soluble OVA protein instead of peptide had been used as model antigen, amounts of 100-500 µg or up to several milligrams were described to induce a PDC-mediated T cell response [Mouries J, unpublished data; #PB-2497, ECI congress, Paris 2006]. However, the amount needed for the induction of CD4⁺ T cell proliferation was clearly higher for PDCs targeted via mPDCA-1 compared to DEC-205-targeted cDCs [Sapozhnikov A, JEM 2007; Bonifaz LC, JEM 2002 and 2004]. This difference may be due to unique natures of the receptors but more likely due to distinct priming or processing capacities of PDCs and cDCs [Salio M, JEM 2004; Sapozhnikov A, JEM 07].

It was demonstrated that mouse PDCs induced a strong proliferation of naïve CD4⁺ T cells after taking up OVA antigen via mPDCA-1 *in vitro*. In previous experiments we had already demonstrated that antigen delivery via mPDCA-1 PDCs induced a persistent response of naïve CD4⁺ T cells *in vivo*, shown by the presence of IFN γ -producing effector memory T cells [Sapozhnikov A, JEM 2007]. To test whether the *in vitro* PDC-induced T cell expansion was associated with the generation of productive but not anergic T effector cells, the proliferation and cytokine production was studied after expansion [Hawiger D, JEM 2001; Itano A, Nat Imm 2003; Sporri R, Nat Imm 2005]. In these experiments restimulation of PDC-primed T cells resulted in a strong IL-2 and IFN γ production and also TNF α secretion, which was comparable but not identical if splenocytes or cDCs were used as APCs. This cytokine profile as well as the

absence of IL-4 producing CD4⁺ T cells suggests a T_H1 polarization [Openshaw P, JEM 1995]. This phenotype was expected as the CpG stimulus needed for optimal priming resulted in the production of IFN α (and IL-12) by PDCs, and the presence of these cytokines typically favored a T_H1 polarization. Interestingly, about 10-20% IFN γ and IL-10 producing CD4⁺ T cells were detected if PDCs but not cDCs primed naïve T cells. In the past several groups also demonstrated the generation of IFN γ IL-10 double-positive CD4⁺ T cells after PDC-priming, probably caused by IFN-I [Dzionek A, Hum Immunol. 2002; Kadowaki N, Hum Immunol 2002; Ito T, JEM 2007; Bochtler P, JI 08;Rutz S, PNAS 2008]. The data of the *in vitro* cytokine production clearly showed that PDCs are able to stimulate naïve CD4⁺ T cells after mPDCA-1 targeting, resulting in a productive response that includes IFN γ -producing effector T cells, comparable to a cDC-induced T_H reaction.

In the past it was shown that PDCs present peptides to antigen-specific CD4⁺ T cells but were less competent to take up and process exogenous proteins for efficient cross-presentation to CD8⁺ T cells in contrast to cDCs [Schlecht G, Blood 2004; Lou Y, JI 2007; Liu C, J Clin Invest. 2008]. As in this work PDCs efficiently process antigens and prime naïve CD4⁺ T cells *in vitro*, next the cross-priming capacity of PDC after antigen-delivery via mPDCA-1 was investigated. It was shown that after mPDCA-1 receptor-mediated uptake PDCs efficiently cross-present exogenous antigens *in vitro*. Compared to soluble or isotype control targeted antigen, significantly lower antigen amounts were needed to induce maximum T cell response, underlining the efficiency of mPDCA-1 mediated antigen uptake. This cross-priming of CD8⁺ T cells could be prevented by blocking of the receptor with excess of unconjugated anti-mPDCA-1 mAb. Identical results were obtained for CD4⁺ T cells, underlining the specificity of antigen delivery via mPDCA-1. In contrast to other reports that propose only a synergistic role for PDCs in the activation of CD8⁺ T cells by production of IFN-I but no direct effect on T cells, these *in vitro* data clearly showed the cross-priming capacity of PDCs [Lou Y, JI 2007]. These different results may be based on different experimental settings, highlighting mPDCA-1-mediated antigen delivery. It was further shown that the receptor pathway is critical for the direction of antigens into distinct processing compartments, i.e. for subsequent MHC-I or MHC-II presentation [Dudziak D, Science 07; Burgdorf S, Science 07]. The result of the work presented here impressively demonstrated that OVA antigen was presented on both MHC-I and II molecules after mPDCA-1 targeting. No prevalence for the processing compartment was observed.

Similar to the CD4⁺ T cell priming, cross-presentation of OVA protein to CD8⁺ T cells required an additional stimulus. The importance of PDC activation has been also described for Siglec-H eliciting a cytotoxic CD8⁺ T cell response [Zhang, J, Blood 06]. Interestingly, compared to the CD4⁺ T cell priming higher antigen amounts were necessary for the induction of CD8⁺ T cell proliferation. This effect might be explained either by differential requirements for the cross-presentation pathway or by the fact that the cross-presentation process is less efficient and only a part of the antigens gains access to this pathway. For example for cross-presentation via the

TAP-dependent pathway the endocytosed antigen has to be exported from the phagosome into the cytosolic proteasome. Degraded antigens were then transported into the endoplasmic reticulum, where they bind to MHC-I molecules [Kovacsovics-Bankowski M, Science 1995]. Using specific proteasome inhibitors, e.g. MG132 or epoxomicin [Burgdorf S, Nat Immunol 2008], it could be tested whether PDCs use this pathway for cross-presentation of mPDCA-1 targeted antigen. Salio *et al.* suggest that PDCs might lack essential prerequisites for the cross-presentation of exogenous antigens [Salio M, JEM 2004], but the data shown here indicate that PDCs possess functional cross-priming machinery.

The priming capacity of PDCs from different lymphoid organs was investigated. PDCs from LNs, spleen, and BM as well as *in vitro* generated PDCs were able to prime CD4⁺ T cells. They also demonstrated an almost identical cross-priming capacity. These results are conflicting with other reports that demonstrated differences between PDCs from several lymphoid organs. It was shown that LN-PDCs but not spleen PDCs could induce a CD4 response *in vivo*, probably due to functional specialization [Sapozhnikov A, JEM 2007]. Interestingly, only LN but not spleen PDCs were able to take up DQ-OVA *in vivo*. Also differences between liver and spleen PDCs in antigen uptake, cytokine production and their allo-activation potential had been reported [Shu S-A, Clinical and Experimental Immunology 2007]. In this study the induced T cell response depends on mPDCA-1 mediated antigen delivery. The influence of the antigen-uptake receptor for adaptive immune responses has been described earlier [Jähn P, EJI 08, Bonifaz L, JEM 2002 and 2004; Zhang J, Blood 06; Dzionek, JEM 2001]. On the other hand the uptake of soluble or untargeted antigen was less efficient. It is speculative whether PDCs from different organs have in general an unequal endocytic capacity that affects their T cell response. As PDCs poorly take up antigen unspecifically, e.g. by macropinocytosis, but rather receptor-mediated [Dzionek A, JI 2000; Dzionek, JEM 2001; Jähn PS, EJI 2008], the conflicting results can be explained more likely with either their maturation state [Toma-Hirano M, EJI 2007; Toyama-Sorimachi N, JI 2005] or by differentially regulated antigen processing machinery [Kamogawa-Schifter Y, Blood 2005]. In this work a stimulus was applied. This may imply that PDCs from several lymphoid organs basically differ in their priming capacities, e.g. are differentially matured or do not have the identical cellular equipment for an adaptive immune response. After receiving an activation stimulus they become synchronized. These considerations may explain the contradictory reports about their general priming capacity in the past, and explain that after activation PDCs are able to elicit the same T cell priming.

The data presented in this work clearly suggest the importance of additional PDC stimulation for optimal T cell response *in vitro* after uptake via mPDCA-1. The relevance of an additional activation of PDCs was reported previously, as only activated PDCs were able to induce an adaptive T cell response [Schlecht G, Blood 2004; Lou Y, JI 2007; Liu C, J Clin Invest. 2008]. Interestingly, as also unstimulated cells internalized the receptor-antibody complex, the activation did not influence the antigen-uptake. The expression of mPDCA-1 on PDCs was not

affected upon activation or culture condition. The precise mechanism of an additional stimulus for T cell priming remains elusive: Stimulation resulted on the one hand in upregulation of co-stimulatory and MHC molecules on PDCs, on the other hand it is not implausible that the processing and presentation machinery is turned on.

In the past it was reported that IFN α -matured cDCs showed an increased cross-presentation capacity, suggesting a “licensing” by IFN-I, which increases the presentation of viral peptides on MHC-I. This mechanism facilitates the recognition of infected cells by cytotoxic T cells [Lapenta C, EJI 2006; Le Bon A, Nat Immunol 03]. In this work it has been demonstrated that upon activation co-stimulatory markers such as CD40, CD80, and CD86 and also MHC-I and -II were upregulated on PDCs. These data suggested that the priming also depends on the “second signal”, provided by co-stimulatory molecules [Bonifaz LC, JEM 2002 and 2004; Steinman RM, Ann N Y Acad Sci. 2003]. Conflicting with this hypothesis, it was shown that peptide-loaded PDCs could prime T cells without additional activation. As it was still possible that a strong and superior first signal, as represented by the huge amount of OVA peptide, would supersede the need for co-stimulation [shown by the activation of CD8⁺ T cells; Wang B, JI 2000], the impact of an additional CpG-stimulus was assessed by titration of the peptide amount. It could be demonstrated that also in lower peptide concentrations the stimulus had no positive effect upon PDC-mediated T cell stimulation, which argues against the requirement of additional co-stimulation.

In the second hypothesis the additional stimulus activates the antigen processing and presentation machinery, resulting in an increased presentation of OVA antigen onto MHC molecules. In order to monitor the MHC-I restricted presentation of OVA-derived peptide on the cell surface of PDC targeted with anti-mPDCA-1F(ab')₂-OVA, cells were stained with mAb recognizing the OVA peptide in the context of MHC-I (H-2k^b) molecules [Porgador A, Immunity 1997]. After CpG-activation MHC-I molecules were upregulated on PDCs, which could be due to the auto- and paracrine effect of IFN α , which was produced by PDCs after CpG stimulation. The upregulated MHC-I expression was also detected by increased anti-SIINFEKL:H-2k^b mAb staining of peptide-loaded PDCs. Unfortunately, processed OVA protein was not detected on MHC-I molecules on PDCs, possibly due to the low number of presented peptides. Although PDCs were incubated with up to 25 μ g/ml OVA protein (mPDCA-1-OVA) or up to 2 mg/ml soluble OVA, no processed OVA could be detected on surface MHC-I. One reason can be that the immunogenic sequence (SIINFEKL) is only about 2.5% of the complete OVA protein. Thus, proteolytic degradation of the protein results in the generation of many irrelevant peptides but few immuno-dominant peptides [Boscardin SB, JEM 2006], which elucidates the differential outcome between loading with OVA protein and OVA peptide. Another explanation addresses the limited sensitivity of the antibody. Although several staining methods were applied to enhance the signal intensity (Fluorescence amplification by the FASER system [Shimizu K, JI 2006]) or magnetofluorescent liposomes [Kunkel D, Cytometry A. 2003], no processed antigen was detectable. Obviously, the peptide amount that could be achieved via the targeting of OVA-anti-mPDCA-1 mAb constructs were dramatically lower than the quantity required for the

detection of processed antigen by the specific antibody. Other groups used highly unphysiologic concentrations of OVA protein. Burgdorf *et al.* exposed DCs to 5 mg/ml soluble OVA to visualize processed antigen by immunofluorescence, thereby underlining the limited sensitivity of the antibody [Burgdorf S, Science 2007]. The hypothesis that the stimulus activates the antigen processing machinery was further underlined by the finding that also in lower peptide concentrations the stimulus had no positive effect upon PDC-mediated T cell stimulation. In this situation the co-stimulus can be disregarded, as the amount of antigen was critical, which could be increased by activation of the processing machinery. Due to a limited readout system the exact impact of an additional activation cannot be revealed at this point and further experiments are necessary that show sensitivity as high as the antigen-specific T cells, e.g. detection of MHC-peptide complexes by recombinant TCRs.

In contrast to the *in vitro* priming experiments presented in this study, we did not need an additional activation for CD4⁺ T cell priming *in vivo* (which has been performed in collaboration with Steffen Jung, Israel). For these experiments a recently developed diphtheria toxin receptor (DTR)-based system was applied that allowed the conditional ablation of CD11c^{high} cDCs. In these transgenic mice the DTR is co-expressed with the *Ilgax* gene, which encodes the α_x subunit of the CD11c integrin leading to the expression in CD11c⁺ cells. Administration of Diphtheria toxin resulted in the depletion of all cDCs but not PDCs [Jung S, Immunity 2002; Sapoznikov A, JEM 2007]. After depletion of cDCs, mice were immunized with mPDCA-1-OVA or DEC-205-OVA targeting constructs after adoptive transfer of OVA-specific T cells. Surprisingly, also in the absence of cDCs a strong proliferation of CD4⁺ T cells but not CD8⁺ T cells could be detected, when OVA was targeted to PDC via mPDCA-1 but not via DEC-205 [Sapoznikov A, JEM 2007]. The priming of naïve CD4⁺ T cells was also observed if mPDCA-1-OVA was administrated, and PDCs or cDCs were subsequently isolated and *in vitro* co-cultured with OVA-specific CD4⁺ T cells. Interestingly, after targeting OVA via mPDCA-1 only PDCs but not cDCs induced a strong T cell response, further underlining the specificity of the targeting procedure and the priming capacity of PDCs. Only LN but not spleen derived PDCs could induce a CD4⁺ T cell response, contradictory to the *in vitro* data presented in this work, in which an equal priming capacity was shown for all PDCs tested. Further experiments are necessary to resolve these conflicting results, e.g. further functional characterization of the PDCs used for these studies. In the work presented here PDCs from different lymphoid tissues were *in vitro* activated for efficient priming. In the *in vivo* experiment no activation signal was applied. It is speculative whether the activated PDCs *in vitro* were actually comparable to the “untreated” PDCs *in vivo*, which also might receive other signals from the environment. Thus, the experimental setups might be a reason for the opposing results. A major difference between the results obtained in this work and in collaboration with Steffen Jung was observed for the activation of CD8⁺ T cells. On the one hand we described that PDCs were not able to cross-present exogenous antigens *in vivo*, either soluble or targeted via mPDCA-1. These data were explained by the lack of the phagosome-to-cytosol pathway required for cross-presentation

[Sapozhnikov A, JEM 2007; Salio M, JEM 2004]. As in this work, PDCs efficiently cross-prime CD8⁺ T cells after antigen targeting via mPDCA-1 *in vitro*, the former conclusion had to be revised: PDCs do have the ability to present exogenous antigen on MHC-I molecules, but for the initiation of a CD8⁺ T cell response an additional activation of PDCs is obligatory. The missing activation signal clearly distinguished these two experimental setups. As a consequence these new data indicate that PDCs have an overall capacity to process antigens for CD4⁺ and CD8⁺ T cell priming. Thus, the cross-presentation of exogenous antigen is no longer considered as a unique property of CD8 α ⁺ cDCs but PDCs and cDCs are able to generate cytotoxic T cells. This study provides evidence that PDCs may represent an attractive target to boost the efficacy of vaccines by induction of a CD8⁺ T cell response.

In summary, in this work it was shown that PDCs have not only a secretory function by production of IFN α but also the role of mPDCA-1 as novel antigen-uptake receptor was highlighted. The mPDCA-1-mediated antigen uptake resulted in significant priming and cross-priming of antigen-specific CD4⁺ and CD8⁺ T cells.

5.3 Heterogeneous expression of Sca-1 defines functionally different PDC subsets

The characterization of PDCs by the classical cell surface receptors B220, Ly-6C, and CD11c as well by specific markers mPDCA-1 and Siglec-H demonstrated a homogeneous population [data not shown; Blasius A, Blood 2004]. Further phenotyping revealed that PDCs exhibited a differential expression of the Sca-1 antigen, describing two subpopulations, Sca-1⁺ and Sca-1⁻ PDCs.

The Sca-1 protein, also termed lymphocyte activation protein 6A (Ly-6A), is a small molecule of about 18 kDa in size and was originally identified on activated lymphocytes, in particular T cells [Yotoku M, JI 1974]. Sca-1 is a member of the Ly-6 multigene family encoding several highly homologous, glycosylphosphatidylinositol (GPI)-anchored membrane proteins [Sinclair AM, Blood 1993; Reiser H, PNAS 1988]. It has been mainly used as "stem cell or progenitor marker" to describe Sca-1⁺, c-kit⁺ lineage⁻ hematopoietic stem cells [Ito M, Stem cells 1996]. There was only one report in which PDCs had been shown to be positive for this marker [O'Keeffe M, JEM 2002]. But neither a differential expression pattern within the PDC population nor functional implications of the expression had been shown.

Interestingly, the percentage of Sca-1⁺ PDCs differed depending on their localization. In BM only 10% to 15% of PDCs expressed Sca-1. In contrast, in blood and spleen the percentage of Sca-1⁺ PDC increased to 25% and 50%, reaching the highest proportion in lymph nodes (>80%). Sca-1⁺ PDCs also showed the highest Sca-1 expression level compared to other cells of tested tissues. As DCs generally develop from CD34⁺ progenitors in the BM and then migrate into the periphery [Banchereau J, Nature 1998], the heterogeneous expression in differential lymphoid tissues might imply a transition of Sca-1⁻ to Sca-1⁺ PDCs during their hematopoietic development. It is speculative whether Sca-1⁻ PDCs in the BM were the earlier, immature subsets, compared to the more differentiated Sca-1⁺ PDCs that were found in the periphery.

Thus, expression of Sca-1 might reflect developmental stages of PDCs and Sca-1⁻ appear earlier in the development. To underline this hypothesis the following *in vivo* proliferation experiments were performed. Within the Sca-1⁻ compartment of BM and spleen PDCs, a higher BrdU incorporation could be demonstrated. These preliminary data implicated that PDCs were negative for Sca-1 at the beginning of their development and upregulated this marker later. Additional pulse/chase experiments should then demonstrate the transition of Sca-1⁻ into Sca-1⁺ PDCs. Immediately after the BrdU pulse, a higher incorporation of BrdU was detected in Sca-1⁻ PDCs of all organs. The greatest discrepancy between Sca-1⁺ and Sca-1⁻ PDCs was observed in spleen and LNs. These results indicate that Sca-1⁻ PDCs were the first population of PDCs, supporting the preliminary data. Hypothesizing that Sca-1⁻ PDCs develop into Sca-1⁺ PDCs, at a later time a higher BrdU proportion was expected within Sca-1⁺ PDCs. After BrdU removal, a shift in the proportion for BrdU⁺ cells between Sca-1⁺ and Sca-1⁻ PDCs was detected first in the BM, followed by spleen. At this point the highest BrdU contingent was found in Sca-1⁺ PDCs, according to the above hypothesis. This tendency was detected in LN-PDCs not until a later point. These data suggested the transition of Sca-1⁻ to Sca-1⁺ PDCs by upregulation of this marker during their post-proliferation phase or by maturing PDCs. Transfer experiments, showing that grafted Sca-1⁻ PDCs become predominately Sca-1⁺, also supported the development of Sca-1⁺ PDCs from Sca-1⁻ cells. These data also excluded the possibility that Sca-1 expression characterizes distinct or separated PDC subsets.

Other groups recently investigated the development of PDCs by differential expression of cell surface makers. In the BM, immature PDCs (Ly-49Q⁻) as well as mature PDCs (Ly-49Q⁺) were described, whereas in the periphery only Ly-49Q⁺ PDCs were found [Omatsu Y, J Immunol 2005; Toyama-Sorimachi N, J Immunol 2005; Kamogawa-Schifter Y, Blood 2005]. For Sca-1 also low expression in the BM and an increased expression on PDCs in the periphery could be detected. Collectively, these data show that the expression of Ly-49Q and Sca-1 tends to be regulated in a similar way. In contrast, both Sca-1⁺ and Sca-1⁻ PDCs are found in the periphery. This heterogeneity is not restricted to the BM like Ly-49Q. Thus, Sca-1 defines developmental PDC subsets in the whole organism. In general, a co-regulated expression of both markers was not found. Another report showed the existence of CD4⁻ and CD4⁺ PDCs and it was hypothesized whether these are two distinct subsets or rather reflect two developmental stages of the same population [O'Keeffe M, JEM 2002]. They could show that PDCs up-regulated the expression of the CD4 molecule upon activation and demonstrated that CD4⁻ PDCs were the immediate precursors of CD4⁺ PDCs.

It was hypothesized that organ-dependent differences of the Sca-1 expression correlate not only with the development but also with the activation status of PDCs. As Sca-1⁻ PDCs appear earlier they might reflect a rather immature stage, whereas Sca-1⁺ PDCs comprise the more mature form of these cells. The differential Sca-1 regulation on PDCs from different organs was subsequently investigated under activating conditions. Although in steady state no correlation to the expression of co-stimulatory molecules was detected, it has been shown that PDCs

upregulated Sca-1 upon TLR7 or TLR9 stimulation both *in vitro* and *in vivo*. Upon CpG activation the expression of Sca-1 as well as CD40, CD80, and CD86 were upregulated. These co-stimulatory molecules are known to be upregulated upon activation [O’Keeffe M, JEM 2002; O’Keeffe M, Blood 2003]. In a different context it was shown that Sca-1 expressed on T cells was involved in activation or differentiation [Codias EK, JI 1990; Flood M, JEM 1990; Bamezai A, JI 1995], Sca-1 might indeed serve as an activation marker and Sca-1⁺ PDCs reflect a more activated form of PDCs. As in steady state Sca-1⁻ and Sca-1⁺ PDCs exist, the latter might be inadequately activated, express only low levels of co-stimulatory molecules.

The results from these proliferation and activation experiments led to the following theory, depicted in Fig. 5.2. After development from PDC progenitors so-called pre-PDCs are found in the BM, which further develop into immature PDCs, characterized by the expression of mPDCA-1, Siglec-H and other PDC markers, but lack the expression of Sca-1. Immature PDCs migrate into the periphery where they persist in a non-dividing form [O’Keeffe, M, JEM 2002]. During this process and upon further activation signals PDCs upregulate the expression of Sca-1. As an activation is normally the signal for accumulation in the LNs, the dominate presence of Sca-1⁺ cells in LNs might reflect an activated status of these cells.

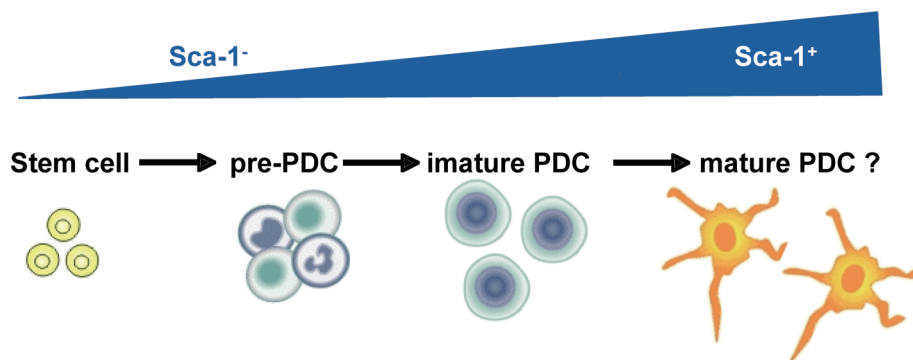


Fig. 5.2 Model of the Sca-1 expression during PDC development

In contrast to highly proliferative PDC precursors, early PDCs (as defined by mPDCA-1 and Siglec-H expression) do not proliferate. They reflect a rather immature phenotype, do not express Sca-1 and migrate into the periphery. Upon stimulation, immature PDCs upregulate the expression of Sca-1. In this activated or matured stage, PDCs mainly found in peripheral lymphoid organs such as the LNs.

It was speculated whether the expression of Sca-1 is associated with functional differences, in particular whether it correlated with the cytokine secretion. In the human system it has been shown that the ability of PDCs to produce IFN- α depends on their activation and maturation status [Krug A, EJI 2001]. Immature PDCs secrete IFN- α upon TLR activation but are not able to respond if restimulated in the matured stage [Jähn P, EJI 2008; Krug A, EJI 2001]. In this work in the Sca-1⁻ PDC compartment more IFN- α -producers were detected upon TLR stimulation and Sca-1⁻ PDCs also had a higher capacity to produce TNF- α . No significant differences could be observed regarding the IL-12 production. The differential cytokine production between Sca-1⁺ and Sca-1⁻ PDCs corresponded to the maturation status of PDCs, according to the above theory, which suggests that only immature PDCs are capable to produce IFN- α . Other observations revealed that PDCs with immature dendritic cell characteristics produced IFN- α .

upon activation and acquired a more mature phenotype and dendritic morphology [Zuniga EI, Nature Immunol 2004]. Sca-1⁻ PDCs predominantly located in the BM were regarded as more immature and were the major IFN α producers. On the other hand, matured Sca-1⁺ PDCs were mainly located in the LNs and produced less cytokines. A differential production of pro-inflammatory cytokines within the PDC population had been observed: For example after viral stimulation not all but only 15% to 20% of PDCs secreted IFN α . IL-12 was produced by 15% to 35% and between 10% and 60% of PDC responded with TNF α secretion [Zucchini N, Int Immunol. 2008]. Heterogeneous PDC responses were also reported by others [Jomantaite I, EJI 2004; Chen L, JI 2006]. These differences might be explained by compartmentation of PDC responses to infections or by lack of TLR expression [Jomantaite I, EJI 2004]. Iparaguierre *et al.* reported about two different types of murine PDCs, depending on either CpG or Influenza activation [Iparaguierre A, J Leukoc Biol. 2008]. They showed that virally activated PDCs respond with high IFN-I production whereas CpG-stimulated PDCs produce less interferon and acquire a more matured and DC-like phenotype. For human PDCs also heterogeneity between IFN α production and antigen presentation capacity was observed depending on the kind of activation [Jähn PS, EJI 2008]. The reason for the differential cytokine responses might be that Sca-1⁺ and Sca-1⁻ PDCs are equipped with a different set of cell surface or adapter signaling molecules necessary for appropriate responses against microbial challenge [Kamogawa-Schifter Y, Blood 2005]. Alternatively, PDCs have already downregulated these molecules after upregulation of Sca-1. Sca-1⁺ PDCs, that contain matured PDCs or PDCs in a later developmental stage, might have a different function as the Sca-1⁻ counterpart, for example a higher T cell stimulatory capacity. In collaboration with Steffen Jung we demonstrated that only LN-PDCs but not spleen PDCs were capable of priming naïve CD4⁺ T cells both *in vitro* and *in vivo* [Sapoznikov A, JEM 2007]. In the *in vitro* experiments of the work described here, PDCs from all organs were able to prime PDCs. These conflicting results might be explained by the application of an additional TLR stimulus that subsequently led to the upregulation of Sca-1 expression. As LN-PDCs were highly positive for Sca-1 it was planned to compare the priming capacities of Sca-1^{+/-} PDCs directly. Although this would be a good opportunity to assess a differential priming capacity, the experiments are critical as for efficient T cell priming an activation of PDCs was mandatory. Thus, all PDCs would upregulate Sca-1 and discrimination between both subsets would be difficult.

To find further functional differences, gene expression profiles of both PDC subpopulations were investigated. By microarray analysis a set of genes was found, significantly over-represented in Sca-1⁺ or Sca-1⁻ PDCs. Differentially transcribed cell surface receptors were e.g. CD22 and CD163 on Sca-1⁻ PDCs and CD44, CD69, EGRI, PROCR, and TNFR1 on Sca-1⁺ PDCs. Upon Gene Ontology Clustering several biologically and immunologically relevant pathways were analyzed. In Sca-1⁺ PDCs a variety of genes were observed, belonging to cell adhesion and migration, stress, immunity and inflammation pathways as well as TLR/cytokine signaling. As Sca-1⁺ PDCs are regarded to be the more mature cells, which already received a stimulus, these results could support the higher differentiation level. On the other hand relatively

more genes involved in metabolic processes were present in Sca-1⁻ PDCs. This might indicate the earlier developmental stage of this subset and the focus on cytokine secretion. As the regulation of the obtained genes was only shown by microarray analysis, further validation either by quantitative PCR or in particular on protein level by ELISA or flow cytometric analysis is mandatory. The confirmation might demonstrate if the differential Sca-1 expression substantially correlates with the presence of specifically expressed or regulated proteins representing a distinct function.

In conclusion, it was demonstrated that the expression of Sca-1 defines two functionally different populations, which are spatially separated in different lymphoid organs. The consequence of this heterogeneity was not answered conclusively. Immature Sca-1⁻ PDCs, possessing the higher ability to produce IFN-I, might have a strong role in innate immunity. In contrast, further differentiated Sca-1⁺ PDCs might be involved in adaptive immunity, possibly by interaction with T cells. Sca-1 can be regarded as an appropriate marker to detect activated PDCs. Although Sca-1 is commonly used as stem cell marker, its function on terminally differentiated cells, PDCs, is still unclear. Proliferation and transfer experiments indicated that the Sca-1⁻ population appears earlier in the development of PDCs.

6. OUTLOOK

This work revealed central aspects of the mPDCA-1 receptor, including the inhibition of IFN-I production, signal transduction, endocytosis, and a potential role as antigen-uptake receptor.

PDC-derived IFN-I is considered to be a pathophysiological factor in several autoimmune diseases, such as SLE or psoriasis. The abrogation of IFN α by mPDCA-1 triggering *in vivo* would be an attractive therapeutic target, which can be tested in several murine lupus models. The mechanism of TLR-induced inhibition of interferon production had not been resolved. Cross-linking of mPDCA-1 resulted in overall protein-tyrosine phosphorylation and calcium mobilization. To identify key molecules of the involved signal transduction pathway, it could be tested whether specific inhibitors of protein-tyrosine kinases, such as PP1 and PP2 that inhibit members of the src-family, or PTK, might abrogate the signaling [Dzionic A, JEM 2001]. The mPDCA-1 signaling pathway could be further investigated by identification of adaptor molecules, such as AP1+2, since the receptor lacked classical signal motifs [Rollason R, J Cell Sci 2007; Röck, EJI 2007]. The signaling pathway might be involved in the inhibition of IFN α or could also affect the endocytosis of the receptor. Since some anti-mPDCA-1 clones internalized but others not, it should be investigated whether the non-internalizing clones also induce phosphorylation and calcium flux. In other reports using BST2 transfected cells, the internalization of the receptor-antibody complex was caused by clathrin-mediated endocytosis (CME) [Kupzig S, Traffic 2003; Rollason R, J Cell Sci 2007]. It has to be shown whether this is also the responsible mechanism in isolated PDCs. After mPDCA-1 ligation the modification of clathrin heavy chain or cytoskeleton modulation could be investigated [Röck J, EJI 2007]. The future identification of the natural ligand of mPDCA-1 will help to understand the *in vivo* function of this receptor. Currently, two ligands of human BST2 are reported, suggesting on the one hand an antagonistic interaction with the HIV accessory molecule Vpu [Neil SJ, Nature 2008; van Damme N, Cell Host Microbiol 2008] and on the other hand binding of the ILT7 receptor expressed on human PDCs [Cao W, unpublished data]. Further studies have to show whether this is also true in the murine system. The generation of a recombinant mPDCA-1 fusion protein might be useful to identify cells expressing the ligand, which then can be used to create a cDNA library for further screenings. For the isolation of the ligand and further exploration of the mPDCA-1 signalosome the generated mPDCA-1/BST2 transfectants might be a promising tool. The generation of an mPDCA-1 knockout mouse might further reveal its function.

As several cell surface receptors expressed on DCs have a role in the uptake of antigens, it is currently elusive whether mPDCA-1 is also endocytosed after binding of the natural ligand. It has been shown that using the antibody as vector the mPDCA-1-mediated uptake of exogenous antigens resulted in processing and loading on MHC-I and -II molecules for efficient priming of naïve CD4⁺ and CD8⁺ T cells. The anti-mPDCA-1-F(ab')₂-OVA targeting system could be used to target e.g. tumor antigens directly to PDCs to assess their capacity in the generation of CTL or other anti-tumor responses. The B16 melanoma (OVA-) tumor model is an attractive target to study the role of PDCs and define if these cells directly induce a CTL response against the

tumor cells *in vivo* [Lou Y, JI 2007; Liu C, J Clin Invest. 2008]. Also the delivery of other antigens including viral proteins should be investigated to assess the potential of PDCs in vaccination trials. Future approaches might also involve the spatiotemporal co-localization of antigen and stimulus. Thus, a nano-particle system consisting of anti-mPDCA-1 mAb, TLR agonists, and model antigens would be a promising tool to study the capacity of PDCs to enhance immune responses [Zhang XQ, J Pharm Sci. 2007; Hao S, Immunology. 2007; Suzuki Y, Cancer Res. 2004].

Highly important for the outcome of these studies is the activation stage of the PDCs, since it was shown that the priming capacity of PDCs clearly depends on appropriate stimulation. Two distinct subsets of murine PDCs can be defined by differential expression of Sca-1, which also indicates heterogeneity in developmental and maturation stages as well as in their capacity to produce cytokines. Other reports showed a functional dichotomy for both human and mouse PDCs in the induction of innate or adaptive immune responses [Iparagirre A, J Leukoc Biol. 2008; Jähn PS, EJI 2008; O'Keeffe M, JEM 2002; Omatsu Y, JI 2005]. As Sca-1⁻ PDCs produce higher amounts of IFN α , it might be interesting whether the Sca-1⁺ PDC subset is characterized by a superior T cell priming capacity. Further studies are required to assign the precise role of Sca-1 in the functional outcome of PDC responses. For example a dissimilar localization or migratory capacity of Sca-1⁺ and Sca-1⁻ PDCs could be assessed. To track PDCs *in vivo*, in these experiments the expression of a fluorescent protein (GFP) under the mPDCA-1 promoter would be beneficial.

In summary, additional information of the exact function of the mPDCA-1 molecule and functional experiments will be crucial for understanding the role of PDCs both in steady state and (auto-) immunity.

7. APPENDIX

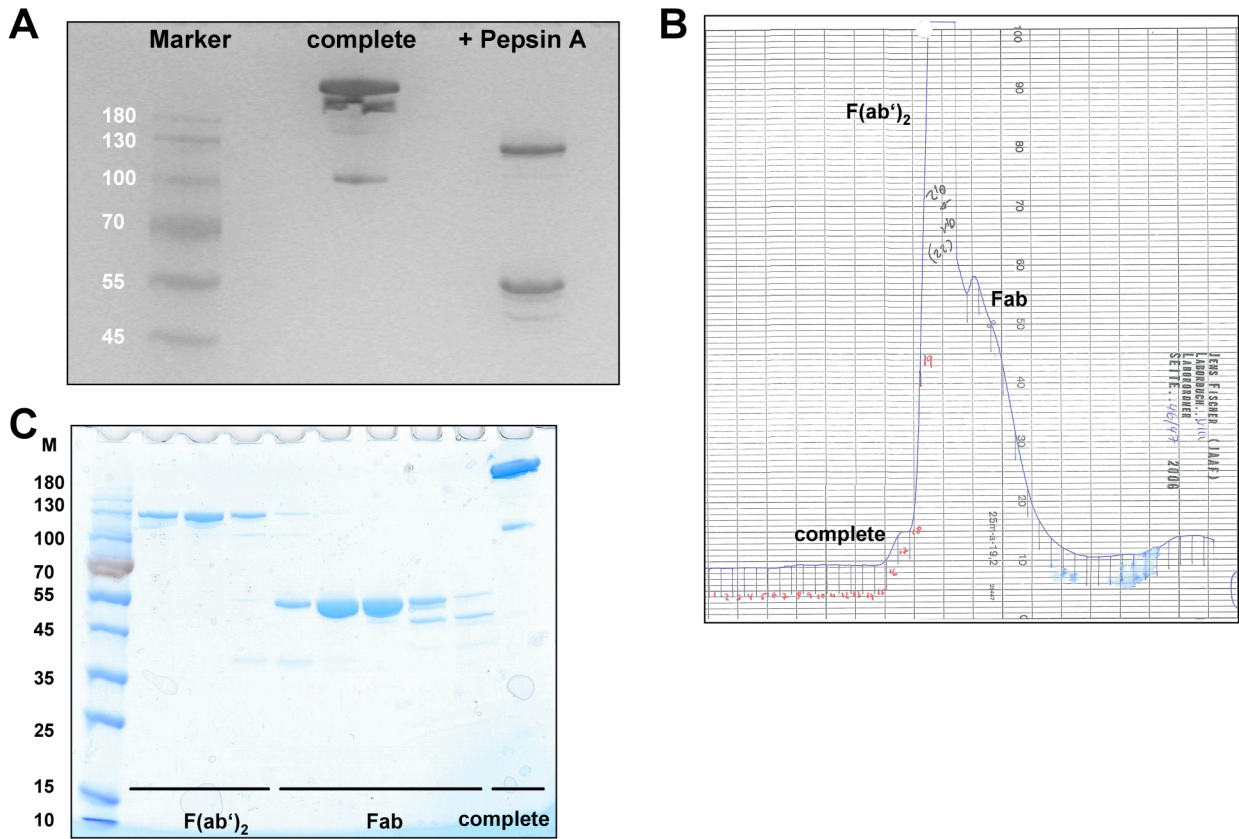


Fig.7.1 Pepsin digestion of anti-mPDCA-1 mAb to generate F(ab')₂ fragments.

(A) Anti-mPDCA-1 mAb (clone JF05-1C2) was re-buffered in 0.1 M sodium acetate buffer (pH 4.2). The antibody was then incubated for 48 hrs at 37°C in the presence of 10% Pepsin A (Sigma). To check the progress of fragmentation aliquots were subjected to SDS-PAGE and visualized by Coomassie staining. (B) Digested anti-mPDCA-1- fragments were then size-fractionated by gel filtration using a Superdex-200 column. (C) Individual fractions were again subjected to SDS-PAGE analysis and visualized by Coomassie staining.

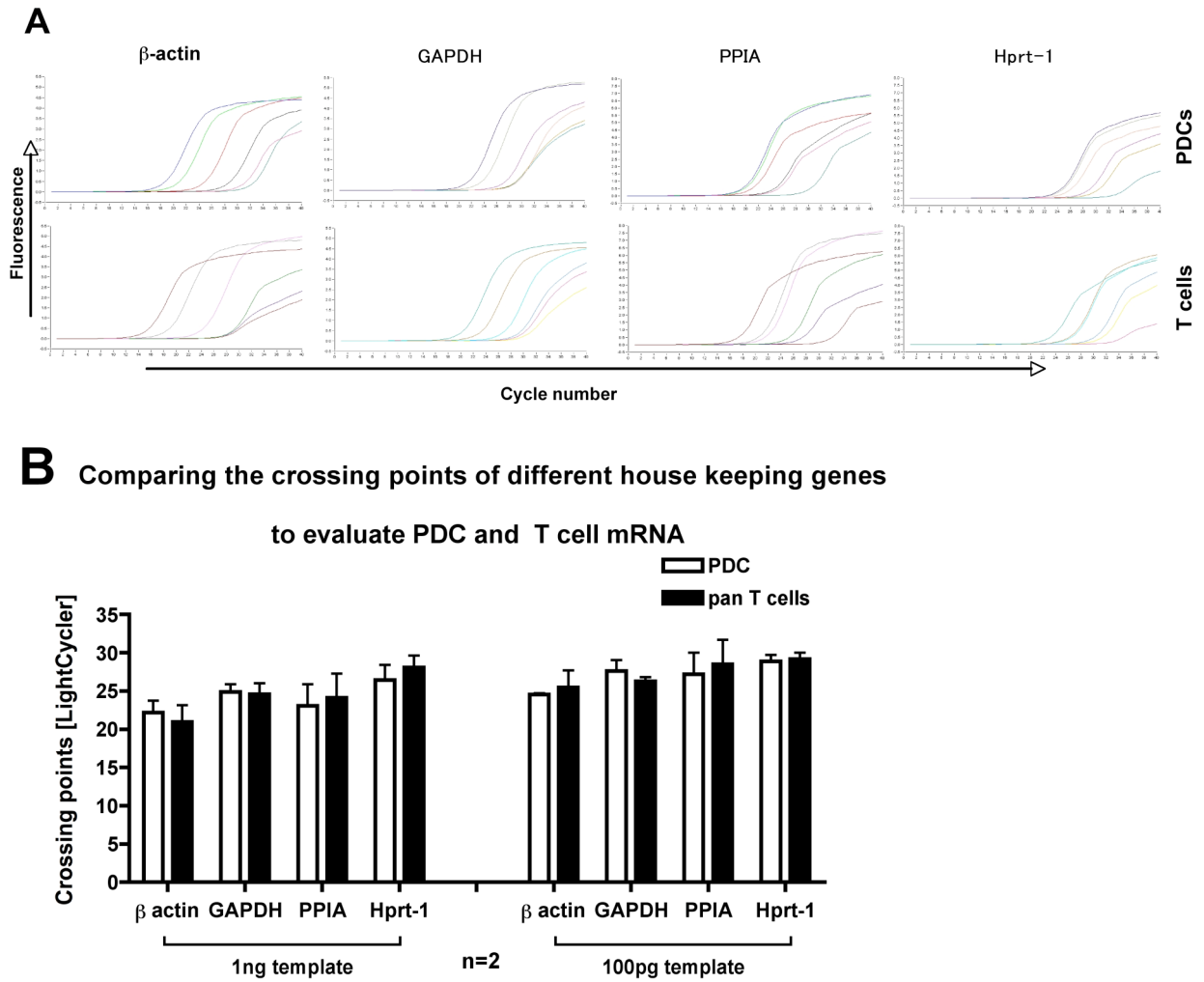


Fig. 7.2 LightCycler standard curves for four murine house keeping genes: β -actin, GAPDH, PPIA, and Hprt-1
 (A) Representative standard curves for house keeping genes. RT-PCRs were performed with titrated amounts of mRNA (ranging from 1pg to 5ng) isolated from PDCs and T cells, respectively, using the LightCycler[®] RNA Master SYBR Green I kit (Roche Diagnostics). All assays were performed at least in duplicates.
 (B) Table gives an overview of the above LightCycler runs and obtained crossing points (given is the mean +/- SEM of the crossing points of indicated housekeeping genes for two amounts of PDC and T cell mRNA).

Tables 7.1 Primer sequences

Table 7.1A Primer for housekeeping genes

#	Gene Acc. No.	Gene name	sense primer	sense primer	Product size (bp)	Comment
1	beta-actin (1)	murine beta-actin	GAAATCGTGCCTGACATCAAAG	TGTAGTTTCATGGATGCCACAG	156	side product of 264 bp
2	beta-actin (2)	murine beta-actin	TTCTTTGCAGCTCCTTCGTTGCCG	TGGATGGCTACGTACATGGCTGGG	218	
3	mGAPDH	murine Glyceraldehyd-3-phosphat-Dehydrogenase	ATCACTGCCACCCAGAAGAC	ACACATTGGGGGTAGGAACA	182	
4	mPPIA (2)	murine Peptidylprolyl Isomerase A	CACAAACGGTCCCAGTTTT	TTACAGGACATTGCGAGCAG	273	
5	mHprt-1	murine Hypoxanthine phosphoribosyltransferase 1	AAGCTTGCTGGTAAAAGGA	TTGCGCTCATCTTAGGCTTT	188	

Table 7.1B Primer for real time RT-PCR (LightCycler)

Primers were selected for an optimal melting temperature (T_m) of 60°C

#	Gene Acc. No.	Gene name	sense primer	sense primer	Product size (bp)	Comment
1	AF017175	liver carnitine palmitoyltransferase I mRNA,	CTATGCGTACTCGCTGAAGG	GGCTTTTCACCCGAGAAGA	126	syn. NM_013495
2	AK010014	ALPHA-INTERFERON INDUCIBLE PROTEIN	CCTGGTAGCCACACTCCAAT	TGAAGTGCCCTTTTGGAACT	182	
3	AK030414	GUANYLATE BINDING PROTEIN 5	AAAGGCCATTGGTCACACTAG	AAGCATCCGCGTCTTCTTA	223	
4	AK037025 E1	2,5-OLIGOADENYLATE SYNTHETASE-LIKE 5	CTGCACAAAATGCTCCAAAA	GCACGCATCACAGTTCCTAA	158	
5	AK046674	9130002C22RIK PROTEIN homolog	CCAACATAACCCGCTTCAGT	GGGCTTTCCACAAATCTGA	233	
6	AK050122	RIKEN full-length enriched library, clone:C730018G06	ACTAGGGGCTGTGTTGTGCT	AACAGGTCCTGGGCTGTTTA	211	
7	AK054410 E	UBIQUITIN-ACTIVATING ENZYME E1	GCGGCTGTAGAGTCTGATT	GTCTGTGCTGCTACCACAA	184	
8	AK077641	TUDOR REPEAT ASSOCIATOR WITH PCTAIRE 2	AGTGCTGCTTGGCTGATCTT	CGGGAAGTTATTGGGAGTGA	170	syn. NM_146142
9	AK077880	THYRO1000270 PROTEIN	GTACACCCAATACCCGATCC	TGCATCTTGCAAAACCAAGAG	209	
10	AK079685	interferon regulatory factor 7	TGGAAGCATTTTCGGTCTGAGG	GCACACCGGAAGTTGGTCT	173	syn. NM_016850
11	AK080076	unknown EST	AAAGCTTCTGGGTCGACGTAT	ATCTTAGAGATGGCCCCACA	179	
12	AK083376 E1	H-2 CLASS I HISTOCOMPATIBILITY ANTIGEN, D-37	GATGTTGCTTTTTGCCCACT	AGTCTCCCGCTCCCAATACT	255	
13	BB684123	hypothetical protein MGC7868 (LOC224133)	CTGAAGCCTTGAGACCTTGG	TATTCAGCCTTGCCCTGAGT	195	
14	BC021340	Parp14 (poly ADP-ribose polymerase 14)	TCTGGTGAATCTGCAAACCA	CTGTCCCATGGAAGAGATGC	200	
15	BC021821	RIKEN cDNA 5033415K03 gene, clone MGC:7873	AGAAGTGGCAGACCTGGAGA	CATCCCTCTTGAGCTTTTGC	163	
16	BC025170	clone IMAGE:4013674, mRNA	ACACACCCAGGACCTGTCTC	GGAGTCGGCCTTAGGATTTTC	181	
17	BC027328	bone marrow stromal cell antigen 2, BST2	CAATCTACTTCGCCGTCACA	TCTTCTCCAGGGACTCCCTGA	194	mPDCA-1
18	BC029209 E	DEXH (Asp-Glu-X-His) box polypeptide 58	GGTGCCCTTTCATACCCAG	TCCTCGCAGCAGATAAAGG	193	
19	BC052532	cDNA sequence BC006779	GGTCCGCATCATAAAGCAGT	GGTGTAGGCCACGTTTACTT	298	
20	L20315 E3	MPS1 gene	TGTAGACATGGGACGGGTGAT	ACTCTGGTAATTCATCCAGGACT	162	
21	M55219	HSR mRNA, clone pMmHSRc-[1,3,3E,10 and 10E]	TGGAGAAAGTACCCGATTTG	CCTCAGCTGCAGACTCTGTG	221	
22	NM_008326	interferon inducible protein 1 (Ifi1),	TTTCATCAATGCACITTCGAGTCAT	AATCCAGGTAAGTCCCACAGC	140	
23	NM_008329	interferon activated gene 204 (Ifi204),	AAAGGAGCCTGCTAAGGAAGA	CGTTCACATCAGAGACACAGGA	274	
24	NM_008331	interferon-induced protein with tetratricopeptide repeats 1	AGGCTGGAGTGTGCTGAGAT	TCTGGATTTAACCCGGACAGC	226	
25	NM_008332	interferon-induced protein with tetratricopeptide repeats 2	GCCTTGATATCTTGGCATT	GGTGAGGGCTTTCTTTTTC	182	
26	NM_008452	Kruppel-like factor 2 (lung) (Klf2),	GGACCTAAACAACGTGTTGGA	CTCCGGGTAGTAGAAGGCAG	117	
27	NM_009099	tripartite motif protein 30 (Trim30),	CCTCGGATTAATGACGGAAAGT	CTGGAATTTGGGGTATAGAACA	197	
28	NM_010255	guanidinoacetate methyltransferase (Gamt),	TGGAAGTGGGCTTCGGTATG	AGGGAACAACCTTATGTGGCT	147	
29	NM_010260	guanylate nucleotide binding protein 2 (Gbp2),	ACCAGCTGCATATGTGATG	TCAGAAGTGACGGGTTTTC	174	
30	NM_010392	histocompatibility 2, Q region locus 2 (H2-Q2),	ACATGGAGCTTGTGGAGACC	CAAGGACAACCAGAACAGCA	204	
31	NM_010393 E	histocompatibility 2, Q region locus 5 (H2-Q5),	ACATGGAGCTTGTGGAGACC	AGCTCCAAGGATGACCCAG	224	
32	NM_010394 E	histocompatibility 2, Q region locus 7 (H2-Q7),	GGGAGCCTCCTCCATCACT	AGGACAAGACCCATCACTG	170	
33	NM_010397	histocompatibility 2, T region locus 22 (H2-T22),	CTCACCTTCTGGCTCAAGG	CCATTGATCCCAATTTGACC	183	
34	NM_010398	histocompatibility 2, T region locus 23 (H2-T23),	TCCATCCACTGTCTCCAACA	GGGATTTTCATGCCTCTGA	193	
35	NM_010501	interferon-induced protein with tetratricopeptide repeats 3	GAGGACAACCCGAAAGTGTGT	GGATGAGCAGAGGAGTCAGG	201	
36	NM_010741	lymphocyte antigen 6 complex, locus C (Ly6c),	CTTGCTCTGATGGTCTCTCC	ACTTACCAGCAGGGCTAT	168	
37	NM_011637	three prime repair exonuclease 1 (Trex1),	CGTCAACGCTTCGATGACAAC	GCTCAGCCTAGCAAGCTCT	140	
38	NM_011909	ubiquitin specific protease 18 (Usp18),	AAGGACAGATCACGGACAC	CACATGTCGGAGCTTGCTAA	230	
39	NM_021430	RIKEN cDNA 2900002H16 gene	AGGAACGAGCTCAAGTCCAA	CCCGGGAGAAAAAGCTAAAC	174	
40	NM_023386	RIKEN cDNA 5830458K16 gene	GTGGGGAGCAGAGCTATGAG	TCCTGGGACCTAGGCTTAT	191	
41	NM_025821	RIKEN cDNA 1200011K09 gene	TTCTTTCTGATGGCCTTGT	CCTGGGCTATACAGCAGGAG	229	
42	NM_029803	interferon alpha-inducible protein 27 (Ifi27)	CTGCCATAGGAGGAGCTCTG	GATGGCATTTGTTGATGTGG	212	
43	NM_031367	histocompatibility 28 (H28),	TTAAACCTGATTGCCCAAG	GGATGGTTTCATGAGCCTGTT	229	
44	NM_133871	expressed sequence AW261460 (AW261460),	CCAAGTACTGCTCGCAATA	TAGGACCCAGCAGCAGAACT	190	
45	NM_146114	SNM1-like (Snm1),	GCCCACGATCAATGTGTTTT	TTGGGTCACAGAAAGTCGTG	166	
46	NM_199146	expressed sequence AI451617	CATTTGAAGGGCTCATGGAT	TGCCCATTTCTTCTTTGAG	290	

Table 7.1C Primer for real time RT-PCR (LightCycler) designed by Miltenyi Biotec

Reference: LIMS v1.3, Miltenyi Biotec, Bergisch Gladbach (former name: Memorec Biotec), unpublished data

#	Gene Acc. No.	Gene name	sense primer	sense primer	Product size	Comment
					(bp)	
1	AK077176	PHF11 (BRCA1, BCAP)	AGGACCACCAGGTCAGATG	GCAGCTTTACTATCAGGGG	191	
2	NM_007609	CASP11 (ICH3, CASPL)	CATTGTCCAGGCCTGCAGAG	TTCTGGAAGCATGTGATGAG	243	
3	NM_008327	IFI202A (IFI202B, IFI202)	TGACACACTCTGCCTTGTTG	TAGGTCCAGGAGAGGCTTG	241	
4	NM_010846	IFI-GBP (MX1)	AATTCTCCGATTAACCAGGC	GTACAAAACCAGAAGCCGAC	301	
5	NM_013606	MX2	CCCCTGTACACAACACTACTC	TGCTGTGCACCAACAAGAAC	299	
6	NM_013673	HMG1-SP100 (HMGB1, HMG1)	CCCCTGTACACAACACTACTC	TGCTGTGCACCAACAAGAAC	232	syn: NM_010439
7	NM_019963	STAT-2	CTCAGTTGGCAGTTCTCTCTC	TCATCCTGGTGCTCCACCC	362	
8	NM_020583	ISG20 (HEM45)	AACATCCAGAACAACACTGGCG	AACATCCAGAACAACACTGGCG	242	
9	NM_021274	CXCL10 (SCYB10)	CCACGTGTTGAGATCATTGC	CTACAGGAGTAGTAGCAGCTG	287	
10	NM_023141	DYT1 (TOR1A, DQ2)	GACTACTACCTGGATGACTG	TCACAAGTCCAGAATGCTGG	221	syn: NM_144884
11	AK045368	MAPRE2	CCCAGCAGTGTGATAGAGC	GAGGAAGAGGGAAGAGGCA	273	
12	NAP000805	unknown AGILENT annotation				
13	NM_008328	IFI203	AAAACTCCCCAGAATGAGG	TCAGTCACCTCACCTTCTC	291	
14	NM_009283	STAT1	<i>no primer sequence available</i>		200	
15	NM_025992	HERC5	TGTTTCTGATTTGGGAAAGG	CTCTGCCACCGTTTAGTCTC	300	syn: NM_016323
16	NM_199015	PHF11 (BCAP)	AGGACCACCAGGTCAGATG	GCAGCTTTACTATCAGGGG	191	

Table 7.1D Cloning primer for MPG1 and BST2

#	Gene Acc. No.	Gene name	sense primer	sense primer	Comment
Macrophage Specific Gene (MPG1, MPS1)					
1	L20315_BglII_FWD	"	AATCAGATCTACCACTGGATTTCAAATATGC		BglII restriction site
2	L20315_Sall_REV	"		CAATGAGTCGACCTATGGTGACTCCCAAAGTGA	Sall restriction site
3	L20315_Sall_FWD	"	AATCGTCGACACCACCATGAACAGCTTCATG GCCTT		Sall restriction site
4a	L20315_XhoI_REV	"		ATGACTCGAGTTGGTGACTCCCAAAGTATT	XhoI restriction site
4b	L20315_NotI_REV	"		ATGAGCGGCCGCTGGTGACTCCCAAAGTATT	NotI restriction site
Murine Bone marrow stromal antigen 2					
5a	Bst2_EcoRV-ATG_FWD	"	GGCGATATCACCACCATGGCGCCCTCTTTCT ATCA		EcoRV restriction site + ATG codon
5b	Bst2_EcoRV_FWD	"		GGCGATATCGCGCCCTCTTTCTATCACTA	EcoRV restriction site
6	Bst2_NotI_REV	"		GCCGCGGCCGCTCAAAGAGCAGGAACAGTGA	NotI restriction site
7	Random-hexamers		5'-NNN-NNN-Wobbles-3'		

129	DCP1_1	(DCP1 OR DCP OR ACE) ANGIOTENSIN-CONVERTING ENZY (EC 3.2.2.5)	0.14/12 %	0.37/- %	0.33/12 %	194	CD37	(CD37) LEUKOCYTE ANTIGEN CD37.	0.92/17 %	0.63/12 %	0.86/- %	0.67/24 %
130	CDH5	(CDH5) VASCULAR ENDOTHELIAL-CADHERIN PRECURSOR (V2.71.6 %)	0.46/16 %	1.60/- %	0.77/21 %	195	CD38	(CD38) ADP-RIBOSYL CYCLASE 1 (EC 3.2.2.5) (CYCLIC ADP-RIF 0.92/17 %)	0.72/18 %	0.60/11 %	0.90/1 %	0.60/11 %
131	MCAM	(MCAM OR MUC18) CELL SURFACE GLYCOPROTEIN MUC18 (0.95/7 %)	2.05/10 %	0.67/8 %	0.67/8 %	196	CD39	(ENTPD1 OR CD39) VASCULAR ATP-DIPHOSPHOHYDROLASE	1.39/10 %	0.83/9 %	1.92/2 %	0.82/9 %
132	PTPRU	(PTPRU OR DEP1 OR BPP OR SCC1) PROTEIN-TYROSINE PH-1 (1.16/15 %)	2.24/27 %	1.38/10 %	1.44/9 %	197	CD39	(CD39 OR TSD1) T-CELL SURFACE GLYCOPROTEIN CD39 DELT.0.93/12 %	1.10/29 %	0.87/21 %	1.11/- %	0.87/21 %
133	CD151	(CD151) PLATELET-ENDOTHELIAL TETRASPAN ANTIGEN 3 (P.0.62/14 %)	0.83/12 %	0.80/12 %	0.58/23 %	198	CD39	(CD39 OR T3E) T-CELL SURFACE GLYCOPROTEIN CD39 EPISL.0.91/12 %	0.86/44 %	0.78/- %	0.75/11 %	0.75/11 %
134	CTLA4	(CTLA4 OR CD152) CYTOTOXIC T-LYMPHOCYTE PROTEIN 4 (-0.91/15 %)	0.95/17 %	1.06/24 %	0.71/15 %	199	CD32-CD3H	(CD32 OR TR2 OR TR22) T-CELL SURFACE GLYCOPROTEIN CD39 (T.1.54/15 %)	1.41/14 %	1.53/1 %	1.34/37 %	0.75/16 %
135	CN3H	(CN3H) CYCLIN H (M015 ASSOCIATED PROTEIN) (P37) (P34)	0.86/15 %	0.28/12 %	0.32/15 %	200	CD4	(CD4) T-CELL SURFACE GLYCOPROTEIN CD4 PRECURSOR (IT.1.54/15 %)	1.41/14 %	1.41/14 %	1.36/37 %	0.75/16 %
136	ADAM8	(ADAM8 OR WS2) ADAM 8 PRECURSOR (EC 3.4.24.-) (A DISIN 0.90/13 %)	0.79/11 %	0.81/- %	0.65/6 %	201	ITGA2B	(ITGA2B OR ITGAB OR GP2B) PLATELET MEMBRANE GLYCOPROTEIN CD4 PRECURSOR (IT.1.54/15 %)	1.32/51 %	1.32/51 %	1.32/51 %	0.75/16 %
137	BST1	(BST1 OR BP3 OR LY65) ADP-RIBOSYL CYCLASE 2 (P.0.79/19 %)	0.83/14 %	0.81/- %	0.81/- %	202	ITGA2B	(ITGA2B OR ITGAB OR GP2B) PLATELET MEMBRANE GLYCOPROTEIN CD4 PRECURSOR (IT.1.54/15 %)	1.32/51 %	1.32/51 %	1.32/51 %	0.75/16 %
138	SELPLG	(SELPLG) P-SELECTIN GLYCOPROTEIN LIGAND 1 PRECURSOR (0.99/12 %)	1.39/12 %	0.58/1 %	0.54/10 %	203	SPN	(SPN OR CD43) LEUKOSIALIN PRECURSOR (LEUCOCYTE SIAL.1.28/16 %)	1.35/11 %	0.90/1 %	0.90/1 %	1.01/8 %
139	ITCAM	(ITCAM OR VNRD) CD166 ANTIGEN PRECURSOR (ACTIVATOR 0.85/9 %)	0.63/13 %	0.62/1 %	0.55/4 %	204	CD44	(CD44 OR LHR) CD44 ANTIGEN PRECURSOR 2.19/10 %	0.59/16 %	0.89/14 %	0.89/14 %	0.66/23 %
140	ITGAV	(ITGAV OR VIM) VITRONECTIN RECEPTOR ALPHA SUBUNIT 2 (1.27/2 %)	0.59/19 %	0.49/5 %	0.49/5 %	205	CD45	(CD45 EX10-12 MOUSE; (CD44 OR LHR) CD44 ANTIGEN PRECURSOR 2.19/10 %)	0.59/16 %	0.89/14 %	0.89/14 %	0.66/23 %
141	CD52	(CD52 OR CD52 OR HE5 OR MB7 OR RB7) CAMPATH-1 ANTIC.1.20/14 %	0.95/16 %	1.00/- %	0.98/8 %	206	CD45	(CD45 EX10-12 MOUSE; (CD44 OR LHR) CD44 ANTIGEN PRECURSOR 2.19/10 %)	0.59/16 %	0.89/14 %	0.89/14 %	0.66/23 %
142	CD53	(CD53 OR MOX44 OR OR-44) LEUKOCYTE SURFACE ANTIGEN 1 (2.0/18 %)	1.70/15 %	0.74/- %	2.53/12 %	207	CD48	(CD48 OR BCL1 OR BCL2) B-LYMPHOCYTE ACTU.1.46/21 %	1.40/8 %	1.04/12 %	1.12/23 %	1.12/23 %
143	DAF	(DAF OR CR OR CD55) COMPLEMENT DEACCELERATING 1 (0.97/8 %)	0.89/14 %	0.89/1 %	0.82/17 %	208	ITGA1	(ITGA1) INTEGRIN ALPHA-1 (LAMININ AND COLLAGEN RECI.0.94/15 %)	0.91/10 %	1.01/17 %	1.08/11 %	0.82/13 %
144	NCAM1	(NCAM1 OR NCAM) NEURAL CELL ADHESION MOLECULE 1 (0.87/12 %)	0.83/14 %	1.17/- %	0.88/19 %	209	ITGA1	(ITGA1) INTEGRIN ALPHA-1 (LAMININ AND COLLAGEN RECI.0.94/15 %)	0.91/10 %	1.01/17 %	0.98/16 %	0.82/13 %
145	ITGB3	(ITGB3 OR GP3A) INTEGRIN BETA-3 PRECURSOR (PLATELET 1.99/14 %)	1.99/14 %	1.55/1 %	1.12/15 %	210	ITGA3	(ITGA3) INTEGRIN ALPHA-3 PRECURSOR (GALACTOPROTEIN 1.07/17 %)	0.88/17 %	1.02/19 %	1.02/19 %	0.90/8 %
146	SELE	(SELE OR ELAM1 OR ELAM-1) E-SELECTIN PRECURSOR (END 0.69/8 %)	0.84/7 %	0.82/3 %	0.65/25 %	211	ITGA4	(ITGA4 OR VLA-4) INTEGRIN ALPHA-4 PRECURSOR (INTEGRIN 2.73/19 %)	0.93/29 %	2.70/4 %	2.70/4 %	0.82/14 %
147	SELL	(SELL OR LYAM1 OR LHM-1) L-SELECTIN PRECURSOR 1 (2.5/11 %)	2.32/4 %	0.90/5 %	3.32/11 %	212	ITGA5	(ITGA5 OR FNRA) INTEGRIN ALPHA-5 PRECURSOR (FIBRONE 1.45/39 %)	0.19/6 %	1.24/1 %	1.24/1 %	0.24/14 %
148	CD63	(CD63 OR MLA1) CD63 ANTIGEN (MELANOMA-ASSOCIATED AN 0.64/6 %)	0.57/3 %	0.49/13 %	0.74/12 %	213	ITGA6	(ITGA6) INTEGRIN ALPHA-6 PRECURSOR (VLA-6) (CD49F) (INI.0.69/16 %)	0.71/13 %	0.71/37 %	0.71/37 %	0.76/5 %
149	FCGR1A	(FCGR1A OR FCGR1 OR FCGR) HIGH AFFINITY I.1.12/8 %	0.83/1 %	0.81/68 %	0.81/68 %	214	CD5	(CD5 OR LEU1) T-CELL SURFACE GLYCOPROTEIN CD5 PRECURSOR (0.73/18 %)	3.82/21 %	2.51/2 %	2.51/2 %	1.03/10 %
150	CD68	(CD68) MACROSIALIN PRECURSOR (CD88 ANTIGEN) (EP110)	0.65/17 %	0.62/0 %	0.70/17 %	215	ICAM1	(ICAM1 OR ICAM-1) INTERCELLULAR ADHESION MOLECULE 1 (0.71/17 %)	3.05/17 %	3.05/17 %	3.05/17 %	0.29/31 %
151	CD69	(CD69) EARLY ACTIVATION ANTIGEN CD69 (EARLY T-CELL AC 2.73/12 %)	5.89/75 %	0.95/- %	5.21/14 %	216	CD6	(CD6) T-CELL DIFFERENTIATION ANTIGEN CD6 PRECURSOR (T.0.71/15 %)	0.80/14 %	0.66/1 %	0.66/1 %	0.71/15 %
152	TNFSF7	(TNFSF7 OR CD70 OR CD27L) TUMOR NECROS 1 (1.6/1 %)	0.83/1 %	0.47/1 %	0.55/15 %	217	CD7	(CD7) T-CELL DIFFERENTIATION ANTIGEN CD7 PRECURSOR (GP40) (T-CELL LEUK.0.81/18 %)	1.00/15 %	0.87/1 %	0.87/1 %	0.88/19 %
153	TRC	(TRC) TRANSFERIN RECEPTOR PROTEIN (TFR1) (0.38/32 %)	0.60/7 %	0.61/1 %	0.40/40 %	218	CD8A	(CD8A OR MAL OR LY2) T-CELL SURFACE GLYCOPROTEIN CD8A (0.81/18 %)	1.86/16 %	2.81/3 %	2.81/3 %	1.11/19 %
154	CD72	(LY-32 OR LYB-2 OR CD72) B-CELL DIFFERENTIATION ANTIGEN (TFR1) (0.38/32 %)	0.60/7 %	0.61/1 %	0.40/40 %	219	CD8B	(CD8B OR LYT-3 OR CD8B1 OR LYT3) T-CELL SURFACE GLYCOPROTEIN CD8B (0.81/18 %)	1.86/16 %	2.81/3 %	2.81/3 %	1.11/19 %
155	NT5	(NT5 OR NT5 OR NTE) 5-NUCLEOTIDASE PRECURSOR (EC 3.1.1.06/14 %)	1.02/18 %	1.42/18 %	1.01/10 %	220	CD9	(CD9 OR MIC3) CD9 ANTIGEN (P24) (LEUKOCYTE ANTIGEN MIC 0.77/17 %)	0.78/1 %	0.78/1 %	0.78/1 %	0.86/26 %
156	CD74	(CD74 OR DHLG OR IL) HLA CLASS-II HISTOCOMPATIBILITY A 1.50/10 %	1.50/10 %	1.68/12 %	1.17/18 %	221	GAP1M	(RAS2A OR RASG OR GAP1M) RAS GTPASE-ACTIVATING 3 (GAP 1.74/15 %)	0.65/11 %	0.73/10 %	0.65/11 %	0.73/10 %
157	CD79A	(CD79A OR IGA OR MB1) B-CELL ANTIGEN RECEPTOR (1.50/11 %)	0.93/14 %	0.93/1 %	1.14/4 %	222	GAP1	(GAP1 OR RAS3) RAS GTPASE-ACTIVATING PROTEIN 3 (GAP 1.74/15 %)	0.65/11 %	0.73/10 %	0.65/11 %	0.73/10 %
158	CD79B	(CD79B OR IGB OR B29) B-CELL ANTIGEN RECEPTOR COMP.0.15/21 %	1.15/11 %	0.54/- %	0.31/15 %	223	ICGAP1	(ICGAP1) RAS GTPASE-ACTIVATING-LIKE PROTEIN (ICGAP1 2.12/16 %)	1.23/7 %	2.47/13 %	2.47/13 %	1.20/13 %
159	CD80	(CD80 OR CD28LG1 OR CD28LG OR LAB7 OR B7) T LYMPHOC.1.14/3 %	7.46/41 %	0.98/1 %	0.82/14 %	224	ICGAP2	(ICGAP2) RAS GTPASE-ACTIVATING-LIKE PROTEIN (ICGAP2 0.68/16 %)	0.75/3 %	0.51/4 %	0.51/4 %	1.66/15 %
160	CD81	(CD81 OR TAPAT) CD81 ANTIGEN (26 KDA CELL SURFACE PR.0.94/17 %)	0.97/14 %	0.87/20 %	0.87/20 %	225	INF1	(INF1) NEUROFIBROMIN (NEUROFIBROMATOSIS-RELATED PRO.0.22/17 %)	2.07/13 %	1.47/15 %	1.47/15 %	4.56/6 %
161	KAH1	(KAH1 OR CD82 OR SAR2) CD82 ANTIGEN (INDUCIBLE MEMBR.1.23/22 %)	1.83/70 %	2.09/4 %	0.26/22 %	226	RAS1	(RAS1) (RAS1) GTPASE-ACTIVATING PROTEIN (GAP) (1.16/37 %)	1.31/18 %	1.41/1 %	1.41/1 %	0.82/19 %
162	CD83	(CD83) ANTIGEN PRECURSOR (CELL SURFACE PROTEIN HB1.1.21/22 %)	1.83/70 %	1.11/17 %	1.11/17 %	227	HTR1A	(HTR1A) 5-HYDROXYTRYPTAMINE 1A RECEPTOR (5-HT1A) (0.86/16 %)	0.93/16 %	0.93/16 %	0.93/16 %	0.93/16 %
163	CD84	(CD84) LEUKOCYTE DIFFERENTIATION ANTIGEN CD84	2.93/19 %	1.37/- %	0.70/43 %	228	CCR1	(CCR1 OR CR31 OR AZ3B OR HNFAG0) C3A ANAPHYLATO.0.67/13 %	0.80/19 %	0.78/20 %	0.78/20 %	0.83/16 %
164	CD86	(CD86 OR CD28LG2) T LYMPHOCYTE ACTIVATION ANTIGEN C1.04/11 %	1.01/17 %	1.37/- %	0.70/43 %	229	CCR3	(CCR3 OR CMKBR3 OR CMKBR1/2) C-C CHEMOKINE RECEPTOR 1 (1.17/16 %)	0.90/14 %	1.07/- %	1.07/- %	0.98/19 %
165	PLAUR	(PLAUR OR UPAR OR MO3) UROKINASE PLASMINOGEN ACT 0.65/27 %	1.87/7 %	0.46/3 %	2.68/11 %	230	CCR4	(CCR4 OR CMKBR4) C-C CHEMOKINE RECEPTOR TYPE 4 (C-C-0.86/18 %)	0.90/6 %	0.90/6 %	0.90/6 %	0.74/7 %
166	CBR1	(CBR1 OR C5AR) ANAPHYLATOXIN CHEMOTACTIC REC 0.99/13 %	0.93/16 %	1.00/19 %	0.70/13 %	231	CCR5	(CCR5 OR CMKBR5) C-C CHEMOKINE RECEPTOR TYPE 1 (6.7/16 %)	3.61/14 %	1.10/2 %	1.10/2 %	5.32/3 %
167	THY1	(THY1) THY-1 MEMBRANE GLYCOPROTEIN PRECURSOR (THY 0.67/25 %)	1.08/18 %	0.55/1 %	1.57/7 %	232	FPRI	(FPRI) FET-LIKE-UPHRE RECEPTOR (FMLP RECEPTOR (NF-FOR 0.81/11 %)	0.91/9 %	0.93/17 %	0.93/17 %	0.73/22 %
168	LRP1	(LRP1 OR A2M) LOW-DENSITY LIPOPROTEIN RECEPTOR-REL 3.84/23 %	0.62/10 %	1.52/4 %	1.65/15 %	233	HR23R	(HR23R) HISTAMINE H2 RECEPTOR (GASTRIC RECEPTOR 1)	2.31/11 %	5.62/22 %	5.62/22 %	0.77/9 %
169	KLRD1	(KLRD1 OR CD94) NATURAL KILLER CELLS ANTIGEN CD94 (P.0.79/16 %)	0.97/7 %	1.06/7 %	0.56/21 %	234	CALB2	(CALB2 OR CAB29) CART CALRETININ (CR) (29 KD CALBINDIN 1.00/19 %)	0.98/20 %	1.20/- %	1.20/- %	0.84/4 %
170	CD96	(TACTILE OR CD96) T-CELL SURFACE PROTEIN TACTILE PRE1.1.62/11 %	4.59/25 %	2.19/49 %	1.65/11 %	235	GJA1_2	(GJA1_2) GAP JUNCTION ALPHA-1 PROTEIN (CONNEXIN 43) (C.0.71/19 %)	0.91/19 %	0.60/18 %	0.60/18 %	0.89/8 %
171	CD97	(CD97) LEUKOCYTE ANTIGEN CD97 PRECURSOR	1.46/10 %	0.82/1 %	1.10/15 %	236	PAR3	(PAR3 OR PAR3) PROTEINASE ACTIVATED RECEPTOR 3 PRE.4.26/20 %	0.70/16 %	7.64/37 %	7.64/37 %	0.29/11 %
172	MDU1	(SLC3A2 OR MDU1) 4F2 CELL SURFACE ANTIGEN HEAVY CH.0.44/17 %	1.32/16 %	0.38/1 %	1.35/15 %	237	TSR	(TSR) THYROTROPIN RECEPTOR PRECURSOR (TSH-R) (TH.0.69/20 %)	0.76/10 %	0.73/15 %	0.73/15 %	0.74/2 %
173	MME	(MME OR EPN) NEPRILYSIN (EC 3.2.4.11) (NEUTRAL ENDOPEI.0.90/12 %)	0.95/14 %	1.01/12 %	0.85/15 %	238	AGTR1	(AGTR1 OR APJ) PROBABLE G PROTEIN-COUPLED RECF.0.97/17 %	1.00/25 %	0.98/22 %	0.98/22 %	0.70/14 %
174	ITGAL	(ITGAL OR CD11A OR LFA-1) INTEGRIN ALPHA-L PRECURSOR (T-CELL 1.02/18 %)	1.02/18 %	0.96/3 %	1.68/23 %	239	CALCR	(CALCR) CALCITONIN RECEPTOR PRECURSOR (CT-R)	0.84/28 %	0.82/28 %	0.82/28 %	0.56/20 %
175	ANPEP	(ANPEP OR PEPI OR APN OR CD13 OR LAP1 OR LAP-1) AMI.0.96/16 %	1.92/7 %	1.01/1 %	0.60/50 %	240	CNR1	(CNR1 OR CNR) CANNABINOID RECEPTOR 1 (CB1) (CB-R) (0.94/13 %)	0.82/22 %	0.89/- %	0.89/- %	0.61/25 %
176	CD14	(CD14) MONOCYTE DIFFERENTIATION ANTIGEN CD14 PRECU.2.27/16 %	2.38/31 %	5.76/19 %	1.68/10 %	241	CMKLR1	(CMKLR1 OR DEZ OR CHEMR23) CHEMOKINE RECEPTOR 1 (CB1) (CB-R) (0.94/13 %)	0.82/22 %	0.89/- %	0.89/- %	0.61/25 %
177	ITGB2	(ITGB2 OR CD18) INTEGRIN BETA-2 PRECURSOR (CELL SUR.0.89/17 %)	0.92/18 %	0.75/0 %	0.93/15 %	242	FY	(FY OR DFY OR GDP OR DARCO) DUFFY ANTIGEN/HEMOKINE RE.1.46/42 %	1.44/1 %	1.30/1 %	1.30/1 %	1.34/9 %
178	CD19	(CD19) B-LYMPHOCYTE ANTIGEN CD19 PRECURSOR (B-LYMPH.0.70/16 %)	0.84/10 %	0.81/10 %	0.65/10 %	243	EMR1	(EMR1) CELL SURFACE GLYCOPROTEIN EMR1 PRECURSOR (0.87/15 %)	0.86/6 %	0.74/29 %	0.74/29 %	0.66/8 %
179	CD2	(CD2) T-CELL SURFACE ANTIGEN CD2 PRECURSOR (T-CELL.1.02/18 %)	1.35/21 %	0.74/10 %	0.73/20 %	244	EMR2	(EMR2 OR GPR2) C-C CHEMOKINE RECEPTOR TYPE 10 (C.4.0/18 %)	1.00/15 %	2.18/7 %	2.18/7 %	1.89/16 %
180	MS4A1	(MS4A1 OR CD20 OR LY-44 OR MS4A2) B-LYMPHOCYTE ANT 0.93/47 %	0.87/32 %	0.26/7 %	0.12/23 %	245	P2RY14	(P2RY14 OR GPR105 OR KIAA0001) P2Y PURINOCYTORECEPTOR 14 (8.6/9 %)	1.86/9 %	0.54/13 %	0.54/13 %	0.76/7 %
181	CD2	(CD2 OR CD3R) COMPLEMENT RECEPTOR TYPE 2 PRECURSOR (0.87/43 %)	0.94/5 %	0.26/7 %	0.12/23 %	246	PTAFR	(PTAFR OR PAFR) PLATELET ACTIVATING FACTOR RECEPTOR (0.68/11 %)	1.14 %	0.54/13 %	0.54/13 %	0.89/12 %
182	CD22	(CD22) B-CELL RECEPTOR CD22 PRECURSOR (LEU-14) (B-LY.0.32/27 %)	0.08/16 %	1.20/- %	0.52/15 %	247	PTGDR	(PTGDR) PROSTAGLANDIN D2 RECEPTOR (PROSTANOI.DF.1.08/11 %)	0.89/25 %	1.59/28 %	1.59/28 %	0.69/12 %
183	FCER2	(FCER2 OR IGE2B OR FCER2A) LOW AFFINITY IMMUNOGLOBULIN 2 (0.75/13 %)	0.89/11 %	1.20/- %	0.52/15 %	248	PTGER2	(PTGER2) PROSTAGLANDIN E2 RECEPTOR, EP2 SUBTYPE 0.93/13 %	0.65/22 %	0.90/47 %	0.90/47 %	0.95/30 %
184	CD24	(CD24 OR CD24A) SIGNAL TRANSDUCER CD24 PRECURSOR (1.13/15 %)	1.20/11 %	0.45/26 %	0.80/11 %	249	PTGFR	(PTGFR) PROSTAGLANDIN F2 ALPHA RECEPTOR (PROSTAN.1.17/18 %)	1.31/50 %	0.95/32 %	0.95/32 %	0.94/13 %
185	IL2RA	(IL2RA OR IL2R) INTERLEUKIN-2 RECEPTOR ALPHA CHAIN PR.0.93/21 %	1.02/10 %	0.96/13 %	0.83/14 %	250	PTGIR	(PTGIR OR PRIPI) PROSTACYCLIN RECEPTOR (PROSTANOI.0.97/10 %)	1.16/22 %	1.00/41 %	1.00/41 %	0.89/11 %
186	DP4	(DP4 OR ADP2 OR CD26) DIPEPTIDYL PEPTIDASE IV (EC 3.3.0.21/3 %)	1.97/15 %	2.10/0 %	2.33/14 %	251	RDC1	(RDC1 OR RDC1) G PROTEIN-COUPLED RECEPTOR RDC1 (0.95/22 %)	0.90/1 %	0.90/1 %	0.90/1 %	0.97/29 %
187	TNFRSF7	(TNFRSF7 OR CD27) TUMOR NECROSIS FACTOR RECEPTOR 0.46/16 %	1.24/20 %	0.42/5 %	0.97/11 %	252	GPRC25	(GPRC25 OR TDA68) PROBABLE G PROTEIN-COUPLED RE.0.51/21 %	0.20/13 %	0.29/5 %	0.29/5 %	0.56/6 %
188	CD28	(CD28) T-CELL-SPECIFIC SURFACE GLYCOPROTEIN CD28 PRI.2.49/15 %	1.50/17 %	2.86/20 %	1.42/13 %	253	SALTB2	(SALTB2 OR KIAA0245) SOLUTE CARRIER FAMILY 7 (CATIOT.0.75/19 %)	0.14/10 %	0.14/10 %	0.14/10 %	0.85/10 %
189	ITGB1	(ITGB1 OR FNBR) INTEGRIN BETA-1 PRECURSOR (FIBRONEC.1.27/16 %)	1.27/14 %	0.89/1 %	1.32/24 %	254	BARD1	(BARD1) BRCA1-ASSOCIATED RING DOMAIN PROTEIN (BARI.0.74/19 %)	0.80/22 %	0.74/- %	0.74/- %	0.85/10 %
190	PCAM1	(PCAM1 OR PECAM-1 OR PECAM) PLATELET ENDOTHELI.0.57/16 %	0.50/10 %	0.52/1 %	0.66/13 %	255	FBXW1A	(FBXW1A OR FBW1A OR BTSPC OR BTFC) F-BOX/WD-REP 1 (0.21/13 %)	1.14/13 %	1.21/12 %	1.21/12 %	0.88/29 %
191	CD34	(CD34) HEMATOPOIETIC PROGENITOR CELL ANTIGEN CD34 F.0.73/7 %	1.00/27 %	0.77/7 %	0.78/9 %	256						

259	LIG4; (LIG4) DNA LIGASE IV (EC 6.5.1.1) (POLYDEOXYRIBONUCLEOTI 2.30/42 %	2.05/14 %	2.26/19 %	4.12/16 %	2.33/- %	3.81/1 %
260	ECT2; (ECT2) ECT2 PROTEIN (EC2 ONCOGENE), (DKFZP434C0523) 0.60/22 %	0.76/1 %	1.08/29 %	1.04/14 %	1.43/- %	0.61/34 %
261	KIB7; (MK167) ANTIGEN K167, 1.18/20 %	1.13/- %	0.78/8 %	1.39/15 %	1.44/2 %	1.38/23 %
262	KIAA0042; (KIAA042 OR KIF14) KINESIN-LIKE PROTEIN KIF14, 0.82/23 %	0.80/10 %	0.71/26 %	1.03/17 %	0.68/- %	1.65/6 %
263	TOPBP1; (TOPBP1 OR KIAA0259) DNA TOPOISOMERASE II BINDING 1.17/15 %	2.39/1 %	6.70/8 %	0.69/10 %	1.04/5 %	1.19/14 %
264	FBXW1; (FBXW1 OR FBXW1B OR BTRCP2 OR KIAA0696) 1.34/17 %	1.38/3 %	5.95/28 %	0.65/20 %	0.80/15 %	0.66/16 %
265	KIF1C; (KIF1C OR KIF1D) KINESIN-LIKE MOTOR PROTEIN 0.69/17 %	1.27/1 %	1.15/28 %	2.42/15 %	1.71/0 %	0.66/16 %
266	FBXW2; (FBXW2 OR FBW2 OR FBW2) F-BOXW2-REPEAT PROTEIN 2.0/7.7 %	0.47/13 %	0.87/32 %	1.17/36 %	1.11/12 %	0.84/23 %
267	MNF; (FOXK1 OR MNF) FORKHEAD BOX PROTEIN K1 (MYOCYTE NUCLEO 0.46/15 %	0.21/5 %	1.80/5 %	1.06/13 %	0.52/33 %	0.84/10 %
268	MSF36; (MCRS1 OR MSF36) MICROSPHERE PROTEIN 1 (68 KDA M0.75/10 %	0.75/15 %	1.21/14 %	1.43/46 %	1.69/- %	1.51/27 %
269	NBS1; (NBS1 OR NBS) NIBIN (NIMJEGEN BREAKAGE SYNDROME P1 1.87/42 %	1.08/24 %	1.46/11 %	0.87/12 %	1.15/31 %	0.83/25 %
270	TP53BP1; (TP53BP1) TUMOR SUPPRESSOR P53-BINDING PROTEIN 1.68/11 %	0.60/12 %	0.26/43 %	2.26/13 %	0.54/3 %	2.93/9 %
271	SFR2; (SFR2 OR FKS2) SECRETED FRIZZLE 1.06/14 %	1.06/14 %	0.74/22 %	2.64/11 %	3.07/- %	1.67/41 %
272	SFRP1; (SFRP1 OR FRP OR SARP2) SECRETED FRIZZLE 0.96/16 %	1.21/19 %	0.75/- %	1.01/44 %	1.46/- %	0.20/17 %
273	FBXL1; (SKP2 OR FBXL1) S-Phase Kinase-Associated Protein 2 0.84/25 %	1.09/- %	1.18/9 %	0.86/16 %	1.23/1 %	1.00/12 %
274	XRCC1; (XRCC1) DNA-REPAIR PROTEIN XRCC1, 2.14/15 %	1.13/20 %	1.13/20 %	1.43/46 %	1.69/- %	1.51/27 %
275	BMP2; (BMP2 OR BMP2A OR BMP-2) BONE MORPHOGENETIC PROTEIN 0.92/17 %	0.98/34 %	1.12/8 %	0.87/12 %	1.15/31 %	0.83/25 %
276	BMP6; (BMP6 OR BMP-6 OR VGR1) BONE MORPHOGENETIC PROTEIN 1.08/14 %	0.85/19 %	0.69/27 %	2.05/28 %	3.07/- %	1.67/41 %
277	BMP8A-BMP8B; (BMP8) BONE MORPHOGENETIC PROTEIN 0.91/15 %	0.83/21 %	0.75/17 %	2.64/11 %	3.07/- %	1.67/41 %
278	CTGF; (CTGF OR HCS24) CONNECTIVE TISSUE GROWTH-FACTOR P10.89/14 %	0.85/19 %	0.67/13 %	1.62/44 %	1.09/- %	1.28/3 %
279	CYR61; (CYR61 OR IGFBP10 OR GIG1 OR CCN1) CYR61 PROTEIN PR 0.72/10 %	1.05/32 %	1.22/34 %	1.62/44 %	1.09/- %	1.28/3 %
280	NBL1; (NBL1 OR DAN) NEUROBLASTOMA SUPPRESSOR OF TUMOR1 1.07/15 %	1.40/32 %	2.11/16 %	1.61/19 %	1.96/2 %	0.97/10 %
281	GDF1; (GDF1 OR GDF-1) EMBRYONIC GROWTH/DIFFERENTIATION F 0.99/14 %	0.92/16 %	0.80/5 %	1.17/4 %	1.25/1 %	1.39/12 %
282	GDF3; 1; (GDF3) GROWTH DIFFERENTIATION FACTOR 3; (GDF3 OR C0.95/13 %	0.77/13 %	0.82/21 %	1.01/25 %	1.02/1 %	0.81/11 %
283	GDF6; (GDF6 OR GDF-6) GROWTH/DIFFERENTIATION FACTOR 6 PRE 1.09/15 %	1.15/57 %	0.88/18 %	0.88/18 %	0.99/16 %	0.87/17 %
284	GDF8; (GDF8 OR MSTIN) GROWTH/DIFFERENTIATION FACTOR 8 PRE 0.63/17 %	0.82/5 %	0.61/9 %	1.01/25 %	0.65/1 %	1.72/11 %
285	GDF9; (GDF9) GROWTH/DIFFERENTIATION FACTOR 9 PRECURSOR 10.87/14 %	0.80/34 %	0.80/34 %	0.77/8 %	0.79/1 %	0.60/28 %
286	GDNF; (GDNF) GLEE CELL GROWTH NEUROTROPHIC FACTOR 0.75/13 %	0.85/19 %	0.91/8 %	1.61/19 %	1.96/2 %	0.97/10 %
287	CGA; (CGA OR CGAL) GLYCOPROTEIN HORMONES ALPHA CHAIN PF 1.25/23 %	1.88/17 %	0.90/2 %	1.17/4 %	1.25/1 %	1.39/12 %
288	INH4; (INH4) INHIBIN ALPHA CHAIN PRECURSOR, 1.19/20 %	1.48/21 %	0.95/16 %	0.34/11 %	2.95/21 %	0.81/11 %
289	INHBB; (INHBB) INHIBIN BETA B CHAIN PRECURSOR (ACTIVIN BETA- 1.06/21 %	0.87/46 %	1.06/16 %	0.90/26 %	0.65/1 %	1.72/11 %
290	INHBC; (INHBC) INHIBIN BETA C CHAIN PRECURSOR (ACTIVIN BETA- 1.03/22 %	0.91/16 %	1.03/1 %	0.77/8 %	0.79/1 %	0.60/28 %
291	NR1N; (NR1N OR NTN) NEURTURIN PRECURSOR, 0.84/18 %	0.70/23 %	0.92/13 %	0.71/6 %	0.88/- %	0.85/8 %
292	PDGF; (PDGF OR RPA1 OR PDGF-1) PDGF PLATELET-DERIVED GRK 0.53/19 %	0.83/22 %	1.77/8 %	1.33/13 %	0.64/6 %	1.55/9 %
293	PDGF; (PDGF OR C-SIS OR PDGF-2 OR PDGF-3) PDGF PLATELET-DERIVED GR 1.09/19 %	1.30/88 %	0.89/12 %	0.59/21 %	0.68/3 %	0.43/8 %
294	PTH; (PTH OR FTHL) FERRETIN HEAVY CHAIN (FERRETIN H) 0.82/13 %	1.23/11 %	1.16/11 %	1.03/7 %	0.88/4 %	0.88/14 %
295	SOD1; (SOD1) SUPEROXIDE DISMUTASE [CU-ZN] (EC 1.15.1.1), 0.69/23 %	1.00/10 %	0.72/29 %	0.73/11 %	0.88/4 %	0.88/14 %
296	TGF; (TGF OR TGF-1) TRANSFORMING GROWTH FACTOR BETA 0.73/17 %	1.07/0 %	0.94/3 %	0.73/11 %	0.74/0 %	0.61/10 %
297	TGF; (TGF3 OR TGF-3) TRANSFORMING GROWTH FACTOR BETA 0.83/16 %	0.95/19 %	1.84/7 %	0.38/23 %	0.26/2 %	0.76/15 %
298	VEGF; (VEGF OR VRF) VASCULAR ENDOTHELIAL GROWTH FACTOR 0.88/7 %	0.90/16 %	0.66/10 %	1.00/8 %	0.94/- %	0.75/9 %
299	VEGF; (VEGF OR VEGF-D) VASCULAR ENDOTHELIAL GROWTH FACTOR 0.83/22 %	0.86/19 %	0.66/10 %	0.60/8 %	1.02/3 %	0.44/33 %
300	VWF; (F8WF OR VWF) VON WILLEBRAND FACTOR PRECURSOR, 0.85/24 %	1.03/8 %	1.07/10 %	1.28/24 %	1.10/- %	0.91/29 %
301	WISP3; (WISP3 OR CCN6 OR DJ42L7.3 OR LINC) WNT1 INDUCIBLE S 1.02/19 %	0.92/3 %	0.73/16 %	1.92/16 %	1.13/- %	1.85/22 %
302	GREM1; (GREM1 OR CKTSF1B1 OR DRM) (GREM1 PROTEIN) I10.79/24 %	0.82/7 %	0.62/48 %	0.85/20 %	0.96/16 %	0.90/4 %
303	GREM2; (GREM2 OR CKTSF1B2 OR DRND3 OR PRDC) GREM1IN-2 PR 0.85/17 %	0.97/16 %	0.80/17 %	0.80/9 %	0.37/1 %	0.57/6 %
304	VEGF; (VEGF OR VEGF-D) VASCULAR ENDOTHELIAL GROWTH FAC 0.53/6 %	0.77/15 %	0.40/22 %	1.01/9 %	1.39/4 %	0.41/20 %
305	ABR; (ABR) ACTIVE BREAKPOINT CLUSTER REGION-RELATED PROT 1.72/22 %	0.65/7 %	0.83/18 %	2.76/42 %	2.76/42 %	0.40/32 %
306	PK3CG; (PK3CG) PHOSPHATIDYLINOSITOL 3-KINASE C2 DOMAIN 0.98/11 %	3.04/57 %	1.40/50 %	0.56/18 %	0.79/- %	0.82/7 %
307	CAPN6; (CAPN6 OR DJ814P14.1 OR CAPA6 GENE OR CALPM) CAPNXP 1.46/10 %	1.38/25 %	0.64/10 %	0.71/5 %	0.53/- %	0.63/16 %
308	DOC2A; (DOC2A OR MDOC2) DOUBLE C2-LIKE DOMAIN CONTAINING 1.46/10 %	0.64/10 %	1.21/31 %	3.14/14 %	0.41/- %	10.29/11 %
309	DOC2B; (DOC2B) DOC2B, 0.95/19 %	1.38/66 %	0.91/24 %	1.02/18 %	1.44/- %	0.89/12 %
310	RASA1; 2; (RASA1 OR RASA) GTPASE-ACTIVATING PROTEIN (GAP) (1.71/21 %	1.13/23 %	1.89/6 %	6.39/12 %	2.28/14 %	2.98/3 %
311	ITCH; (ITCH) ITCHY HOMOLOG E3 UBIQUITIN PROTEIN LIGASE (EC 3.4.20/29 %	7.12/2 %	5.49/27 %	2.58/4 %	2.58/4 %	2.98/3 %
312	SYT11; (SYT11 OR KIAA0080) SYNAPTOTAGMIN-11 (SYNAPTOTAGMIN0.92/12 %	0.67/3 %	1.05/62 %	0.94/15 %	0.75/8 %	0.84/19 %
313	HEDWI; (HEDWI OR KIAA0322 OR NEDL1) NEDD4-LIKE UBIQUITIN L1.107/13 %	0.88/12 %	1.00/14 %	1.69/13 %	1.05/3 %	1.09/7 %
314	NEDD4; (NEDD4L OR NEDD4L OR NEDD4B) NEDD4L UBIQUITIN 2.93/14 %	0.51/18 %	1.09/19 %	1.13/14 %	0.41/1 %	10.29/11 %
315	CPNE3; (CPNE3 OR CPN3 OR KIAA0636) COPINE III, 1.44/6 %	1.68/18 %	1.19/15 %	3.67/14 %	2.73/28 %	1.48/13 %
316	PKCE; (PKCE OR PKCE) PROTEIN KINASE C, EPSILON TYPE (EC 2.7.1.77/15 %	1.72/36 %	2.04/34 %	2.12/3 %	2.13/15 %	0.89/15 %
317	PRKCK; (PRKCK OR PKCL) PROTEIN KINASE C, ETA TYPE (EC 2.7.1.1-0.56/18 %	1.15/26 %	1.14/7 %	0.66/6 %	1.10/8 %	0.96/22 %
318	CAPN5; (CAPN5) CALPAIN-5 (EC 3.4.22.17) (NCL-3) (HTRA-3), 1.27/23 %	1.29/18 %	0.78/1 %	0.93/9 %	1.37/2 %	0.51/28 %
319	NEDD4; (NEDD4 OR KIAA0093) UBIQUITIN-PROTEIN LIGASE NEDD-4 1.07/25 %	0.39/19 %	0.84/1 %	1.13/3 %	1.30/4 %	1.22/14 %
320	SYT17; (SYT17) SYNAPTOTAGMIN XVII (254P9.1) (BPK PROTEIN), 3.04/25 %	0.70/13 %	0.81/8 %	2.10/8 %	1.16/- %	0.96/13 %
321	PRF1; (PRF1) PERFORIN 1 PRECURSOR (P1) (LYMPHOCYTE 0.98/7 %	0.81/8 %	1.01/20 %	0.86/24 %	1.08/- %	0.89/16 %
322	PK3CA; (GPK-M OR PK3CA) PHOSPHOINOSITIDE 3-KINASE, 0.26/11 %	2.98/41 %	0.64/18 %	0.71/20 %	0.21/2 %	0.88/24 %
323	PLCL1; (PLC-L OR PLC-L OR PLC-EPSILON) PHOSPHOLIPID-0.96/17 %	0.82/19 %	0.64/18 %	0.77/8 %	0.75/8 %	0.75/8 %
324	PRK2; (PRK2 OR PRK2) PROTEIN KINASE C-LIKE 2 (EC 2.7.1.-) (PRI 3.23/17 %	4.12/16 %	1.04/14 %	0.84/23 %	1.43/- %	0.61/34 %
325	RPHA3; (RPHA3) RABPHILIN-3A (FRAGMENT), 1.04/14 %	1.39/15 %	1.39/15 %	1.44/2 %	1.44/2 %	1.38/23 %
326	UVRAG; (UVRAG OR UVRAGL) UV RADIATION RESISTANCE ASSOCIAT 1.20/26 %	0.68/1 %	1.65/6 %	0.58/- %	1.65/6 %	1.65/6 %
327	WWP2; 1; (WWP2) NEDD4-LIKE E3 UBIQUITIN-PROTEIN LIGASE WW 1.03/17 %	1.07/2 %	1.07/2 %	0.69/10 %	1.04/5 %	1.19/14 %
328	MLL2; (MLL2 OR AF6) AFADIN (AF-6 PROTEIN), 0.69/10 %	1.04/5 %	0.65/20 %	0.80/15 %	0.71/0 %	0.66/16 %
329	APL1; (APL1) APICAL-LIKE PROTEIN (APXL PROTEIN), 0.65/20 %	0.65/20 %	0.80/15 %	2.42/15 %	1.11/12 %	0.84/23 %
330	WPI1; (WPI1 OR EMP55) 55 KD ERYTHROCYTE MEMBRANE PROTEIN 0.59/19 %	2.42/15 %	1.06/13 %	1.06/13 %	0.52/33 %	0.84/10 %
331	MP2; (MP2 OR DLG2) MAGUK P55 SUBFAMILY MEMBER 2 (MPP2 P 1.17/36 %	1.43/46 %	1.36/12 %	1.43/46 %	1.69/- %	1.51/27 %
332	MPP3; (MPP3 OR DLG3) MAGUK P55 SUBFAMILY MEMBER 3 (MPP3 P 0.74/15 %	1.43/46 %	1.36/12 %	1.43/46 %	1.69/- %	1.51/27 %
333	RL; (RL) LIMPK3 PROTEIN, 1.43/46 %	1.36/12 %	1.43/46 %	1.43/46 %	1.69/- %	1.51/27 %
334	SLC3A3R2; 1; (SLC3A3R2 OR NHERF2) NA(+)/JH(+)-EXCHANGE REGUL 0.87/11 %	0.87/12 %	1.15/31 %	0.83/25 %	0.54/3 %	2.93/9 %
335	SPAI1; (SPAI1 OR SPA1) GTPASE-ACTIVATING PROTEIN S10.82/14 %	2.26/13 %	2.64/11 %	3.07/- %	1.67/41 %	0.20/17 %
336	SDCBP; (SDCBP OR CYL OR MD49) SYNTENIN 1 (SYNDECAN BINDI 2.05/28 %	2.64/11 %	2.64/11 %	3.07/- %	1.67/41 %	0.20/17 %
337	TIAM; (TIAM) T-LYMPHOMA INVASION AND METASTASIS INDUCING F 0.84/31 %	0.21/44 %	0.21/44 %	1.46/- %	1.46/- %	1.00/12 %
338	TJPI; (TJPI OR ZO1) TIGHT JUNCTION PROTEIN ZO1 (ZONULIN OCC 0.87/17 %	0.21/44 %	0.21/44 %	1.46/- %	1.46/- %	1.00/12 %
339	WAG1; (BAIAP1 OR WWP3 OR BAP1 OR WAG1 OR TNRC19 OR GUKI 0.84/19 %	0.75/23 %	0.78/1 %	0.82/36 %	0.78/1 %	0.82/36 %
340	GBP; (PSCDBP OR GBP) CYTOSHEIN BINDING PROTEIN HE (PLECKS 2.24/22 %	1.23/13 %	1.23/13 %	1.23/15 %	2.29/21 %	0.92/21 %
341	PDLIM7; (PDLIM7 OR ENIGMA) PDZ AND LIM DOMAIN PROTEIN 7 (LIM 1.15/10 %	1.36/1 %	1.36/1 %	1.36/1 %	0.96/44 %	0.96/44 %
342	CIPP; (INADL OR CIPP) CIPP PDZ DOMAIN PROTEIN (INADL_C-TERM 1.62/44 %	1.09/- %	1.09/- %	1.09/- %	1.59/- %	0.92/33 %
343	PRSS11; (PRSS11 OR HTRA1 OR HTRA) SERINE PROTEASE HTRA1 F.0.93/13 %	0.76/10 %	0.76/10 %	0.76/10 %	0.70/1 %	0.72/15 %
344	PTP; (PTPN13 OR PTP1E OR PTP1) PROTEIN TYROSINE P.0.78/16 %	0.79/9 %	0.79/9 %	2.02/24 %	2.02/24 %	0.48/15 %
345	HPT; (HPT11 OR HPT1) HYPOXANTHINE-GUANINE PHOSPHORIBO: 1.85/12 %	0.76/21 %	0.76/21 %	3.36/5 %	3.36/5 %	1.08/49 %
346	ACTB; (ACTB) BETA1, CYTOPLASMIC (BETA-ACTIN) ACTIN, CYTOPLA 2.05/10 %	2.17/6 %	2.17/6 %	1.31/67 %	0.99/16 %	0.87/17 %
347	IL4; (IL4 OR IL-4) INTERLEUKIN-4 PRECURSOR (IL-4) (B-CELL STIMUL 1.10/25 %	1.01/25 %	1.01/25 %	1.31/67 %	0.99/16 %	0.87/17 %
348	WAPT; (WAPT OR MTBT1; OR TAU) MICROTUBULE-ASSOCIATED PRO 1.08/18 %	0.88/12 %	0.88/12 %	0.88/12 %	0.99/16 %	0.87/17 %
349	ZAK1; (ZAK14 OR USCR1L1) ZAK1-L4 PROTEIN, CALCIUM-INDUCED 1.12/20/11 %	1.53/29 %	1.53/29 %	1.53/29 %	1.36/1 %	0.97/10 %
350	HSPCA; (HSPCA OR HSPC1) OR HSP90A OR HSP86-1) HEA 1.11/22 %	1.61/19 %	1.61/19 %	1.61/19 %	1.96/2 %	0.97/10 %
351	WHAH; (WHAH) 14-3-3 PROTEIN EPSILON (MITOCHONDRIAL MPFO 0.97/13 %	1.76/18 %	1.76/18 %	1.76/18 %	1.25/1 %	1.39/12 %
352	MATRIN3; (MATR3) MATRIN3 RNA BINDING PROTEIN KIAA0723 PRO: 1.17/11 %	0.65/35 %	0.65/35 %	1.02/- %	1.02/- %	0.81/11 %
353	PREPL; (PREPL OR KIAA0436 OR D030028016R1K) PROLYL ENDOPEP 1.56/10 %	0.34/11 %	0.34/11 %	2.95/21 %	2.95/21 %	0.81/11 %
354	GDI1; (ARHGDI1 OR GDI1) RHO GDP-DISSOCIATION INHIBITOR 1 (1.13/16 %	0.90/26 %	0.90/26 %	0.65/1 %	0.65/1 %	1.72/11 %
355	SRM2; (SRM2 OR KIAA0324) KIAA0324 (SRM300) (SPLICING COAC 0.71/12 %	0.77/8 %	0.77/8 %	0.77/8 %	0.79/1 %	0.60/28 %
356	BLK; (BLK) TYROSINE-PROTEIN KINASE BLK (EC 2.7.1.112) (B-LYMPH 1.33/13 %	0.71/6 %	0.71/6 %	0.88/- %	0.88/- %	0.85/8 %
357	CSK; (CSK) TYROSINE-PROTEIN KINASE CSK (EC 2.7.1.112) (C-SRCL 1.06/13 %	0.96/25 %	0.96/25 %	0.68/3 %	0.68/3 %	0.43/8 %
358	FAK1; (FAK1 OR FAK OR PTK2) FOCAL ADHESION KINASE 1 (EC 2.7.10.46/17 %	0.59/21 %	0.59/21 %	0.59/21 %	0.68/3 %	0.43/8 %
359	FGR; (FGR OR SRC2) PROTO-ONCOGENE TYROSINE-PROTEIN KINA 0.85/10 %	1.03/7 %	1.03/7 %	0.88/4 %	0.88/4 %	0.88/14 %
360	FYN; (FYN) PROTO-ONCOGENE TYROSINE-PROTEIN KINASE FYN (E 0.47/18 %	0.73/11 %	0.73/11 %	0.73/11 %	0.88/4 %	0.88/14 %
361	GRB2; (GRB2 OR ASH) GROWTH FACTOR RECEPTOR-BOUND PROTI 0.73/16 %	0.38/23 %	0.38/23 %	0.74/0 %	0.74/0 %	0.61/10 %
362	HCK; (HCK) TYROSINE-PROTEIN KINASE HCK (EC 2.7.1.112) (P59-HC 0.59/19 %	0.63/16 %	0.63/16 %	0.26/2 %	0.26/2 %	0.76/15 %
363	ITK; (ITK OR LYK OR EMT) TYROSINE-PROTEIN KINASE ITK/TSK (EC: 0.90/16 %	1.00/8 %	1.00/8 %	0.94/- %	0.94/- %	0.75/9 %
364	PKCD; (PKCD OR PKCD) PROTEIN KINASE C, DELTA TYPE (EC 2.7.10.83/14 %	0.				

389	CCR6: (CCR6 OR CMKBR6 OR STRL22 OR GPR29 OR CKRL3) C-C CH 1.80/21 %	0.94/19 %	2.13/4 %	0.64/14 %	0.92/10 %	0.98/11 %	0.87/18 %
390	CCR8: (CCR8 OR CMKBR8 OR CKRL1 OR TER1) C-C CHEMOKINE RE0.74/18 %	0.81/17 %	0.68/- %	0.71/7 %	0.93/12 %	0.94/14 %	0.77/16 %
391	CALB1: (CALB1 OR CAB27) CALBINDIN (VITAMIN D-DEPENDENT CALB) 0.72/15 %	0.74/17 %	0.62/25 %	0.77/8 %	1.84/- %	2.03/65 %	0.83/21 %
392	ADCVYPIR1: (ADCVYPIR1) PITUITARY ADENYLATE CYCLASE ACTIV 0.98/16 %	0.79/16 %	0.81/- %	0.69/14 %	0.87/0 %	0.91/23 %	0.92/12 %
393	VIPRI: (VIPRI) VASOACTIVE INTESTINAL POLYPEPTIDE RECEPTOR 0.77/17 %	0.94/18 %	1.06/15 %	0.82/9 %	0.82/26 %	1.01/23 %	1.11/16 %
394	AC15: (RFC1 OR RFC14 OR RECC1) (ACTIVATOR 1 140 KD SUBUNIT 1.87/13 %)	0.48/19 %	0.76/18 %	1.40/9 %	1.07/7 %	0.84/24 %	1.20/15 %
395	PARP1: (PARP1 OR APRD OR PPOL) POLY (ADP-RIBOSE) POLYMER0.36/21 %	1.31/15 %	0.28/13 %	2.05/4 %	0.94/2 %	0.67/24 %	0.98/45 %
396	TD: (DNIT OR TDT) DNA NUCLEOTIDYLTRANSFERASE (EC 2.7.1.00/10 %)	0.72/19 %	0.98/14 %	0.79/19 %	1.00/1 %	2.35/6 %	1.00/1 %
397	BM38: (GDF10 OR BMP38) BONE MORPHOGENETIC PROTEIN 3B PR1 1.02/16 %	1.01/12 %	1.10/18 %	0.88/14 %	1.73/18 %	1.06/18 %	0.81/24 %
398	GDF5: (GDF5 OR COMIP) BONE MORPHOGENETIC PROTEIN 5 PR 1.02/16 %	0.90/14 %	1.13/- %	0.85/14 %	1.46/- %	0.87/24 %	0.74/24 %
399	INHBA: (INHBA) INHIBIN BETA A CHAIN PRECURSOR (ACTIVIN BETA 1.33/17 %)	0.83/53 %	1.29/8 %	1.29/8 %	1.41/2 %	0.88/12 %	0.81/24 %
400	TGF2: (TGFB2) TRANSFORMING GROWTH FACTOR BETA 2 PRECU0.93/16 %	1.24/35 %	0.77/6 %	0.77/6 %	1.31/20 %	1.57/10 %	0.97/15 %
401	LEFTY1: (LEFTY1) MOUSE: (EBAF OR TGF4 OR LEFTA OR LEFTY) 1.82/10 %	2.00/17 %	2.28/11 %	3.44/23 %	1.06/13 %	1.01/13 %	1.01/13 %
402	VEGF: (VEGFC) VASCULAR ENDOTHELIAL GROWTH FACTOR C PRE 2.68/19 %	5.76/27 %	2.78/15 %	3.44/23 %	0.82/2 %	0.68/7 %	0.82/2 %
403	STMT1: (STMT1) STATHMIN (PHOSPHOPROTEIN) 0.93/16 %	1.01/4 %	1.10/- %	0.65/17 %	1.40/18 %	1.55/17 %	1.55/17 %
404	PLA2G4: (PLA2G4 OR PLA2G4 OR CPLA2) CYTOSOLIC PHOSPHOLIP 1.51/15 %	0.17/13 %	0.27/13 %	0.27/13 %	0.27/13 %	0.27/13 %	0.27/13 %
405	PLCB3: (PLCB3) 1-PHOSPHATIDYLINOSITOL-4,5-BISPHOSPHATE PHK 1.13/15 %	0.79/19 %	1.11/15 %	1.11/15 %	0.97/19 %	0.97/19 %	0.97/19 %
406	PLCG1: (PLCG1 OR PLC1) 1-PHOSPHATIDYLINOSITOL-4,5-BISPHOSPHATE PHK 0.37/28 %	1.22/11 %	0.45/- %	0.96/6 %	0.09/18 %	1.11/27 %	0.09/18 %
407	PLD1: (PLD1) 1-PHOSPHATIDYLINOSITOL-4,5-BISPHOSPHATE PHK 0.98/9 %	0.88/13 %	1.35/1 %	0.95/20 %	0.85/19 %	0.91/18 %	0.91/18 %
408	SOS2: (SOS2) SON OF SEVENLESS PROTEIN HOMOLOG 2 (SOS-2) 1.01/12 %	1.24/16 %	0.96/10 %	0.95/20 %	0.85/19 %	1.00/23 %	0.93/36 %
409	GAPD: (GAPD) GLYCERALDEHYDE 3-PHOSPHATE DEHYDROGENAS1.01/14 %	1.28/16 %	0.96/10 %	1.44/17 %	0.85/19 %	1.00/23 %	0.93/36 %
410	COL1A1: (COL1A1) COLLAGEN ALPHA 1(I) CHAIN PRECURSOR 0.85/25 %	1.00/16 %	0.93/15 %	0.98/12 %	0.88/16 %	0.88/16 %	0.88/16 %
411	COL10A1: (COL10A1) COLLAGEN ALPHA 1(X) CHAIN PRECURSOR 2.02/31 %	0.48/19 %	1.18/19 %	0.63/27 %	1.70/11 %	1.05/22 %	1.05/22 %
412	COL11A1: (COL11A1) COLLAGEN ALPHA 1(XI) CHAIN PRECURSOR 1.04/12 %	0.88/18 %	0.91/- %	0.91/- %	0.82/93 %	0.88/27 %	0.88/27 %
413	COL12A1: (COL12A1) COLLAGEN ALPHA 1(XII) CHAIN PRECURSOR 1.22/10 %	0.98/10 %	1.09/- %	0.85/17 %	0.69/21 %	1.87/6 %	0.61/22 %
414	COL13A1: (COL13A1 OR COL4A2) ALPHA-1 TYPE XIII COLLAGEN 0.69/19 %	0.85/10 %	0.76/- %	0.78/22 %	0.87/12 %	0.87/12 %	0.87/12 %
415	COL15A1: (COL15A1) COLLAGEN ALPHA 1(XV) CHAIN PRECURSOR 1.36/12 %	1.40/14 %	1.35/4 %	1.35/4 %	0.97/14 %	0.87/13 %	0.87/13 %
416	COL16A1: (COL16A1) COLLAGEN ALPHA 1(XVI) CHAIN PRECURSOR 1.08/22 %	0.69/18 %	0.79/- %	0.79/- %	0.83/12 %	0.83/12 %	0.83/12 %
417	COL17A1: (COL17A1 OR BP180 OR BPA2) COLLAGEN ALPHA-1(XVII) CHAIN PRECURSOR 1.07/16 %	0.88/12 %	1.24/10 %	0.91/28 %	0.80/16 %	1.03/18 %	1.03/18 %
418	COL18A1_2: (COL18A1) COLLAGEN ALPHA 1(XVIII) CHAIN 1.04/17 %	0.87/50 %	0.89/0 %	0.85/14 %	1.11/25 %	0.98/- %	1.11/25 %
419	COL2A1: (COL2A1) COLLAGEN ALPHA 1(II) CHAIN PRECURSOR (CON) 0.78/21 %	0.90/13 %	0.89/0 %	0.85/14 %	0.96/19 %	1.00/6 %	0.87/19 %
420	COL3A1: (COL3A1) COLLAGEN ALPHA 1(III) CHAIN PRECURSOR 0.90/24 %	0.96/15 %	0.97/1 %	0.87/6 %	1.01/44 %	1.01/44 %	0.96/18 %
421	COL4A1: (COL4A1) COLLAGEN ALPHA 1(IV) CHAIN PRECURSOR (ARF) 0.73/12 %	0.99/17 %	0.82/13 %	0.90/7 %	0.82/13 %	0.82/13 %	0.82/13 %
422	COL5A1: (COL5A1) PRO-ALPHA-1 TYPE V COLLAGEN 0.97/12 %	0.99/17 %	0.85/1 %	0.97/1 %	0.93/17 %	0.93/17 %	0.93/17 %
423	COL6A1: (COL6A1) COLLAGEN (VI) ALPHA-1 CHAIN (FRAGMENT) COL 0.93/18 %	0.93/1 %	1.25/- %	1.08/15 %	0.92/17 %	0.92/17 %	0.92/17 %
424	COL7A1: (COL7A1) COLLAGEN ALPHA 1(VII) CHAIN PRECURSOR (LO) 0.57/14 %	0.38/20 %	0.22/- %	1.15/12 %	0.95/16 %	0.95/16 %	0.95/16 %
425	COL8A1: (COL8A1) COLLAGEN ALPHA 1(VIII) CHAIN PRECURSOR (E) 0.91/12 %	0.73/28 %	1.01/10 %	0.85/20 %	1.00/9 %	1.26/22 %	1.26/22 %
426	COL9A1_1: (COL9A1) COLLAGEN ALPHA 1(IX) CHAIN PRECURSOR 1.10/27 %	1.07/10 %	1.01/10 %	0.85/20 %	0.90/8 %	1.05/16 %	0.84/14 %
427	COL12A2: (COL12A2) COLLAGEN ALPHA 2(II) CHAIN PRECURSOR 0.96/13 %	0.92/16 %	0.71/26 %	0.84/14 %	0.91/25 %	0.84/8 %	0.84/8 %
428	COL11A2: (COL11A2) COLLAGEN ALPHA 2(XI) CHAIN PRECURSOR 0.26/22 %	0.55/12 %	0.36/- %	0.40/22 %	2.71/- %	1.08/7 %	1.08/7 %
429	COL4A2: (COL4A2) COLLAGEN ALPHA 2(IV) CHAIN PRECURSOR 0.77/7 %	0.80/20 %	0.83/5 %	0.83/5 %	0.83/21 %	0.89/15 %	0.89/15 %
430	COL5A2: (COL5A2) COLLAGEN ALPHA 2(V) CHAIN PRECURSOR 1.00/21 %	0.95/4 %	1.00/- %	0.93/12 %	0.95/5 %	0.73/2 %	0.83/19 %
431	COL6A2: (COL6A2) COLLAGEN ALPHA 2(VI) CHAIN PRECURSOR C 0.96/15 %	0.95/15 %	1.13/22 %	0.84/14 %	18.50/92 %	0.24/4 %	3.88/28 %
432	COL8A2: (COL8A2) COLLAGEN ALPHA 2(VIII) CHAIN (ENDOTHELIAL C) 0.82/10 %	0.98/16 %	0.73/7 %	0.84/13 %	0.90/11 %	2.07/77 %	0.79/22 %
433	COL9A2: (COL9A2) COLLAGEN TYPE IX ALPHA 2 CHAIN (ALPHA-2 IX) 1.06/26 %	1.00/7 %	0.81/- %	0.88/7 %	0.81/10 %	2.07/77 %	0.90/4 %
434	COL4A3: (COL4A3) COLLAGEN ALPHA 3(IV) CHAIN PRECURSOR 1.38/41 %	1.30/56 %	2.11/78 %	1.32/14 %	1.01/32 %	1.00/13 %	1.00/13 %
435	COL6A3: (COL6A3) COLLAGEN ALPHA 3(VI) CHAIN PRECURSOR 1.11/14 %	1.19/11 %	1.38/14 %	0.90/4 %	1.15/42 %	0.96/55 %	1.17/8 %
436	COL9A3: (COL9A3) ALPHA-3 TYPE IX COLLAGEN 0.95/12 %	1.07/11 %	3.33/18 %	0.23/34 %	1.45/16 %	1.45/16 %	1.45/16 %
437	ITGA7: (ITGA7) INTEGRIN ALPHA-7 (INTEGRIN ALPHA 7 CHAIN) (NITE) 1.08/19 %	0.84/54 %	1.00/- %	0.75/1 %	1.62/12 %	1.80/- %	1.00/10 %
438	ITGA8: (ITGA8) INTEGRIN ALPHA-8 (INTEGRIN A8) 1.25/36 %	0.59/73 %	1.00/- %	0.83/28 %	0.85/17 %	0.97/3 %	0.79/8 %
439	ITGA9: (ITGA9) INTEGRIN ALPHA-9 PRECURSOR (INTEGRIN ALPHA-9 PRECURSOR) 1.50/6 %	0.91/7 %	1.00/- %	0.83/28 %	0.85/17 %	0.97/3 %	0.79/8 %
440	ITGB5: (ITGB5) INTEGRIN BETA-5 PRECURSOR (INTEGRIN B5) 1.03/18 %	1.02/12 %	0.91/5 %	1.12/17 %	0.87/13 %	0.87/13 %	0.87/13 %
441	ITGB6: (ITGB6) INTEGRIN BETA-6 PRECURSOR (INTEGRIN B6) 0.90/16 %	0.84/18 %	0.79/21 %	0.81/3 %	2.54/- %	1.34/9 %	1.34/9 %
442	ITGB7: (ITGB7) INTEGRIN BETA-7 PRECURSOR (INTEGRIN B7) 0.62/18 %	0.61/16 %	0.74/13 %	0.53/20 %	0.90/27 %	0.85/6 %	0.85/6 %
443	ITGB8: (ITGB8) INTEGRIN BETA-8 PRECURSOR 1.03/12 %	0.86/15 %	1.00/- %	0.83/28 %	0.75/11 %	0.75/11 %	0.75/11 %
444	PA1: (SERPINE1 OR PA1 OR PLANH1) PLASMINOGEN ACTIVATOR IF 1.19/10 %	0.72/14 %	1.33/- %	0.85/9 %	0.68/21 %	0.85/16 %	0.67/16 %
445	SERPINB2: (SERPINB2 OR PA2 OR PLANH2) PLASMINOGEN ACTIVATOR 0.94/29 %	0.85/7 %	0.81/14 %	0.66/35 %	0.73/6 %	0.73/6 %	0.73/6 %
446	TACE: (ADAM17 OR TACE OR C5V) ADAM 17 PRECURSOR (EC 3.4.21.89/19 %)	2.85/9 %	0.81/14 %	0.86/35 %	0.74/14 %	0.49/80 %	0.49/80 %
447	TIMP1: (TIMP1 OR TIMP OR CLG1) METALLOPROTEINASE INHIBITOR 1.11/16 %	0.95/19 %	0.61/- %	0.59/16 %	1.05/6 %	1.05/6 %	1.05/6 %
448	TIMP2: (TIMP2) METALLOPROTEINASE INHIBITOR 2 PRECURSOR (TH1) 0.81/10 %	0.30/18 %	1.10/- %	0.52/25 %	1.18/30 %	1.18/30 %	1.18/30 %
449	TIMP3: (TIMP3) METALLOPROTEINASE INHIBITOR 3 PRECURSOR (TH1) 1.41/25 %	1.24/17 %	0.97/10 %	1.10/19 %	0.97/9 %	1.01/1 %	0.97/9 %
450	TIMP4: (TIMP4) METALLOPROTEINASE INHIBITOR 4 PRECURSOR (TH1) 1.01/21 %	1.35/30 %	0.97/10 %	1.10/19 %	0.88/10 %	1.51/- %	0.88/10 %
451	PLAT: (PLAT) TISSUE-TYPE PLASMINOGEN ACTIVATOR PRECURSOR (PG-S2) 0.93/11 %	0.86/13 %	0.77/23 %	0.77/23 %	0.88/11 %	0.88/11 %	0.88/11 %
452	UPA: (PLAU) UROKINASE-TYPE PLASMINOGEN ACTIVATOR PRECUR 1.14/16 %	0.13/8 %	1.24/- %	0.12/5 %	0.60/3 %	0.60/3 %	0.60/3 %
453	BMP7: (BMP7 OR BMP-7 OR OP1) BONE MORPHOGENETIC PROTEIN 1.14/12 %	1.03/19 %	0.91/2 %	0.91/2 %	0.91/2 %	0.91/2 %	0.91/2 %

779	BNIP3; (BNIP3 OR NIP3) BCL2/ADENOVIRUS E1B 19-KDA PROTEIN-IN 1.16 / 12 %	2.33 / 29 %	0.95 / - %	0.23 / 22 %	844	BIRC2_5PRIME; (BIRC2 OR AP11 OR IAP2 OR MIHB) BACULOVIRAL IA 6.42 / 12 %	6.26 / 12 %
780	BNIP3L; (BNIP3L OR BNIP3) BCL2/ADENOVIRUS 1.98 / 6 %	0.35 / 13 %	1.90 / 6 %	0.29 / 22 %	845	KSR1; (KSR OR KSR1 OR HB) KINASE SUPPRESSOR OF RAS-1 (KINASE SUPPRESSOR OF RAS-1)	0.85 / - %
781	BTG1; (BTG1 OR BTG1) BTG1 TRANSCRIPTION GENE 1 PRC 1.48 / 10 %	0.81 / 19 %	1.30 / 3 %	0.86 / 41 %	846	MAP2K2; (MAP2K2 OR PRKMK2 OR MEK2) DUAL SPECIFIC(K) 0.67 / 15 %	1.94 / 6 %
782	BTG2; (BTG2 OR PC3) BTG2 PROTEIN PRECURSOR (NGF-INDUCIBLE) 1.52 / 12 %	0.73 / 6 %	0.86 / - %	0.94 / 18 %	847	P53R2; (P53R2) RIBONUCLEOTIDE REDUCTASE (DKFZ761E1312)	0.83 / - %
783	BTG3; (BTG3 OR T0B5 OR ANA) BTG3 PROTEIN (T0B5-INDUCIBLE) 1.54 / 15 %	5.42 / 29 %	0.89 / - %	0.37 / 17 %	848	RAG1; (RAG1 OR RNF4) V(D)J RECOMBINATION ACTIVATING PROTI 0.92 / 9 %	1.04 / 14 %
784	CC3; (CC3) COMPLEMENT C3 PRECURSOR	0.90 / 21 %	1.09 / - %	1.45 / 23 %	849	RAG2; (RAG2) V(D)J RECOMBINATION ACTIVATING PROTI 0.87 / 9 %	0.80 / 6 %
785	CLU; (CLU) CLUSTERIN PRECURSOR	0.89 / 8 %	0.89 / 9 %	3.52 / 14 %	850	AIM2; (AIM2) INTERFERON-INDUCIBLE PROTEIN AIM2 (ABSENT IN ME-10.09 / 20 %)	0.48 / 9 %
786	E2F5; (E2F5) TRANSCRIPTION FACTOR E2F5 (E2F-5)	1.27 / 7 %	0.93 / 24 %	1.68 / 22 %	851	IFNB1; (IFNB1 OR IFNB OR IFB) INTERFERON BETA PRECURSOR (IFN 1.02 / 15 %)	1.03 / 9 %
787	EGR1; (EGR1 OR ZNF225) EARLY GROWTH RESPONSE PROTEIN 1 (1.13, 48 / 24 %)	53.82 / 145 %	15.06 / 70 %	33.18 / 78 %	852	ZMDA1; (IL19 OR ZMDA1) INTERLEUKIN-19 PRECURSOR (IL-19) (MEL 0.89 / 19 %)	0.57 / - %
788	ENFAP8; (ENFAP8 OR GG2-1 OR MDC-3.13 OR SCC-S2) TNFAIP8 TUI 1.64 / 18 %	1.81 / 14 %	1.14 / - %	2.52 / 16 %	853	CTSP; (CTSP) CATHEPSIN D PRECURSOR (EC 3.4.23.5)	0.35 / - %
789	HMOX1; (HMOX1 OR HO1) HEME OXYGENASE 1 (EC 1.14.99.3.0.41 / 38 %)	1.10 / 20 %	1.75 / 3 %	0.63 / 6 %	854	CD163; (CD163) M130 ANTIGEN PRECURSOR (MACROPHAGE HEMOX 0.37 / 22 %)	0.43 / 13 %
790	HMOX2; (HMOX2 OR HO2) HEME OXYGENASE 2 (EC 1.14.99.3.0.2 / 10 %)	1.10 / 20 %	0.76 / - %	1.23 / 34 %	855	ACVR1; (ACVR1 OR ACVR1K2) ACTIVIN RECEPTOR TYPE I PRECURSOR 0.32 / 15 %	1.13 / - %
791	PIP; (PIP OR CVPB) PEPTIDYL-PROLYL CIS-TRANS ISOMERASE B 0.84 / 7 %	0.82 / 7 %	0.43 / 0 %	1.01 / 6 %	856	ACVR2; (ACVR2) ACTIVIN RECEPTOR TYPE II PRECURSOR 0.27 / 1.49 / 17 %	2.86 / 28 %
792	RHOA; (ARHA OR ARH12 OR RHOA OR RHO12) TRANSFORMING PRC 1.87 / 33 %	0.49 / 32 %	2.43 / 0 %	0.31 / 26 %	857	ACVRL1; (ACVRL1 OR ACVRLK1) SEPRIN/THREONINE-PRO-1.89 / 13 %	0.89 / 23 %
793	B2M; (B2M) BETA-2-MICROGLOBULIN PRECURSOR (HDCMA22P)	1.53 / 15 %	1.26 / 12 %	2.22 / - %	858	ADCY8; (ADCY8) ADENYLATE CYCLASE, TYPE VIII (EC 4.6.1.1) (ATP F 1.04 / 14 %)	0.85 / 12 %
794	CDM; (BCAP31 OR BAP31) B-CELL RECEPTOR-ASSOCIATED PROTI 0.25 / 24 %	0.35 / 13 %	0.55 / 2 %	0.21 / 12 %	859	AID; (AID) ACTIVATION-INDUCED CYTIDINE DEAMINASE	0.99 / 25 %
795	FRAP; (FRAP) FKBP-RAPAMYCIN ASSOCIATED PROTI (FRAP) (RAI0 0.51 / 6 %)	18.96 / 64 %	0.47 / - %	0.28 / 39 %	860	AIOLOS; (ZNFN1A3) ZINC FINGER PROTEIN AIOLOS	1.12 / 18 %
796	G22P1; (G22P1) ATP-DEPENDENT DNA HELICASE II, 70 KDA SUBUNIT 3.02 / 12 %	3.33 / 23 %	1.43 / 31 %	1.98 / 21 %	861	ACOC3; (ACOC3 OR VAP1) MEMBRANE COPPER AMINE OXIDASE (EC 1.1.45 / 48 %)	1.84 / 18 %
797	P1M1; (P1M1) PROTO-ONCOGENE SERINE/THREONINE-PROTEIN KIN 3.05 / 11 %	1.43 / 31 %	0.98 / 14 %	2.79 / 18 %	862	AP1G2; (AP1G2) ADAPTER-RELATED PROTEIN COMPLEX 1 GAMMA 2.68 / 23 %	0.71 / 10 %
798	ORM2; (ORM2 OR AGP2) AND (ORM1 OR ASP1)) ALPHA-1-ACI 0.99 / 6 %	0.98 / 14 %	0.45 / 23 %	1.72 / 12 %	863	CD274; (CD274 OR B7H1 OR PDCCD1L1 OR PDCL1) PRO 0.66 / 19 %	1.02 / 12 %
799	MLL3; (MLL3 OR HALR OR KIAA1506) MYELOIDILYMPHOID OR MIXED 4.15 / 23 %	1.10 / 10 %	3.45 / 8 %	0.26 / 12 %	864	CD276; (CD276 OR B7H3 OR PSEC0249) CD276 ANTIGEN PRECURSOR 1.18 / 20 %	0.26 / 10 %
800	BCL6; (BCL6 OR ZNF51 OR LAZ3 OR BCL-6) B-CELL LYMPHOID 0.48 / 22 %	0.06 / 8 %	2.03 / - %	0.76 / 18 %	865	CEACAM1-CEACAM2; ((CEACAM1 OR BGF OR BGP1 OR BGP2) AND 1.74 / 14 %)	1.33 / 5 %
801	BLIMP1; (PRDM1 OR BLIMP1) B LYMPHOCYTE INDUCED MATURATIO 1.05 / 19 %	59.80 / 137 %	0.97 / 2 %	63.19 / 44 %	866	BMP15; (BMP15 OR GDF9B) BONE MORPHOGENETIC PROTEIN 15 PF 0.94 / 18 %	0.92 / - %
802	ZBTB18; (ZBTB18 OR ZFP238 OR RP58 OR TAZ1) ZINC FINGER PROT 1.61 / 23 %	4.10 / 30 %	0.34 / 28 %	3.50 / 16 %	867	BMPRIA; (BMPRIA OR ACVRLK3) BONE MORPHOGENETIC PROTEIN 1.33 / 41 %	1.78 / 12 %
803	BACH2; (BACH2) TRANSCRIPTION REGULATORY PROTEIN BACH2 (BT 0.46 / 31 %)	0.21 / 35 %	0.09 / 51 %	1.35 / 9 %	868	BMPRI1B; (BMPRI1B OR ACVRLK6) BONE MORPHOGENETIC PROTEIN 1.33 / 32 %	1.58 / - %
804	ZBTB19; (ZBTB19 OR ZNF278 OR PATZ OR RIAZ OR ZSG) ZINC FINGER 0.33 / 16 %	1.40 / 9 %	0.90 / 12 %	1.50 / 28 %	869	CD164; (CD164 OR MMGC-24) PUTATIVE MUCIN CORE PROTEIN 24 P 1.70 / 21 %	2.49 / 9 %
805	PCAF; (PCAF) P300/CBP-ASSOCIATED FACTOR (PCAF) PCAF ACETY 1.27 / 10 %	1.40 / 9 %	0.45 / 11 %	0.50 / 39 %	870	CD44; (CD44, EX13-15, MOUSE; (CD44 OR LHR) CD44 ANTIGEN PRECURSOR 1.42 / 16 %)	49.52 / - %
806	TNFI; (TNF1 OR PCM1) METHYL-CPG BINDING PROTEIN 1 (METHYL 2.83 / 18 %)	0.45 / 11 %	1.29 / 25 %	0.50 / 39 %	871	CD44; (CD44, EX16-20, MOUSE; (CD44 OR LHR) CD44 ANTIGEN PRECURSOR 1.03 / 21 %)	2.16 / 14 %
807	MBP1; (MBP1 OR TNFIP1) OR EDP1) EDP1 PROTEIN	1.03 / 9 %	11.52 / 68 %	0.70 / 1 %	872	CD44; (CD44 OR LHR) CD44 ANTIGEN PRECURSOR (1.72 / 21 %)	2.03 / 8 %
808	DL1; (DL1) DELTA-LIKE PROTEIN 1 PRECURSOR (DROSOPHILA DE 5.29 / 17 %)	15.00 / - %	3.89 / - %	4.98 / 27 %	873	CDH3; (CDH3 OR CDHP) CADHERIN-3 PRECURSOR (PLACENTAL-CAI 1.47 / 17 %)	1.27 / 5 %
809	HJ1; (HJ1) JAGGED1 PRECURSOR (JAGGED1) (HJ1) NOTCH LIGAN 1.06 / 8 %	2.48 / 16 %	1.01 / - %	0.88 / 35 %	874	CRKL; (CRKL) CRK-LIKE PROTEIN	0.48 / 21 %
810	NFKB2; (NFKB2) IKAPPA-B-RELATED PROTI (IKAPB) (IKAF 0.53 / 19 %)	2.48 / 16 %	1.01 / - %	0.98 / 7 %	875	EXCL16; (091000IK24RIK) SR-PSOX (TRANSMEMBRANE CHEMOKINE 0.92 / 22 %)	0.77 / 13 %
811	NOTCH1; (NOTCH1 OR TANI) NEUROGENIC LOCUS NOTCH PROTEIN 1.73 / 16 %	0.38 / 13 %	0.75 / 6 %	0.83 / 18 %	876	DAPK1; (DAPK1 OR DAPK) DEATH-ASSOCIATED PROTI KINASE 1 (1.33 / 13 %)	0.69 / - %
812	NOTCH2; (NOTCH2) NEUROGENIC LOCUS NOTCH PROTEIN 2.81 / 13 %	3.04 / 13 %	2.13 / 6 %	3.53 / 26 %	877	TNFRSF21; (TNFRSF21 OR DR6) TUMOR NECROSIS FACTOR RECEP 0.87 / 18 %	0.77 / 7 %
813	NOTCH4; (NOTCH4) NOTCH4	0.82 / 24 %	1.36 / 10 %	0.96 / 10 %	878	EGR2; (EGR2 OR KROX20) EARLY GROWTH RESPONSE PROTEIN 2 (0.86 / 51 %)	0.59 / 16 %
814	ECF1; (ECF1) ENDOTHELIN-CONVERTING ENZYME 1 (EC 3.4.24.71) (1.46 / 14 %)	0.46 / 14 %	0.45 / 16 %	0.76 / 11 %	879	EGR3; (EGR3 OR PILOT) EARLY GROWTH RESPONSE PROTEIN 3 (E0.70 / 24 %)	0.61 / 29 %
815	ECE2; (ECE2) ENDOTHELIN-CONVERTING ENZYME 2 (EC 3.4.24.71) (1.17 / 10 %)	1.55 / 29 %	0.91 / 46 %	1.22 / 10 %	880	EPHB2; (EPHB2 OR EPH3 OR ERK OR DRT OR HEK5) EPHRIN TYPE 1.55 / 10 %	0.80 / 14 %
816	EPOR; (EPOR) ERYTHROPOIETIN RECEPTOR PRECURSOR (EPOR) 1.44 / 4 %	1.83 / 47 %	2.20 / 22 %	1.12 / 23 %	881	FCP1; (FCP1) SERINE PHOSPHATASE FCP1A (CTDMP1) RNA POLYME 0.81 / 12 %	0.41 / 11 %
817	IGFBP1; (IGFBP1 OR IBP1) INSULIN-LIKE GROWTH FACTOR BINDING 1.18 / 12 %	0.78 / 20 %	1.26 / 19 %	0.93 / 9 %	882	FLT3LG; (FLT3LG) SL CYTOKINE PRECURSOR (FLT3) RNA POLYME 0.78 / 16 %	0.69 / 19 %
818	POU2F1; (POU2F1 OR OTF1 OR OCT1) POU DOMAIN, CLASS 2, TR 4.12 / 9 %	1.65 / 8 %	3.23 / 9 %	1.59 / 12 %	883	GATA3; (GATA3) TRANS-ACTING T-CELL SPECIFIC TRANSCRIPTION 1.21 / 14 %	1.36 / 19 %
819	BMP10; (BMP10) BONE MORPHOGENETIC PROTEIN 10	1.26 / 26 %	1.21 / 32 %	0.97 / 28 %	884	GZMB; (GZMB OR CTLA1 OR GRB OR CSFB OR CGL1) GR 0.65 / 26 %	0.62 / 11 %
820	F2R; (F2R OR PAR1 OR TR OR CF2R) PROTEINASE ACTIVATED RECI 4.21 / 64 %	1.45 / - %	1.10 / - %	3.82 / 38 %	885	HEXA; (HEXA) BETA-HEXOSAMINIDASE ALPHA CHAIN PRECURSOR (1.57 / 24 %)	1.60 / 19 %
821	MGST3; (MGST3) MICROSOMAL GLUTATHIONE S-TRANSFERASE 3 (1.04 / 8 %)	0.86 / 36 %	0.26 / 18 %	0.93 / 22 %	886	HHEX; (HHEX OR PRHX OR PRH OR HEX) HOMEOBOX PROTI PR-0.82 / 12 %	0.75 / 13 %
822	NRP1; (NRP1 OR NRP OR VEGF165R) NEUROPLIN-1 PRECURSOR (V 1.43 / 35 %)	1.37 / - %	1.37 / - %	1.92 / 16 %	887	HLX1; (HLX1) HOMEOBOX PROTI HLX1 (HOMEOBOX PROTI HB; 1.85 / 22 %)	0.87 / 6 %
823	PAFAH1B1; (PAFAH1B1 OR PAFAH1 OR LIST OR MDCR) PLATELET-A 2.73 / 15 %	1.89 / 6 %	3.37 / - %	1.76 / 12 %	888	ICOS; (ICOS) ACTIVATION-INDUCIBLE LYMPHOCYTE IMMUNOMEDIA 0.78 / 16 %	0.95 / 10 %
824	PAFAH1B2; (PAFAH1B2 OR PAFAHB) PLATELET-ACTIVATING FACTO 0.47 / 25 %	1.22 / 18 %	0.24 / - %	2.54 / 12 %	889	IL10RB; (IL10RB OR CRFB4) INTERLEUKIN-10 RECEPTOR BETA CHAI 1.21 / 16 %	2.40 / 25 %
825	PAFAH1B3; (PAFAH1B3 OR PAFAHG) PLATELET-ACTIVATING FACTO 0.47 / 10 %	0.74 / 7 %	0.59 / - %	0.57 / 22 %	890	IL12RB1; (IL12RB1 OR IL12RB OR IL12R) INTERLEUKIN-12 RECEPT 0.90 / 30 %	1.49 / 61 %
826	PAFAH2; (PAFAH2) PLATELET-ACTIVATING FACTOR ACETYLYHYDRO 0.58 / 9 %	0.82 / 16 %	0.86 / - %	1.15 / 4 %	891	IL12RB2; (IL12RB2) INTERLEUKIN-12 RECEPTOR BETA-2 CHAIN PREC 0.11 / 19 %	1.74 / 18 %
827	SPAZL2; (PLA2-XII OR PLA2G13 OR FKSFG7) GROUP XII SECRETOR 1.26 / 29 %	1.09 / - %	1.63 / - %	1.56 / 24 %	892	IL17R; (IL17R) INTERLEUKIN-17 RECEPTOR PRECURSOR (IL-17 RECI 1.46 / 23 %)	2.61 / 8 %
828	TRAP; (TRAP OR DJ30M3.3 OR EAP2 OR AD-022) DJ30M3.3 (NOVEL 1.04 / 23 %)	1.51 / 17 %	1.63 / - %	0.80 / 22 %	893	IL21; (IL21) INTERLEUKIN 21	0.69 / 28 %
829	USP2; (USP2 OR UBPA1) UBIQUITIN CARBOXYL-TERMINAL HYDROL 1.13 / 16 %	0.60 / 10 %	0.53 / - %	0.74 / 9 %	894	INPP4A; (INPP4A) TYPE I INOSITOL-3,4-BISPHOSPHATE 4-PHOSPHAT 0.70 / 76 %	0.71 / 29 %
830	ALOX12E; (ALOX12E OR ALOX12-PS2 OR ALOXE) ARACHIDIC 1.59 / 3 %	1.19 / 14 %	0.59 / - %	1.04 / 7 %	895	IRAK1; (IRAK1 OR IRAK) INTERLEUKIN-1 RECEPTOR-ASSOCIATED KINASE 3 (10.78 / 14 %)	1.19 / - %
831	ALOX5; (ALOX5) EPIDERMAL LIPOXYGENASE (LIPOXYGENASE) 0.89 / 16 %	0.33 / 11 %	0.63 / - %	0.41 / 3 %	896	IRAK2; (IRAK2) INTERLEUKIN-1 RECEPTOR-ASSOCIATED KINASE-2 (0.80 / 21 %)	2.84 / 25 %
832	IPAZ2; (IPAZ2) CALCIUM-INDEPENDENT PHOSPHOLIPASE A2 (MEMBR 3.54 / 9 %)	3.61 / 4 %	0.86 / - %	27.67 / 31 %	897	IRAK2; (IRAK2) INTERLEUKIN-1 RECEPTOR-ASSOCIATED KINASE-2 (0.68 / 10 %)	2.60 / 17 %
833	MGST1; (MGST1 OR GSTG OR GSTT1) GLUTATHIONE S-TRANSFERASE 1.36 / 17 %	0.97 / 11 %	1.67 / 16 %	1.96 / 19 %	898	IRF3; (IRF3) INTERFERON REGULATORY FACTOR 3 (IRF-3)	0.37 / 7 %
834	MGST2; (MGST2 OR GSTG) MICROSOMAL GLUTATHIONE S-TRANSFERASE 1.76 / 24 %	1.67 / 11 %	2.76 / - %	1.26 / 16 %	899	IRF5; (IRF5) INTERFERON REGULATORY FACTOR 5 (IRF-5)	0.81 / 17 %
835	NTE; (NTE) NEUROPATHY TARGET ESTERASE	4.06 / 14 %	4.13 / 26 %	2.55 / 9 %	900	IRF6; (IRF6) INTERFERON REGULATORY FACTOR 6 (IRF-6)	0.18 / 14 %
836	SLASH; (PLA2G3D OR SLASH) GROUP IID SECRETORY PHOSPHO 1.01 / 22 %	0.52 / 28 %	0.84 / - %	0.94 / 28 %	901	IRF7; (IRF7) INTERFERON REGULATORY FACTOR 7 (IRF-7)	1.65 / 13 %
837	AKAP1; (AKAP1 OR AKAP149) A KINASE ANCHOR PROTEIN 1 (AKINA 3.20 / 18 %)	0.35 / 15 %	0.84 / - %	1.09 / 12 %	902	KLRK1; (KLRK1 OR NKG2D) NKG2D TYPE II INTEGRAL MEMBRANE P 3.09 / 20 %	2.73 / 16 %
838	OACT5; (OACT5 OR C3F) O-ACTYLTRANSFERASE (MEMBRANE BOUNI 2.25 / 9 %)	53.40 / 294 %	12.92 / - %	1.63 / 22 %	903	KNSL1; (KNSL1 OR EG5) KINESIN-RELATED MOTOR PROTIEN EG5 (K 0.88 / 13 %)	0.84 / 59 %
839	PLCB4; (PLCB4) PHOSPHOLIPASE C BETA 4	1.24 / 22 %	0.94 / 6 %	2.67 / 24 %	904	LAG3; (LAG3 OR FDC) LYMPHOCYTE ACTIVATION GENE-3 PROTIEN 0.68 / 13 %	0.94 / 20 %
840	PLCE; (PLCE OR P1CE1 OR PLC-EPSILON) PHOSPHOINOSITIDE-SPE 0.91 / 25 %	1.63 / - %	1.10 / - %	0.89 / 16 %	905	LEF1; (LEF1) LYMPHOID ENHANCER BINDING FACTOR 1 (LEF-1) (T C 0.72 / 4 %)	0.85 / 22 %
841	HRA5L; (HRA5L OR HRA5R) HRA5-LIKE SUPPRESSOR (A-C1)	1.08 / 22 %	1.07 / - %	0.96 / 21 %	906	LGA3L3; (LGA3L3 OR MAC2) GALECTIN-3 (GALACTOSE-SPECIFIC LE 0.69 / 5 %)	0.58 / 18 %
842	LRA1; (LRA1) LECTININ RETINOL ACYLTRANSFERASE	1.23 / 37 %	0.95 / - %	1.21 / 8 %	907	LMO4; (LMO4) LIM DOMAIN TRANSCRIPTION FACTOR LMO4 (LIM-ONI 0.58 / 20 %)	0.81 / 13 %
843	ITGA3_5PRIME; (ITGA3) INTEGRIN ALPHA-3 PRECURSOR (GALACTO10.91 / 12 %)	1.14 / 24 %	0.68 / - %	1.00 / 16 %	908	LTY5; (LTY5) RECEPTOR DEC205 (DEC-205) (CD205)	0.89 / 21 %

1039	ABIN-2: (ABIN-2) A20-BINDING INHIBITOR OF NF-KAPPAB ACTIVATIOI	0.70 / 11 %	0.92 / 21 %	0.81 / 1 %	0.91 / 6 %
1040	APAF1: (APAF1 OR KIAA0413) APOPTOTIC PROTEASE ACTIVATING F	3.63 / 19 %	4.64 / 20 %	1.96 / 5 %	4.87 / 9 %
1041	CASP9: (CASP9 OR MCH6) CASPASE-9 PRECURSOR (EC 3.4.22.-) (CA	0.28 / 15 %	1.78 / 70 %	0.53 / - %	0.95 / 10 %
1042	TNFAIP3: (TNFAIP3 OR A20) TUMOR NECROSIS FACTOR, ALPHA-IND	0.75 / 14 %	0.66 / 6 %	0.78 / - %	0.63 / 6 %
1043	AKAP11_1: (AKAP11 OR AKAP220 OR KIAA0629) A-KINASE ANCHOR F	0.81 / 18 %	1.76 / 27 %	0.61 / - %	1.32 / 15 %
1044	SRCAP: (SRCAP) TRANSCRIPTIONAL ACTIVATOR SRCAP (FLJ46149)	2.02 / 7 %	0.77 / 9 %	2.25 / 3 %	0.55 / 19 %
1045	TKT1: (TKT1 OR TKT) TRANSKETOLASE (EC 2.2.1.1) (TK).	0.73 / 10 %	0.65 / 8 %	0.63 / 4 %	0.77 / 12 %
1046	IKAP: (IKAP OR IKBKAP) IKB KINASE COMPLEX ASSOCIATED PROTE	2.39 / 31 %	1.77 / 24 %	1.38 / 21 %	2.59 / 10 %
1047	TNFRSF19L: (TNFRSF19L OR RELT) TUMOR NECROSIS FACTOR REC	0.36 / 15 %	2.23 / 7 %		1.56 / 13 %
1048	IRF1: (IRF1) INTERFERON REGULATORY FACTOR 1 (IRF-1).	0.72 / 21 %	2.93 / 8 %	1.57 / - %	1.24 / 7 %
1049	TGFBR2: (TGFBR2) TGF-BETA RECEPTOR TYPE II PRECURSOR (EC	2.92 / 29 %	0.58 / 10 %	0.92 / 17 %	1.35 / 1 %
1050	KLF6: (COPEB OR KLF6 OR BCD1 OR CPBP) CORE PROMOTER ELEN	0.40 / 11 %	0.98 / 6 %	0.59 / 1 %	0.68 / 18 %
1051	FSTL1: (FSTL1 OR FRP) FOLLISTATIN-RELATED PROTEIN 1 PRECUR	1.00 / 24 %	1.15 / 39 %		0.99 / 14 %
1052	FYCO1: (FYCO1) FYVE AND COILED-COIL DOMAIN CONTAINING 1 (2E	3.64 / 12 %	0.94 / 7 %	4.31 / - %	0.66 / 15 %
1053	KITLG: (KITLG OR MGF OR SCF) KIT LIGAND PRECURSOR (C-KIT LIG	1.09 / 15 %	1.27 / 14 %	1.40 / 2 %	0.96 / 15 %
1054	LSP1: (LSP1 OR WP34 OR S37 OR PP52) LYMPHOCYTE-SPECIFIC PR	1.00 / 19 %	1.01 / 6 %	0.88 / 1 %	1.29 / 16 %
1055	SELENBP2-SELENBP1: (SELENBP2 OR LPSB2) SELENIUM-BINDING P	1.71 / 8 %			4.08 / 33 %
1056	CLEC4A-DCIR2: ((CLEC4A OR CLECSF6 OR DCIR OR LLIR) AND (DCIF	0.71 / 11 %	1.56 / 87 %	0.73 / 7 %	0.91 / 5 %
1057	IDD: (IDD OR DGCR2 OR KIAA0163) INTEGRAL MEMBRANE PROTEIN	2.57 / 21 %	3.69 / 33 %	1.41 / 3 %	5.82 / 23 %
1058	BY55: (BY55) NATURAL KILLER CELL RECEPTOR BY55 PRECURSOR	0.85 / 12 %	0.74 / 37 %	0.72 / 14 %	0.85 / 13 %
1059	CBLN1: (CBLN1) CEREBELLIN PRECURSOR (PRECEREBELLIN).	1.21 / 18 %			1.08 / 13 %
1060	IL18BP: (IL18BP) INTERLEUKIN-18 BINDING PROTEIN PRECURSOR (II	5.83 / 38 %	1.93 / - %		3.42 / 13 %
1061	IL1RN: (IL1RN OR IL1RA) INTERLEUKIN-1 RECEPTOR ANTAGONIST P	1.09 / 73 %	1.13 / 40 %	0.75 / - %	1.15 / 14 %
1062	IL21R: (IL21R OR NILR) INTERLEUKIN 21 RECEPTOR PRECURSOR (IL	0.12 / 12 %	9.63 / 49 %	0.34 / 5 %	1.92 / 39 %
1063	LITAF: (LITAF OR PIG7 OR 3222402J11RIK) LIPOPOLYSACCHARIDE-IN	1.21 / 15 %	2.15 / 6 %	1.27 / 1 %	1.79 / 19 %
1064	MAPK8IP1: (MAPK8IP1 OR JIP1 OR IB1)C-JUN-AMINO-TERMINAL KINA	0.75 / 13 %	0.95 / 37 %	0.83 / - %	1.05 / 12 %
1065	MAPK8IP2: (MAPK8IP2 OR JIP2 OR IB2) C-JUN-AMINO-TERMINAL KIN	0.72 / 23 %	0.93 / 19 %	0.67 / 17 %	0.77 / 33 %
1066	TNFAIP2: (TNFAIP2) TUMOR NECROSIS FACTOR, ALPHA-INDUCED P	0.84 / 31 %	0.84 / 19 %	0.93 / - %	0.84 / 31 %
1067	EDEM1: (EDEM1 OR EDEM OR KIAA0212) ER DEGRADATION-ENHANC	16.53 / 104 %	6.80 / 46 %	2.98 / - %	6.79 / 18 %
1068	TANK_1: (TANK OR ITRAF) TRAF FAMILY MEMBER-ASSOCIATED NF-I	1.13 / 17 %	0.77 / 20 %	0.83 / - %	1.00 / 12 %
1069	TLR3: (TLR3) TOLL-LIKE RECEPTOR 3.	0.86 / 17 %	0.94 / 10 %	0.93 / - %	0.82 / 16 %
1070	IL1RL1_1: (IL1RL1 OR ST2 OR STE2 OR LY84 OR DER4 OR T1) INTERI	1.45 / 9 %			

Sorted Sca-1⁻ PDCs and Sca-1⁺ PDCs we hybridized on a PIQOR mouse immunology chip. A value below “1” demonstrates an over-representation of the mRNA transcript in Sca-1⁻ PDCs. A value over “1” indicates a predominant transcription in Sca-1⁺ PDCs. Values represent mean regulation of four replicates on different positions of the array. Standard error is given in parenthesis.

REFERENCES

- Aarnoudse CA**, Bax M, Sánchez-Hernández M, García-Vallejo JJ, van Kooyk Y (2008) Glycan modification of the tumor antigen gp100 targets DC-SIGN to enhance dendritic cell induced antigen presentation to T cells. *Int J Cancer* 122:839-846.
- Abe M**, Colvin BL, Thomson AW (2005) Plasmacytoid dendritic cells: in vivo regulators of alloimmune reactivity? *Transplant Proc* 37:4119-4121.
- Abe M**, Wang Z, de Creus A, Thomson AW (2005) Plasmacytoid dendritic cell precursors induce allogeneic T-cell hyporesponsiveness and prolong heart graft survival. *Am J Transplant* 5:1808-1819.
- Abts H**, Emmerich M, Miltenyi S, Radbruch A, Tesch H (1989) CD20 positive human B lymphocytes separated with the magnetic cell sorter (MACS) can be induced to proliferation and antibody secretion in vitro. *J Immunol Methods* 125:19-28.
- Afzali B**, Lombardi G, Lechler RI, Lord GM (2007) The role of T helper 17 (Th17) and regulatory T cells (Treg) in human organ transplantation and autoimmune disease. *Clin Exp Immunol* 148:32-46.
- Agnetto D**, Lankford CS, Bream J, Morinobu A, Gadina M, O'Shea JJ, Frucht DM (2003) Cytokines and transcription factors that regulate T helper cell differentiation: new players and new insights. *J Clin Immunol* 23:147-161.
- Akira S**, Takeda K (2004) Toll-like receptor signalling. *Nat Rev Immunol* 4:499-511.
- Albert ML**, Sauter B, Bhardwaj N (1998) Dendritic cells acquire antigen from apoptotic cells and induce class I-restricted CTLs. *Nature* 392(6671):86-9.
- Albert ML**, Pearce SF, Francisco LM, Sauter B, Roy P, Silverstein RL, Bhardwaj N (1998) Immature dendritic cells phagocytose apoptotic cells via alpha5beta1 and CD36, and cross-present antigens to cytotoxic T lymphocytes. *J Exp Med* 188(7):1359-68.
- Allman D**, Dalod M, Asselin-Paturel C, Delale T, Robbins SH, Trinchieri G, Biron CA, Kastner P, Chan S (2006) Ikaros is required for plasmacytoid dendritic cell differentiation. *Blood* 108:4025-4034.
- Ariizumi K**, Shen GL, Shikano S, Ritter R, Zukas P, Edelbaum D, Morita A, Takashima A (2000) Cloning of a second dendritic cell-associated C-type lectin (dectin-2) and its alternatively spliced isoforms. *J Biol Chem* 275:11957-11963.
- Ariizumi K**, Shen GL, Shikano S, Xu S, Ritter R, Kumamoto T, Edelbaum D, Morita A, Bergstresser PR, Takashima A (2000) Identification of a novel, dendritic cell-associated molecule, dectin-1, by subtractive cDNA cloning. *J Biol Chem* 275:20157-20167.
- Asselin-Paturel C**, Boonstra A, Dalod M, Durand I, Yessaad N, Dezutter-Dambuyant C, Vicari A, O'Garra A, Biron C, Brière F, Trinchieri G (2001) Mouse type I IFN-producing cells are immature APCs with plasmacytoid morphology. *Nat Immunol* 2:1144-1150.
- Asselin-Paturel C**, Brizard G, Pin JJ, Brière F, Trinchieri G (2003) Mouse strain differences in plasmacytoid dendritic cell frequency and function revealed by a novel monoclonal antibody. *J Immunol* 171:6466-6477.
- Asselin-Paturel C**, Trinchieri G (2005) Production of type I interferons: plasmacytoid dendritic cells and beyond. *J Exp Med* 202:461-465.
- Asseman C**, Mauze S, Leach MW, Coffman RL, Powrie F (1999) An essential role for interleukin 10 in the function of regulatory T cells that inhibit intestinal inflammation. *J Exp Med* 190:995-1004.
- Backer R**, van Leeuwen F, Kraal G, den Haan JM (2008) CD8- dendritic cells preferentially cross-present *Saccharomyces cerevisiae* antigens. *Eur J Immunol* 38:370-380.
- Baechler EC**, Batliwalla FM, Karypis G, Gaffney PM, Ortmann WA, Espe KJ, Shark KB, Grande WJ, Hughes KM, Kapur V, Gregersen PK, Behrens TW (2003) Interferon-inducible gene expression signature in peripheral blood cells of patients with severe lupus. *Proc Natl Acad Sci U S A* 100(5):2610-5.
- Bailey-Bucktrout SL**, Caulkins SC, Goings G, Fischer JA, Dzionek A, Miller SD (2008) Cutting edge: central nervous system plasmacytoid dendritic cells regulate the severity of relapsing experimental autoimmune encephalomyelitis. *J Immunol* 180:6457-6461.
- Bamezai A**, Palliser D, Berezovskaya A, McGrew J, Higgins K, Lacy E, Rock KL (1995) Regulated expression of Ly-6A.2 is important for T cell development. *J Immunol* 154:4233-4239.
- Banchereau J**, Steinman RM (1998) Dendritic cells and the control of immunity. *Nature* 392:245-252.
- Banchereau J**, Briere F, Caux C, Davoust J, Lebecque S, Liu YJ, Pulendran B, Palucka K (2000) Immunobiology of dendritic cells. *Annu Rev Immunol* 18:767-811.

- Banchereau J**, Pascual V (2006) Type I interferon in systemic lupus erythematosus and other autoimmune diseases. *Immunity* 25:383-392.
- Barchet W**, Krug A, Cella M, Newby C, Fischer JA, Dzionek A, Pekosz A, Colonna M (2005) Dendritic cells respond to influenza virus through TLR7- and PKR-independent pathways. *Eur J Immunol* 35:236-242.
- Barchet W**, Cella M, Colonna M (2005) Plasmacytoid dendritic cells--virus experts of innate immunity. *Semin Immunol.* 17(4):253-61
- Barrat FJ**, Meeker T, Chan JH, Guiducci C, Coffman RL (2007). Treatment of lupus-prone mice with a dual inhibitor of TLR7 and TLR9 leads to reduction of autoantibody production and amelioration of disease symptoms. *Eur J Immunol.* 37(12):3582-6
- Barry M**, Bleackley RC (2002) Cytotoxic T lymphocytes: all roads lead to death. *Nat Rev Immunol* 2:401-409.
- Becker M**, Sommer A, Krätzschar JR, Seidel H, Pohlenz HD, Fichtner I (2005) Distinct gene expression patterns in a tamoxifen-sensitive human mammary carcinoma xenograft and its tamoxifen-resistant subline MaCa 3366/TAM. *Mol Cancer Ther* 4:151-168.
- Belz GT**, Shortman K, Bevan MJ, Heath WR (2005) CD8alpha+ dendritic cells selectively present MHC class I-restricted noncytolytic viral and intracellular bacterial antigens in vivo. *J Immunol* 175:196-200.
- Biron CA**, Nguyen KB, Pien GC, Cousens LP, Salazar-Mather TP (1999) Natural killer cells in antiviral defense: function and regulation by innate cytokines. *Annu Rev Immunol* 17:189-220.
- Björck P** (2001) Isolation and characterization of plasmacytoid dendritic cells from Flt3 ligand and granulocyte-macrophage colony-stimulating factor-treated mice. *Blood* 98:3520-3526.
- Blanco P**, Palucka AK, Gill M, Pascual V, Banchereau J (2001) Induction of dendritic cell differentiation by IFN-alpha in systemic lupus erythematosus. *Science* 294:1540-1543.
- Blasius A**, Vermi W, Krug A, Facchetti F, Cella M, Colonna M (2004) A cell-surface molecule selectively expressed on murine natural interferon-producing cells that blocks secretion of interferon-alpha. *Blood* 103:4201-4206.
- Blasius AL**, Cella M, Maldonado J, Takai T, Colonna M (2006) Siglec-H is an IPC-specific receptor that modulates type I IFN secretion through DAP12. *Blood* 107:2474-2476.
- Blasius AL**, Giurisato E, Cella M, Schreiber RD, Shaw AS, Colonna M (2006) Bone marrow stromal cell antigen 2 is a specific marker of type I IFN-producing cells in the naive mouse, but a promiscuous cell surface antigen following IFN stimulation. *J Immunol* 177:3260-3265.
- Blasius AL**, Barchet W, Cella M, Colonna M (2007) Development and function of murine B220+CD11c+NK1.1+ cells identify them as a subset of NK cells. *J Exp Med* 204:2561-2568.
- Blomberg S**, Eloranta ML, Cederblad B, Nordlin K, Alm GV, Rönnblom L (2001) Presence of cutaneous interferon-alpha producing cells in patients with systemic lupus erythematosus. *Lupus* 10:484-490.
- Bochtler P**, Kröger A, Schirmbeck R, Reimann J (2008) Type I IFN-induced, NKT cell-mediated negative control of CD8 T cell priming by dendritic cells. *J Immunol* 181:1633-1643.
- Bonifaz L**, Bonnyay D, Mahnke K, Rivera M, Nussenzweig MC, Steinman RM (2002) Efficient targeting of protein antigen to the dendritic cell receptor DEC-205 in the steady state leads to antigen presentation on major histocompatibility complex class I products and peripheral CD8+ T cell tolerance. *J Exp Med* 196:1627-1638.
- Bonifaz LC**, Bonnyay DP, Charalambous A, Darguste DI, Fujii S, Soares H, Brimnes MK, Moltedo B, Moran TM, Steinman RM (2004) In vivo targeting of antigens to maturing dendritic cells via the DEC-205 receptor improves T cell vaccination. *J Exp Med* 199:815-824.
- Boonstra A**, Asselin-Paturel C, Gilliet M, Crain C, Trinchieri G, Liu YJ, O'Garra A (2003) Flexibility of mouse classical and plasmacytoid-derived dendritic cells in directing T helper type 1 and 2 cell development: dependency on antigen dose and differential toll-like receptor ligation. *J Exp Med* 197:101-109.
- Boscardin SB**, Hafalla JC, Masilamani RF, Kamphorst AO, Zebroski HA, Rai U, Morrot A, Zavala F, Steinman RM, Nussenzweig RS, Nussenzweig MC (2006) Antigen targeting to dendritic cells elicits long-lived T cell help for antibody responses. *J Exp Med.* 20;203(3):599-606.
- Bradley LM** and Watson SR (1996) Lymphocyte migration into tissue: the paradigm derived from CD4 subsets. *Curr. Opin. Immunol.* 8:312
- Brawand P**, Fitzpatrick DR, Greenfield BW, Brasel K, Maliszewski CR, De Smedt T (2002) Murine plasmacytoid pre-dendritic cells generated from Flt3 ligand-supplemented bone marrow cultures are

immature APCs. *J Immunol* 169:6711-6719.

Brode S, Macary PA (2004) Cross-presentation: dendritic cells and macrophages bite off more than they can chew!. *Immunology* 112:345-351.

Brooks PC, Lin JM, French DL, Quigley JP (1993) Subtractive immunization yields monoclonal antibodies that specifically inhibit metastasis. *J Cell Biol* 122:1351-1359.

Brown GD (2006) Dectin-1: a signalling non-TLR pattern-recognition receptor. *Nat Rev Immunol* 6:33-43.

Brown MG, Driscoll J, Monaco JJ (1993) MHC-linked low-molecular mass polypeptide subunits define distinct subsets of proteasomes. Implications for divergent function among distinct proteasome subsets. *J Immunol* 151:1193-1204.

Burgdorf S, Kautz A, Böhnert V, Knolle PA, Kurts C (2007) Distinct pathways of antigen uptake and intracellular routing in CD4 and CD8 T cell activation. *Science* 316:612-616.

Burgdorf S, Schölz C, Kautz A, Tampé R, Kurts C (2008) Spatial and mechanistic separation of cross-presentation and endogenous antigen presentation. *Nat Immunol*. 9(5):558-66.

Butcher EC and Picker L J (1996) Lymphocyte homing and homeostasis. *Science* 272:60

Caminschi I, Lucas KM, O'Keeffe MA, Hochrein H, Laâbi Y, Brodnicki TC, Lew AM, Shortman K, Wright MD (2001) Molecular cloning of a C-type lectin superfamily protein differentially expressed by CD8 α (-) splenic dendritic cells. *Mol Immunol* 38:365-373.

Caminschi I, Ahmet F, Heger K, Brady J, Nutt SL, Vremec D, Pietersz S, Lahoud MH, Schofield L, Hansen DS, O'Keeffe M, Smyth MJ, Bedoui S, Davey GM, Villadangos JA, Heath WR, Shortman K (2007) Putative IKDCs are functionally and developmentally similar to natural killer cells, but not to dendritic cells. *J Exp Med* 204:2579-2590.

Cantor H, Simpson E, Sato VL, Fathman CG, Herzenberg LA (1975) Characterization of subpopulations of T lymphocytes. I. Separation and functional studies of peripheral T-cells binding different amounts of fluorescent anti-Thy 1.2 (theta) antibody using a fluorescence-activated cell sorter (FACS). *Cell Immunol* 15:180-196.

Cao W, Rosen DB, Ito T, Bover L, Bao M, Watanabe G, Yao Z, Zhang L, Lanier LL, Liu YJ (2006) Plasmacytoid dendritic cell-specific receptor ILT7-Fc epsilonRI gamma inhibits Toll-like receptor-induced interferon production. *J Exp Med* 203:1399-1405.

Cao W, Zhang L, Rosen DB, Bover L, Watanabe G, Bao M, Lanier LL, Liu YJ (2007) BDCA2/Fc epsilon RI gamma complex signals through a novel BCR-like pathway in human plasmacytoid dendritic cells. *PLoS Biol* 5:e248.

Cao W (2008). *Experimental Biology 2008*, San Diego. The FASEB Journal;22:1065.17; unpublished data

Carbone FR, Hosken NA, Moore MW, Bevan MJ (1989) Class I MHC-restricted cytotoxic responses to soluble protein antigen. *Cold Spring Harb Symp Quant Biol* 54 Pt 1:551-555.

Cavanagh LL, Boyce A, Smith L, Padmanabha J, Filgueira L, Pietschmann P, Thomas R (2005) Rheumatoid arthritis synovium contains plasmacytoid dendritic cells. *Arthritis Res Ther* 7:R230-R240.

Cederblad B, Blomberg S, Vallin H, Perers A, Alm GV, Rönnblom L (1998) Patients with systemic lupus erythematosus have reduced numbers of circulating natural interferon-alpha-producing cells. *J Autoimmun* 11:465-470.

Cella M, Scheidegger D, Palmer-Lehmann K, Lane P, Lanzavecchia A, Alber G (1996) Ligation of CD40 on dendritic cells triggers production of high levels of interleukin-12 and enhances T cell stimulatory capacity: T-T help via APC activation. *J Exp Med* 184:747-752.

Cella M, Jarrossay D, Facchetti F, Alebardi O, Nakajima H, Lanzavecchia A, Colonna M (1999) Plasmacytoid monocytes migrate to inflamed lymph nodes and produce large amounts of type I interferon. *Nat Med* 5:919-923.

Cella M, Facchetti F, Lanzavecchia A, Colonna M (2000) Plasmacytoid dendritic cells activated by influenza virus and CD40L drive a potent TH1 polarization. *Nat Immunol* 1:305-310.

Chan CW, Crafton E, Fan HN, Flook J, Yoshimura K, Skarica M, Brockstedt D, Dubensky TW, Stins MF, Lanier LL, Pardoll DM, Housseau F (2006) Interferon-producing killer dendritic cells provide a link between innate and adaptive immunity. *Nat Med* 12:207-213.

Chen L, Arora M, Yarlagadda M, Oriss TB, Krishnamoorthy N, Ray A, Ray P (2006) Distinct responses of lung and spleen dendritic cells to the TLR9 agonist CpG oligodeoxynucleotide. *J Immunol*. 15;177(4):2373-83.

- Chen W**, Antonenko S, Sederstrom JM, Liang X, Chan ASH, Kanzler H, Blom B, Blazar BR, Liu YJ (2004) Thrombopoietin cooperates with FLT3-ligand in the generation of plasmacytoid dendritic cell precursors from human hematopoietic progenitors. *Blood* 103:2547-2553.
- Cho M**, Ishida K, Chen J, Ohkawa J, Chen W, Namiki S, Kotaki A, Arai N, Arai K, Kamogawa-Schifter Y (2008) SAGE library screening reveals ILT7 as a specific plasmacytoid dendritic cell marker that regulates type I IFN production. *Int Immunol* 20:155-164.
- Christensen SR**, Shupe J, Nickerson K, Kashgarian M, Flavell RA, Shlomchik MJ (2006) Toll-like receptor 7 and TLR9 dictate autoantibody specificity and have opposing inflammatory and regulatory roles in a murine model of lupus. *Immunity* 25:417-428.
- Codias EK**, Cray C, Baler RD, Levy RB, Malek TR (1989) Expression of Ly-6A/E alloantigens in thymocyte and T-lymphocyte subsets: variability related to the Ly-6a and Ly-6b haplotypes. *Immunogenetics* 29:98-107.
- Codias EK**, Malek TR (1990) Regulation of B lymphocyte responses to IL-4 and IFN-gamma by activation through Ly-6A/E molecules. *J Immunol* 144:2197-2204.
- Codias EK**, Rutter JE, Fleming TJ, Malek TR (1990) Down-regulation of IL-2 production by activation of T cells through Ly-6A/E. *J Immunol* 145:1407-1414.
- Colonna M**, Trinchieri G, Liu YJ (2004) Plasmacytoid dendritic cells in immunity. *Nat Immunol* 5:1219-1226.
- Cotton RG**, Milstein C (1973) Letter: Fusion of two immunoglobulin-producing myeloma cells. *Nature* 244:42-43.
- D'Amico A**, Wu L (2003) The early progenitors of mouse dendritic cells and plasmacytoid predendritic cells are within the bone marrow hemopoietic precursors expressing Flt3. *J Exp Med* 198:293-303.
- Dalod M**, Salazar-Mather TP, Malmgaard L, Lewis C, Asselin-Paturel C, Brière F, Trinchieri G, Biron CA (2002) Interferon alpha/beta and interleukin 12 responses to viral infections: pathways regulating dendritic cell cytokine expression in vivo. *J Exp Med* 195:517-528.
- Dalod M**, Hamilton T, Salomon R, Salazar-Mather TP, Henry SC, Hamilton JD, Biron CA (2003) Dendritic cell responses to early murine cytomegalovirus infection: subset functional specialization and differential regulation by interferon alpha/beta. *J Exp Med* 197:885-898.
- de Heer HJ**, Hammad H, Soullié T, Hijdra D, Vos N, Willart MA, Hoogsteden HC, Lambrecht BN (2004) Essential role of lung plasmacytoid dendritic cells in preventing asthmatic reactions to harmless inhaled antigen. *J Exp Med* 200:89-98.
- de la Rosa M**, Rutz S, Dorninger H, Scheffold A (2004) Interleukin-2 is essential for CD4+CD25+ regulatory T cell function. *Eur J Immunol* 34:2480-2488.
- De Maeyer E**, De Maeyer-Guignard J (1998) Type I interferons. *Int Rev Immunol* 17:53-73.
- Decalf J**, Fernandes S, Longman R, Ahloulay M, Audat F, Lefrerre F, Rice CM, Pol S, Albert ML (2007) Plasmacytoid dendritic cells initiate a complex chemokine and cytokine network and are a viable drug target in chronic HCV patients. *J Exp Med* 204:2423-2437.
- del Hoyo GM**, Martín P, Vargas HH, Ruiz S, Arias CF, Ardavin C (2002) Characterization of a common precursor population for dendritic cells. *Nature* 415:1043-1047.
- den Haan JM**, Lehar SM, Bevan MJ (2000) CD8(+) but not CD8(-) dendritic cells cross-prime cytotoxic T cells in vivo. *J Exp Med* 192:1685-1696.
- Der SD**, Zhou A, Williams BR, Silverman RH (1998) Identification of genes differentially regulated by interferon alpha, beta, or gamma using oligonucleotide arrays. *Proc Natl Acad Sci U S A.* 2;95(26):15623-8.
- Di Gaetano N**, Cittera E, Nota R, Vecchi A, Grieco V, Scanziani E, Botto M, Introna M, Golay J (2003) Complement activation determines the therapeutic activity of rituximab in vivo. *J Immunol* 171:1581-1587.
- Diacovo TG**, Blasius AL, Mak TW, Cella M, Colonna M (2005) Adhesive mechanisms governing interferon-producing cell recruitment into lymph nodes. *J Exp Med* 202:687-696.
- Diebold SS**, Kaisho T, Hemmi H, Akira S, Reis e Sousa C (2004) Innate antiviral responses by means of TLR7-mediated recognition of single-stranded RNA. *Science* 303:1529-1531.
- Duan XZ**, Wang M, Li HW, Zhuang H, Xu D, Wang FS (2004) Decreased frequency and function of circulating plasmacytoid dendritic cells (pDC) in hepatitis B virus infected humans. *J Clin Immunol* 24:637-646.
- Dudziak D**, Kamphorst AO, Heidkamp GF, Buchholz VR, Trumppfeller C, Yamazaki S, Cheong C, Liu K,

- Lee HW, Park CG, Steinman RM, Nussenzweig MC (2007) Differential antigen processing by dendritic cell subsets in vivo. *Science* 315:107-111.
- Dunn GP**, Koebel CM, Schreiber RD (2006) Interferons, immunity and cancer immunoediting. *Nat Rev Immunol* 6:836-848.
- Dzionic A**, Fuchs A, Schmidt P, Cremer S, Zysk M, Miltenyi S, Buck DW, Schmitz J (2000) BDCA-2, BDCA-3, and BDCA-4: three markers for distinct subsets of dendritic cells in human peripheral blood. *J Immunol* 165:6037-6046.
- Dzionic A**, Sohma Y, Nagafune J, Cella M, Colonna M, Facchetti F, Günther G, Johnston I, Lanzavecchia A, Nagasaka T, Okada T, Vermi W, Winkels G, Yamamoto T, Zysk M, Yamaguchi Y, Schmitz J (2001) BDCA-2, a novel plasmacytoid dendritic cell-specific type II C-type lectin, mediates antigen capture and is a potent inhibitor of interferon alpha/beta induction. *J Exp Med* 194:1823-1834.
- Dzionic A**, Inagaki Y, Okawa K, Nagafune J, Röck J, Sohma Y, Winkels G, Zysk M, Yamaguchi Y, Schmitz J (2002) Plasmacytoid dendritic cells: from specific surface markers to specific cellular functions. *Hum Immunol* 63:1133-1148.
- Eberwine J** (1996) Amplification of mRNA populations using aRNA generated from immobilized oligo(dT)-T7 primed cDNA. *Biotechniques* 20:584-591.
- Edwards AD**, Diebold SS, Slack EM, Tomizawa H, Hemmi H, Kaisho T, Akira S, Reis e Sousa C (2003) Toll-like receptor expression in murine DC subsets: lack of TLR7 expression by CD8 alpha+ DC correlates with unresponsiveness to imidazoquinolines. *Eur J Immunol* 33:827-833.
- Eisen MB**, Spellman PT, Brown PO, Botstein D (1998) Cluster analysis and display of genome-wide expression patterns. *Proc Natl Acad Sci U S A* 95:14863-14868.
- Engering A**, Geijtenbeek TB, van Vliet SJ, Wijers M, van Liempt E, Demaurex N, Lanzavecchia A, Fransen J, Figdor CG, Piguët V, van Kooyk Y (2002) The dendritic cell-specific adhesion receptor DC-SIGN internalizes antigen for presentation to T cells. *J Immunol* 168:2118-2126.
- English A**, Kosoy R, Pawlinski R, Bamezai A (2000) A monoclonal antibody against the 66-kDa protein expressed in mouse spleen and thymus inhibits Ly-6A.2-dependent cell-cell adhesion. *J Immunol* 165:3763-3771.
- Fallarino F**, Asselin-Paturel C, Vacca C, Bianchi R, Gizzi S, Fioretti MC, Trinchieri G, Grohmann U, Puccetti P (2004) Murine plasmacytoid dendritic cells initiate the immunosuppressive pathway of tryptophan catabolism in response to CD200 receptor engagement. *J Immunol* 173:3748-3754.
- Fallarino F**, Gizzi S, Mosci P, Grohmann U, Puccetti P (2007) Tryptophan catabolism in IDO+ plasmacytoid dendritic cells. *Curr Drug Metab* 8:209-216.
- Fanning SL**, George TC, Feng D, Feldman SB, Megjugorac NJ, Izaguirre AG, Fitzgerald-Bocarsly P (2006) Receptor cross-linking on human plasmacytoid dendritic cells leads to the regulation of IFN-alpha production. *J Immunol* 177:5829-5839.
- Farkas L**, Beiske K, Lund-Johansen F, Brandtzaeg P, Jahnsen FL (2001) Plasmacytoid dendritic cells (natural interferon- alpha/beta-producing cells) accumulate in cutaneous lupus erythematosus lesions. *Am J Pathol* 159:237-243.
- Figdor CG**, van Kooyk Y, Adema GJ (2002) C-type lectin receptors on dendritic cells and Langerhans cells. *Nat Rev Immunol* 2:77-84.
- Fitzgerald-Bocarsly P**, Dai J, Singh S (2008) Plasmacytoid dendritic cells and type I IFN: 50 years of convergent history. *Cytokine Growth Factor Rev* 19:3-19.
- Fleming TJ**, Fleming ML, Malek TR (1993) Selective expression of Ly-6G on myeloid lineage cells in mouse bone marrow. RB6-8C5 mAb to granulocyte-differentiation antigen (Gr-1) detects members of the Ly-6 family. *J Immunol* 151:2399-2408.
- Flood PM**, Dougherty JP, Ron Y (1990) Inhibition of Ly-6A antigen expression prevents T cell activation. *J Exp Med* 172:115-120.
- Galiana-Arnoux D**, Imler J-LL (2006) Toll-like receptors and innate antiviral immunity. *Tissue Antigens* 67:267-276.
- Ge Y**, Dombkowski AA, LaFiura KM, Tatman D, Yedidi RS, Stout ML, Buck SA, Massey G, Becton DL, Weinstein HJ, Ravindranath Y, Matherly LH, Taub JW (2006) Differential gene expression, GATA1 target genes, and the chemotherapy sensitivity of Down syndrome megakaryocytic leukemia. *Blood* 107:1570-1581.
- Geijtenbeek TB**, van Duijnhoven GC, van Vliet SJ, Krieger E, Vriend G, Figdor CG, van Kooyk Y (2002) Identification of different binding sites in the dendritic cell-specific receptor DC-SIGN for intercellular

adhesion molecule 3 and HIV-1. *J Biol Chem* 277:11314-11320.

Germain RN (1994) MHC-dependent antigen processing and peptide presentation: providing ligands for T lymphocyte activation. *Cell* 76:287-299.

Gilliet M, Boonstra A, Paturel C, Antonenko S, Xu XL, Trinchieri G, O'Garra A, Liu YJ (2002) The development of murine plasmacytoid dendritic cell precursors is differentially regulated by FLT3-ligand and granulocyte/macrophage colony-stimulating factor. *J Exp Med* 195:953-958.

Golay J, Zaffaroni L, Vaccari T, Lazzari M, Borleri GM, Bernasconi S, Tedesco F, Rambaldi A, Introna M (2000) Biologic response of B lymphoma cells to anti-CD20 monoclonal antibody rituximab in vitro: CD55 and CD59 regulate complement-mediated cell lysis. *Blood* 95(12):3900-8.

Goto T, Kennel SJ, Abe M, Takishita M, Kosaka M, Solomon A, Saito S (1994) A novel membrane antigen selectively expressed on terminally differentiated human B cells. *Blood* 84:1922-1930.

Grohmann U, Volpi C, Fallarino F, Bozza S, Bianchi R, Vacca C, Orabona C, Belladonna ML, Ayroldi E, **Nocentini G**, Boon L, Bistoni F, Fioretti MC, Romani L, Riccardi C, Puccetti P (2007) Reverse signaling through GITR ligand enables dexamethasone to activate IDO in allergy. *Nat Med* 13:579-586.

Groothuis TAM, Neefjes J (2005) The many roads to cross-presentation. *J Exp Med* 202:1313-1318.

Grouard G, Risoan MC, Filgueira L, Durand I, Banchereau J, Liu YJ (1997) The enigmatic plasmacytoid T cells develop into dendritic cells with interleukin (IL)-3 and CD40-ligand. *J Exp Med* 185:1101-1111.

Groux H, Sornasse T, Cottrez F, de Vries JE, Coffman RL, Roncarolo MG, Yssel H (1997) Induction of human T helper cell type 1 differentiation results in loss of IFN-gamma receptor beta-chain expression. *J Immunol* 158:5627-5631.

Grundy MA, Zhang T, Sentman CL (2007) NK cells rapidly remove B16F10 tumor cells in a perforin and interferon-gamma independent manner in vivo. *Cancer Immunol Immunother* 56:1153-1161.

Guermonprez P, Valladeau J, Zitvogel L, Théry C, Amigorena S (2002) Antigen presentation and T cell stimulation by dendritic cells. *Annu Rev Immunol* 20:621-667.

Hao S, Bai O, Li F, Yuan J, Laferte S, Xiang J (2007) Mature dendritic cells pulsed with exosomes stimulate efficient cytotoxic T-lymphocyte responses and antitumour immunity. *Immunology* 120:90-102.

Harrington LE, Mangan PR, Weaver CT (2006) Expanding the effector CD4 T-cell repertoire: the Th17 lineage. *Curr Opin Immunol* 18:349-356.

Hartmann E, Wollenberg B, Rothenfusser S, Wagner M, Wellisch D, Mack B, Giese T, Gires O, Endres S, Hartmann G (2003) Identification and functional analysis of tumor-infiltrating plasmacytoid dendritic cells in head and neck cancer. *Cancer Res* 63:6478-6487.

Hawiger D, Inaba K, Dorsett Y, Guo M, Mahnke K, Rivera M, Ravetch JV, Steinman RM, Nussenzweig MC (2001) Dendritic cells induce peripheral T cell unresponsiveness under steady state conditions in vivo. *J Exp Med* 194:769-779.

Heath WR, Carbone FR (2001) Cross-presentation in viral immunity and self-tolerance. *Nat Rev Immunol* 1:126-134.

Hegde RS, Mastrianni JA, Scott MR, DeFea KA, Tremblay P, Torchia M, DeArmond SJ, Prusiner SB, Lingappa VR (1998) A transmembrane form of the prion protein in neurodegenerative disease. *Science* 279:827-834.

Hegde RS, Tremblay P, Groth D, DeArmond SJ, Prusiner SB, Lingappa VR (1999) Transmissible and genetic prion diseases share a common pathway of neurodegeneration. *Nature* 402:822-826.

Heil F, Hemmi H, Hochrein H, Ampenberger F, Kirschning C, Akira S, Lipford G, Wagner H, Bauer S (2004) Species-specific recognition of single-stranded RNA via toll-like receptor 7 and 8. *Science* 303:1526-1529.

Henri S, Vremec D, Kamath A, Waithman J, Williams S, Benoist C, Burnham K, Saeland S, Handman E, Shortman K (2001) The dendritic cell populations of mouse lymph nodes. *J Immunol* 167:741-748.

Hidvegi T, Mirnics K, Hale P, Ewing M, Beckett C, Perlmutter DH (2007) Regulator of G Signaling 16 is a marker for the distinct endoplasmic reticulum stress state associated with aggregated mutant alpha1-antitrypsin Z in the classical form of alpha1-antitrypsin deficiency. *J Biol Chem* 282:27769-27780.

Hochrein H, Shortman K, Vremec D, Scott B, Hertzog P, O'Keeffe M (2001) Differential production of IL-12, IFN-alpha, and IFN-gamma by mouse dendritic cell subsets. *J Immunol* 166:5448-5455.

Hofmann K, and Stoffel W (1993). TMbase - A database of membrane spanning proteins segments. *Biol. Chem. Hoppe-Seyler* 374,166

Hogquist KA, Jameson SC, Heath WR, Howard JL, Bevan MJ, Carbone FR (1994) T cell receptor

antagonist peptides induce positive selection. *Cell* 76:17-27.

Honda K, Ohba Y, Yanai H, Negishi H, Mizutani T, Takaoka A, Taya C, Taniguchi T (2005) Spatiotemporal regulation of MyD88-IRF-7 signalling for robust type-I interferon induction. *Nature* 434:1035-1040.

Honda K, Yanai H, Negishi H, Asagiri M, Sato M, Mizutani T, Shimada N, Ohba Y, Takaoka A, Yoshida N, Taniguchi T (2005) IRF-7 is the master regulator of type-I interferon-dependent immune responses. *Nature* 434:772-777.

Honda K, Taniguchi T (2006) IRFs: master regulators of signalling by Toll-like receptors and cytosolic pattern-recognition receptors. *Nat Rev Immunol* 6:644-658.

Iparraquirre A, Tobias JW, Hensley SE, Masek KS, Cavanagh LL, Rendl M, Hunter CA, Ertl HC, von Andrian UH, Weninger W (2008) Two distinct activation states of plasmacytoid dendritic cells induced by influenza virus and CpG 1826 oligonucleotide. *J Leukoc Biol* 83:610-620.

Ishikawa J, Kaisho T, Tomizawa H, Lee BO, Kobune Y, Inazawa J, Oritani K, Itoh M, Ochi T, Ishihara K (1995) Molecular cloning and chromosomal mapping of a bone marrow stromal cell surface gene, BST2, that may be involved in pre-B-cell growth. *Genomics* 26:527-534.

Itano AA, Jenkins MK (2003) Antigen presentation to naive CD4 T cells in the lymph node. *Nat Immunol* 4:733-739.

Ito CY, Li CY, Bernstein A, Dick JE, Stanford WL (2003) Hematopoietic stem cell and progenitor defects in Sca-1/Ly-6A-null mice. *Blood* 101:517-523.

Ito M, Anan K, Misawa M, Kai S, Hara H (1996) In vitro differentiation of murine Sca-1+Lin- cells into myeloid, B cell and T cell lineages. *Stem Cells* 14:412-418.

Ito T, Amakawa R, Inaba M, Ikehara S, Inaba K, Fukuhara S (2001) Differential regulation of human blood dendritic cell subsets by IFNs. *J Immunol* 166:2961-2969.

Ito T, Amakawa R, Inaba M, Hori T, Ota M, Nakamura K, Takebayashi M, Miyaji M, Yoshimura T, Inaba K, Fukuhara S (2004) Plasmacytoid dendritic cells regulate Th cell responses through OX40 ligand and type I IFNs. *J Immunol* 172:4253-4259.

Ito T, Kanzler H, Duramad O, Cao W, Liu YJ (2006) Specialization, kinetics, and repertoire of type 1 interferon responses by human plasmacytoid predendritic cells. *Blood* 107:2423-2431.

Ito T, Yang M, Wang YH, Lande R, Gregorio J, Perng OA, Qin XF, Liu YJ, Gilliet M (2007) Plasmacytoid dendritic cells prime IL-10-producing T regulatory cells by inducible costimulator ligand. *J Exp Med* 204:105-115.

Ivanov V, Fleming TJ, Malek TR (1994) Regulation of nuclear factor-kappa B and activator protein-1 activities after stimulation of T cells via glycosylphosphatidylinositol-anchored Ly-6A/E. *J Immunol* 153:2394-2406.

Iwasaki A, Medzhitov R (2004) Toll-like receptor control of the adaptive immune responses. *Nat Immunol* 5:987-995.

Jacob J and Kelsoe G (1992) In situ studies of the primary immune response to (4-hydroxy-3-nitrophenyl)acetyl. II. A common clonal origin for periaarteriolar lymphoid sheath-associated foci and germinal centers. *J. Exp. Med.* 176:679

Jaehn PS, Zaenker KS, Schmitz J, Dzionek A (2008) Functional dichotomy of plasmacytoid dendritic cells: antigen-specific activation of T cells versus production of type I interferon. *Eur J Immunol* 38:1822-1832.

Janeway CA (1989) Approaching the asymptote? Evolution and revolution in immunology. *Cold Spring Harb Symp Quant Biol* 54 Pt 1:1-13.

Janeway CA, Travers P, Walport M, and Shlomchik MJ [eds.]. (2001) *Immunobiology: the immune system in health and disease*. 5th ed, Garland Publishing New York

Janssen EM, Lemmens EE, Wolfe T, Christen U, von Herrath MG, Schoenberger SP (2003) CD4+ T cells are required for secondary expansion and memory in CD8+ T lymphocytes. *Nature* 421:852-856.

Jego G, Palucka AK, Blanck JP, Chalouni C, Pascual V, Banchereau J (2003) Plasmacytoid dendritic cells induce plasma cell differentiation through type I interferon and interleukin 6. *Immunity* 19:225-234.

Jomantaite I, Dikopoulos N, Kröger A, Leithäuser F, Hauser H, Schirmbeck R, Reimann J (2004). Hepatic dendritic cell subsets in the mouse. *Eur J Immunol.* 34(2):355-65.

Jung S, Unutmaz D, Wong P, Sano G, De los Santos K, Sparwasser T, Wu S, Vuthoori S, Ko K, Zavala F, Pamer EG, Littman DR, Lang RA (2002) In vivo depletion of CD11c(+) dendritic cells abrogates

- priming of CD8(+) T cells by exogenous cell-associated antigens. *Immunity* 17:211-220.
- Kaczorowski DJ**, Mollen KP, Edmonds R, Billiar TR (2008) Early events in the recognition of danger signals after tissue injury. *J Leukoc Biol* 83:546-552.
- Kadowaki N**, Antonenko S, Lau JY, Liu YJ (2000) Natural interferon alpha/beta-producing cells link innate and adaptive immunity. *J Exp Med* 192:219-226.
- Kadowaki N**, Ho S, Antonenko S, Malefyt RW, Kastelein RA, Bazan F, Liu YJ (2001) Subsets of human dendritic cell precursors express different toll-like receptors and respond to different microbial antigens. *J Exp Med* 194:863-869.
- Kadowaki N**, Liu YJ (2002) Natural type I interferon-producing cells as a link between innate and adaptive immunity. *Hum Immunol* 63:1126-1132.
- Kaliński P**, Hilkens CM, Wierenga EA, Kapsenberg ML (1999) T-cell priming by type-1 and type-2 polarized dendritic cells: the concept of a third signal. *Immunol Today* 20:561-567.
- Kamath AT**, Pooley J, O'Keefe MA, Vremec D, Zhan Y, Lew AM, D'Amico A, Wu L, Tough DF, Shortman K (2000) The development, maturation, and turnover rate of mouse spleen dendritic cell populations. *J Immunol* 165:6762-6770.
- Kamogawa-Schifter Y**, Ohkawa J, Namiki S, Arai N, Arai K, Liu Y (2005) Ly49Q defines 2 pDC subsets in mice. *Blood* 105:2787-2792.
- Kang HK**, Liu M, Datta SK (2007) Low-dose peptide tolerance therapy of lupus generates plasmacytoid dendritic cells that cause expansion of autoantigen-specific regulatory T cells and contraction of inflammatory Th17 cells. *J Immunol* 178:7849-7858.
- Kapsenberg ML** (2003) Dendritic-cell control of pathogen-driven T-cell polarization. *Nat Rev Immunol* 3:984-993.
- Karsunky H**, Merad M, Mende I, Manz MG, Engleman EG, Weissman IL (2005) Developmental origin of interferon-alpha-producing dendritic cells from hematopoietic precursors. *Exp Hematol* 33:173-181.
- Kawai T**, Sato S, Ishii KJ, Coban C, Hemmi H, Yamamoto M, Terai K, Matsuda M, Inoue J, Uematsu S, Takeuchi O, Akira S (2004) Interferon-alpha induction through Toll-like receptors involves a direct interaction of IRF7 with MyD88 and TRAF6. *Nat Immunol* 5:1061-1068.
- Kearney ER**, Pape KA, Loh DY, Jenkins MK (1994) Visualization of peptide-specific T cell immunity and peripheral tolerance induction in vivo. *Immunity* 1:327
- Kirstetter P**, Thomas M, Dierich A, Kastner P, Chan S (2002) Ikaros is critical for B cell differentiation and function. *Eur J Immunol* 32:720-730.
- Koch F**, Stanzl U, Jennewein P, Janke K, Heufler C, Kämpgen E, Romani N, Schuler G (1996) High level IL-12 production by murine dendritic cells: upregulation via MHC class II and CD40 molecules and downregulation by IL-4 and IL-10. *J Exp Med* 184:741-746.
- Köhler G**, Milstein C (1975) Continuous cultures of fused cells secreting antibody of predefined specificity. *Nature* 256:495-497.
- Kovacsovics-Bankowski M**, and Rock KL (2005). A phagosome-to-cytosol pathway for exogenous antigens presented on MHC class I molecules. *Science* 307(5715):243-6.
- Kreisel FH**, Blasius A, Kreisel D, Colonna M, Cella M (2006) Interferon-producing cells develop from murine CD31(high)/Ly6C(-) marrow progenitors. *Cell Immunol* 242:91-98.
- Krieg AM** (2008) Toll-like receptor 9 (TLR9) agonists in the treatment of cancer. *Oncogene* 27:161-167.
- Krug A**, Rothenfusser S, Hornung V, Jahrsdörfer B, Blackwell S, Ballas ZK, Endres S, Krieg AM, Hartmann G (2001) Identification of CpG oligonucleotide sequences with high induction of IFN-alpha/beta in plasmacytoid dendritic cells. *Eur J Immunol* 31:2154-2163.
- Krug A**, Towarowski A, Britsch S, Rothenfusser S, Hornung V, Bals R, Giese T, Engelmann H, Endres S, Krieg AM, Hartmann G (2001) Toll-like receptor expression reveals CpG DNA as a unique microbial stimulus for plasmacytoid dendritic cells which synergizes with CD40 ligand to induce high amounts of IL-12. *Eur J Immunol* 31:3026-3037.
- Krug A**, Uppaluri R, Facchetti F, Dorner BG, Sheehan KC, Schreiber RD, Cella M, Colonna M (2002) IFN-producing cells respond to CXCR3 ligands in the presence of CXCL12 and secrete inflammatory chemokines upon activation. *J Immunol* 169:6079-6083.
- Krug A**, Veeraswamy R, Pekosz A, Kanagawa O, Unanue ER, Colonna M, Cella M (2003) Interferon-producing cells fail to induce proliferation of naive T cells but can promote expansion and T helper 1 differentiation of antigen-experienced unpolarized T cells. *J Exp Med* 197:899-906.

- Krug A**, French AR, Barchet W, Fischer JA, Dzionek A, Pingel JT, Orihuela MM, Akira S, Yokoyama WM, Colonna M (2004) TLR9-dependent recognition of MCMV by IPC and DC generates coordinated cytokine responses that activate antiviral NK cell function. *Immunity* 21:107-119.
- Krug A**, Luker GD, Barchet W, Leib DA, Akira S, Colonna M (2004) Herpes simplex virus type 1 activates murine natural interferon-producing cells through toll-like receptor 9. *Blood* 103:1433-1437.
- Kunkel D**, Kirchhoff D, Volkmer-Engert R, Radbruch A, Scheffold A (2003) Sensitive visualization of peptide presentation in vitro and ex vivo. *Cytometry A* 54:19-26.
- Kupzig S**, Korolchuk V, Rollason R, Sugden A, Wilde A, Banting G (2003) Bst-2/HM1.24 is a raft-associated apical membrane protein with an unusual topology. *Traffic* 4:694-709.
- Kuwajima S**, Sato T, Ishida K, Tada H, Tezuka H, Ohteki T (2006) Interleukin 15-dependent crosstalk between conventional and plasmacytoid dendritic cells is essential for CpG-induced immune activation. *Nat Immunol* 7:740-746.
- Kuwana M** (2002) Induction of anergic and regulatory T cells by plasmacytoid dendritic cells and other dendritic cell subsets. *Hum Immunol* 63:1156-1163.
- Laemmli UK** (1970) Cleavage of structural proteins during the assembly of the head of bacteriophage T4. *Nature* 227:680-685.
- Lande R**, Giacomini E, Serafini B, Rosicarelli B, Sebastiani GD, Minisola G, Tarantino U, Ricciari V, Valesini G, Coccia EM (2004) Characterization and recruitment of plasmacytoid dendritic cells in synovial fluid and tissue of patients with chronic inflammatory arthritis. *J Immunol* 173:2815-2824.
- Lapenta C**, Santini SM, Spada M, Donati S, Urbani F, Accapezzato D, Franceschini D, Andreotti M, Barnaba V, Belardelli F (2006) IFN-alpha-conditioned dendritic cells are highly efficient in inducing cross-priming CD8(+) T cells against exogenous viral antigens. *Eur J Immunol* 36:2046-2060.
- Le Bon A**, Etchart N, Rossmann C, Ashton M, Hou S, Gewert D, Borrow P, Tough DF (2003) Cross-priming of CD8+ T cells stimulated by virus-induced type I interferon. *Nat Immunol* 4:1009-1015.
- LeibundGut-Landmann S**, Waldburger JM, Reis e Sousa C, Acha-Orbea H, Reith W (2004) MHC class II expression is differentially regulated in plasmacytoid and conventional dendritic cells. *Nat Immunol* 5:899-908.
- Lennert K**, Remmele W (1958) [Karyometric research on lymph node cells in man. I. Germinoblasts, lymphoblasts & lymphocytes.]. *Acta Haematol* 19:99-113.
- Lennert K**, Kaiserling E, Müller-Hermelink HK (1975) Letter: T-associated plasma-cells. *Lancet* 1:1031-1032.
- Li X**, Kaloyanova D, van Eijk M, Eerland R, van der Goot G, Oorschot V, Klumperman J, Lottspeich F, Starkuviene V, Wieland FT, Helms JB (2007) Involvement of a Golgi-resident GPI-anchored protein in maintenance of the Golgi structure. *Mol Biol Cell* 18:1261-1271.
- Lin ML**, Zhan Y, Villadangos JA, Lew AM (2008) The cell biology of cross-presentation and the role of dendritic cell subsets. *Immunol Cell Biol* 86:353-362.
- Liu C**, Lou Y, Lizée G, Qin H, Liu S, Rabinovich B, Kim GJ, Wang YH, Ye Y, Sikora AG, Overwijk WW, Liu YJ, Wang G, Hwu P (2008) Plasmacytoid dendritic cells induce NK cell-dependent, tumor antigen-specific T cell cross-priming and tumor regression in mice. *J Clin Invest* 118:1165-1175.
- Liu YJ** (2001) Dendritic cell subsets and lineages, and their functions in innate and adaptive immunity. *Cell* 106:259-262.
- Liu YJ** (2005) IPC: professional type 1 interferon-producing cells and plasmacytoid dendritic cell precursors. *Annu Rev Immunol* 23:275-306.
- Ljunggren HG**, Kärre K (1990) In search of the 'missing self': MHC molecules and NK cell recognition. *Immunol Today* 11:237-244.
- Lo D**, Feng L, Li L, Carson MJ, Crowley M, Pauza M, Nguyen A, Reilly CR (1999) Integrating innate and adaptive immunity in the whole animal. *Immunol Rev* 169:225-239.
- Lou Y**, Liu C, Kim GJ, Liu YJ, Hwu P, Wang G (2007) Plasmacytoid dendritic cells synergize with myeloid dendritic cells in the induction of antigen-specific antitumor immune responses. *J Immunol* 178:1534-1541.
- Lund JM**, Alexopoulou L, Sato A, Karow M, Adams NC, Gale NW, Iwasaki A, Flavell RA (2004) Recognition of single-stranded RNA viruses by Toll-like receptor 7. *Proc Natl Acad Sci U S A* 101:5598-5603.
- Macagno A**, Gilliet M, Sallusto F, Lanzavecchia A, Nestle FO, Groettrup M (1999) Dendritic cells up-

- regulate immunoproteasomes and the proteasome regulator PA28 during maturation. *Eur J Immunol* 29:4037-4042.
- MacMicking J**, Xie QW, Nathan C (1997) Nitric oxide and macrophage function. *Annu Rev Immunol* 15:323-350.
- Mahnke K**, Guo M, Lee S, Sepulveda H, Swain SL, Nussenzweig M, Steinman RM (2000) The dendritic cell receptor for endocytosis, DEC-205, can recycle and enhance antigen presentation via major histocompatibility complex class II-positive lysosomal compartments. *J Cell Biol* 30;151(3):673-84.
- Malek TR**, Danis KM, Codias EK (1989) Tumor necrosis factor synergistically acts with IFN-gamma to regulate Ly-6A/E expression in T lymphocytes, thymocytes and bone marrow cells. *J Immunol* 142:1929-1936.
- Malek TR**, Shevach EM, Danis KM (1989) Activation of T lymphocytes through the Ly-6 pathway is defective in A strain mice. *J Immunol* 143:439-445.
- Matsuda A**, Suzuki Y, Honda G, Muramatsu S, Matsuzaki O, Nagano Y, Doi T, Shimotohno K, Harada T, Nishida E, Hayashi H, Sugano S (2003) Large-scale identification and characterization of human genes that activate NF-kappaB and MAPK signaling pathways. *Oncogene* 22:3307-3318.
- Matzinger P** (2002) The danger model: a renewed sense of self. *Science* 296:301-305.
- Medzhitov R**, Janeway CA (1998) Innate immune recognition and control of adaptive immune responses. *Semin Immunol* 10:351-353.
- Medzhitov R**, Janeway C (2000) Innate immune recognition: mechanisms and pathways. *Immunol Rev* 173:89-97.
- Medzhitov R** (2007) Recognition of microorganisms and activation of the immune response. *Nature* 449:819-826.
- Meyer-Wentrup F**, Benitez-Ribas D, Tacke PJ, Punt CJ, Figdor CG, de Vries IJ, Adema GJ (2008) Targeting DCIR on human plasmacytoid dendritic cells results in antigen presentation and inhibits IFN-alpha production. *Blood* 111:4245-4253.
- Miltenyi S**, Müller W, Weichel W, Radbruch A (1990) High gradient magnetic cell separation with MACS. *Cytometry* 11:231-238.
- Mouries J** (2006). ECI congress, #PB-2497, Paris 2006 unpublished data
- Munn DH**, Sharma MD, Hou D, Baban B, Lee JR, Antonia SJ, Messina JL, Chandler P, Koni PA, Mellor AL (2004) Expression of indoleamine 2,3-dioxygenase by plasmacytoid dendritic cells in tumor-draining lymph nodes. *J Clin Invest* 114:280-290.
- Naik SH**, Corcoran LM, Wu L (2005) Development of murine plasmacytoid dendritic cell subsets. *Immunol Cell Biol* 83:563-570.
- Naik SH**, Sathe P, Park HY, Metcalf D, Proietto AI, Dakic A, Carotta S, O'Keeffe M, Bahlo M, Papenfuss A, Kwak JY, Wu L, Shortman K (2007) Development of plasmacytoid and conventional dendritic cell subtypes from single precursor cells derived in vitro and in vivo. *Nat Immunol* 8:1217-1226.
- Nakano H**, Yanagita M, Gunn MD (2001) CD11c(+)B220(+)Gr-1(+) cells in mouse lymph nodes and spleen display characteristics of plasmacytoid dendritic cells. *J Exp Med* 194:1171-1178.
- Neil SJ**, Zang T, Bieniasz PD (2008) Tetherin inhibits retrovirus release and is antagonized by HIV-1 Vpu. *Nature* 451:425-430.
- Nestle FO**, Conrad C, Tun-Kyi A, Homey B, Gombert M, Boyman O, Burg G, Liu YJ, Gilliet M (2005) Plasmacytoid predendritic cells initiate psoriasis through interferon-alpha production. *J Exp Med* 202:135-143.
- O'Doherty U**, Peng M, Gezelter S, Swiggard WJ, Betjes M, Bhardwaj N, Steinman RM (1994) Human blood contains two subsets of dendritic cells, one immunologically mature and the other immature. *Immunology* 82:487-493.
- O'Keeffe M**, Hochrein H, Vremec D, Caminschi I, Miller JL, Anders EM, Wu L, Lahoud MH, Henri S, Scott B, Hertzog P, Tatarczuch L, Shortman K (2002) Mouse plasmacytoid cells: long-lived cells, heterogeneous in surface phenotype and function, that differentiate into CD8(+) dendritic cells only after microbial stimulus. *J Exp Med* 196:1307-1319.
- O'Keeffe M**, Hochrein H, Vremec D, Scott B, Hertzog P, Tatarczuch L, Shortman K (2003) Dendritic cell precursor populations of mouse blood: identification of the murine homologues of human blood plasmacytoid pre-DC2 and CD11c+ DC1 precursors. *Blood* 101:1453-1459.
- Ohbayashi M**, Manzouri B, Flynn T, Toda M, Ikeda Y, Nakamura T, Ono SJ (2007) Dynamic changes in

- conjunctival dendritic cell numbers, anatomical position and phenotype during experimental allergic conjunctivitis. *Exp Mol Pathol.* 83(2):216-23.
- Ochando JC**, Homma C, Yang Y, Hidalgo A, Garin A, Tacke F, Angeli V, Li Y, Boros P, Ding Y, Jessberger R, Trinchieri G, Lira SA, Randolph GJ, Bromberg JS (2006) Alloantigen-presenting plasmacytoid dendritic cells mediate tolerance to vascularized grafts. *Nat Immunol* 7:652-662.
- Ohtomo T**, Sugamata Y, Ozaki Y, Ono K, Yoshimura Y, Kawai S, Koishihara Y, Ozaki S, Kosaka M, Hirano T, Tsuchiya M (1999) Molecular cloning and characterization of a surface antigen preferentially overexpressed on multiple myeloma cells. *Biochem Biophys Res Commun* 258:583-591.
- Omatsu Y**, Iyoda T, Kimura Y, Maki A, Ishimori M, Toyama-Sorimachi N, Inaba K (2005) Development of murine plasmacytoid dendritic cells defined by increased expression of an inhibitory NK receptor, Ly49Q. *J Immunol* 174:6657-6662.
- Openshaw P**, Murphy EE, Hosken NA, Maino V, Davis K, Murphy K, O'Garra A (1995) Heterogeneity of intracellular cytokine synthesis at the single-cell level in polarized T helper 1 and T helper 2 populations. *J Exp Med* 182:1357-1367.
- Ortega G**, Korty PE, Shevach EM, Malek TR (1986) Role of Ly-6 in lymphocyte activation. I. Characterization of a monoclonal antibody to a nonpolymorphic Ly-6 specificity. *J Immunol* 137:3240-3246.
- Ozaki S**, Kosaka M, Wakahara Y, Ozaki Y, Tsuchiya M, Koishihara Y, Goto T, Matsumoto T (1999) Humanized anti-HM1.24 antibody mediates myeloma cell cytotoxicity that is enhanced by cytokine stimulation of effector cells. *Blood* 93:3922-3930.
- Palamara F**, Meindl S, Holcmann M, Lühns P, Stingl G, Sibilio M (2004) Identification and characterization of pDC-like cells in normal mouse skin and melanomas treated with imiquimod. *J Immunol* 173:3051-3061.
- Palucka AK**, Blanck JP, Bennett L, Pascual V, Banchereau J (2005) Cross-regulation of TNF and IFN-alpha in autoimmune diseases. *Proc Natl Acad Sci U S A.* 1;102(9):3372-7.
- Pestka S**, Langer JA, Zoon KC, Samuel CE (1987) Interferons and their actions. *Annu Rev Biochem* 56:727-777.
- Pestka S**, Krause CD, Walter MR (2004) Interferons, interferon-like cytokines, and their receptors. *Immunol Rev* 202:8-32.
- Picker LJ** and Butcher EC (1992) Physiological and molecular mechanisms of lymphocyte homing. *Annu. Rev. Immunol.* 10:561
- Poeck H**, Wagner M, Battiany J, Rothenfusser S, Wellisch D, Hornung V, Jahrsdorfer B, Giese T, Endres S, Hartmann G (2004) Plasmacytoid dendritic cells, antigen, and CpG-C license human B cells for plasma cell differentiation and immunoglobulin production in the absence of T-cell help. *Blood* 103:3058-3064.
- Porgador A**, Yewdell JW, Deng Y, Bennink JR, Germain RN (1997) Localization, quantitation, and in situ detection of specific peptide-MHC class I complexes using a monoclonal antibody. *Immunity* 6(6):715-26.
- Proietto AI**, O'Keeffe M, Gartlan K, Wright MD, Shortman K, Wu L, Lahoud MH (2004) Differential production of inflammatory chemokines by murine dendritic cell subsets. *Immunobiology* 209:163-172.
- Radbruch A** (ed.) (1992). *Flow Cytometry and Cell Sorting*. Ed. Radbruch, A., Springer-Verlag, Berlin
- Radbruch A**, Mechtold B, Thiel A, Miltenyi S, Pflüger E (1994) High-gradient magnetic cell sorting. *Methods Cell Biol* 42 Pt B:387-403.
- Ramirez MC**, Sigal LJ (2004) The multiple routes of MHC-I cross-presentation. *Trends Microbiol* 12:204-207.
- Reiner SL**, Sallusto F, Lanzavecchia A (2007) Division of labor with a workforce of one: challenges in specifying effector and memory T cell fate. *Science* 317:622-625.
- Reis e Sousa C** (2001) Dendritic cells as sensors of infection. *Immunity* 14:495-498.
- Reiser H**, Coligan J, Palmer E, Benacerraf B, Rock KL (1988) Cloning and expression of a cDNA for the T-cell-activating protein TAP. *Proc Natl Acad Sci U S A* 85:2255-2259.
- Ridderstad A** and Tarlinton DM (1998) Kinetics of establishing the memory B cell population as revealed by CD38 expression. *J. Immunol.* 160:4688
- Robertson JM**, Jensen PE, Evavold BD (2000) DO11.10 and OT-II T cells recognize a C-terminal ovalbumin 323-339 epitope. *J Immunol* 164:4706-4712.
- Rollason R**, Korolchuk V, Hamilton C, Schu P, Banting G (2007) Clathrin-mediated endocytosis of a lipid-raft-associated protein is mediated through a dual tyrosine motif. *J Cell Sci* 120:3850-3858.

- Romani N**, Gruner S, Brang D, Kämpgen E, Lenz A, Trockenbacher B, Konwalinka G, Fritsch PO, Steinman RM, Schuler G (1994) Proliferating dendritic cell progenitors in human blood. *J Exp Med* 180:83-93.
- Romani N**, Lenz A, Glassel H, Stössel H, Stanzl U, Majdic O, Fritsch P, Schuler G (1989) Cultured human Langerhans cells resemble lymphoid dendritic cells in phenotype and function. *J Invest Dermatol* 93:600-609.
- Romani N**, Schuler G (1989) Structural and functional relationships between epidermal Langerhans cells and dendritic cells. *Res Immunol* 140:895-8; discussion 918-26.
- Röck J**, Schneider E, Grün JR, Grützkau A, Küppers R, Schmitz J, Winkels G (2007) CD303 (BDCA-2) signals in plasmacytoid dendritic cells via a BCR-like signalosome involving Syk, Slp65 and PLCgamma2. *Eur J Immunol* 37:3564-3575.
- Rönblom L**, Alm GV (2003) Systemic lupus erythematosus and the type I interferon system. *Arthritis Res Ther* 5:68-75.
- Rutz S**, Janke M, Kassner N, Hohnstein T, Krueger M, Scheffold A (2008) Notch regulates IL-10 production by T helper 1 cells. *Proc Natl Acad Sci U S A* 105:3497-3502.
- Sambrook J**, Fritsch EF, Maniatis T (eds.) (1989). *Molecular Cloning - A Laboratory Manual* (Second Edition), Vol. 1-3. *New York, Cold Spring Harbor Laboratory Press*
- Sambrook J**, Russell DW (2001). *Molecular Cloning. A Laboratory Manual*. 3rd edition. Cold Spring Harbor Laboratory Press
- Saeed AI**, Sharov V, White J, Li J, Liang W, Bhagabati N, Braisted J, Klapa M, Currier T, Thiagarajan M, Sturn A, Snuffin M, Rezantsev A, Popov D, Ryltsov A, Kostukovich E, Borisovsky I, Liu Z, Vinsavich A, Trush V, Quackenbush J (2003) TM4: a free, open-source system for microarray data management and analysis. *Biotechniques* 34:374-378.
- Salio M**, Palmowski MJ, Atzberger A, Hermans IF, Cerundolo V (2004) CpG-matured murine plasmacytoid dendritic cells are capable of in vivo priming of functional CD8 T cell responses to endogenous but not exogenous antigens. *J Exp Med* 199:567-579.
- Samuel CE** (2001) Antiviral actions of interferons. *Clin Microbiol Rev* 14:778-809, table of contents.
- Sancho D**, Mourão-Sá D, Joffre OP, Schulz O, Rogers NC, Pennington DJ, Carlyle JR, Reis e Sousa C (2008) Tumor therapy in mice via antigen targeting to a novel, DC-restricted C-type lectin. *J Clin Invest* 118:2098-2110.
- Sapozhnikov A**, Fischer JA, Zaft T, Krauthgamer R, Dzionek A, Jung S (2007) Organ-dependent in vivo priming of naive CD4+, but not CD8+, T cells by plasmacytoid dendritic cells. *J Exp Med* 204:1923-1933.
- Schiavoni G**, Mattei F, Sestili P, Borghi P, Venditti M, Morse HC, Belardelli F, Gabriele L (2002) ICSBP is essential for the development of mouse type I interferon-producing cells and for the generation and activation of CD8alpha(+) dendritic cells. *J Exp Med* 196:1415-1425.
- Schlecht G**, Garcia S, Escriou N, Freitas AA, Leclerc C, Dadaglio G (2004) Murine plasmacytoid dendritic cells induce effector/memory CD8+ T-cell responses in vivo after viral stimulation. *Blood* 104:1808-1815.
- Schleicher U**, Liese J, Knippertz I, Kurzmann C, Hesse A, Heit A, Fischer JA, Weiss S, Kalinke U, Kunz S, Bogdan C (2007) NK cell activation in visceral leishmaniasis requires TLR9, myeloid DCs, and IL-12, but is independent of plasmacytoid DCs. *J Exp Med* 204:893-906.
- Schnorrer P**, Behrens GM, Wilson NS, Pooley JL, Smith CM, El-Sukkari D, Davey G, Kupresanin F, Li M, Maraskovsky E, Belz GT, Carbone FR, Shortman K, Heath WR, Villadangos JA (2006) The dominant role of CD8+ dendritic cells in cross-presentation is not dictated by antigen capture. *Proc Natl Acad Sci U S A* 103:10729-10734.
- Sharma MD**, Baban B, Chandler P, Hou DY, Singh N, Yagita H, Azuma M, Blazar BR, Mellor AL, Munn DH (2007) Plasmacytoid dendritic cells from mouse tumor-draining lymph nodes directly activate mature Tregs via indoleamine 2,3-dioxygenase. *J Clin Invest* 117:2570-2582.
- Shen H**, Iwasaki A (2006) A crucial role for plasmacytoid dendritic cells in antiviral protection by CpG ODN-based vaginal microbicide. *J Clin Invest* 116:2237-2243.
- Shigematsu H**, Reizis B, Iwasaki H, Mizuno S, Hu D, Traver D, Leder P, Sakaguchi N, Akashi K (2004) Plasmacytoid dendritic cells activate lymphoid-specific genetic programs irrespective of their cellular origin. *Immunity* 21:43-53.
- Shortman K** (2000) Burnet oration: dendritic cells: multiple subtypes, multiple origins, multiple functions. *Immunol Cell Biol* 78:161-165.

- Shortman K**, Liu YJ (2002) Mouse and human dendritic cell subtypes. *Nat Rev Immunol* 2:151-161.
- Shortman K**, Naik SH (2007) Steady-state and inflammatory dendritic-cell development. *Nat Rev Immunol* 7:19-30.
- Shu SA**, Lian ZX, Chuang YH, Yang GX, Moritoki Y, Comstock SS, Zhong RQ, Ansari AA, Liu YJ, Gershwin ME (2007) The role of CD11c(+) hepatic dendritic cells in the induction of innate immune responses. *Clin Exp Immunol* 149:335-343.
- Siegal FP**, Kadowaki N, Shodell M, Fitzgerald-Bocarsly PA, Shah K, Ho S, Antonenko S, Liu YJ (1999) The nature of the principal type 1 interferon-producing cells in human blood. *Science* 284:1835-1837.
- Sinclair AM**, Dzierzak EA (1993) Cloning of the complete Ly-6E.1 gene and identification of DNase I hypersensitive sites corresponding to expression in hematopoietic cells. *Blood* 82:3052-3062.
- Smit JJ**, Rudd BD, Lukacs NW (2006) Plasmacytoid dendritic cells inhibit pulmonary immunopathology and promote clearance of respiratory syncytial virus. *J Exp Med* 203:1153-1159.
- Smit JJ**, Lindell DM, Boon L, Kool M, Lambrecht BN, Lukacs NW (2008) The balance between plasmacytoid DC versus conventional DC determines pulmonary immunity to virus infections. *PLoS ONE* 3:e1720.
- Smyth MJ**, Hayakawa Y, Takeda K, Yagita H (2002) New aspects of natural-killer-cell surveillance and therapy of cancer. *Nat Rev Cancer* 2:850-861.
- Soumelis V**, Scott I, Gheyas F, Bouhour D, Cozon G, Cotte L, Huang L, Levy JA, Liu YJ (2001) Depletion of circulating natural type 1 interferon-producing cells in HIV-infected AIDS patients. *Blood* 98:906-912.
- Spörri R**, Reis e Sousa C (2005) Inflammatory mediators are insufficient for full dendritic cell activation and promote expansion of CD4+ T cell populations lacking helper function. *Nat Immunol* 6:163-170.
- Stary G**, Bangert C, Tauber M, Strohal R, Kopp T, Stingl G (2007) Tumoricidal activity of TLR7/8-activated inflammatory dendritic cells. *J Exp Med* 204:1441-1451.
- Stefanová I**, Horejsí V, Ansoategui IJ, Knapp W, Stockinger H (1991) GPI-anchored cell-surface molecules complexed to protein tyrosine kinases. *Science* 254:1016-1019.
- Steinman L** (2007) A brief history of T(H)17, the first major revision in the T(H)1/T(H)2 hypothesis of T cell-mediated tissue damage. *Nat Med* 13:139-145.
- Steinman RM**, Cohn ZA (1973) Identification of a novel cell type in peripheral lymphoid organs of mice. I. Morphology, quantitation, tissue distribution. *J Exp Med* 137:1142-1162.
- Steinman RM** (1991) The dendritic cell system and its role in immunogenicity. *Annu Rev Immunol* 9:271-296.
- Steinman RM**, Hawiger D, Liu K, Bonifaz L, Bonnyay D, Mahnke K, Iyoda T, Ravetch J, Dhodapkar M, Inaba K, Nussenzweig M (2003) Dendritic cell function in vivo during the steady state: a role in peripheral tolerance. *Ann N Y Acad Sci* 987:15-25.
- Sung SS**, Fu SM, Rose CE, Gaskin F, Ju ST, Beaty SR (2006) A major lung CD103 (alphaE)-beta7 integrin-positive epithelial dendritic cell population expressing Langerin and tight junction proteins. *J Immunol* 176:2161-2172.
- Suzuki Y**, Wakita D, Chamoto K, Narita Y, Tsuji T, Takeshima T, Gyobu H, Kawarada Y, Kondo S, Akira S, Katoh H, Ikeda H, Nishimura T (2004) Liposome-encapsulated CpG oligodeoxynucleotides as a potent adjuvant for inducing type 1 innate immunity. *Cancer Res* 64:8754-8760.
- Swiecki MK**, Colonna M (2007) Running to stand still: BCR-like signaling suppresses type I IFN responses in pDC. *Eur J Immunol* 37:3327-3329.
- Taieb J**, Chaput N, Ménard C, Apetoh L, Ullrich E, Bonmort M, Péquignot M, Casares N, Terme M, Flament C, Opolon P, Lecluse Y, Métivier D, Tomasello E, Vivier E, Ghiringhelli F, Martin F, Klatzmann D, Poynard T, Tursz T, Raposo G, Yagita H, Ryffel B, Kroemer G, Zitvogel L (2006) A novel dendritic cell subset involved in tumor immunosurveillance. *Nat Med* 12:214-219.
- Takeda K**, Kaisho T, Akira S (2003) Toll-like receptors. *Annu Rev Immunol* 21:335-376.
- Tao MH**, Smith RI, Morrison SL (1993) Structural features of human immunoglobulin G that determine isotype-specific differences in complement activation. *J Exp Med* 1;178(2):661-7.
- Tarlinton D** (1998) Germinal centers: form and function. *Curr Opin Immunol* 10:245
- Toma-Hirano M**, Namiki S, Miyatake S, Arai K, Kamogawa-Schifter Y (2007) Type I interferon regulates pDC maturation and Ly49Q expression. *Eur J Immunol* 37:2707-2714.
- Tong JC**, Tan TW, Ranganathan S (2004) Modeling the structure of bound peptide ligands to major

histocompatibility complex. *Protein Sci* 13:2523-2532.

Toyama-Sorimachi N, Omatsu Y, Onoda A, Tsujimura Y, Iyoda T, Kikuchi-Maki A, Sorimachi H, Dohi T, Taki S, Inaba K, Karasuyama H (2005) Inhibitory NK receptor Ly49Q is expressed on subsets of dendritic cells in a cellular maturation- and cytokine stimulation-dependent manner. *J Immunol* 174:4621-4629.

Toyama-Sorimachi N, Tsujimura Y, Maruya M, Onoda A, Kubota T, Koyasu S, Inaba K, Karasuyama H (2004) Ly49Q, a member of the Ly49 family that is selectively expressed on myeloid lineage cells and involved in regulation of cytoskeletal architecture. *Proc Natl Acad Sci U S A* 101:1016-1021.

Treilleux I, Blay JY, Bendriss-Vermare N, Ray-Coquard I, Bachelot T, Guastalla JP, Bremond A, Goddard S, Pin JJ, Barthelemy-Dubois C, Lebecque S (2004) Dendritic cell infiltration and prognosis of early stage breast cancer. *Clin Cancer Res* 10:7466-7474.

Trinchieri G, Santoli D (1978) Anti-viral activity induced by culturing lymphocytes with tumor-derived or virus-transformed cells. Enhancement of human natural killer cell activity by interferon and antagonistic inhibition of susceptibility of target cells to lysis. *J Exp Med* 147:1314-1333.

Trinchieri G, Santoli D, Dee RR, Knowles BB (1978) Anti-viral activity induced by culturing lymphocytes with tumor-derived or virus-transformed cells. Identification of the anti-viral activity as interferon and characterization of the human effector lymphocyte subpopulation. *J Exp Med* 147:1299-1313.

Trombetta ES, Mellman I (2005) Cell biology of antigen processing in vitro and in vivo. *Annu Rev Immunol* 23:975-1028.

Ulsenheimer A, Gerlach JT, Jung MC, Gruener N, Wächtler M, Backmund M, Santantonio T, Schraut W, Heeg MH, Schirren CA, Zachoval R, Pape GR, Diepolder HM (2005) Plasmacytoid dendritic cells in acute and chronic hepatitis C virus infection. *Hepatology* 41:643-651.

Vallin H, Perers A, Alm GV, Rönnblom L (1999) Anti-double-stranded DNA antibodies and immunostimulatory plasmid DNA in combination mimic the endogenous IFN-alpha inducer in systemic lupus erythematosus. *J Immunol* 163:6306-6313.

Van Damme N, Goff D, Katsura C, Jorgenson RL, Mitchell R, Johnson MC, Stephens EB, Guatelli J (2008) The interferon-induced protein BST-2 restricts HIV-1 release and is downregulated from the cell surface by the viral Vpu protein. *Cell Host Microbe* 3:245-252.

Van den Eynde BJ, Morel S (2001) Differential processing of class-I-restricted epitopes by the standard proteasome and the immunoproteasome. *Curr Opin Immunol* 13:147-153.

Van Gelder RN, von Zastrow ME, Yool A, Dement WC, Barchas JD, Eberwine JH (1990) Amplified RNA synthesized from limited quantities of heterogeneous cDNA. *Proc Natl Acad Sci U S A* 87:1663-1667.

van Kooyk Y, Geijtenbeek TB (2003) DC-SIGN: escape mechanism for pathogens. *Nat Rev Immunol* 3:697-709.

van Vliet C, Thomas EC, Merino-Trigo A, Teasdale RD, Gleeson PA (2003) Intracellular sorting and transport of proteins. *Prog Biophys Mol Biol* 83:1-45.

Vermi W, Bonocchi R, Facchetti F, Bianchi D, Sozzani S, Festa S, Berenzi A, Cella M, Colonna M (2003) Recruitment of immature plasmacytoid dendritic cells (plasmacytoid monocytes) and myeloid dendritic cells in primary cutaneous melanomas. *J Pathol* 200:255-268.

Veugelers K, Motyka B, Goping IS, Shostak I, Sawchuk T, Bleackley RC (2006) Granule-mediated killing by granzyme B and perforin requires a mannose 6-phosphate receptor and is augmented by cell surface heparan sulfate. *Mol Biol Cell* 17:623-633.

Vidal-Laliena M, Romero X, March S, Requena V, Petriz J, Engel P (2005) Characterization of antibodies submitted to the B cell section of the 8th Human Leukocyte Differentiation Antigens Workshop by flow cytometry and immunohistochemistry. *Cell Immunol* 236(1-2):6-16.

Vosshenrich CA, Lesjean-Pottier S, Hasan M, Richard-Le Goff O, Corcuff E, Mandelboim O, Di Santo JP (2007) CD11c^{lo}B220⁺ interferon-producing killer dendritic cells are activated natural killer cells. *J Exp Med* 204:2569-2578.

Wallace RB, Shaffer J, Murphy RF, Bonner J, Hirose T, Itakura K (1979) Hybridization of synthetic oligodeoxyribonucleotides to phi chi 174 DNA: the effect of single base pair mismatch. *Nucleic Acids Res* 6:3543-3557.

Wang B, Maile R, Greenwood R, Collins EJ, Frelinger JA (2000) Naive CD8⁺ T cells do not require costimulation for proliferation and differentiation into cytotoxic effector cells. *J Immunol* 164:1216-1222.

Wang B, Pelletier J, Massaad MJ, Herscovics A, Shore GC (2004) The yeast split-ubiquitin membrane protein two-hybrid screen identifies BAP31 as a regulator of the turnover of endoplasmic reticulum-associated protein tyrosine phosphatase-like B. *Mol Cell Biol* 24:2767-2778.

- Wang J**, Zhang Y, Wei J, Zhang X, Zhang B, Zhu Z, Zou W, Wang Y, Mou Z, Ni B, Wu Y (2007) Lewis X oligosaccharides targeting to DC-SIGN enhanced antigen-specific immune response. *Immunology* 121:174-182.
- Wang RF** (2001) The role of MHC class II-restricted tumor antigens and CD4+ T cells in antitumor immunity. *Trends Immunol* 22:269-276.
- Watarai H**, Sekine E, Inoue S, Nakagawa R, Kaisho T, Taniguchi M (2008) PDC-TREM, a plasmacytoid dendritic cell-specific receptor, is responsible for augmented production of type I interferon. *Proc Natl Acad Sci U S A* 105:2993-2998.
- Watson SR** and Bradley LM (1998) The recirculation of naive and memory lymphocytes. *Cell. Adhes. Commun.* 6:105
- Weigert M**, Perry R, Kelley D, Hunkapiller T, Schilling J, Hood L (1980) The joining of V and J gene segments creates antibody diversity. *Nature* 283:497-499.
- Wendland M**, Czeloth N, Mach N, Malissen B, Kremmer E, Pabst O, Förster R (2007) CCR9 is a homing receptor for plasmacytoid dendritic cells to the small intestine. *Proc Natl Acad Sci U S A* 104(15):6347-52.
- Weslow-Schmidt JL**, Jewell NA, Mertz SE, Simas JP, Durbin JE, Flaño E. (2007). Type I interferon inhibition and dendritic cell activation during gammaherpesvirus respiratory infection. *J Virol.* 81(18):9778-89.
- Wu L**, D'Amico A, Hochrein H, O'Keeffe M, Shortman K, Lucas K (2001) Development of thymic and splenic dendritic cell populations from different hemopoietic precursors. *Blood* 98:3376-3382.
- Xu Y**, Oomen R, Klein MH (1994) Residue at position 331 in the IgG1 and IgG4 CH2 domains contributes to their differential ability to bind and activate complement. *J Biol Chem.* 4;269(5):3469-74.
- Yang GX**, Lian ZX, Kikuchi K, Liu YJ, Ansari AA, Ikehara S, Gershwin ME (2005) CD4- plasmacytoid dendritic cells (pDCs) migrate in lymph nodes by CpG inoculation and represent a potent functional subset of pDCs. *J Immunol* 174:3197-3203.
- Yang L**, Kobie JJ, Mosmann TR (2005) CD73 and Ly-6A/E distinguish in vivo primed but uncommitted mouse CD4 T cells from type 1 or type 2 effector cells. *J Immunol* 175:6458-6464.
- Yin AH**, Miraglia S, Zanjani ED, Almeida-Porada G, Ogawa M, Leary AG, Olweus J, Kearney J, Buck DW (1997) AC133, a novel marker for human hematopoietic stem and progenitor cells. *Blood* 90:5002-5012.
- Yoneyama H**, Matsuno K, Toda E, Nishiwaki T, Matsuo N, Nakano A, Narumi S, Lu B, Gerard C, Ishikawa S, Matsushima K (2005) Plasmacytoid DCs help lymph node DCs to induce anti-HSV CTLs. *J Exp Med* 202:425-435.
- Yoneyama H**, Matsuno K, Zhang Y, Nishiwaki T, Kitabatake M, Ueha S, Narumi S, Morikawa S, Ezaki T, Lu B, Gerard C, Ishikawa S, Matsushima K (2004) Evidence for recruitment of plasmacytoid dendritic cell precursors to inflamed lymph nodes through high endothelial venules. *Int Immunol* 16:915-928.
- York IA**, Rock KL (1996) Antigen processing and presentation by the class I major histocompatibility complex. *Annu Rev Immunol* 14:369-396.
- Yutoku M**, Grossberg AL, Pressman D (1974) Preparation and properties of rabbit anti-mouse plasmacyte serum purified by in vivo absorption: further evidence for a new antigenic determinant on plasmacytes. *J Immunol* 112:911-918.
- Zhang J**, Raper A, Sugita N, Hingorani R, Salio M, Palmowski MJ, Cerundolo V, Crocker PR (2006) Characterization of Siglec-H as a novel endocytic receptor expressed on murine plasmacytoid dendritic cell precursors. *Blood* 107:3600-3608.
- Zhang XQ**, Dahle CE, Weiner GJ, Salem AK (2007) A comparative study of the antigen-specific immune response induced by co-delivery of CpG ODN and antigen using fusion molecules or biodegradable microparticles. *J Pharm Sci* 96:3283-3292.
- Zheng B**, Xue W, Kelsoe G (1994) Locus-specific somatic hypermutation in germinal centre T cells. *Nature* 372:556-559.
- Zou W**, Machelon V, Coulomb-L'Hermin A, Borvak J, Nome F, Isaeva T, Wei S, Krzysiek R, Durand-Gasselin I, Gordon A, Pustilnik T, Curiel DT, Galanaud P, Capron F, Emilie D, Curiel TJ (2001) Stromal-derived factor-1 in human tumors recruits and alters the function of plasmacytoid precursor dendritic cells. *Nat Med* 7:1339-1346.
- Zucchini N**, Bessou G, Robbins SH, Chasson L, Raper A, Crocker PR, Dalod M (2008) Individual plasmacytoid dendritic cells are major contributors to the production of multiple innate cytokines in an organ-specific manner during viral infection. *Int Immunol* 20:45-56.

Zuniga EI, McGavern DB, Pruneda-Paz JL, Teng C, Oldstone MB (2004) Bone marrow plasmacytoid dendritic cells can differentiate into myeloid dendritic cells upon virus infection. *Nat Immunol* 5:1227-1234.

9. PUBLICATIONS, POSTERS, AND ABSTRACTS**9.1 Publications in peer-reviewed journals:****Immunity. 2004 Jul;21(1):107-19.****TLR9-dependent recognition of MCMV by IPC and DC generates coordinated cytokine responses that activate antiviral NK cell function.**Krug A¹, French AR², Barchet W¹, Fischer JA⁵, Dzionek A⁵, Pingel JT³, Orihuela MM³, Akira S⁴, Yokoyama WM³, Colonna M¹.¹Department of Pathology and Immunology, Washington University School of Medicine, St. Louis, MO 63110 USA, ²Department of Pediatrics, Washington University School of Medicine, St. Louis, MO 63110 USA, ³Department of Medicine and Howard Hughes Medical Institute, Washington University School of Medicine, St. Louis, USA, ⁴Department of Host Defense, Research Institute for Microbial Diseases, Osaka University, Osaka, Japan, ⁵Miltenyi Biotec, Bergisch Gladbach, Germany

Natural interferon-producing cells (IPC) respond to viruses by secreting type I interferon (IFN) and interleukin-12 (IL-12). Toll-like receptor (TLR) 9 mediates IPC recognition of some of these viruses in vitro. However, whether TLR9-induced activation of IPC is necessary for an effective antiviral response in vivo is not clear. Here, we demonstrate that IPC and dendritic cells (DC) recognize murine cytomegalovirus (MCMV) through TLR9. TLR9-mediated cytokine secretion promotes viral clearance by NK cells that express the MCMV-specific receptor Ly49H. Although depletion of IPC leads to a drastic reduction of the IFN-alpha response, this allows other cell types to secrete IL-12, ensuring normal IFN-gamma and NK cell responses to MCMV. We conclude that the TLR9/MyD88 pathway mediates antiviral cytokine responses by IPC, DC, and possibly other cell types, which are coordinated to promote effective NK cell function and MCMV clearance.

Eur J Immunol. 2005 Jan;35(1):236-42.**Dendritic cells respond to influenza virus through TLR7- and PKR-independent pathways.**Barchet W¹, Krug A¹, Cella M¹, Newby C, Fischer JA³, Dzionek A³, Pekosz A^{1,2}, Colonna M¹.¹Department of Pathology and Immunology, Washington University School of Medicine, St. Louis, Missouri, USA, ²Department of Microbiology, Washington University School of Medicine, St. Louis, Missouri, USA, ³Miltenyi Biotec, Bergisch Gladbach, Germany

Natural interferon-producing cells (IPC) secrete type I IFN (IFN-alpha and -beta) in response to influenza virus. This process is independent of viral replication and is mediated by Toll-like receptor 7 (TLR7), which recognizes single-stranded RNA (ssRNA). DC also express TLR7 but its function in DC response to influenza virus is unknown. To address this, we compared the DC and IPC responses to influenza virus and ssRNA oligoribonucleotides (ORN) that activate TLR7. When stimulated by ORN in vitro and in vivo, DC matured and produced inflammatory cytokines but not IFN-alpha. DC did secrete IFN-alpha in response to influenza virus. However, this response was independent of TLR7 signaling and required viral replication but not dsRNA-activated protein kinase (PKR). We conclude that DC and IPC are hard-wired to secrete IFN-alpha via different pathways, reflecting their complementary but distinct roles in anti-viral immunity.

J Exp Med. 2007 Apr 16;204(4):893-906.**NK cell activation in visceral leishmaniasis requires TLR9, myeloid DCs, and IL-12, but is independent of plasmacytoid DCs.**Ulrike Schleicher^{1,2}, Jan Liese¹, Ilka Knippertz², Claudia Kurzmann¹, Andrea Hesse^{1,2}, Antje Heit³, Jens A. A. Fischer⁴, Siegfried Weiss⁵, Ulrich Kalinke⁶, Stefanie Kunz¹, and Christian Bogdan^{1,2}¹Institute of Medical Microbiology and Hygiene, University of Freiburg, D-79104 Freiburg, Germany, ²Institute of Clinical Microbiology, Immunology and Hygiene, University of Erlangen, 91054 Erlangen, Germany, ³Institute of Medical Microbiology, Immunology and Hygiene, Technical University of Munich, 81675 München, Germany, ⁴Department of Research and Development, Miltenyi Biotec GmbH, 51429 Bergisch-Gladbach, Germany, ⁵Department of Molecular Immunology, Helmholtz Zentrum für Infektionsforschung, D-38124 Braunschweig, Germany, ⁶Department of Immunology, Paul Ehrlich Institute, 63225 Langen, Germany

Natural killer (NK) cells are sentinel components of the innate response to pathogens, but the cell types, pathogen recognition receptors, and cytokines required for their activation in vivo are poorly defined. Here, we investigated the role of plasmacytoid dendritic cells (pDCs), myeloid DCs (mDCs), Toll-like receptors (TLRs), and of NK cell stimulatory cytokines for the induction of an NK cell response to the protozoan parasite *Leishmania infantum*. In vitro, pDCs did not endocytose *Leishmania* promastigotes but nevertheless released interferon (IFN)-alpha/beta and interleukin (IL)-12 in a TLR9-dependent manner. mDCs rapidly internalized *Leishmania* and, in the presence of TLR9, produced IL-12, but not IFN-alpha/beta. Depletion of pDCs did not impair the activation of NK cells in *L. infantum*-infected mice. In contrast, *L. infantum*-induced NK cell cytotoxicity and IFN-gamma production were abolished in

mDC-depleted mice. The same phenotype was observed in TLR9(-/-) mice, which lacked IL-12 expression by mDCs, and in IL-12(-/-) mice, whereas IFN-alpha/beta receptor(-/-) mice showed only a minor reduction of NK cell IFN-gamma expression. This study provides the first direct evidence that mDCs are essential for eliciting NK cell cytotoxicity and IFN-gamma release in vivo and demonstrates that TLR9, mDCs, and IL-12 are functionally linked to the activation of NK cells in visceral leishmaniasis.

J Exp Med. 2007 Aug 6;204(8):1923-33.

Organ-dependent in vivo priming of naive CD4+, but not CD8+, T cells by plasmacytoid dendritic cells.

Anita Sapozhnikov¹, Jens A. A. Fischer², Tami Zaft¹, Rita Krauthgamer¹, Andrzej Dzionek², and Steffen Jung¹

¹Department of Immunology, The Weizmann Institute of Science, 76100 Rehovot, Israel, ²Miltenyi Biotec GmbH, 51429 Bergisch Gladbach, Germany

Plasmacytoid dendritic cells (PDCs) play a pivotal role as cytokine-secreting accessory cells in the antimicrobial immune defense. In contrast, the capacity of PDCs to act as antigen-presenting cells in naive T cell priming remains unclear. By studying T cell responses in mice that lack conventional DCs (cDCs), and by the use of a PDC-specific antigen-targeting strategy, we show that PDCs can initiate productive naive CD4(+) T cell responses in lymph nodes, but not in the spleen. PDC-triggered CD4(+) T cell responses differed from cDC-driven responses in that they were not associated with concomitant CD8(+) T cell priming. Our results establish PDCs as a bona fide DC subset that initiates unique CD4(+) Th cell-dominated primary immune responses.

Cutting Edge: The Journal of Immunology. May 2008; 180: 6457 - 6461

CNS Plasmacytoid Dendritic Cells Regulate the Severity of Relapsing Experimental Autoimmune Encephalomyelitis

Samantha L. Bailey-Bucktrout¹, Sarah C. Caulkins¹, Gwendolyn Goings¹, Jens A. A. Fischer², Andrzej Dzionek², and Stephen D. Miller¹

¹Department of Microbiology-Immunology and the Interdepartmental Immunobiology Center, Feinberg School of Medicine, Northwestern University, Chicago, IL 60611 USA,

²Miltenyi Biotec GmbH, 51429 Bergisch Gladbach, Germany.

Plasmacytoid dendritic cells (pDC) have both stimulatory and regulatory effects on T cells. pDCs are a major CNS-infiltrating DC population during experimental autoimmune encephalomyelitis (EAE), but unlike myeloid DCs (mDC) have a minor role in T cell activation and epitope spreading. We show that depletion of pDCs during either the acute or relapse phases of EAE resulted in exacerbation of disease severity. pDC depletion significantly enhanced CNS but not peripheral CD4⁺ T cell activation, as well as IL-17 and IFN- γ production. Moreover, CNS pDCs suppressed CNS mDC-driven production of IL-17, IFN- γ and IL-10 in an IDO-independent manner. The data demonstrate that pDCs play a critical regulatory role in negatively regulating pathogenic CNS CD4⁺ T cell responses highlighting a new role for pDCs in inflammatory autoimmune disease.

9.2 Publications in submission/preparation:

Manuscript in submission:

Heterogeneous Sca-1 expression on murine plasmacytoid dendritic cells defines developmental and functional differences

Jens A. A. Fischer, Jürgen Schmitz, and Andrzej Dzionek

Manuscript in preparation:

Identification and functional characterization of mPDCA-1 as a novel antigen-uptake receptor for murine PDCs enabling (cross-) priming of naïve CD4+ and CD8+ T cells.

Jens A. A. Fischer, Jürgen Schmitz, and Andrzej Dzionek

9.3 Posters & Abstracts:**Joint Annual Meeting of Immunology of the Austrian and German Societies, September 3-6, 2008, Vienna, Austria****Cross-priming capacity of activated and mPDCA-1-targeted Plasmacytoid Dendritic cells (#2008-A-488-OEGAI)**

Jens A. A. Fischer^{1 2}, Sonja Schmucker^{1 3}, Stefan A. Kaden¹, Tobias Voelkel¹, Jürgen Schmitz¹, and Andrzej Dzionek¹

¹Miltenyi Biotec, Bergisch Gladbach, Germany; ²University of Cologne, Cologne, Germany; ³Presenting author

Plasmacytoid Dendritic cells (PDCs) are a distinct subset of dendritic cells and have a central role as sentinels for pathogens. PDCs produce large amounts of interferons upon microbial stimulation and are believed to link innate and adaptive immune responses. However, their exact function as antigen-presenting cells for the initiation of adaptive immune responses is controversially discussed and it remains unclear whether PDC are in fact able to prime naïve T cells. In this study we investigated the function of the recently described PDC-specific receptor mPDCA-1. Cross-linking of mPDCA-1 resulted in a rapid internalization. Targeting of PDCs with OVA-conjugated anti-mPDCA-1 mAb, but not with an equivalent amount of soluble OVA or OVA conjugated to isotype control antibody, resulted in strong proliferation of OVA-specific naïve CD4⁺ T cells. PDCs were also able to cross-present mPDCA-1-targeted OVA protein to naïve CD8⁺ T cells. Blocking the receptor with excess of unconjugated anti-mPDCA-1 mAb inhibited priming of CD4⁺ and CD8⁺ T cells. These results indicate that mPDCA-1 may serve as an antigen uptake receptor for efficient priming of CD4⁺ and CD8⁺ T cells. Interestingly, processing and presentation of antigens taken up via mPDCA-1 was strongly dependent on stimulation, since only activated but not immature PDC were able to prime naïve antigen-specific T cells. In contrast, antigen uptake was independent on activation as unstimulated PDC also internalized the mAb-receptor-complex. Our results demonstrate that PDCs take up and process antigens, delivering its ligands for MHC-I and MHC-II presentation and thus combine innate and adaptive functions.

**2eme Journee Scientifique Miltenyi Biotec - Cancer Immunotherapy, July 2008 in Paris, France
Biological functions of plasmacytoid dendritic cells: Antigen-specific activation of T cells versus production of type I interferon.**

Peter S. Jähn, Jens A. A. Fischer, Andrzej Dzionek and Jürgen Schmitz

Miltenyi Biotec GmbH, Bergisch Gladbach, Germany

Plasmacytoid dendritic cells (PDC) also referred to as type I interferon producing cells (IPC) are believed to act as a link between innate and adaptive immunity by producing type I interferon, and subsequently triggering adaptive T cell mediated immunity by differentiating into mature DC. However, it remains controversial to which degree PDC play a direct role as APC in the activation of naïve and memory CD4⁺ and CD8⁺ T cells and to which degree APC functions and production of type I interferon are directly linked.

To analyze whether human and mouse PDC can act as APC, we decided to adopt a strategy involving antibody mediated targeting of antigen to PDC-specific receptors: BDCA-2 (CD303) for human PDC and mPDCA-1 (BST-2, CD317) for murine PDC. Independent on Toll-like receptor (TLR) ligand stimulation antigen is rapidly endocytosed by these receptors and traffics via early sorting endosomes to emerging MHC-enriched compartments (MIIC). In vitro restimulation of human CMV-specific CD4⁺ effector memory T cells and in vitro priming of murine naïve ovalbumin (OVA)-specific T-cell receptor transgenic CD4⁺ and CD8⁺ T cells, however, are dependent on appropriate TLR ligand stimulation of PDC.

Most interestingly, at least in human PDC processing and presentation of CMV antigen and production of type I interferon are mutually exclusively induced by distinct CpG oligonucleotides. Type B CpG oligonucleotide (CpG-B)-stimulated PDC efficiently process and present CMV antigen and are thus capable of stimulating CMV-specific CD4⁺ effector memory T cells. CpG-A stimulated PDC produce large amounts of type I interferon and express programmed death-1 ligand 1 (PD-1L), a molecule which is known to inhibit T cell activation via PD-1 ligation. CpG-A plus CpG-B co-stimulated PDC behave like CpG-B stimulated PDC, indicating that CpG-B induction of antigen processing and presentation in PDC concurrently inhibits type I interferon production.

Our results suggest that innate and adaptive immunity are not linked at the level of individual PDC which first produce type I interferon and then differentiate in mature DC, but rather at the population level, where depending on the stimulation received, individual PDC either contribute to the innate response by production of IFN-alpha or to the

adaptive response by antigen presentation and stimulation of T cells.

Experimental Biology 2008 in combination with AAI 2008, San Diego, USA (The FASEB Journal. 2008;22:1068.23)

Plasmacytoid Dendritic cells prime naïve CD4+ and CD8+ T cells after antigen uptake via mPDCA-1

Jens A. A. Fischer^{1,2}, Monika Janz¹, Tobias Voelkel¹, Jürgen Schmitz¹, and Andrzej Dzionek¹

¹R&D, Miltenyi Biotec GmbH, Bergisch Gladbach, Germany; ²University of Cologne, Germany

Plasmacytoid Dendritic cells (PDC) produce large amounts of IFN upon microbial stimulation and are believed to link innate and adaptive immune responses. However, it remains controversial whether PDC are in fact able to prime naïve T cells. Here we investigated the function of the recently described PDC-specific receptor mPDCA-1. Ligation of mPDCA-1 with specific mAb resulted in a rapid internalization of the complex. Targeting of PDC with OVA-conjugated anti-mPDCA-1 mAb, but not with an equivalent amount of soluble OVA or OVA conjugated to isotype control antibody, resulted in strong proliferation of OVA-specific naïve CD4+ T cells. The same was also observed for OVA-specific naïve CD8+ T cells. Blocking the receptor with excess of unconjugated anti-mPDCA-1 mAb inhibited priming of CD4+ and CD8+ T cells. These results indicate that mPDCA-1 may serve as an antigen uptake receptor delivering its ligands for MHC-I and MHC-II presentation. Interestingly, processing and presentation of antigens taken up via mPDCA-1 was strongly dependent on stimulation, since only activated but not immature PDC were able to prime naïve antigen-specific T cells. In contrast, antigen uptake was independent on activation as unstimulated PDC also internalized the mAb-receptor complex. Our results demonstrate that PDC take up and process antigen for efficient priming of CD4+ and CD8+ T cells and thus combine innate and adaptive function.

DC2007 (Dendritic Cell Vaccination and other Strategies to tip the Balance of the Immune System), 2007 in Bamberg, Germany

Highly efficient antigen targeting to murine plasmacytoid dendritic cells (PDC) using mPDCA-1-specific antibody conjugates: PDC activation dependent priming of naïve CD4+ T cells

Jens A. A. Fischer, Jürgen Schmitz, and Andrzej Dzionek

Miltenyi Biotec, Bergisch Gladbach, Germany

PDC represent a distinct subset of dendritic cells characterised by their plasmacytoid morphology and the ability to produce large amounts of IFN-alpha in response to viruses and microbial compounds. It is still controversial to which degree PDC are capable of taking up exogenous antigens and play a role in priming of naïve T cells.

Here we investigated the function of the recently described PDC marker mPDCA-1 as an antigen-uptake receptor. Using a monoclonal antibody (mAb) against mPDCA-1 we were able to specifically target PDC both in vivo and in vitro. Ligation of mPDCA-1 leads to a rapid internalisation of the antibody-receptor complex, indicating that mPDCA-1 might serve as a PDC-specific antigen-uptake receptor. Furthermore, targeting PDC with OVA-conjugated anti-mPDCA-1 mAb, but not with an equivalent amount of soluble OVA, or OVA conjugated to an isotype control mAb resulted in efficient proliferation of naïve OVA-specific CD4+ T cell receptor transgenic T cells in vitro. However, this was clearly dependent on CpG oligonucleotide activation of PDC, since non-activated PDC were not able to prime OVA-specific T cells. Our results indicate that efficient processing and presentation of antigen by PDC for stimulation of naïve CD4+ T cells requires appropriate PDC stimulation. Currently we investigate, whether PDC may further contribute to adaptive immunity by cross-presenting antigens taken up via mPDCA-1 to naïve CD8+ T cell receptor transgenic T cells.

International Symposium of Dendritic Cells, 2006 in Edinburgh, UK

Murine Plasmacytoid Dendritic Cells: Heterogeneous Expression Of Sca-1 Characterises Functional Differences

Fischer, J A A; Janz, M; Schmitz, J; Dzionek, A

Miltenyi Biotec GmbH, Bergisch Gladbach, Germany

Murine plasmacytoid dendritic cells (PDC) represent a distinct leukocyte population capable of secreting large amounts of type I interferon in response to microbial stimuli. In lymphoid organs all PDC show a homogenous expression profile for following markers: B220⁺, Ly-6C⁺, CD11c^{int}, mPDCA-1⁺, CD3⁻, CD4^{+/-}, CD8a⁻, CD11b⁻, CD19⁻,

CD49b⁻, CD123⁻, CD40⁻, CD80^{low}, and CD86⁻, and MHC-II⁺. Here we demonstrate differential expression levels of the stem cell antigen 1 (Sca-1) on PDC from different organs. In bone marrow (BM) and blood only 15-20% of PDC express Sca-1. In contrast, about 35% of liver PDC and about 50% of splenic PDC are positive for Sca-1. In lymph nodes (LN) up to 80% of PDC are positive for Sca-1. Phenotyping study of both, Sca-1⁺ and Sca-1⁻ PDC in BALB/c mice revealed no significant differences between the subsets in expression level of any surface marker tested. The expression of Sca-1 on Sca-1⁻ PDC from BM and spleen was up-regulated after the culture and could be further increased, when stimulated with CpG. Interestingly, when stimulated with the TLR7 ligand Loxoribine the activation-dependent up-regulation of Sca-1 was decelerated. Furthermore, CpG induced IFN α production correlated inversely with the expression level of Sca-1 as we could show by intracellular staining. Analysing the total amount of IFN α in culture supernatants, Sca-1⁻ PDC produced strongly elevated IFN α levels compared to Sca-1 positive PDC. These results correlate with further data showing higher IFN α production of BM-PDC (mainly Sca-1⁻) compared to LN-PDC (predominantly Sca-1⁺). Additionally, bromodeoxyuridine labeling *in vivo* demonstrate that the Sca-1⁻ population appeared earlier in the development of PDC. On the basis of the shown association of Sca-1 expression with the development stage and Interferon production capacity, we are currently investigating further functional aspects of the differential Sca-1 expression on PDC.

ECI, 2006 in Paris, France

Murine Plasmacytoid Dendritic Cells: Differential expression of Sca-1 (Ly-6A/E) in spleen defines two subsets

Fischer J. A. A., Janz, M., Schmitz J. and Dzionek A.

Miltenyi Biotec GmbH, Bergisch Gladbach, Germany

Murine Plasmacytoid dendritic cells (PDC) represent a distinct leukocyte population capable of secreting large amounts of type I interferon in response to viruses and bacteria and are defined by a unique phenotype: B220⁺, Ly-6C⁺, CD11c^{int}. In lymphoid organs the mPDCA-1 antigen is specifically expressed on cells which are CD11c^{int}, B220, Ly-6C⁺, CD3⁻, CD4⁺, CD8a^{dim}, CD11b⁻, CD19⁻, CD49b⁻, CD90⁻, CD123⁻, CD40⁻, CD80^{low}, and CD86⁻, and therefore phenotypically identical to PDC.

Here we demonstrate differential expression levels of the stem cell antigen 1 (Sca-1 [Ly-6A/E]) on PDC from different organs. In bone marrow (BM) and peripheral blood the Sca-1 expression on PDC is very low: only 15-20% express the marker. In contrast, about 35% liver PDC and 45-55% of splenic PDC are positive for Sca-1. In lymph nodes (LN) the majority (up to 80%) of PDC are positive for Sca-1. Analysing splenic PDC of several mouse strains, the Sca-1 expression is not uniform: C57BL/6, Sv129, and CD1 mice show predominantly Sca-1⁺ PDC, whereas BALB/c and FVB mice show heterogeneous Sca-1 expression, and the majority of DBA/1 PDC are Sca-1⁻. Phenotyping both PDC subsets of BALB/c mice, we observe no difference for all cell surface markers tested. After culture of Sca-1⁺ and Sca-1⁻ PDC, we detect an upregulation of Sca-1 on primary Sca-1⁻ mPDC. After CpG-stimulation PDC become Sca-1⁺. *In vivo* activation with CpG ODN also enhances Sca-1 expression on PDC both in BM and spleen, whereas ligation of mPDCA-1 has no effect on Sca-1 or co-stimulatory/-inhibitory molecule expression. To show IFN α production depending on the Sca-1 change, we performed intracellular IFN α stainings by FACS analysis as well as IFN α ELISA. Our results show that the percentage of IFN α producers is much higher in *ex vivo* Sca-1⁻ PDC compared to Sca-1⁺ PDC. Analysing the total amount of IFN α , Sca-1⁻ PDC also produce strongly elevated IFN α levels. These results support previous data when we compared the IFN α production of PDC from both LN and BM. Hypothesising that the upregulation of Sca-1 correlates with the maturation or activation status of PDC, we are currently investigating the biological function of the differential Sca-1 expression on both PDC subpopulations.

AAI, 2006 in Boston, USA**Differential Expression Of Sca-1 Defines Two Subsets Of Murine Plasmacytoid Dendritic Cells in Spleen**

Fischer J. A. A., Janz, M., Schmitz J. and Dzionek A.

Miltenyi Biotec GmbH, Bergisch Gladbach, Germany

Murine Plasmacytoid dendritic cells (PDC) represent a distinct leukocyte population capable of secreting large amounts of type I interferon in response to viruses and bacteria and are defined by a unique phenotype: B220⁺, Ly-6C⁺, CD11c^{int}.

We have generated a panel of monoclonal antibodies that all identify a single, presumably novel antigen, which we have termed Murine Plasmacytoid Dendritic Cell Antigen 1 (mPDCA-1). In lymphoid organs as well as in peripheral blood, liver, and lung mPDCA-1 is exclusively expressed on cells, which are CD11c^{int}, B220, Ly-6C^{high}, CD3⁻, CD4⁺, CD8a^{dim}, CD11b⁻, CD19⁻, CD49b⁻ (DX-5), CD90⁻ (Th-1.2), CD123, CD40⁻, CD80^{low}, and CD86⁻, and therefore phenotypically identical to PDC.

In past, PDC were described as a homogenous population. Now we demonstrated differential expression levels of the stem cell antigen 1 (Sca-1) in mPDC. In bone marrow (BM) and peripheral blood the Sca-1 expression on PDC is very low: only 15% express the marker. In contrast, about 40-50% of splenic PDC are positive for Sca-1. This expression can be enhanced following *in vivo* activation with CpG ODN both in BM and spleen.

Recently Ly-49Q has been described as a development marker for PDC in BM. It was shown that Ly-49Q and MHC-II were heterogeneously expressed on PDC in BM. Nevertheless in spleen only a homogenous Ly-49Q⁺ MHC-II⁺ PDC fraction could be detected. Therefore Sca-1 is an appropriate marker discriminating PDC subsets in spleen. Gating on mPDCA-1⁺ cells we found MHC-II⁺ Ly-49Q⁺ Sca-1⁺ as well as MHC-II⁺ Ly-49Q⁺ Sca-1⁻ mPDC in spleen.

Functional differences between both splenic mPDC subpopulations are currently under investigation.

Australian Society of Immunology: The 8th HLDA Workshop & Conference, December 12-16, 2004, Adelaide, Australia**mPDCA-1: A Presumably Novel Antigen Exclusively Expressed by Murine Plasmacytoid Dendritic Cells**

Talk presented by Dr. Jürgen Schmitz, Miltenyi Biotec

International Symposium of Dendritic Cells, 2004 in Brugge, Belgium**mPDCA-1: A presumably novel antigen exclusively expressed by murine plasmacytoid dendritic cells (mPDC)**

Fischer J. A. A., Schmitz J. and Dzionek A.

Miltenyi Biotec GmbH, Bergisch Gladbach, Germany

PDC represent a unique leukocyte population capable of secreting large amounts of type I interferon (IFN) in response to viruses and bacteria. In humans, PDC have been shown to specifically express BDCA-2 and BDCA-4, but in mouse, no such specific markers are available to date. Instead, mPDC are typically identified in lymphoid organs as CD45R⁺ (B220⁺), Ly-6C⁺, CD11c^{int}, CD8alpha^{+/-}, CD11b⁻ cells.

We have generated a panel of mAb that all identify a single, presumably novel antigen, which we have termed mPDC antigen-1 (mPDCA-1). In lymphoid organs, mPDCA-1 is exclusively present on cells, which are CD11c^{int}, CD45R⁺ (B220), Ly-6C^{high}, Gr-1^{int} (Ly-6C/G), CD3⁻, CD8a^{dim}, CD11b⁻, CD19⁻, CD49b⁻ (DX-5), CD90⁻ (Th-1.2), MHC-II^{int}, CD40⁻, CD80^{dim} and CD86⁻, and therefore phenotypically identical to mPDC. In fact, multi-color-staining reveals, that all CD11c^{int}, CD45R⁺ (B220), Ly-6C^{high} mPDC are mPDCA-1⁺ and that there are no other mPDCA-1⁺ cells present in lymphoid organs apart from mPDCA-1⁺ mPDC. mPDCA-1 is also expressed on mPDC generated from bone marrow-derived hematopoietic progenitors in Flt-3 Ligand/thrombopoietin (TPO) cultures. B cells as well as other types of DC may transiently express mPDCA-1 after *in vitro* stimulation with IFN-alpha. Anti-mPDCA-1 mAb-labeling of mPDC results in signal transduction as is evident by an increase in overall protein-tyrosine phosphorylation. Furthermore, injection of anti-mPDCA-1 mAb (rat IgG_{2b}/kappa; 200-500 µg/ml intraperitoneally) almost completely depletes mPDC *in vivo* (more than 80% are depleted within 24h in spleen, bone marrow and lymph nodes), indicating that mPDCA-1 is not only useful for single-color identification of mPDC by flow cytometry, but also of great value for elucidating the *in vivo* role of mPDC. Disclosure of the molecular nature of mPDCA-1 is currently underway.

FOCIS/IIC, 2004 in Montreal, Canada**A panel of new monoclonal antibodies with specificity for mouse plasmacytoid dendritic cell antigen-1 (mPDCA-1), a presumably novel antigen exclusively expressed by murine plasmacytoid dendritic cells**

Jens Fischer, Jürgen Schmitz, and Andrzej Dzionek

Miltényi Biotec, Bergisch Gladbach, Germany

The immunophenotype of murine PDCs has been reported in several studies. Murine PDC are CD45R⁺ (B220⁺), Ly6C⁺, CD11c⁺, CD8 alpha^{+/+}, CD3⁻, Thy-1.2⁻, CD49b⁻ (DX-5⁻), CD11b⁻, CD19⁻. We have generated a panel of monoclonal antibodies (mAb) that all identify a single presumably novel antigen, mPDCA-1, which in murine spleen, bone marrow and lymph nodes is exclusively present on these cells. Anti PDCA-1 mAb-labeling of PDCs results in signal transduction as is evident by an increase in overall protein-tyrosine phosphorylation. Furthermore, *in vivo* administration of anti PDCA-1 mAb causes depletion of PDC. Disclosure of the molecular nature of PDCA-1 is currently underway.

10. ACKNOWLEDGEMENTS

I would like to express my gratitude to my supervisor, Prof. Dr. Manolis Pasparakis for the supervision of my PhD project and his kind and helpful advice.

I am also very grateful to Professor Dr. Dagmar Knebel-Mörsdorf for her supervision of this PhD thesis.

I would like to thank Dr. Jürgen Schmitz for initiating this project and the opportunity to perform my doctoral thesis at Miltenyi Biotec GmbH. I am very grateful to my internal supervisor at Miltenyi, Dr. Andrzej Dzionek, for being such a competent, accurate and demanding supervisor, for his critical comments, useful advice and the continuous support.

My gratitude goes to my - former and present - colleagues and dear teammates for their constant encourage and motivation, for perpetual optimism, for the exciting and helpful scientific discussions. In particular, I am deeply indebted to (Drs) Tobias Voelkel, Jürgen Röck, Stefan A. Kaden, Sonja S. Schmucker, Björn Kolbe, Alexandra Hoch, Jeannette M. Möbius, Olaf T. Hardt, Peter S. Jähn, and Stefanie Kurig. I appreciate your friendship and encouragement that helped to finish this dissertation!

At Miltenyi I appreciated the warm welcome, helpful assistance, and great teamwork and I would like to mention all the energetic people from the R&D department and especially Monika Janz, Jörg Eilers, Katrin Vasters, Christoph „π“ Piechaczek, Gregor Winkels, Frank N. Single, Michael Birth, Andreas Bosio, Michaela Niemöller, Anna Förster, and Anne Richter. I thank, Olaf Brauns for peptide synthesis, and also Gerd Großhauser, Dirk Dittrich, and Bernhard Gerstmeyer from the MACS molecular business unit for their help my during all my microarray experiments and for bioinformatical support.

I especially thank my collaborators Anne Krug, Winfried Barchet, and especially Marco Colonna for the initiation of fruitful collaborations between Miltenyi and the Development of Pathology and Immunology, Washington University School of Medicine, St. Louis, USA. Furthermore, I am very grateful to Ulrike Schleicher from the Institute of Medical Microbiology and Hygiene, University of Freiburg, for the prosperous co-operation about PDC-NK cell interactions. I thank Anita Sapoznikov and Steffen Jung, Department of Immunology, Weizmann Institute of Science, Rehovot, Israel, for the close and long standing collaboration and for finally revealing the priming capacity of murine PDCs. I would like to thank Samantha Bailey-Bucktrout and Steve Miller from the Department of Microbiology-Immunology, Feinberg School of Medicine, Northwestern University, Chicago, USA, for outstanding experimental collaboration about the regulatory role of PDCs in EAE. My thanks go Christoph Göttlinger from the University of Cologne for countless hours of FACS sorting. In addition, I would like to thank Dennis Kirchhof, Sascha Rutz and in particular Dr. Alexander Scheffold for the opportunity to stay in his laboratory at the DRFZ, Berlin. I also thank PD Dr. Stefan Arnold, Institute I for Anatomy, University Hospital of Cologne, and Lars Ohl, Institute of Immunology, Hannover Medical School, Hannover, for assistance and generation of cryo-sections. I would like to thank Sven Burgdorf (Institute of Molecular Medicine and Experimental Immunology, Bonn), Sandra Gerecht, Sandra Balkow and Professor Stephan Grabbe (Institute of Immunology and Hautklinik des Universitätsklinikums, Johannes Gutenberg Universität Mainz) for transgenic mice and first insights into T cell interaction. I would empathize the current and ongoing collaborations with Ahmed Hegazy and Professor Max Löhning (Experimentelle Immunologie, Charite

Berlin) and Dr. Andreas Bergthaler, Department of Pathology and Immunology, University of Geneva, Switzerland, as well as Professor Dr. Ari Waisman (I. Medizinische Klinik und Poliklinik, Johannes Gutenberg-Universität Mainz) who introduced me first into the field of immunology.

At last but not no less intensively I would like to thank everybody who encouraged me; notably my friends and in particular my family. Without these people this work couldn't have been done, and I am very grateful for their trust and continuous support as well as the never-ending interest, solicitousness, and love.

Finally, there is one person whom I owe most gratitude: Virginia, thanks for all your love, consolation, patience, encouragement, and support during this stage of my life. I am looking forward to our life after this PhD thesis.

Ich danke von Herzen allen, die mich unterstützt und ermutigt haben, vor allem meinen besten Freunden sowie meiner Familie, insbesondere meinen Eltern, meinen Großeltern und Geschwistern Kristiane und Hendrik. Ohne diese Menschen würde mein Leben sicher ganz anders ausschauen und ich danke Euch für Euer Vertrauen und immerwährende Unterstützung sowie Euer fortwährendes Interesse!

Zum Abschluß möchte ich dem wichtigsten Menschen danken und in dessen Schuld ich am meisten stehe: Virginia, danke für all Deine Liebe, Trost, Geduld, Ermutigung und unendliche Unterstützung in dieser schweren aber mit Dir immer schönen Zeit. Ich freue mich auf unseres gemeinsames Leben in der Zeit „danach“.

11. ERKLÄRUNG

Ich versichere,

- dass ich die von mir vorgelegte Dissertation selbständig angefertigt, die benutzten Quellen und Hilfsmittel
- vollständig angegeben und die Stellen der Arbeit – einschließlich Tabellen, Karten und Abbildungen –, die anderen Werken im Wortlaut oder dem Sinn nach entnommen sind, in jedem Einzelfall als Entlehnung kenntlich gemacht habe;
- dass diese Dissertation noch keiner anderen Fakultät oder Universität zur Prüfung vorgelegen hat;
- dass sie – abgesehen von unten angegebenen Teilpublikationen – noch nicht veröffentlicht worden ist sowie,
- dass ich eine solche Veröffentlichung vor Abschluss des Promotionsverfahrens nicht vornehmen werde.

Die Bestimmungen der Promotionsordnung sind mir bekannt. Die von mir vorgelegte Dissertation ist von Herrn Professor Dr. Manolis Pasparakis betreut worden. Diese Arbeit wurde in der Forschungs- und Entwicklungsabteilung der Firma Miltenyi Biotec GmbH, Bergisch Gladbach, angefertigt.

Jens A. A. Fischer

Köln, im August 2008

Teilpublikationen:

Immunity 2004 Jul;21(1):107-19.

TLR9-dependent recognition of MCMV by IPC and DC generates coordinated cytokine responses that activate antiviral NK cell function.

A Krug, AR French, W Barchet, JAA Fischer, A Dzionek, JT Pingel, MM Orihuela, S Akira, WM Yokoyama, and M Colonna

Eur J Immunol. 2005 Jan;35(1):236-42.

Dendritic cells respond to influenza virus through TLR7- and PKR-independent pathways.

W Barchet, A Krug, M Cella, C Newby, JAA Fischer, A Dzionek, A Pekosz, and M Colonna

J Exp Med. 2007 Apr 16;204(4):893-906.

NK cell activation in visceral leishmaniasis requires TLR9, myeloid DCs, and IL-12, but is independent of plasmacytoid DCs.

U Schleicher, J Liese, I Knippertz, C Kurzmann, A Hesse, A Heit, JAA Fischer, S Weiss, U Kalinke, S Kunz, and C Bogdan

J Exp Med. 2007 Aug 6;204(8):1923-33.

Organ-dependent in vivo priming of naive CD4⁺, but not CD8⁺, T cells by plasmacytoid dendritic cells.

A Sapozhnikov, JAA Fischer, T Zaft, R Krauthgamer, A Dzionek, and S Jung

Cutting Edge: The Journal of Immunology May 2008; 180: 6457 - 6461

CNS Plasmacytoid Dendritic Cells Regulate the Severity of Relapsing Experimental Autoimmune Encephalomyelitis

SL Bailey-Bucktrout, SC Caulkins, G Goings, JAA Fischer, A Dzionek, and SD Miller

Manuscript in submission (August 2008)

Heterogeneous Sca-1 expression on murine plasmacytoid dendritic cells defines developmental and functional differences

Jens A. A. Fischer, Jürgen Schmitz, and Andrzej Dzionek

Manuscript in preparation (October 2008)

Identification and functional characterization of mPDCA-1 as a novel antigen-uptake receptor on murine plasmacytoid dendritic cells for (cross-) priming of naïve CD4⁺ and CD8⁺ T cells.

Jens A. A. Fischer, Jürgen Schmitz, and Andrzej Dzionek

12. LEBENS LAUF (*Curriculum vitae*)Persönliche Daten

Name: Jens A. A. Fischer
 Geburtsdatum und -ort: 31. Mai 1977 in Leverkusen
 Familienstand: verheiratet
 Staatsangehörigkeit: deutsch

Schule

1983 – 1987 Gemeinschaftsgrundschule Hebborn, Bergisch Gladbach
 1987 – 1996 Nicolaus-Cusanus-Gymnasium, Bergisch Gladbach,
 Abschluß mit allgemeiner Hochschulreife (Abitur)

Zivildienst

1996 – 1997 Evangelische Kirchengemeinde Bergisch Gladbach und Stadtkirchenverband
 Köln

Hochschulausbildung

Oktober 1997 – **Studium der Biologie** an der Universität zu Köln
 Oktober 2001 Hauptfach Genetik, Nebenfächer Biochemie und Pharmakologie
 1999 – 2000 **Praktikum** in der Arbeitsgruppe von Professor Maria Leptin, Institut für Genetik,
 Universität zu Köln
 WS 1999/2000 **Vordiplomsprüfung** Biologie in den Fächern Botanik, Zoologie, Physik und
 Chemie
 Sommer 2000 **Praktikum** in der Arbeitsgruppe von Priv.-Doz. Dr. Reinhard Berkels, Institut für
 Pharmakologie, Universitätsklinikum Köln
 Sommer 2001 **Praktikum** in der Arbeitsgruppe von Professor Stefan Kochanek, Zentrum für
 Molekulare Medizin Köln (ZMMK), Universität zu Köln
 Oktober 2001 – **Diplomarbeit** am Zentrum für Molekulare Medizin Köln (ZMMK) und Institut für
 Januar 2003 Genetik, Universität zu Köln
 Titel der Diplomarbeit: Synthese und Charakterisierung rekombinanter
 adenoviraler Fiber-Proteine mit heterologen Trimerisierungsdomänen mit dem
 Ziel einer gerichteten Tropismusmodifikation adenoviraler Gentransfer-Vektoren
 Betreuer: Professor Stefan Kochanek (gegenwärtige Adresse: Universität Ulm)
 Januar 2003 Verleihung des **Diplomzeugnisses** (Gesamtnote: sehr gut)
 Februar 2003 – **Promotionsarbeit** am Institut für Genetik, Universität zu Köln; Universitärer Be-
 Oktober 2008 treuer: Professor Manolis Pasparakis. Durchführung der praktischen Arbeiten
 als externer Promotionsstudent in der Firma Miltenyi Biotec GmbH, Bergisch
 Gladbach, unter der Anleitung von Dr. Andrzej Dzionek und Dr. Jürgen
 Schmitz; Titel der Promotion: "Identification and functional characterization of
 mPDCA-1 as a novel antigen-uptake receptor for murine plasmacytoid dendritic
 cells enabling (cross-) priming of naïve CD4⁺ and CD8⁺ T cells."
 August 2006 **Praktikum** in der Arbeitsgruppe von Dr. Alexander Scheffold, Deutsches
 Rheumaforschungszentrum (DRFZ) Berlin
 Oktober 2008 **Voraussichtlicher Abschluß der Promotion** an der Universität zu Köln

Jens A. A. Fischer

Bergisch Gladbach, im August 2008